Effect of future CO_2 and temperature regimes on phytoplankton community composition, biomass and photosynthetic rates in the western English Channel

By Matthew E. Keys

A thesis submitted to the School of Biological Sciences of the University of Essex in partial fulfilment of the requirements for the degree of Doctor of Philosophy, Marine Biology

In collaboration with Plymouth Marine Laboratory

October 2017

To my wife, who thought this day would never come,

and to my Mother who would have enjoyed this moment.

Abstract

CO_2 storage in the oceans is strongly affected by biological processes. Production of organic matter through phytoplankton photosynthesis drives CO_2 sequestration, which feeds back to atmospheric CO_2 and global climate. The ongoing increase in atmospheric CO_2 and temperature is strongly associated with changes in ocean chemistry and increasing seawater temperatures. To investigate these impacts on coastal phytoplankton under conditions predicted for the year 2100 (pCO_2 elevated to 800 µatm and +4 °C temperature), three factorial experiments were conducted with natural communities sampled from the western English Channel (WEC). Elevated pCO_2 increased phytoplankton biomass by up to 20-fold while elevated temperature resulted in an increase of up to 14-fold. Light-saturated photosynthetic carbon fixation rates increased > 6-fold under elevated pCO_2 while an increase of up to 3-fold resulted from elevated temperature. The combined effects of elevated pCO_2 and temperature reduced biomass in late summer and had no effects on biomass in the autumn with no significant effects on photosynthetic carbon fixation rates in either season. Individual treatments of elevated pCO_2 and temperature resulted in near mono-specific communities: diatoms in late summer and nanophytoplankton in autumn. Combined effects of both factors resulted in the most diverse phytoplankton communities and promoted increased dinoflagellate and *Synechococcus* biomass at the expense of diatoms and nanophytoplankton. Elevated pCO_2 alone promoted dominance of the harmful algal bloom (HAB) species, *Phaeocystis* in spring and autumn, while the combination of elevated pCO_2 and temperature promoted biomass of the HAB species, *Prorocentrum minimum* in autumn. The results indicate that experimental simulations of year 2100 pCO_2 and temperature may significantly modify phytoplankton community structure with a positive feedback on atmospheric CO_2 in late summer and no change on feedback in autumn. In either scenario, no increase in phytoplankton productivity during a period of changes in bulk carbonate chemistry resulting from ongoing anthropogenic carbon uptake, may be expected to negatively influence carbon biogeochemistry in the WEC.

Acknowledgements

I am particularly grateful to the project supervisors Gavin Tilstone, Helen Findlay, Claire Widdicombe and Tracy Lawson for their help, encouragement, positive input and advice.

Special thanks and gratitude go to Glen Tarran for helpful training and insight in flow cytometry, Denise Cummings for training and assistance with CHN analysis, Paul Rooks for his help, knowledge, humour and assistance with microscopy, Elaine Fileman for imparting taxonomic knowledge and training on the FlowCam, Malcolm Woodward and Carolyn Harris for the kind assistance with nutrients analysis and to all who contribute to the western Channel Observatory.

I would like to express my sincere gratitude to the Natural Environment Research Council for funding this PhD studentship (grant no. NE/L50189X/1).

Declaration of Authorship

I, Matthew E. Keys, declare that the thesis entitled

Effect of future CO_2 and temperature regimes on phytoplankton community composition, biomass and photosynthetic rates in the western English Channel

And the work presented in it are my own. I confirm that:

This work was done wholly or mainly while in candidature for a research degree at this university;

It has not already been accepted for any degree, and is not being concurrently submitted for any other degree;

Where I have consulted the published work of others, this is always clearly attributed;

All main sources of help have been acknowledged

Word count of main body of thesis: 44769

List of contents

List of Figures

List of tables

Abbreviations

ATP	Adenosine triphosphate
C	Carbon
C:N:P	Ratio of carbon:nitrogen:phosphorus
CA	Carbonic anhydrase
$CaCO_3$	Calcium carbonate
CCM	Carbon concentrating mechanism
Chl *a*	Chlorophyll a
CO_2	Carbon dioxide
CO_3^{2-}	Carbonate ions
DA	Domoic acid
DIC	Dissolved inorganic carbon
DMS	Dimethyl sulphide
DMSP	Dimethylsulphoniopropionate
E_k	Light saturation point of photosynthesis
Fe	Iron
FES	Fluorescence excitation spectra values
F_m	Maximum chlorophyll fluorescence
F_o	Minimum chlorophyll fluorescence
FRRf	Fast Repetition Rate fluorometer
F_v/F_m	Maximum photochemical efficiency of PSII in the dark-adapted state
GLMM	Generalised linear mixed model
GLM	Generalised linear model
GP	Gross photosynthesis
H^+	Hydrogen ion
H_2CO_3	Carbonic acid

HAB	Harmful algal bloom
HCO_3^-	Bicarbonate ion
$HgCl_2$	Mercuric chloride
IPCC	Intergovernmental panel on climate change
JV_{PSII}	Photosystem II flux per unit volume
MODIS	Moderate resolution Imaging spectroradiometer
N	Nitrogen
N_2	Nitrogen gas
NADPH	Nicotinamide adenine dinucleotide phosphate
NCP	Net community production
NEODAAS	NERC Earth Observation Data Acquisition Service
nMDS	Non-metric multidimensional scaling
NPP	Net primary production
OA	Ocean acidification
P	Phosphate
PAR	Photosynthetically active radiation
P^B_m	Maximum light-saturated rate of photosynthesis
P_{Bmax}	Maximum biomass-normalised light-saturated carbon fixation rate
PCA	Principal components analysis
pCO_2	Partial pressure of CO_2 in seawater
pH	Logarithmic scale used to specify acidity or basicity of an aqueous solution
PE curve	Photosynthesis vs irradiance curve
PIC	Particulate inorganic carbon
POC	Particulate organic carbon
PON	Particulate organic nitrogen
PSII	Photosystem II
PTFE	Polytetrafluoroethylene

RubisCO	Ribulose-1, 5-bisphosphate carboxylase/oxygenase
Si	Silicate
SST	Sea surface temperature
TA	Total alkalinity
WEC	western English Channel
α^B	Light limited slope of photosynthesis
σ_{PSII}	Functional cross section of photosystem II
$\varphi_{E:C}$	Electron requirement for carbon uptake

Chapter 1 – Phytoplankton, climate change and ocean acidification

Abstract

Atmospheric CO_2 concentration has increased by around 33% over pre-industrial levels, with an on-going annual increase of ~0.4% per annum and the dissolution of this excess CO_2 into the surface ocean is lowering ocean pH. The surface ocean carbonate system is directly affected by increased atmospheric CO_2. In combination with climate warming, predictions imply modification of sea surface temperature, precipitation, ocean stratification and circulation. Further predicted consequences include higher integrated mean irradiance within shallower mixed layers and lower nutrient concentrations due to mixed layer shoaling. The physiological and ecological aspects of the phytoplankton response to changing environmental factors hold the potential to alter phytoplankton community composition, primary productivity and to feedback to biogeochemical cycles. Phytoplankton have been observed to exhibit a wide variety of responses to environmental pressures and a current paucity in data relating combinations of environmental change to outcomes of changes to phytoplankton community structure expose significant knowledge gaps. After more than fifteen years of studies testing sensitivity and physiological performance of phytoplankton in response to elevated CO_2, current research trends show many phytoplankton species to be largely insensitive to increasing CO_2. This may be in part, due to a concerted focus of investigations on single species and testing hypotheses that factor just one environmental variable in isolation. While these studies provide important data, they lack the biological, competitive and environmental interactions that take place in natural systems with mixed communities. More recent studies have expanded the range of experimental treatments tested and are aligning experimental designs with multiple environmental stressors predicted to change in concert with elevated atmospheric CO_2. Additionally, a renewed focus on testing hypotheses at a natural population level has highlighted how responses in tightly controlled laboratory conditions may change significantly in the environment.

1.1 Introduction

Photosynthesis is the formation of organic matter (carbon fixation) in the oceans using energy from sunlight and is carried out chiefly by phytoplankton. Marine phytoplankton are responsible for ~50% of global net primary production (NPP) (Falkowski & Raven, 2007; Beardall *et al.*, 2009) and have played a central role in mitigating and amplifying past climate change as well as contributing to stabilising the climate (Schlesinger, 2005). The oceans take up about one million tons of CO_2 per hour on average and remove a quarter of the CO_2 emitted to the atmosphere by anthropogenic activities (Sabine et al., 2004). While coastal zones account for just 7% of the global ocean surface, their role in the global carbon cycle is critical to NPP (Wollast, 1998). Supporting an estimated 10-15% of global ocean NPP, coastal zones may be responsible for more than 40% of oceanic carbon sequestration (Muller-Karger, 2005).

Atmospheric CO_2 concentration has increased by around 33% over pre-industrial levels, with an on-going increase of ~0.4% per annum. Current pCO_2 concentration has reached ~400 µatm and has been predicted to rise to 700 µatm by the end of this century (Alley *et al.*, 2007), or even values exceeding 1000 µatm (Raupach *et al.*, 2007; Raven *et al.*, 2005), with a corresponding seawater pH decrease of 0.3 units below the present value (8.1) to 7.8 (Wolf-Gladrow et al., 1999). As anthropogenic CO_2 increases in the atmosphere, it dissolves in the surface ocean and aqueous CO_2 (CO_2 (aq)) reacts with water to form the weak carbonic acid (H_2CO_3), a process termed ocean acidification (OA):

$[CO_2]_{(aq)} + [H_2O] = [H_2CO_3]$

Carbonic acid dissociates to hydrogen ions (H^+) and bicarbonate ions (HCO_3^-):

$[H_2CO_3] = [H^+] + [HCO_3^-]$

A large fraction of the additional hydrogen ions combine with carbonate ions (CO^{2}_{3-}) to form bicarbonate ions:

$[H+] + [CO_3^{2-}] = [HCO_3^-]$

The resulting consequence in this relatively straight forward carbonate chemistry is an increase in the concentrations of aqueous carbon dioxide, carbonic acid, hydrogen ions and bicarbonate ions, and a decrease in carbonate ions (**Fig. 1.1 A**). Therefore an increase in H^+ results in a pH decrease, since pH is defined by the negative logarithm of the activity of hydrogen ions (Joint et al., 2011). Thus, a shift in equilibria between CO_2, HCO_3^- and CO_3^{2-} based on a three-fold increase in atmospheric CO_2 from the pre-industrial level (a rise to ~840 µatm) would result in a concentration increase by 17% for HCO_3^- and decrease by 54% for CO_3^{2-} (**Table 1.1**). This shift in dissolved inorganic carbon (DIC) equilibria has wide-ranging implications for photosynthesis and phytoplankton cell growth (Riebesell, 2004), while a reduction in carbonate concentrations results in a decrease in the saturation state of both calcite and aragonite; critical minerals for a range of calcifying planktonic (and non-planktonic) organisms (Riebesell and Zondervan, 2000).

Table 1.1 A shift in equilibria between CO_2, HCO_3^- and CO_3^{2-} would result in a concentration increase by 17% for HCO_3^- and decrease by 54% for CO_3^{2-} (based on Total Alkalinity of 2324 mol kg^{-1} and temperature of 18 °C). (After Raven *et al*., 2005)

Carbonate system parameters	Pre-Industrial	Present day	3 x pre-industrial	4 x pre-industrial
Atmospheric CO_2 (µatm)	280	380	840	1120
H_2CO_3 (mol kg^{-1})	9	13	28	38
HCO_3^- (mol kg^{-1})	1768	1867	2070	2123
CO_3^{2-} (mol kg^{-1})	225	185	103	81
Total DIC (mol kg^{-1})	2003	2065	2201	2242
Surface ocean mean pH	8.18	8.07	7.77	7.65
Calcite saturation	5.3	4.4	2.4	1.9
Aragonite saturation	3.4	2.8	1.6	1.2

Concurrent to changes in carbonate chemistry, elevated concentrations of atmospheric CO_2 along with other climate-active gases are warming the planet. Climate change has been predicted to modify sea surface temperature, precipitation, ocean stratification and circulation (Sarmiento et al., 2004). The global ocean sea surface temperature (SST) has already warmed by an estimated ~0.6°C over the past 100 years (IPCC, 2007) and has been predicted to rise further, between 1.8 to 4 °C by the end of this century (Alley et al., 2007). Phytoplankton are likely to experience higher integrated irradiance due to intensified stratification and mixed

layer shoaling (Boyd and Doney, 2002) and such physical changes in stratification are expected to influence water mass exchange and hence the vertical flux of nutrients, enhancing nutrient limitation in the open ocean photic zone (Beardall et al., 2009) (**Fig. 1.1 B**). Conversely, episodic storm and precipitation events linked to climate warming, together with anthropogenic riverine inputs due to agriculture and changes in land use may increase nutrient loads within coastal zones leading to increased eutrophication episodes (Muller-Karger, 2005). The distribution of phytoplankton biomass and NPP is defined by the availability of inorganic carbon, light and a suite of major and trace nutrients (including nitrogen (N), phosphate (P) and iron (Fe)) (Behrenfeld et al., 2006) . Recent studies show that phytoplankton C:N:P ratios can be responsive to elevated CO_2 (for a full review, see Hutchins *et al.*, 2009) and that additionally, dissolved Fe may decrease in bioavailability, despite no change in the Fe requirements of phytoplankton (Shi et al., 2010). Therefore changes in CO_2, temperature, depth-integrated irradiance and nutrient availability hold significant implications for phytoplankton community composition (Raven et al., 2000; Sarmiento et al., 2004) and consequently NPP (Marinov et al., 2010). High variability in the relative rates of photosynthesis exists amongst the phytoplankton on the basis of significant physiological and ecological differences between the predominant functional groups; cyanobacteria, diatoms, dinoflagellates, prymnesiophytes and flagellates (Widdicombe et al., 2010a) and across a wide size spectrum, broadly categorised into 3 size classes; picophytoplankton (0.2 – 2 μm), nanophytoplankton (2 – 20 μm) and microphytoplankton (20 – 200 μm) (Finkel et al., 2009). Different species have differing requirements for inorganic carbon (as well as light, temperature and nutrients) due to physiological differences (e.g. CO_2-concentrating mechanisms), thus changes in community structure will impact gross photosynthesis (GP) and NPP (Giordano et al., 2005) as well as elemental cycling and food web dynamics (Beardall and Stojkovic, 2006).

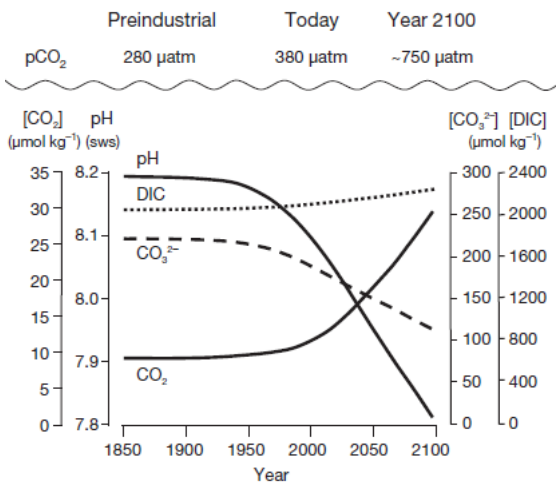

Fig. 1.1 A. Seawater pH and the dissolved carbon dioxide (CO_2) and carbonate ion concentrations (CO_3^{2-}). Dashed lines represent predicted changes in carbonate chemistry under a 'business as usual' anthropogenic CO_2 emission scenario (Alley et al., 2007). (Modified after Wolf-Gladrow *et al.*, 1999)

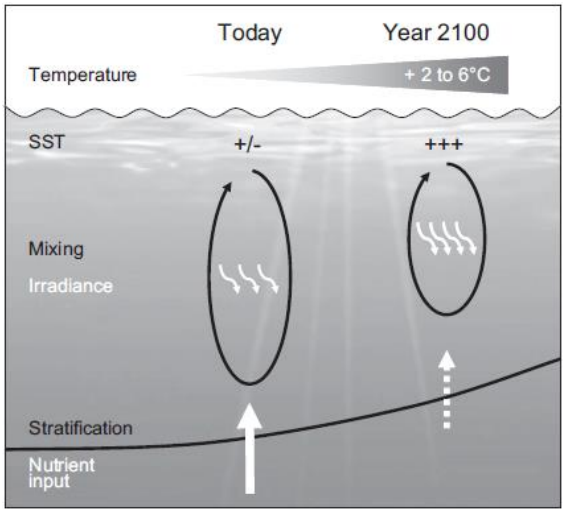

Fig. 1.1 B. Changes in stratification, light and nutrient availability in response to increased sea surface temperatures. (Modified after Rost & Riebesell, 2004)

Innovative early studies on pH in the oceans, its changes with depth, tide, physical and biological processes and its impact on physiological responses were conducted in the early 20th century (Gail, 1919; McClendon, 1918; Prytherch, 1929; Rubey, 1951). Results from these and other early studies are not entirely relevant for assessing the effects of future OA due to the uncertain measurements of the carbonate system and large ranges of pH values tested. Over the past 15 years a concerted research effort has focused on environmental parameter ranges far more within the scope of future global environmental change. More than 260 scientific papers have reported impacts of OA on marine life, the vast majority of which have been performed on individual species (Gunawan and Ng, 2011) and less than 5% of which have been conducted on communities or ecosystems. Predicting impacts at the community and ecosystem level by extrapolating from organism-based responses is difficult and potentially misleading, since the observed responses do not factor in competition, trophic interactions and with low, or no genetic diversity (Riebesell et al., 2011). In the case of marine phytoplankton, responses to OA

have only been examined in a few field-based natural community studies and at a species level, in a small number of taxa, chosen in many cases for their ease of culture in the laboratory. There exists a vast knowledge gap in investigating changes in population-level responses with a range of ecologically relevant species, set within the context of OA together with the complex interactions between all drivers of global climate change including CO_2, temperature, light and nutrient regimes.

1.2 Phytoplankton response to elevated CO_2

1.2.1 Photosynthesis and carbon fixation – Laboratory studies

The inherent CO_2 sensitivity in photosynthesis is primarily a result of the primary carboxylating enzyme ribulose-1, 5-bisphosphate carboxylase/oxygenase (RubisCO). The photosynthetic process starts with capturing light energy, converting it into ATP and NADPH and through the Calvin-Benson cycle, using these compounds to fix CO_2 (Falkowski and Raven, 2007). Approximately 50% of recent photosynthate is allocated to protein synthesis by actively growing marine phytoplankton. This results in a competitive interaction for NADPH and ATP between CO_2 fixation, transport processes, nitrate reduction and protein formation (Geider and MacIntyre, 2008). RubisCO, a highly conserved enzyme which evolved 3 billion years ago during a period of elevated atmospheric CO_2 and low O_2 concentrations, has a low affinity for its CO_2 substrate and is susceptible to this competitive reaction with O_2 (Raven et al., 2012). Despite variation in RubisCO's catalytic properties, the generally poor substrate affinity for CO_2 imposes constraints on assimilation of carbon (C) under present day comparatively low concentrations of CO_2 in seawater (Rost et al., 2008). To avoid C limitation most marine phytoplankton have evolved different mechanisms that enhance the concentration of CO_2 in the close vicinity of RubisCO (Badger et al., 1998; Thoms et al., 2001). CO_2 concentrating mechanisms (CCMs) have been found to be present in many marine phytoplankton species that facilitate the uptake of CO_2 and/or HCO_3-, as well as isoforms of the enzyme carbonic anhydrase (CA), which increase the

inter-conversion rates between these inorganic C species (Price et al., 2008; Roberts et al., 2007).

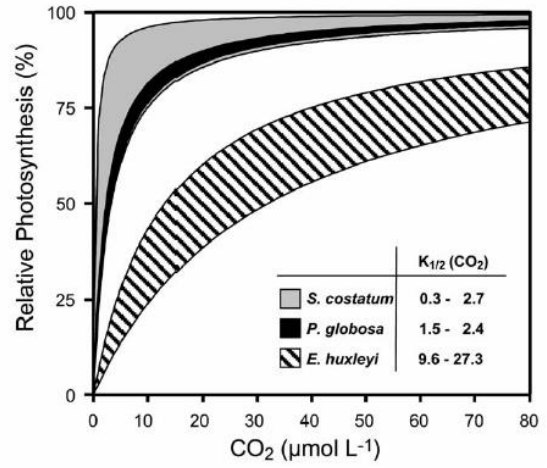

Fig. 1. 2. Effects of CO_2 sensitivity on phytoplankton photosynthesis. *Skeletonema costatum* and *Phaeocystis globosa* are at or close to saturation (present day CO_2 concentrations of 8-20 µmol L^{-1}). Coccolithophores such as *Emiliania huxleyi* with low affinities for inorganic carbon appear to be carbon limited in today's oceans. (From Riebesell, 2004)

Although still poorly understood, a few studies suggest that species differ in the regulation and efficiency of their CCMs (Burkhardt et al., 2001; Rost et al., 2006a; Trimborn et al., 2008). Additionally, dominant marine phytoplankton species differ in their CO_2 requirement, some preferentially using CO_2 as a C source where as other species draw their inorganic C from the large pool of HCO_3- (Elzenga et al., 2000) (**Fig. 1.2**). Species with inefficient CCMs or those that rely on diffusive CO_2 uptake with low affinities for inorganic C, may benefit from an increase in atmospheric CO_2 since they are more highly CO_2 sensitive in photosynthesis. However, while species that operate highly efficient CCMs are at, or close to, rate saturation under current ambient CO_2 concentrations, they may still benefit from increasing atmospheric CO_2 since optimised energy and resource allocation could result from a down regulation of CCMs. Some phytoplankton species grown under ocean acidification conditions have been shown to alter their metabolic pathways, down-regulating their CCMs, up-regulating photorespiration (dark

respiration) and heat- dissipating processes and generating extra energy by degrading accumulated phenolic compounds (Gao, 2017). For example, elevated pCO_2 (1000 ppm) incubations with the diatom *Phaeodactylum tricornutum* resulted in the down-regulation of CCMs leading to increased growth rates, enhanced photoinhibition at high light intensities and stimulation of dark respiration resulting in a 5.8% increase in photosynthetic production (Wu et al., 2010a). Similarly, down-regulation of CCMs in the dinoflagellate *Karenia mikimotoi* under conditions of elevated pCO_2 (1000 and 2000 ppm) resulted in increased dark respiration and a stimulation in growth and photosynthesis (Hu et al., 2017). Group-specific variation is most pronounced within photosynthetic C-fixation rates when comparing certain diatom species tested, as well as the prymnesiophyte *Phaeocystis globosa* (which are at or close to CO_2 saturation at present day values) (Burkhardt et al., 2001; Rost et al., 2003), with the coccolithophores *Emiliania huxleyi* and *Gephyrocapsa oceanica* which are currently well below saturation (Riebesell and Zondervan, 2000; Rost et al., 2003). This suggests significant differences in the physiological response to elevated CO_2 concentrations between major phytoplankton taxonomic groups, indicating that changes in the carbonate system may have profound effects on phytoplankton communities. This may result in a direct effect in productivity and/or changes in community taxonomic composition and species succession.

Photosynthetic reactions are categorised in to light dependent (light reaction) and light independent (dark reaction or Calvin-Benson cycle) phases. The light reactions of photosynthesis generate the energy needed to fuel the dark reaction as well as the CCMs (Falkowski and Raven, 2007). Photosynthetic rates are related to irradiance in a non-linear fashion and photosynthesis vs irradiance (PE) curves are commonly used to parameterise this relationship in phytoplankton species in culture and natural populations in the field. At the lowest irradiances, the absorption of photons is slower than the capacity rate of steady-state electron transport from water to CO_2 (parameterised as the light limited slope: α^B). Photosynthetic rates become increasingly non-linear with increasing irradiance and rise to

saturation level when the rate of photon absorption exceeds the rate of steady-state electron transport from water to CO_2 (parameterised as the maximum light-saturated photosynthetic rate: P^B_m). The light saturation point of photosynthesis is parameterised by the ratio P^B_m: α^B (E_k) and consequently higher values of E_k indicate photosynthesis saturates at higher irradiances. A reduction in photosynthetic rates may occur with further increases in irradiance which is dependent on the irradiance level and duration of exposure (parameterised as photoinhibition: β) (Sakshaug et al., 1997) (**Fig. 1.3**).

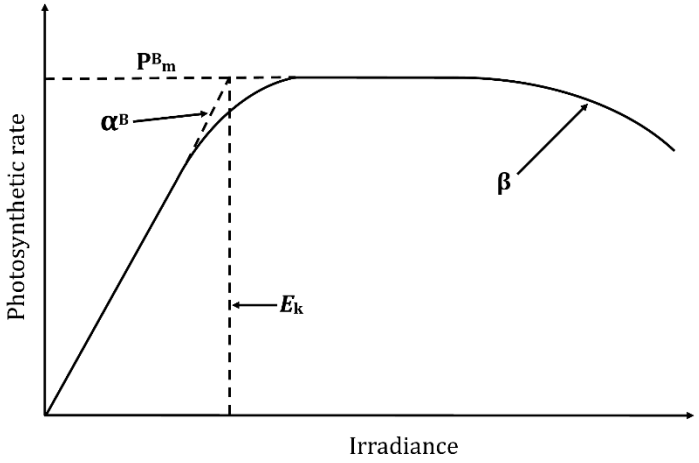

Fig. 1.3 Schematic diagram of PE curve parameters: P^B_m (maximum light-saturated photosynthetic rate), α^B (light limited slope), E_k (light saturation point of photosynthesis) and β (point at which photoinhibition occurs).

The following sections discuss current trends in phytoplankton group- and species-specific responses to elevated CO_2. While the predominant unit used for the concentration of CO_2 in seawater throughout this thesis is the partial pressure of CO_2 in seawater (pCO_2) expressed in units of micro atmospheres (μatm), authors of ocean acidification research papers also commonly use the mole fraction for gaseous species with a unit of parts per million (e.g. moles of CO_2 per million parts of air:PPM or PPMV). Where cited from the published literature in this thesis, these units have not been converted. For clarity, the two units of measure slightly differ.

The mixing ratio in ppm is defined as 'mixing ratio in dry air', i.e. in going from partial pressure you must subtract out the water vapor pressure. The conversion is:

$pCO_2 = xCO_2 * (p(air) - p(H_2O))$

where pCO_2 is the partial pressure of CO_2, xCO_2 is the mixing ratio, p(air) is the air pressure and $p(H_2O)$ is the water vapor partial pressure. Because of this, the value for pCO_2 is somewhat lower compared to xCO_2. The difference depends on temperature and relative humidity, but for an xCO_2 of 360 ppm the value of pCO_2 is around 350 µatm (Riebesell et al., 2010).

1.2.2 Coccolithophores

Stimulation of photosynthesis and C fixation rates through elevated CO_2 has been observed in a variety of phytoplankton species including diatoms, coccolithophores, cyanobacteria and dinoflagellates as well as natural assemblages. While under-saturated at current ambient atmospheric CO_2, it would be intuitive to consider that the calcifying coccolithophores may significantly benefit from increasing CO_2 concentrations, compared to other non-calcifying taxa. The secretion of calcium carbonate [$CaCO_3$] skeletal structures is wide spread across planktonic biota throughout the world oceans (Riebesell et al., 2010). Corals, foraminifera and coccolithophores account for the bulk of global calcification (Mackinder et al., 2010) and coccolithophores alone are believed to contribute up to half of current oceanic $CaCO_3$ production (Milliman, 1993), playing a major biogeochemical role as well as ballast provision for sedimentation of organic carbon production (although estimates vary). HCO_3^- comprises more than 90% of the total dissolved inorganic carbon pool (DIC) in the oceans and most evidence suggests that this is the main carbon source for calcification, the reaction for which shows a net production of CO_2 (Brownlee and Taylor, 2002):

$$\mathbf{Ca^{2+} + 2HCO_3^- \xrightarrow{calcification} CaCO_3 + H_2O + CO_2}$$

Sea surface carbonate chemistry may be influenced by coccolithophore calcification by reducing draw down of atmospheric CO_2 and by reducing sea surface alkalinity (Riebesell et al., 2009).

Among the adverse effects of ocean acidification on marine organisms, reduction in the capacity of calcifiers to build shells has received special attention due to the importance of the global biogeochemical cycle implications (Van Cappellen, 2003). Most planktonic organisms investigated to date exhibit reduced or abnormal calcification in response to elevated CO_2 and the concomitant changes in carbonate chemistry (Delille et al., 2005; Zondervan et al., 2002). The first widely adopted notion was that *Emiliania huxleyi*, the most widely studied coccolithophore in the context of ocean acidification, decrease their calcification rate with increasing CO_2 in a linear fashion (Riebesell and Zondervan, 2000). Subsequent studies showed this not to be the case (Iglesias-rodriguez et al., 2008; Langer et al., 2006), demonstrating that there is no uniform response of coccolithophores to elevated CO_2 (Iglesias-rodriguez et al., 2008). Add to this the known considerable phenotypic and genotypic variation amongst *E. huxleyi* ecotypes together with strain specific responses to a host of experimental conditions (e.g. light saturation, nutrients, temperature, salinity and CO_2), much phenotypic plasticity has been demonstrated (Findlay et al., 2011). The diverging response reported on *E. huxleyi* calcification to changing carbonate chemistry has been recently resolved through the implementation of a model equation describing the dependence of calcification rates on carbonate chemistry speciation (Bach et al., 2015). The model equation considered key factors most relevant to coccolithophore calcification and common to all experimental data: calcification rate scales positively with HCO_3^-, the primary substrate for calcification, and CO_2, which can limit cell growth, whereas it is inhibited by protons (H^+). The model results were highly correlated to culture experiment results and suggested the projected increase in H^+ with only a minor increase in HCO_3- could impede calcification rates. Other variables manipulated inconsistently in culture experiments (temperature, light, nutrients etc.) were excluded from the model, since they are also responsible for variability in calcification rates. While effects of some of these variables on calcification individually (e.g. temperature and irradiance) are well described, other variables have not been studied and there is a lack of knowledge on their interactions. Other coccolithophore studies have taken a multiple-global change stressor

approach in experimental design and have shown how the interaction of elevated CO_2 and increased temperature and irradiance act together to decrease rates of calcification further, as well as the ratio of inorganic to organic C (PIC:POC) with an over-all increase in photosynthetic performance (Feng et al., 2008a). However, the only study to show a decrease in organic matter production at elevated CO_2 was conducted under nitrate limitation (Sciandra et al., 2003). (**Table 1.2**). 90% of the marine biogenic sulfur in the atmosphere, where it affects cloud formation and climate, originates from the production of the marine trace gas dimethyl sulphide (DMS). Measurements of DMS production were taken from *E. huxleyi* cultures grown under conditions of elevated pCO_2 (1000 µatm), elevated temperature (+ 4 °C) and a combination of these two treatments (Arnold et al., 2013). Average DMS production was about 50% lower in the elevated pCO_2 treatment relative to the ambient control. In contrast, elevated temperature and the combination of elevated temperature and pCO_2 had a strong effect, showing significantly higher DMS production with the highest production under elevated temperature alone. While growth of *E. huxleyi* was unaffected by the experimental treatments, cell diameter decreased significantly under elevated temperature.

1.2.3 Diatoms

Since the process of silicification does not appear to be CO_2 sensitive compared to that of calcification (Milligan et al., 2004), diatoms have consequently not been studied in the context of carbonate system manipulations with anywhere near the same intensity as coccolithophores. A much larger proportion of studies have investigated the influence and effects of light and nutrients with this important group of phytoplankton. **Table 1.3** summarises the response of diatoms to elevated CO_2 through experimental investigations dating back to 1993. Earlier studies suggested that diatoms were limited by CO_2 (Riebesell et al., 1993), while later studies have showed that many diatoms in fact use highly regulated and efficient CCMs in order to compensate for low CO_2 conditions, particularly those associated with large bloom formations (Burkhardt et al., 2001; Rost et al., 2003; Trimborn et al., 2008).

More recently, studies on diatoms testing effects of elevated CO_2 have started to show a pattern of physiological responses not previously investigated. Growth and photosynthetic C fixation rates have been shown to increase by a factor of 5% and 12% respectively at elevated CO_2 in the diatom *Phaeodactylum tricornutum,* with dark respiration stimulated by 34% at the same experimental CO_2 concentration (Wu et al., 2010b). The same study also showed a down regulation of CCMs resulting from photoinhibition at high levels of photosynthetically active radiation (PAR) at the high CO_2 concentration. Similarly, Yang and Gao (2012) found increases of 25% and 35% in photosynthetic performance and dark respiration respectively, in a study exposing *Thalassiosira pseudonana* to high CO_2 treatments (1000 µatm pCO_2). They also reported a similar CCM down regulation. This contrasts greatly with a slightly earlier study on exactly the same strain of *T. pseudonana* (CCMP 1335) where continuous cultures over a 3 month period at 760 µatm pCO_2 showed no change in photosynthetic efficiency (F_v/F_m) or functional cross section of photosystem II (σ_{PSII}) (Crawfurd et al., 2011). It is unclear whether this variation in response is a result of differences between experimental CO_2 concentration (i.e. 1000 µatm *vs*. 760 µatm pCO_2) or culture conditions (both studies used a continuous culture system with slight differences in irradiance and both used filtered seawater as growth medium). Maximal photosynthetic capacity has also been shown to increase with elevated CO_2 concentrations at saturating light intensity in a study with *Chaetoceros muelleri* (Ihnken et al., 2011), however no growth effect was observed under the same CO_2 treatment, showing opposite effects to CO_2 availability.

Of particular interest amongst marine phytoplankton are those species associated with harmful algal blooms (HABS) and in particular, how global climate change may impact the occurrence of HAB events. Some members of the diatom genus *Pseudo-nitzschia* are known to produce the toxin domoic acid (DA), responsible through trophic transfer for mass mortalities of shellfish with risks to human health (Andeson et al., 2002). Cultures of the toxic species *Pseudo-nitzschia multiseries* were incubated under a combination of elevated CO_2 treatments, with both phosphate replete and limiting conditions (Sun et al., 2011a). Increasing CO_2 concentrations

Table 1.2. A summary of experimental results showing general responses of coccolithophores to elevated CO_2.

Taxonomic group	CO_2 conc. range tested	Method	Growth	Photosynthetic rate	Carbon assimilation	Elemental composition	Study Authors
Coccolithophores	360-720 µatm	Acid/base	↔	↑	↑	C:N ↔	(Buitenhuis et al., 1999)
	250-800 ppmv	Acid/base & CO_2 Bubbling	↔	↑	↑	n/a	(Riebesell and Zondervan, 2000)
	100-1000 µatm	Acid/Base	↔	↑	↑	n/a	(Rost et al., 2002)
	100-1000 µatm	Acid/Base	↔	↑	↑	n/a	(Zondervan et al., 2002)
	400-700 µatm	CO_2 Bubbling	n/a	↓	↓	n/a	(Sciandra et al., 2003)
	360-2000 ppmv	CO_2 Bubbling	↔	↑	↑	C:N ↑, N:P ↔	(Leonardos and Geider, 2005)
	98-920 µatm	Acid/base	↔	n/a	n/a	n/a	(Langer et al., 2006)
	375-750 ppmv	CO_2 Bubbling	↑	↑	↑	C:N ↑, N:P ↔	(Feng et al., 2008b)
	280-750 ppmv	CO_2 Bubbling	↓	n/a	↑	C:N ↑	(Iglesias-rodriguez et al., 2008)
	380-750 µatm	Acid/Base & CO_2 Bubbling	↑	↑	↑	n/a	(Shi et al., 2009)
	190-1500 µatm	Acid/Base	↓	↑	↑	n/a	(Barcelos e Ramos et al., 2010)
	180-750 ppmv	CO_2 Bubbling	↔	↑	↑	C:N ↑	(De Bodt et al., 2010)
	260-1150 µatm	Acid/base	↓	↑	↑	C:N ↔	(Müller et al., 2010)
	153-1283 µatm	Acid/base & CO_2 Bubbling	↓	n/a	n/a	↔	(Hoppe et al., 2011)
	400-1000 µatm	CO_2 Bubbling	↑↓	n/a	↑	n/a	(Lefebvre et al., 2012)
	380-1000 µatm	CO_2 Bubbling	↔↓	n/a	↑↔	POC:PON ↔	(Rokitta and Rost, 2012)

↑ increase; ↓ decrease; ↔ no change/inconclusive

Table 1.3. A summary of experimental results showing general responses of diatoms to elevated CO_2.

Taxonomic group	CO_2 conc. range tested	Method	Growth	Photosynthetic rate	Carbon assimilation	Elemental composition	Study Authors
Diatoms	180-355 µatm	Acid/base	↑	↑	↑	n/a	(Riebesell et al., 1993)
	30-1000 µatm	Acid/base	↑	↑	↑	C:N ↑ C:P,N:P ↓	(Burkhardt and Riebesell, 1997)
	30-1000 µatm	Acid/base	↑	↑	↑	C:N,C:P ↑↓↔ *Species specific*	(Burkhardt et al., 1999)
	100-600 µatm	Acid/base	↑	↑	↑	↓	(Gervais and Riebesell, 2001)
	36-1800 ppmv	CO_2 Bubbling	n/a	↑	↑	n/a	(Burkhardt et al., 2001)
	384-997 µatm	CO_2 Bubbling	↑	↑	↑	n/a	(Wu et al., 2010b)
	380-760 µatm	CO_2 Bubbling	↔	↔	↔	C:N ↓	(Crawfurd et al., 2011)
	559-2074 µatm	Acid Addition	↑	↑	↑	n/a	(Ihnken et al., 2011)
	220-730 ppmv	CO_2 Bubbling	↑	↑	↑	Si:C ↓, C:P ↑	(Sun et al., 2011a)
	390-1000 µatm	CO_2 Bubbling	↔	↑	↑	n/a	(Yang and Gao, 2012)
	400-1000 ppmv	CO_2 Bubbling	↑	n/a	n/a	n/a	(Hyun et al., 2014a)

↑ increase; ↓ decrease; ↔ no change/inconclusive

stimulated production of DA under both nutrient conditions, particularly under the P-limiting conditions, where DA increased four times over the range of CO_2 concentrations examined (220 ppm – 730 ppm). Growth rates, primary productivity and photosynthesis *vs*. irradiance parameters all increased in line with the increased production of DA at the highest CO_2 treatment, indicating the potential for an escalating negative effect of increased HAB events in future oceans.

1.2.4 Cyanobacteria

Cyanobacteria are the largest and most widely distributed group of photosynthetic prokaryotes in the marine environment (Burns et al., 2005). A large fraction of primary production in tropical and subtropical regions is supported by N_2-fixing cyanobacteria (diazotrophs), as well as providing a significant source of reactive N to the water column over long time scales, further influencing the global carbon cycle (Gruber and Sarmiento, 1997). Cyanobacteria possess RubisCOs with very low CO_2 affinities (Badger et al., 1998) therefore increasing atmospheric CO_2 concentrations could favour this group, either through CCM down regulation or increased carboxylation efficiency of RubisCO. Results from recent studies on C acquisition in response to elevated CO_2 (1000 ppm) with the cyanobacteria *Trichodesmium* showed a stimulation of photosynthesis and N_2 fixation together with higher C and N quotas compared to controls (Kranz et al., 2009). While a direct CO_2 effect was not established on the carboxylation efficiency of RubisCO, the combined results point to a shift in the resource allocation among photosynthesis, C acquisition and N_2 fixation under elevated CO_2 conditions. Other studies have investigated the effects of elevated CO_2 on the bloom forming *Trichodesmium* (Barcelos e Ramos et al., 2007; Hutchins et al., 2007; Levitan et al., 2007) showing strong increases in growth rates, photosynthesis and N_2 fixation at a greater magnitude than previously seen in other photoautotrophs, indicating significant implications in a future high CO_2 global ocean. Barcelos E Ramos *et al.*, (2007) reported a doubling in growth rate at elevated $C0_2$ (850 µatm) and a more than doubling in N_2 fixation rates. Hutchins *et al*., (2007) tested responses of Atlantic and

Pacific *Trichodesmium* isolates at CO_2 concentrations elevated to 750 ppm and found N_2 fixation rates to increase by 35-100% and C fixation rates to increase by 15-128%. They found that the slope of the light limited portion of the P-E curve (α) increased under high CO_2 conditions for both strains, indicating a higher efficiency of light harvesting for photosynthesis under future climatic regimes.

While some non-diazotrophic cyanobacteria have been investigated within the context of climate warming and increased atmospheric CO_2 conditions, the majority of these studies test elevated CO_2 conditions well beyond the range expected for year 2100 and 2150 predictions (see Price *et al.*, 2008 for review) and therefore lack some relevance to environmental evaluation and meta-comparison. Therefore, there is a current paucity of data on the sensitivity of this group to elevated CO_2 concentrations within the range tested for other components of the phytoplankton community. Equally, there is limited data on the response of the picocyanobacteria to elevated CO_2. Picocyanobacteria such as *Synechococcus* and *Prochlorococcus* contribute up to 50% of fixed C in some marine (predominantly oligotrophic) systems, strongly influencing the global carbon cycle (Partensky et al., 1999). Incubations of semi-continuous cultures at present and future CO_2 concentrations (750 ppm) and at present and +4°C temperature regimes revealed significant differences in the response patterns of both species (Fu et al., 2007a). The high CO_2/temperature treatment stimulated growth rates in *Synechococcus* leading to a four-fold increase in chlorophyll *a*-normalised photosynthetic rates (relative to controls). Only temperature influenced an increase in chl *a* (divinyl) in *Prochlorococcus* with no effect seen from elevated CO_2. This species-specific difference in CO_2 sensitivity could influence dominance amongst picoprokaryote ecotypes leading to shifts in community structure.

Table 1.4. A summary of experimental results showing general responses of dinoflagellates and cyanobacteria to elevated CO_2.

Taxonomic group	CO_2 conc. range tested	Method	Growth	Photosynthetic rate	Carbon assimilation	Elemental composition	Study Authors
Dinoflagellates	30-780 µatm	Acid/base	↑	↑	↑	C:N ↔, N:P ↑	(Burkhardt et al., 1999)
	30-660 µatm	Acid/base	n/a	n/a	↑	n/a	(Rost et al., 2006b)
	370-5000 ppmv	CO_2 Bubbling	↑	n/a	n/a	n/a	(Ratti et al., 2007)
	375-750 ppmv	CO_2 Bubbling	↔	↑	↑	C:P, N:P ↔	(Fu et al., 2008)
	260-1500 µatm	CO_2 Bubbling	↔	↓	↓	n/a	(Crawley et al., 2010)
	394-898 µatm	$NaHCO_3$- & CO_2 Bubbling	↔↑ *Phylotype specific*	↔↑ *Phylotype specific*	↔↑ *Phylotype specific*	n/a	(Brading et al., 2011)
	400-977 µatm	CO_2 Bubbling	↔	n/a	n/a	C:N ↓	(Wynn-Edwards et al., 2014)
Cyanobacteria	140-850 µatm	Acid/base	↑	↑	↑	N:P, C:P ↑	(Barcelos e Ramos et al., 2007)
	380-750 ppmv	CO_2 Bubbling	↑↔ *Species specific*	↑↔ *Species specific*	↓↔ *Species specific*	C:N, N:P, C:P ↑ ↔ *Species specific*	(Fu et al., 2007a)
	148-1500 µatm	CO_2 Bubbling	↑	↑	↑	C:N ↔, N:P ↑	(Hutchins et al., 2007)
	250-900 ppmv	CO_2 Bubbling	↑	↑	↑	C:N ↑	(Levitan et al., 2007)
	150-1000 ppmv	CO_2 Bubbling	↑	↑	↑	C:N ↔	(Kranz et al., 2009)
	150-700 ppmv	Acid/base	↓	↔	↔	C:N ↑, N:P ↓	(Czerny et al., 2009)
	315-548 µatm	CO_2 Bubbling	↑	↑	↑	C:N, N:P ↑	(Wannicke et al., 2012)

↑ increase; ↓ decrease; ↔ no change/inconclusive

1.2.5 Dinoflagellates

Dinoflagellates play extremely important ecological roles in the marine environment. The genus *Symbiodinium* is well known for its symbiotic relationships with marine invertebrates , in particular, reef building corals (Iglesias-Prieto et al., 2004). Not an exclusive symbiont, *Symbiodinium* also exists as free-living cells although far less is known of this ecology aspect of the taxonomically diverse genus (Manning and Gates, 2008). Dinoflagellates are also well known for their formation of toxic red tides, giving rise to significant impacts on coastal ecology with socio-economic impacts (Andeson et al., 2002), as is the case with some of the *Prorocentrum* spp. (Fu et al., 2008). Previous studies have suggested that the *Prorocentrum* spp. may be CO_2 limited and that these dinoflagellates are restricted to CO_2 enriched micro-environments (Colman et al., 2002; Dason et al., 2004). However, the primary C source utilised by *Prorocentrum* spp. has since been found to be HCO_3^- (Rost et al., 2006b), suggesting no CO_2 limitation and therefore, ongoing changes with ocean carbonate chemistry will be less likely to affect carbon fixation rates in this species in the open ocean. There could be opposite effects however in more dynamic coastal zones where pH and DIC concentrations may be more highly variable (Hansen, 2002).

Prorocentrum minimum and the raphidophyte *Heterosigma akashiwo* have been studied in the context of elevated CO_2 and temperature (Fu et al., 2008). Elevated CO_2 alone, or in combination with elevated temperature stimulated growth in *Heterosigma* but not *Prorocentrum*. The maximum biomass-normalised light-saturated carbon fixation rate (P_{Bmax}) was increased in *Heterosigma* only with a combination of elevated CO_2 and temperature, while the same rate increased in *Prorocentrum* significantly under elevated CO_2 conditions alone. C:P and N:P ratios increased in *Heterosigma* under elevated CO_2 conditions, but not in *Prorocentrum*, indicating that *Heterosigma* may be more vulnerable to N limitation and that ultimately, changes in environmental temperature and CO_2 concentrations could alter the relative dominance of these two HAB species in the future global ocean.

Brading *et al*., (2011) investigated the effects of elevated CO_2 in four phylotypes of *Symbiodinium* (ITS2 types A1, A13, A2, B1). The response to a doubling of CO_2 concentration (898 µatm) was varied and phylotype specific and showed the growth rate of type A13 and photosynthetic capacity of type A2 to significantly increase by ~60%. Phylotypes A1 and B1 showed no significant response to the altered CO_2 concentration.

An alternative approach to assessing effects of elevated CO_2 concentrations by studying community change was investigated by Tatters *et al*., (2013). Assessment of community structure in a natural mixed dinoflagellate bloom dominated by *Lingulodinium polyedrum*, *Prorocentrum micans*, *Alexandrium* sp. and *Gonyaulax* sp. showed interesting results after a 2 week incubation experiment with a low CO_2 treatment at 230 ppm and high treatment at 765 ppm. The initial bloom composition showed relative abundance as *L. polyedrum* 82.5%, *P. micans* 9.0%, *Gonyaulax* sp. 4.8% and *Alexandrium* sp. 3.7%. Following incubation in the high CO_2 treatment, those relative abundances changed to 67, 13, 8 and 10% respectively, indicating how specific response to elevated CO_2 can change dominance (**Table 1.4**).

1.3 Multiple environmental stressors – Laboratory studies

The vast majority of laboratory studies discussed have examined effects of elevated CO_2 in isolation from any other processes and mechanisms expected to change with global climate warming. Moreover, these studies have predominantly investigated individual species cultures in isolation. To date, few such studies have investigated phytoplankton response to combined and interactive perturbations relevant to predicted future climate change scenarios and no studies have investigated full-factorial perturbations (including elevated CO_2, + temperature, +/- nutrients and + irradiance). By their nature, these types of experiments are complex, labour intense with high replication and the data not straight forward to interpret. **Table 1.5** summarises the few studies that have so far investigated one or more environmental stressor response in concert with elevated CO_2. Understanding how these multiple factors may combine (interactively, synergistically or antagonistically) is critical to our understanding and

Table 1.5. Studies to date that have investigated one or more environmental stressors in combination with elevated CO_2.

Species/genus		+ Temp	- Temp	+ Nutrients	- Nutrients	+ Irradiance	- Irradiance	+ pCO_2	Study Authors
Emiliania huxleyi	Growth Photosynthetic rate Elemental composition				↑	↑↑		↑↑	(Leonardos and Geider, 2005)
Synechococcus	Growth	↑	↔	n/a	n/a	n/a	n/a	↑↑	
	Photosynthetic rate	↑	↔	n/a	n/a	n/a	n/a	↑↑	
	Elemental composition	↔	↔	n/a	n/a	n/a	n/a	C:P, N:P ↑	(Fu et al., 2007a)
Prochlorochoccus	Growth	↔	↔	n/a	n/a	n/a	n/a	↔	
	Photosynthetic rate	↔	↔	n/a	n/a	n/a	n/a	↔	
	Elemental composition	C:N:P ↑ constant stoichiometry	↔	n/a	n/a	n/a	n/a	↔	
Trichodesmium	Growth	↔	↔	n/a	n/a	n/a	n/a	↑	
	Photosynthetic rate	↔ (P- ↑↑)	↔	n/a	P- ↑	n/a	n/a	↑	(Hutchins et al., 2007)
	Elemental composition	↔	↔	n/a	n/a	n/a	n/a	N:P ↑	
	Other	N_2 fixation ↔	↔	n/a	n/a	n/a	n/a	N_2 fixation ↑	
Emiliania huxleyi	Growth	↔	↑↑	n/a	n/a	↑	↔	↔	
	Photosynthetic rate	↑↑	↔	n/a	n/a	↔	↔	↑↑	(Feng et al., 2008a)
	Elemental composition	↔	↔	n/a	n/a	↑↑	↔	C:P ↑	
	Other	↔	↔	n/a	n/a	PIC:POC ↓	↔	PIC:POC ↓↓	
Chaetoceros muelleri	Growth	n/a	n/a	n/a	n/a	↔	↓↓	↓	
	Photosynthetic rate	n/a	n/a	n/a	n/a	↑↑	↔	↑	(Ihnken et al., 2011)
	Elemental composition	n/a	n/a	n/a	n/a	n/a	n/a	n/a	
Pseudo-nitzschia	Growth	n/a	n/a	P + ↑↑	↔	n/a	n/a	↑	
	Photosynthetic rate	n/a	n/a	P+ ↑↑	↔	n/a	n/a	↑	
	Elemental composition	n/a	n/a	n/a	n/a	n/a	n/a	n/a	(Sun et al., 2011b)
	Other	n/a	n/a	DA prod ↔	DA prod P- ↑↑	n/a	n/a	DA prod ↑	
Emiliania huxleyi	Growth	n/a	n/a	$NH4^+$ ↓↓	↔	n/a	n/a	↓	
	Photosynthetic rate	n/a	n/a	$NH4^+$ ↑↑	↔	n/a	n/a	↑	(Lefebvre et al., 2012)
	Elemental composition	n/a	n/a	n/a	n/a	n/a	n/a		
	Other	n/a	n/a	PIC ↓		n/a	n/a	PIC ↓	
Chaetoceros debilis *Chaetoceros didymus*	Growth	↑↓	↔	n/a	n/a	n/a	n/a	↑	
	Photosynthetic rate	n/a	n/a	n/a	n/a	n/a	n/a	n/a	(Hyun et al., 2014a)
	Elemental composition	n/a	n/a	n/a	n/a	n/a	n/a	n/a	

↑ increase; ↑↑ additive increase; ↓ decrease; ↓↓ additive decrease; ↔ no change/inconclusive

predictions of future primary productivity and biogeochemical cycles as well as changing phytoplankton community structure and ecology.

Leonardos and Geider, (2005) were amongst the first to show increased productivity through a multi-factorial experimental approach within the context of ocean acidification research. They investigated CO_2 fixation in a non-calcifying strain of the coccolithophore *E. huxleyi* and showed that C fixation increased through POC production under conditions of elevated CO_2 (2000 ppmv), high irradiance (500 μmol photons m^{-2} s^{-1}) and when N was the limiting nutrient. This increase in production also resulted in deviations to C:N:P stoichiometry with increases in the C:N and C:P ratios.

The interactive effects of elevated CO_2, temperature and irradiance have since been further investigated on a calcifying strain of *E. huxleyi* in semi-continuous laboratory cultures (Feng et al., 2008b). Elevated temperature (+4°C) at low irradiance (50 compared to 400 μmol photons m^{-2} s^{-1}) greatly accelerated growth at ambient CO_2 concentrations (375 ppm). At high and low irradiance, photosynthetic performance was significantly stimulated by both increased CO_2 and temperature. Elevated CO_2 together with increased irradiance resulted in increased C:P ratios, indicating a reduced P requirement, while PIC:POC ratios remained constant at low irradiance, irrespective of CO_2 and temperature conditions. However, PIC:POC ratios and cellular PIC significantly decreased under high irradiance and further decreased by the combination of elevated CO_2 and high irradiance, indicating a combined effect of CO_2 and light on calcification.

1.3.1 Natural population studies

Single and multi-factorial laboratory studies provide critical evidence to add to our knowledge and assist in informing predictions of how future environmental change may impact phytoplankton primary production. However, by their very nature, they utilise phytoplankton strains that are preconditioned to laboratory conditions, in many cases for many years (i.e. culture collections). It is not currently known whether this may introduce bias or variability in experimental results. Single species experimental investigations also lack important

components of natural conditions such as competitive interactions and high genetic diversity. Extrapolating from the individual species response level to community production predictions should be done with caution. Over the past twenty years a number of elevated CO_2 perturbation studies have focussed on natural populations, through shipboard bottle incubations, land based mesocosms and deployed floating mesocosms. **Table 1.6** summarises the key findings of these studies in terms of the overall response to net community production (NCP) as well as how elevated CO_2 conditions have altered phytoplankton community structure.

Amongst the first of these studies, Hein and Sand-Jensen., (1997) experimented with short term bottle incubations with natural populations sampled (in situ) from the nutrient poor central Atlantic Ocean. Using an acid/base approach to elevate CO_2 concentrations, they found that primary production was stimulated by up to 19%. Tortell *et al*., (2002) subsequently incubated natural populations from the Equatorial Pacific, elevating CO_2 concentrations to 750 ppmv (CO_2 gas bubbling). While a significant change in production was not found, significant changes in the community assemblage showed that increased CO_2 conditions can influence competition amongst phytoplankton taxa, thus impacting nutrient cycling with the potential to increase or decrease production. A further shipboard incubation, this time of Ross Sea natural phytoplankton communities at elevated CO_2 concentrations (800 ppm), showed a ~20% increase in growth and productivity (Tortell et al., 2008a). At a community level, this study showed how diatom species composition is sensitive to elevations in CO_2 concentrations resulting in a starting population dominated by smaller diatoms (e.g. *Pseudo-nitzschia subcurvata*) moving to dominance of larger chain forming centric diatoms (*Chaetoceros* spp.). Shipboard semi-continuous incubations of North Atlantic natural populations at elevated CO_2 (690 ppmv) and elevated temperature (+4°C) showed an increase in NCP (chl *a* doubled within the first 3 days) (Feng et al., 2009). In this same study, changes in community structure revealed dominance from diatoms to coccolithophores within the high CO_2, high temperature treatments and a change in relative abundance in diatom species, from *Cylindrotheca* to *Pseudo-nitzschia*. Natural populations sampled from two Bering Sea locations (deep water and shelf) were

Table 1.6. Single and multi-factorial elevated CO_2 studies on natural phytoplankton communities including laboratory incubations, shipboard incubations, floating mesocosm deployments and land based mesocosms. ↑ increased net community production (NCP); ↔ no change in NCP.

Exp. type	Location	CO_2 conc. range tested	Net community production	Community structure	Study authors
Shipboard incubations	Central Atlantic		↑	n/a	(Hein and Sand-Jensen, 1997)
Shipboard incubations	Equatorial Pacific (6° 36'S, 81°01'W)	150-750 ppmv	↔	**Exp. start**: Community dominated by *cryptophytes* (~45%), *prasinophytes*, *prymnesiophytes*, chl*orophytes* and *cyanobacteria* (20, 13, 8 and 7% respectively). **Exp end**: Community dominated by *diatoms* and *prymnesiophytes* (~90%). 40 and 50% respectively in low CO_2 and 60 and 30% in high CO_2 treatments.	(Tortell et al., 2002)
Mesocosm	Raunefjorden, Norway (60.3°N, 5.2°E)	180-700 ppmv	↔	*E. huxleyi* bloom. Rates of net community calcification declined with elevated pCO_2. Onset of calcification delayed by 48 hrs at elevated compared to low pCO_2.	(Delille et al., 2005)
Mesocosm	S. Korean coastal zone (34.6°N and 128.5°W)	250-750 µatm	↔	**Exp. start**: Community dominated by microflagellates, cryptomonads, and the diatoms *Skeletonema costatum* and *Nitzschia* spp. (90% of community). Microflagellates' largest contributor (50% of total community). **Exp end**: *S. costatum* and *Nitzschia* sp. increased substantially after N & P addition; only *S. costatum* showed an increase in growth rate with elevated pCO_2. Microflagellate population declined.	(Kim et al., 2006a)
Community bottle incubations	Bering Sea deep water (55°1.339'N, 179°1.828'W) Bering Sea shelf (56°30.899'N,164° 43.799'W)	370-750ppmv	↑	**Exp start**: Community dominated by diatoms. *Cylindrotheca* sp. was the predominant diatom. **Exp end**: Community shift to nanophytoplankton dominated by haptophytes, pelagophytes and prasinophytes. Main factor, temperature increase. Secondary factor, elevated CO_2.	(Hare et al., 2007a)
Mesocosm	Raunefjorden, Norway (60.3°N, 5.2°E)	350-1050 µatm	↑	**Exp start**: Community dominated by diatoms, subsequently shifted to coccolithophores due to limiting Si (combined biomass 85-90% of community). **Exp end**: Community dominated by prasinophytes, dinoflagellates and cyanobacteria. No community assemblage difference between CO_2 treatments.	(Riebesell et al., 2007)
Shipboard incubations	Ross Sea	100-800 ppmv	↑	**Exp. start**: Spring community dominated by *Phaeocystis Antarctica* (> 90%), summer community various dominant diatom spp. (*Pseudo-nitzschia subcurvata*) and *P. Antarctica*. **Exp. end**: Spring community shift in high CO_2 treatments to the large chain-forming centric diatom *Chaetoceros* spp. Summer	(Tortell et al., 2008a)
Mesocosm	Raunefjorden, Norway (60.3°N, 5.2°E)	375-1150 µatm	↑	**Exp start**: Community dominated by diatoms followed by *E. huxleyi* (following Si depletion and N/P addition). **Exp. end**: Community dominated by *E. huxleyi* and *Synechococcus*. No community shift from diatoms to nano/pico-phytoplankton in response to elevated CO_2.	(Egge et al., 2009)

Table 1.6. continued

Exp. type	Location	CO_2 conc. range tested	Net community production	Community structure	Study authors
Shipboard incubations	North Atlantic 57.58°N, 15.32°W	390-690 ppmv	↑	**Exp start**: Si limiting conditions with diatoms, chrysophytes and coccolithophores. **Exp end**: Community shift to dominance of coccolithophores in high CO_2 and high temp, high CO_2 treatments. Increased diatom abundance in high CO_2, ambient temp treatment with a diatom community shift from Cylindrotheca to *Pseudo-nitzschia spp.* in the high CO2, high temp treatment.	(Feng et al., 2009)
Community bottle incubation	Godavari River Estuary East India	646-1860 µatm	↑	Elevated CO_2 lead to dominance of cyanobacteria over diatoms while N, P & Si were limiting to diatom growth.	(Biswas et al. , 2011)
Shipboard incubations	Western Subarctic Gyre, NW Pacific Ocean (46°N, 160°E)	230-1124 µatm	n/a	Fe addition induced diatom blooms. Diatoms were present in both non-Fe and Fe addition CO_2 treatments, predominantly large pennate *P. nitzschia* spp. Diatoms exhibited little response to elevated CO_2, while coccolithophores decreased in abundance in response to elevated CO_2 treatments. *Synechococcus* increased in abundance at elevated CO_2.	(Endo et al., 2013)
Mesocosm	Kongsfjorden, Svalbard (78°56.2' N, 11°53.6' E)	185-1420 µatm	(I)↑, (II) ↑, (III) ↓	Phase (I) Community production increased with increasing CO_2 based on a community structure of pico phytoplankton (0.8-2.0 µm). The pico community was dominant based on Si limitation and N deficiency. Growth in phase (I) was terminated following viral infection. Phase (II) Following nutrient addition the small size fraction of phytoplankton again dominated the community and responded to elevated CO_2 with increased growth and increased net community production. Growth in phase (II) was again terminated following viral infection. Phase (III) Due to a greater abundance of larger size fraction phytoplankton, net community production was greatest in phase (III). This was not the case however in the high CO_2 treatments, which showed lower growth and community production. This was due to nutrient limitation resulting from high biomass in phase (II), rather than a CO_2 response.	(Silyakova et al., 2013)
Mesocosm (land based)	Marine Biological Field Station, Norway	400-1000 ppmv	↑	Low pH treatments (pH 7.7) accelerated bloom development. This was most significant in diatoms, but not the case with coccolithophores. Chlorophyta were also stimulated by the low pH treatment with highest abundance with *Micromonas* phylotypes. Chryptophytes showed a differential response. *Plagioselmis prolonga* responded with higher concentrations under low pH, ambient temperature, but declined at low pH, high temperature. Ciliates significant declined at low pH. Temperature effects in isolation exerted a positive effect on Prymnesiophytes and an earlier breakdown of diatoms.	(Calbet et al., 2014)

incubated in shipboard continuous culture systems at increased CO_2 concentration (750 ppmv) and increased temperature (+4.7 °C) (Hare et al., 2007a). Maximum biomass-normalized photosynthetic rates increased 2.6 to 3.5 times and throughout the incubations, community structure shifted from a dominance of diatoms, to that of nanophytoplankton, comprising haptophytes, pelagophytes and prasinophytes. Delille et al., (2005) studied a natural coccolithophore bloom dominated by *E. huxleyi* within a mesocosm deployment (Raunefjorden, Norway, PeECE mesocosm studies) at a CO_2 concentration elevated to 700 ppmv. No change in NCP was found to occur, however, compared to an ambient control mesocosm, the onset of calcification was delayed by up to 48 hours and net community calcification decreased by 40% with an enhanced loss of organic carbon to calcium carbonate. In a more recent study utilising nine units of the Kiel Off-Shore Mesocosms for Ocean Simulations (KOSMOS) in Kongsfjorden (Svalbard), amongst other parameters, NCP and community structure were investigated in pelagic natural populations (Schulz et al., 2013a; Silyakova et al., 2013). CO_2 concentration was elevated to a maximum of 1420 µatm and over the period of the study, three peaks in chl *a* were observed, representing three distinct phases. NCP responded to elevated CO_2 with an increase during phases (I) and (II), however despite a third chl *a* peak in phase (III) NCP decreased (relative to controls). While these types of studies and resulting data are highly complex, the analysis revealed a decrease in production (phase III) due to nutrient limitation resulting from high biomass during phase (II), and not as a CO_2 response. In phase (I) the community was dominated by haptophytes, phase (II) prasinophytes, dinoflagellates and cryptophytes and phase (III) haptophytes, prasinophytes, dinoflagellates and chlorophytes. The response of the pelagic phytoplankton community within this study was complex compared to previous similar studies and further knowledge of individual species CO_2 sensitivities as well as trophic interactions will help further future analysis of similar large-scale study projects.

A series of short-term (2-4 days) elevated CO_2 (750 µatm) shipboard bottle incubation experiments using natural communities sampled from eight locations from the northwest European shelf seas showed a contrasting trend of decreased community production (Richier et

al., 2014). Size fractionated assays showed this was due to decreased biomass accumulation within the smaller size fraction (< 10 μm), though in two of the eight experiments when larger cells dominated (> 10 μm), community production increased, albeit with a weaker response compared to the reduction due to smaller cells. These were however, much shorter incubation periods than most natural community studies and it is unclear if the observed response was due to short-term cellular stress due to bottle containment and experimental conditions. More recently, Gao et al., (2016) observed contrasting responses with off-shore and near-shore communities from the South China Sea during multivariate shipboard bottle incubations. With the off-shore community, individual high temperature treatments (+ 3 °C) increased productivity by 64% which increased to 117% when high temperature and elevated pCO_2 (1000 μatm) were combined simultaneously. In contrast, productivity in the near-shore community was not stimulated by high temperature treatments and was reduced relative to ambient controls in the combined elevated temperature and pCO_2 treatments.

While investigations on individual species reveal an overall trend of increased photosynthetic carbon fixation, the results are variable and species, strain and phylotype specific (e.g. Fu *et al.*, 2007b; Langer *et al.*, 2009; Brading *et al.*, 2011). Few phytoplankton species appear to be insensitive to elevated CO_2, however accurate inter-comparison of single species studies is made challenging through different experimental designs and parameters measured. Examination of the studies to date reveals a wide range of CO_2 concentrations tested. A more common approach in experimental design, carbonate system parameters measured, physiological and photo-physiological parameters measured, ambient control and maximum CO_2 concentrations would make for a less ambiguous analysis. The more recent laboratory experiments designed to analyse multiple environmental stress responses from phytoplankton demonstrate a more complete picture, by considering more variables predicted to change. Results such as Feng et al., (2008b) provide new evidence of future trends in parameters such as growth, photosynthesis, nutrient status and cycling and PIC:POC 'rain ratio'. Of the 56 investigation studies examined herein, 12 consider an additional variable other than elevated CO_2. It is therefore clear that

future investigations need to test against more than one global change variable. This will increase the growing data.

The field studies on natural assemblages provide a slightly clearer picture in terms of a more consistent response to elevated CO_2 of increased carbon fixation rates at a net community production level, and changes in phytoplankton community composition. These trends do not completely mirror responses of individual species in culture experiments. Patterns from the experiments discussed and tabulated on the natural community response are summarised in **Fig. 1.4.** It is therefore also critical that more investigations are scaled up to the community level with multi-factorial designs, either field based or in the laboratory. Acquiring experimental results from natural populations at a greater spatial and temporal scale, both coastal and oceanic, would provide a better resolution of both seasonal and geographical trends, of particular importance to models and predicting future change. Still in their infancy, model predictions of global change mediated phytoplankton community shifts and primary production are based on simplistic growth models (Anderson, 2005). An increased focus on identifying shifts in community taxonomic composition is critical to these model predictions of future primary production with global change. Those studies to have done so to date provide further insight to competitive interactions and changes in species succession in response to elevated CO_2 (e.g. Tortell *et al.*, 2008; Schulz *et al.*, 2013b; Silyakova *et al.*, 2013).

The size structure and elemental composition of phytoplankton communities can alter the magnitude of carbon fixed and subsequently exported to the deep (Laws et al., 2000a), thus feeding back to global biogeochemical cycles (Riebesell, 2004). Trajectory studies at the geologic timescale in the size of diatoms and dinoflagellates are consistent with a shift towards smaller cells in a more stratified ocean (Finkel et al., 2005)

However, a cautionary note in interpreting experimental results on natural populations is to consider the simultaneous effect of community composition with environmental change. How these factors compare to each other remains largely unknown. This question was recently

addressed for the first time by Eggers *et al*., (2013) who showed how initial starting experimental communities had a significantly greater impact on phytoplankton biomass than elevated CO_2.

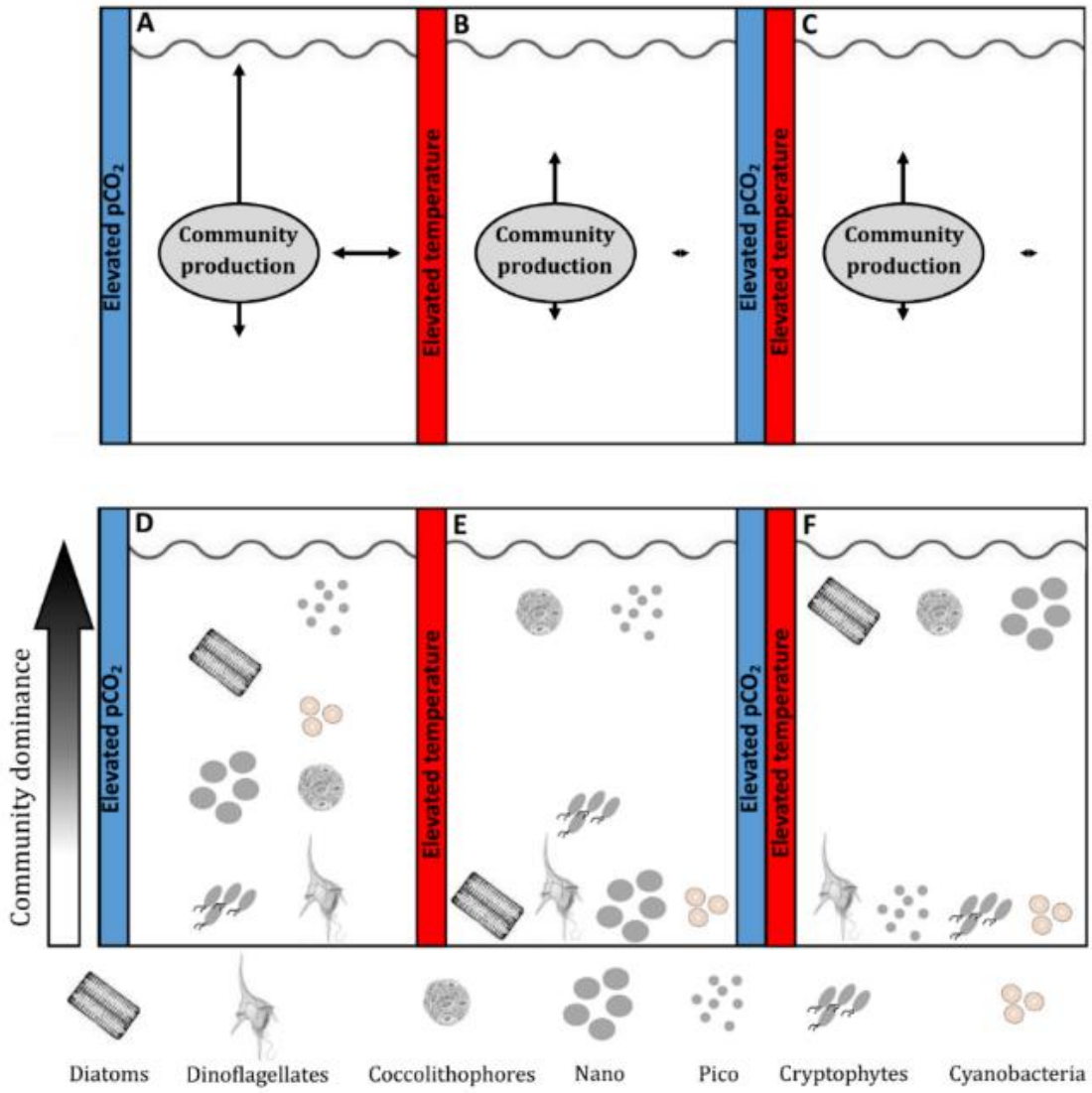

Fig. 1. 4 Schematic representation of the relative differences in the magnitude of the phytoplankton community production response and the relative contributions of groups and species to biomass under elevated pCO_2 (**A & D**), elevated temperature (**B & E**) and the combined influence of both factors (**C & F**) from previous experiments conducted on natural phytoplankton communities over the last 20 years. These experimental results formed the basis of the working hypotheses formulated in this thesis research. Vertical (↕) error bars in panels A, B and C represent the relative number of published studies reporting either increased or decreased production and the horizontal (↔) error bars represent the relative number of studies to report no change in production.

1.4 Aims and Objectives

Addressing the many uncertainties associated with changes in taxonomic composition of phytoplankton communities in response to abiotic variables through laboratory studies is highly challenging. By focussing on natural communities sampled over seasonal cycles, one can better inform global biogeographical and biogeochemical models to improve future estimations of coastal productivity and the cycling of chemical elements such as carbon, nitrogen and phosphorus.

The objectives of the research described in this thesis focussed on investigating the response of natural phytoplankton communities sampled from the western English Channel (WEC), to predicted future levels of elevated pCO_2 and temperature.

The Western Channel Observatory (WCO) in the WEC comprises several long-term sustained time series observations. Coastal Station L4 (50° 15'N, 4° 13'W) (**Fig. 1.5**) is located 13km SSW of Plymouth in a water depth of ~54m (Harris, 2010) and is regarded as one of Europe's principal coastal time series sites. Plymouth Marine Laboratory has sampled the natural phytoplankton community at L4 continuously since 1992. Previous analysis of the phytoplankton species abundance and composition time-series (1992-2007) has identified: (1) seasonal patterns of abundance of seven phytoplankton groups, (2) inter-annual variability in the floristic composition and (3) significant long-term trends showing a decrease in abundance of diatoms with an increase in coccolithophores, the dinoflagellate *Prorocentrum minimum* and some heterotrophic dinoflagellates and ciliates (Widdicombe et al., 2010b). **Fig. 1.6** shows the mean phytoplankton community biomass from weekly sampling between 1993 and 2014, and the successional timing of peak biomass contributions from the seven phytoplankton groups. To complement the biological time series, key environmental parameters are measured weekly including depth profiles of nutrients, seawater temperature, salinity, dissolved oxygen, fluorescence and photosynthetically active radiation.

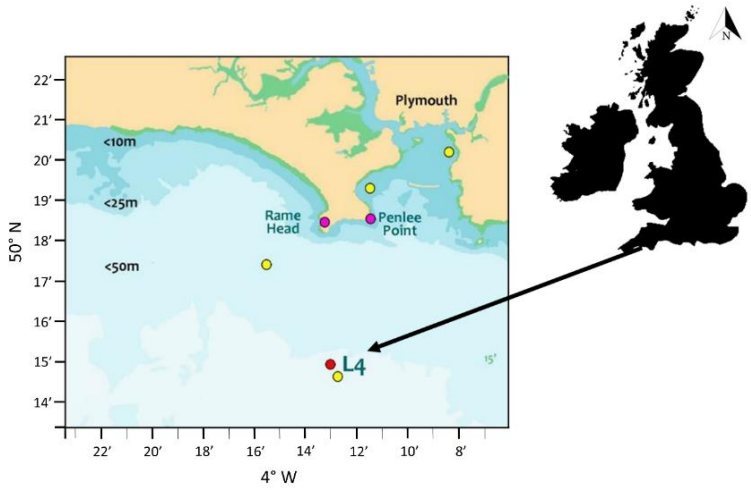

Fig. 1.5 Location of coastal station L4, Western English Channel, 50° 15.00' N, 4° 13.02' W.

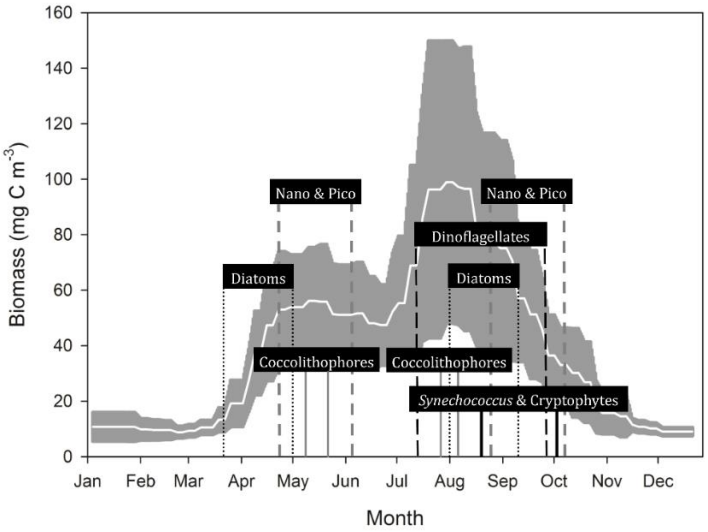

Fig. 1.6 Mean phytoplankton community biomass (white line) at station L4 between 1993 and 2014 (grey area is standard deviation, n = 909). Superimposed over this biomass is a schematic representation of the successional timing of peak biomass contributions from the seven phytoplankton groups identified at the study site.

Over the past 50 years, a 0.5 °C warming has been observed in the WEC (Smyth et al., 2010) and over the period coinciding with phytoplankton community sampling, temperature at 10 m depth at L4 has significantly increased in the month of June (Pearson correlation coefficient 0.431, p <0.05, n = 23) (**Fig 1.7 A-C**). Dissolved inorganic carbon (DIC) and total alkalinity (TA)

has been sampled at station L4 since 2008 and while the time series is relatively short, pCO_2 calculated from the carbonate system parameters has significantly increased in the month of March (Pearson correlation coefficient 0.85, p <0.05, n = 6) (**Fig.1. 7 D-F**).

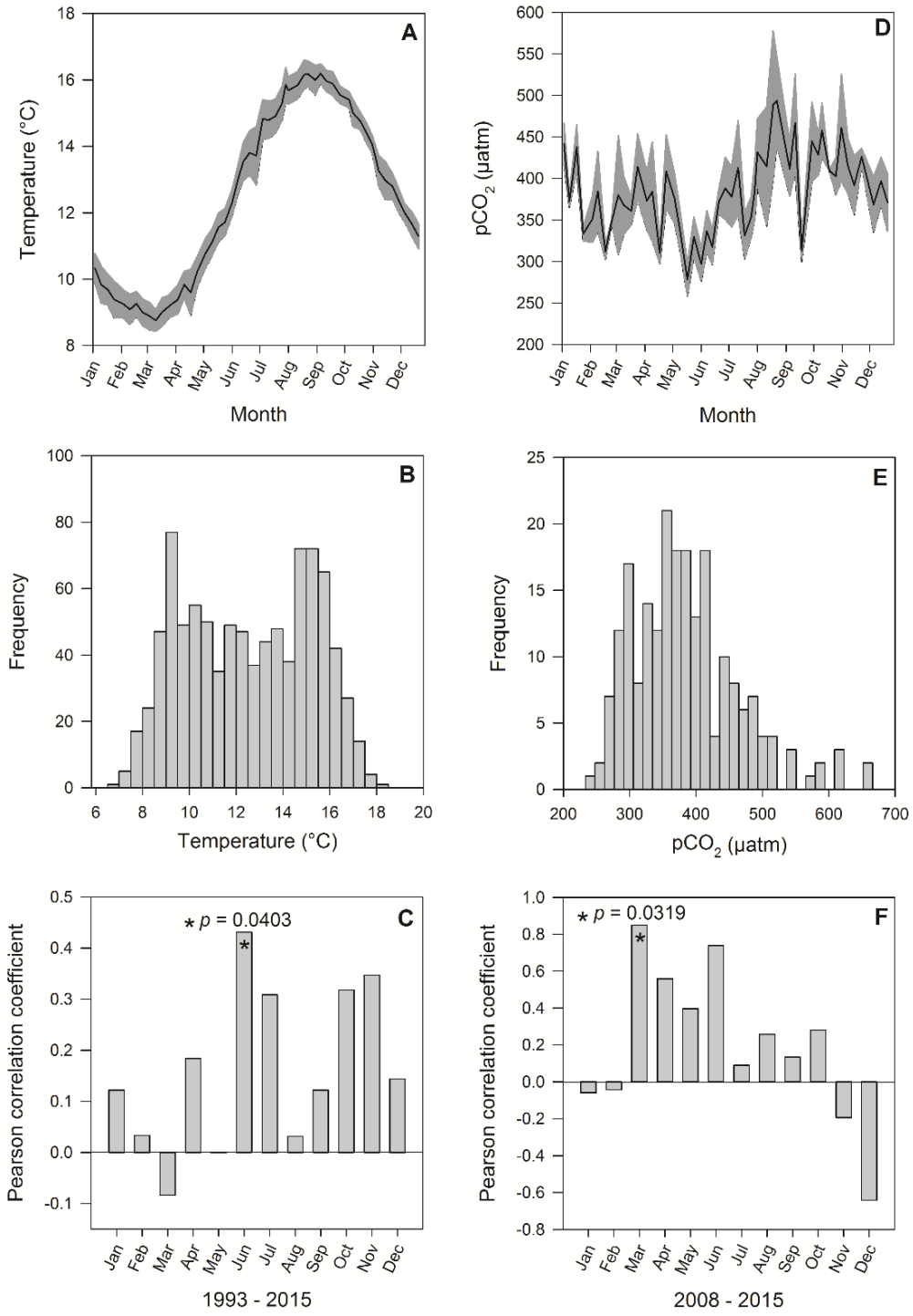

Fig. 1.7 Mean temperature at station L4 (10 m) (1993-2015, n = 920) (**A**), frequency distribution of temperature (**B**), Pearson product moment correlations of changes in monthly temperature over the time series (**C**), mean pCO_2 at station L4 (2008-2015, n = 215) (**D**), frequency distribution of pCO_2 (**E**) and Pearson product moment correlations of changes in monthly pCO_2 over time (**F**).

Based on the summary of experimental results from natural phytoplankton studies in the field, it is clear that the initial community taxonomic composition in CO_2 and temperature perturbation studies has some level of influence over community shifts and biomass accumulation, independent of experimental treatments (**Fig. 1.4**). The working hypotheses for this thesis research are based on the synthesis of response patterns observed in these past studies:

1. Elevated pCO_2 alone will have the greatest influence, increasing total community production and photosynthetic rates significantly, relative to elevated temperature treatments, combined elevated pCO_2 and temperature treatments and ambient controls.
2. Elevated temperature and combined elevated pCO_2 and temperature will increase total community production and photosynthetic rates with equal weight significantly, relative to ambient controls, but will be significantly lower than production under elevated pCO_2 alone.
3. Elevated pCO_2 will select for picophytoplankton-dominated communities with significant contributions from diatoms and cyanobacteria, dependent on the relative abundance in the initial experimental communities.
4. Elevated temperature will select for picophytoplankton and/or coccolithophore-dominated communities with minor contributions from cryptophytes, dependent on the relative abundance in the initial experimental communities.
5. Combined elevated pCO_2 and temperature will select for diatom, nanophytoplankton or coccolithophore-dominated communities, dependent on the relative abundance in the initial experimental communities.

To investigate the response to elevated pCO_2 and temperature at the phytoplankton community-, group- and species-specific levels, measurable parameters were defined to allow for statistical tests for significant differences between experimentally manipulated treatments and ambient controls:

1. Use of established fluorometric techniques to determine community Chl *a* concentration variability.
2. Use of established microscopy and flow cytometry techniques to determine variability in group and species abundance and individual group and species contributions to total community biomass. Use of state-of-the-art flow cytometry coupled with digital imaging microscopy capabilities (FlowCAM) was also tested for the microphytoplankton size fraction (cells < 18 μm).
3. Use of established equations for carbon to volume relationships to estimate species, group and community biomass.
4. Use of established carbon, hydrogen and nitrogen (CHN) analytical techniques to measure total and organic carbon and nitrogen in the particulate phase as a direct phytoplankton community biomass measure and to verify accuracy of estimated phytoplankton biomass.
5. Use of state-of-the-art fast repetition rate fluorometric techniques (FRRf) to investigate variability of the three key parameters of photosynthesis vs irradiance (PE) curves: maximum photosynthetic rates of carbon fixation (P^B_m), the light limited slope of photosynthesis (α^B) and the light saturation point of photosynthesis (E_k).
6. Analysis of the species and groups found to be dominant in experimental treatments, over the L4 time series to determine their relative in situ contributions to group and total phytoplankton biomass relative to their contributions to the experimental communities.
7. Analysis of the species and groups found to be dominant in experimental treatments, over the L4 time series relative to their distribution along the in situ temporal gradients of temperature and pCO_2.

In chapter 4, the effects of elevated pCO_2 alone were investigated during a univariate experiment on a natural community sampled during the 2015 spring bloom transition from

diatoms to nanophytoplankton (15-day incubation under laboratory conditions). In chapter 5, the combined effects of elevated pCO_2 and temperature were investigated during a longer-term multivariate experiment (36 days) on a natural community sampled during the 2015 autumn bloom transition from diatoms and dinoflagellates to nanophytoplankton. This experiment was conducted in an outdoor incubator under natural irradiance to more closely simulate in situ conditions. In chapter 6, the combined effects of elevated pCO_2 and temperature were investigated during a multivariate experiment (30 days in outdoor incubator) on a natural community sampled during the 2016 late summer bloom transition from dinoflagellates to diatoms.

Chapter 2 – materials and methods

Abstract

In this chapter, methods for the collection and analysis of phytoplankton enumeration, total alkalinity, dissolved inorganic carbon and nutrients that contribute to the time series data set for coastal station L4 are presented. These data are used in this thesis though the author did not directly perform the measurements. Development of a simulated in situ incubation system used for multifactorial experimentation is described and the analytical methodologies of experimental samples are presented.

2.1 Phytoplankton time series, coastal station L4 (1992-2014)

Phytoplankton taxonomic composition was enumerated from seawater samples collected from 10m depth, fixed with 2% (final concentration) Lugol's iodine solution and analysed by inverted light microscopy using the Utermöhl counting technique (Utermöhl, 1958; Widdicombe *et al.*, 2010). For phytoplankton carbon biomass values; taxa-specific mean cell bio-volumes were calculated following Kovala & Larrance, (1966) and converted to carbon using the equations of Menden-Deuer & Lessard, (2000).

2.1.1 Dissolved inorganic carbon and total alkalinity time series, coastal station L4 (2008-2014)

Sampling was carried out approximately weekly at station L4. Seawater samples were collected using a 10 x 10 L hydrocast fitted with a SeaBird (SBE 19) conductivity temperature depth probe (CTD). Surface and bottom DIC and TA samples were collected in 250 mL glass bottles and preserved with 50 µL of saturated $HgCl_2$ solution. The samples were analysed within 12 months (Apollo SciTech™ Alkalinity Titrator AS-ALK2; Apollo SciTech AS-C3 DIC analyser, with analytical precision of 3 µmol kg^{-1}). Duplicate measurements were made for TA and triplicate measurements for DIC. Carbonate system parameter values were calculated from TA and DIC measurements using the programme CO_2Sys (Pierrot et al., 2006) with dissociation constants of

carbonic acid of Mehrbach *et al*., (1973) refitted by Dickson and Millero (Dickson and Millero, 1987).

2.1.2 Nutrients time series, coastal station L4 (2000-2014)

Nutrient samples from L4 were taken weekly. They were sampled under clean conditions and returned in the cool and dark to Plymouth Marine Laboratory where triplicate samples were analysed both for filtered (0.2µm Millipore Fluoropore) and non-filtered water. Samples were not stored or frozen unless there were extenuating circumstances making the live analysis impossible. Samples were analysed using a 5-channel Bran and Luebbe segmented flow system. Quality control procedures were carried out using KANSO certified reference materials. This has been the protocol since 2007, and prior to that the samples were stored frozen and then analysed in batches.

2. 2 Sampling for experimental phytoplankton communities

Experimental seawater containing natural phytoplankton communities was sampled at station L4 from 10 m depth (40 L) for pilot experiments described in chapter 3 of this thesis and for the main experiments described in chapters 4, 5 and 6. The experimental seawater was gently pre-filtered through a 200 µm Nitex mesh to remove mesozooplankton grazers, into two 20 L acid-cleaned carboys. While grazers play an important role in regulating phytoplankton community structure (e.g. Strom, 2002), the experimental goals considered only the effects of elevated temperature and pCO_2, though the mesh size used does not remove microzooplankton. In addition, 320 L of seawater was collected into acid-cleaned carboys from the same depth for use as experimental media. Immediately upon return to the laboratory the media seawater was filtered through an in-line 0.2 and 0.1 µm filter (Acropak™, Pall Life Sciences) then stored in the dark at 14 °C until use.

2.2.1 Experimental set-up

The first elevated pCO_2 perturbation experiment (chapter 4) was conducted in an indoor closed incubation system (**Fig.2.1**) under LED lights and temperature was controlled by a flow-through water bath. The subsequent multivariate experiments (chapters 5 and 6) were conducted in an out-door simulated in situ incubation system, the details of which are described below.

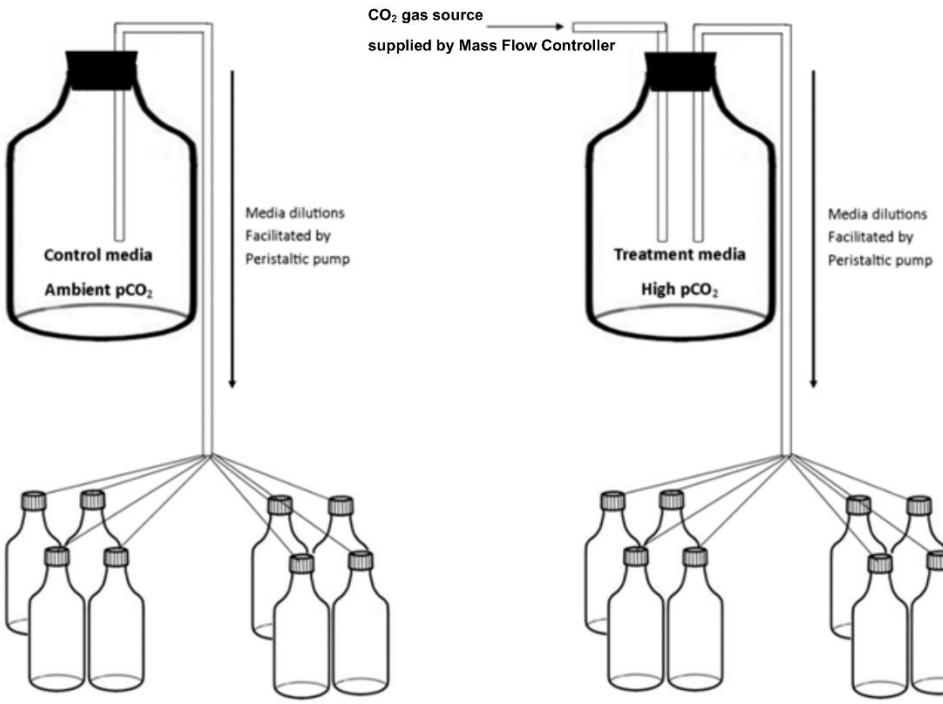

Fig. 2.1 Indoor **e**xperimental set-up to investigate the effects of elevated pCO_2 on phytoplankton community biomass and species composition (1st experiment, chapter 4).

2.3 Design and application of an outdoor simulated in situ incubation system

With the exception of shipboard natural community perturbation experiments, most global change phytoplankton incubation studies are conducted in low volume bottles in temperature-controlled rooms under static laboratory light regimes. Photosynthesis is the biological conversion of light energy to chemical bond energy that is stored in the form of organic carbon compounds (Falkowski and Raven, 2007). The effect of light intensity alone on responses to elevated pCO_2 has already been shown to be particularly important (Gao et al., 2012; Ihnken et al., 2011; Kranz et al., 2009). Natural irradiance in the environment is highly dynamic and

increased costs imposed by continuous photo acclimation and/or time spent under sub-optimal light conditions occur in the environment. Hoppe *et al*, (2015) recently showed in experiments with the Antarctic diatom *Chaetoceros debilis* that dynamic light strongly altered the effects of elevated CO_2 (1000 μatm) when compared to a constant light source (with equal integrated irradiance over a 1 day period in comparison to a static light regime control treatment). This indicates that future multi-stressor studies on phytoplankton, either monocultures or natural communities, in the context of elevated pCO_2 should be performed under dynamic light regimes, if we are to extrapolate response trends to the natural environment. Development and application of a simulated in situ incubation system (SISI) for use outside under natural sunlight is described below. This system enables full factorial studies on phytoplankton within the context of OA under dynamic natural irradiance.

A steel housing was fabricated (length: 2 m, width: 1m, height: 1 m, 316 stainless steel for marine environment corrosion resistance) with a reinforced hinged lid and a steel box section frame was mounted to the lid to cradle an array of five extruded polycarbonate incubation chambers (length: 2 m, diameter: 20 cm). Internally the system was designed to accommodate a bank of aquarium chiller systems (Boyu 500 and 350) (for cooling system temperature control) together with all electronics and power supplies. Six integral manifolds embedded in the steel box provided hose connections to and from the aquarium chillers and incubation chambers in closed circuits, to provide a flow-through system to control the temperature environment for pairs of incubation chambers (**Fig. 2.2 A & B**). Each incubation chamber has capacity to hold four x 2.5L incubation bottles, secured internally within a polycarbonate frame. Multi-port polyvinyl chloride end-caps with silicon double O-rings secured with marine-grade toggle

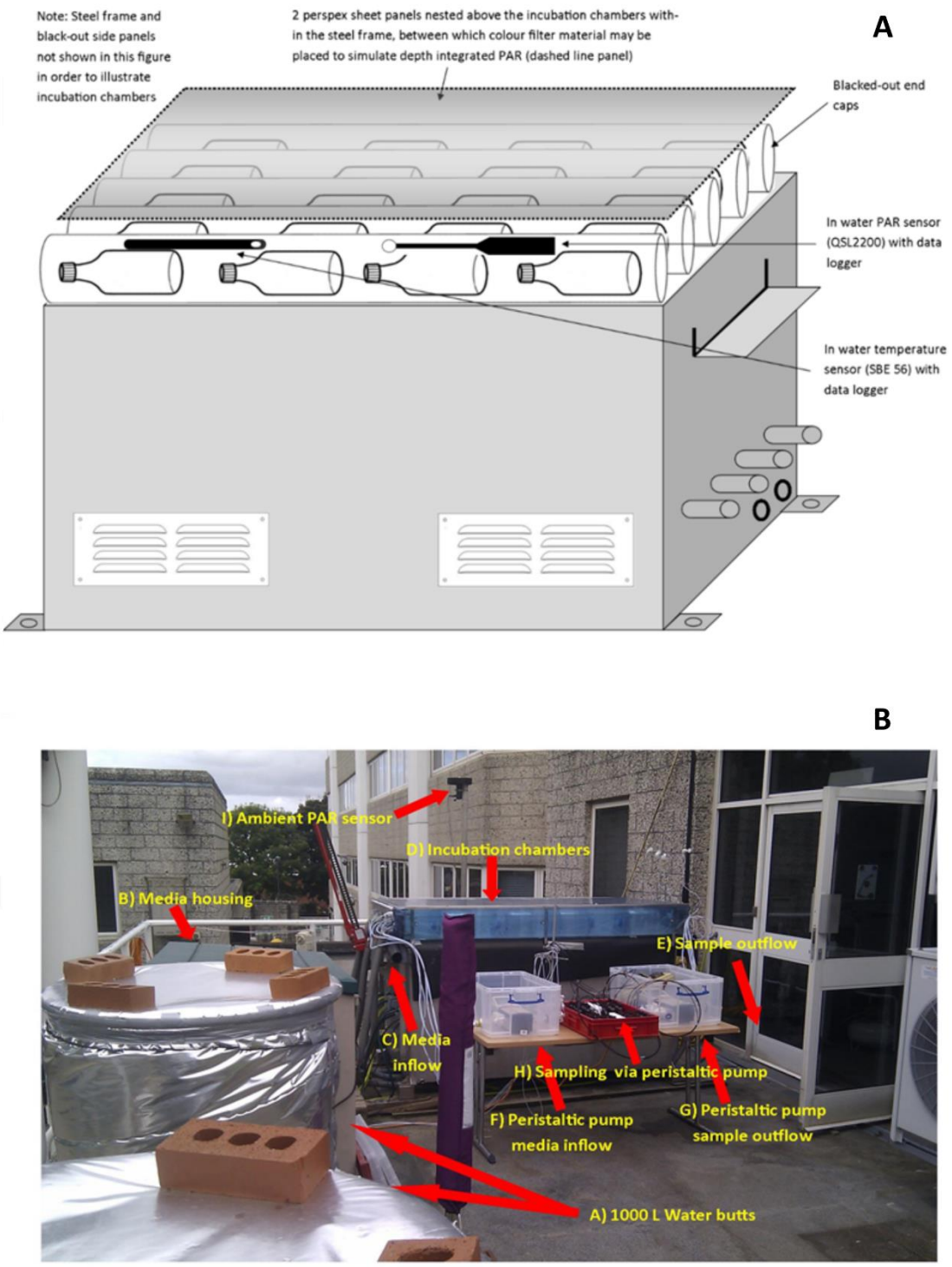

Fig. 2.2 (**A**) Original schematic concept of the SISI system and (**B**) the fabricated system set-up complete with auxiliary components while in use during an experiment. Experimental manipulated medium is pumped from vessels in the media housing B. into incubation bottles via C. housed within the incubation chambers D. Sampling is via outflow E.

latches provided a water tight seal at either end of each incubation chamber. End-cap ports (¼ inch) facilitated an inflow and outflow connector for the cooling water system circulation, which was recirculated via heavily insulated 1000 L water butts. The large volume of thermal mass contained within the water butts maintained temperature stability against diel fluctuations in ambient atmospheric temperature as well as fluctuations in temperature on days of high sunlight. Submersible pumps were located at the bottom of each water butt (Atom 6000 pond pump) and recirculated the cooling-system water via the incubation chambers at a manufacturer stated flow rate of 6000 L hr^{-1}. A reinforced shelf attached to the front end of the steel box supported an electronic scissor jack, the extending arm of which located onto a slider mechanism on the hinged lid. A timer mechanism and relay switch within the electronics control box activated the scissor jack twice every 30 minutes, and the SISI lid was raised and lowered to agitate the incubation bottles to keep phytoplankton cells in suspension. The incubation chambers were also rocked back and forth manually 4 times each day to provide additional mixing.

The full system was located at the most advantageous position outside, on a balcony on the south facing side of the Plymouth Marine Laboratory. Neutral density spectrally-corrected blue filters (Lee Filters) were placed between polycarbonate sheets and mounted to the top, sides and ends of the incubation chamber frame to provide ~50% irradiance, approximating PAR measured at 10m depth at station L4 on the days of sampling prior to starting experimental incubations.

Experimental media for the SISI was dark stored in 4 x 22L media vessels, located in a flow through water-bath within a heavily insulated storage box, and situated next to the SISI unit. One of 3 aquarium chillers (housed within the SISI) controlled the water-bath temperature and cooling water circulation was via a pump (Atom 6000 pond pump). Two 1/8 inch PTFE tube lines carried CO_2- enriched air at a flow rate of 150 ml min^{-1} from a mass flow controller (Bronkhorst UK Ltd) situated inside the main building, to the media vessels (vented with 0.2 µm

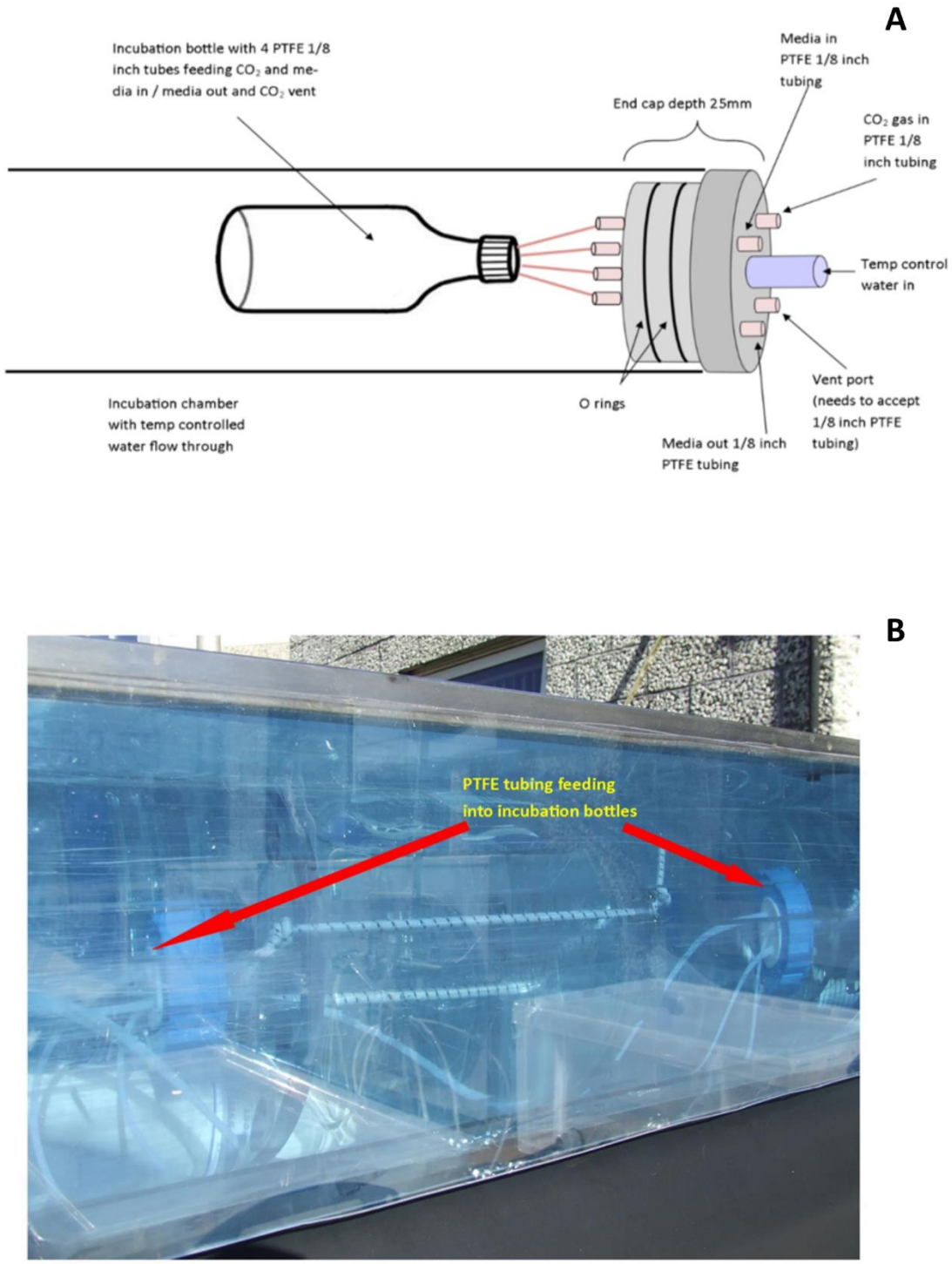

Fig. 2.3 (**A**) Original schematic design of the incubation chambers and multi-ported end-caps. (**B**) 2.5L Duran bottles located within the incubation chambers showing 1/8 inch PTFE tubing supplying media inflow and sample outflow. Neutral density spectrally-corrected blue filters are mounted along the sides, ends and top of the incubation chambers to provide ~50% irradiance.

air filters) and were connected with air-tight seals. Two 16 channel peristaltic pumps (Watson Marlow 205 U) were mounted inside waterproof containers on a bench located next to the SISI, one for media inflow, the other for sample outflow. 1/8 inch PTFE tubing connected the 4 media vessels to the media inflow peristaltic pump via four 1 into 4 manifolds, to supply each of the 16 pump channels (i.e. each media vessel supplied media to each of 4 replicate incubation bottles within each of the incubation chambers). 1/8 inch PTFE tube lines were routed from the media inflow peristaltic pump through port fittings (Kinesis Omnifit) in each incubation chamber end cap, and then fed into each incubation bottle via ported GL45 bottle caps (Dibbafit). The sample outflow set up was the same as the media inflow. Semi continuous batch culture dilutions were conducted at the same time each 24 hour period, when both peristaltic pumps were run simultaneously at low rpm (30 rpm) until the desired dilution and sample volume was reached. This therefore maintained a neutral pressure within the incubation bottles and allowed introduction of CO_2-enriched media as well as sample acquisition each day.

2.3.1 Instrumentation

Temperature loggers with internal memory were placed inside each pair of incubation chambers and programmed to capture internal temperature measurements every 15 minutes (Seabird SBE56). An analogue output aquatic scalar PAR sensor (photosynthetically active radiation) with 1.93cm 4π collector was located within one of the incubation chambers via a water-proof bulkhead fitting in one of the end-caps (Biospherical Instruments QSPL 2200) and a scalar PAR surface reference sensor was located next to the SISI (Biospherical Instruments QSR 2200) together with an ambient temperature probe housed within a weather shield (HygroMet). Both PAR sensors and the ambient temperature sensor were connected to a data logger (housed within the electronics control box) and programmed to measure every 15 minutes (Campbell Scientific 800 series). The instrumentation allowed ambient and incubation treatment profiles of temperature and PAR to be recorded over the course of incubation experiments. **Figs. 2.3 & 2.4** provide detailed annotated images of the full apparatus.

A

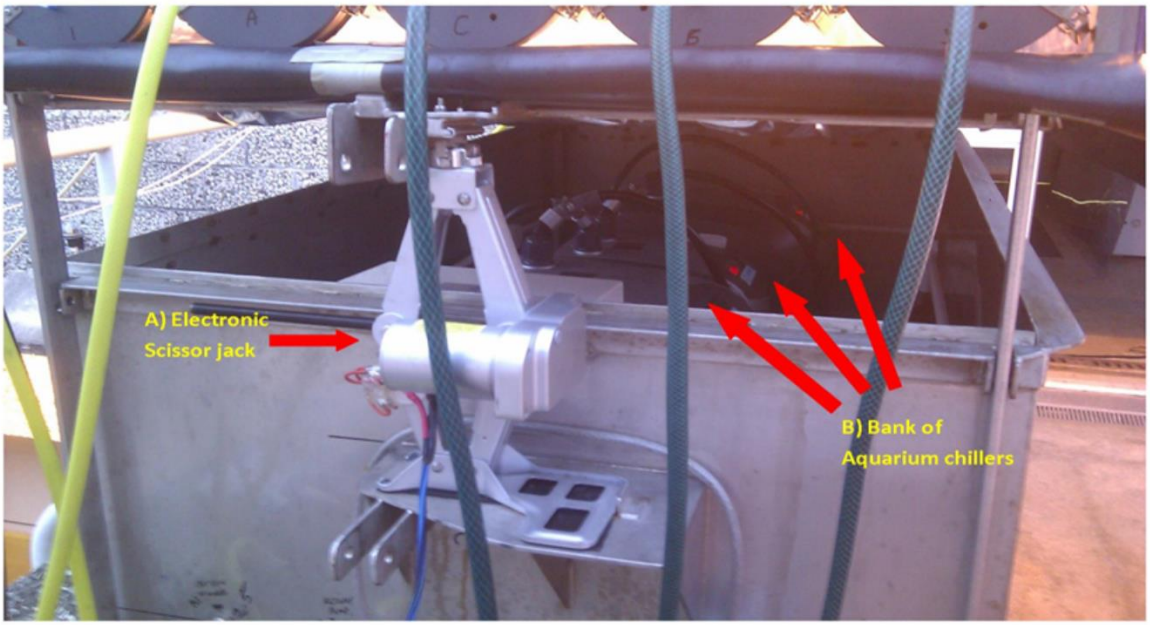

B

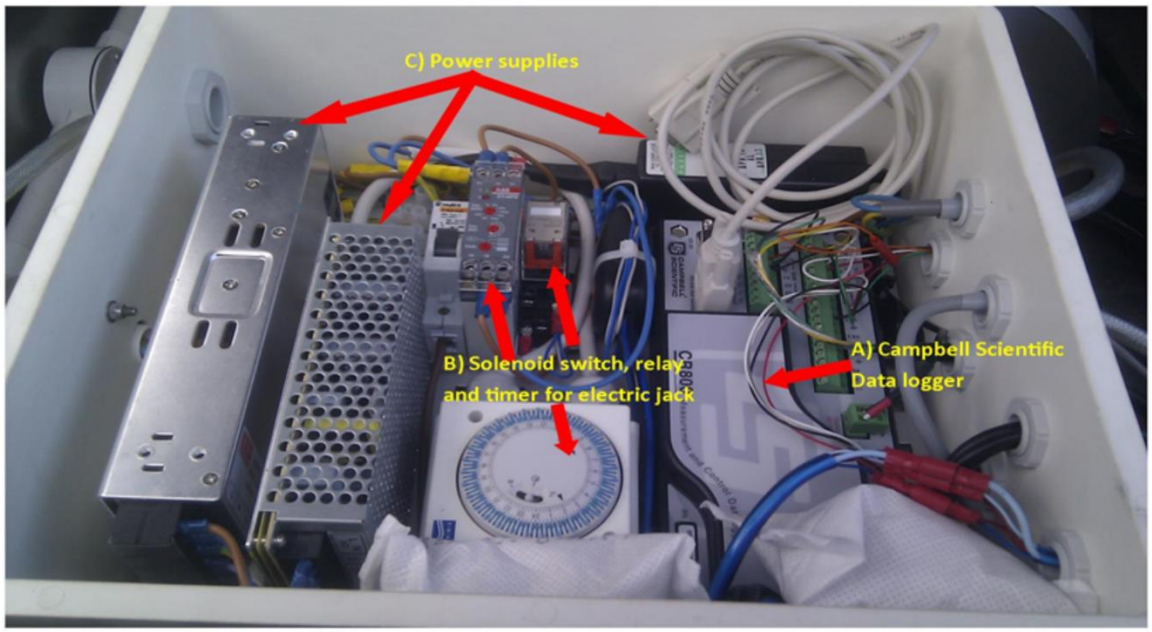

Fig. 2.4 (**A**) Front elevation of the SISI with the electronic jack activated and lid in raised position for incubation bottle agitation. A bank of 3 aquarium chillers is housed within the system for temperature control of the incubation chambers and media flow through water cooling system. (**B**) Electronic control box housed within the main system provides power to all instrumentation, timer mechanism for the electronic jack and data logger linked to all instruments.

2.4 Analytical methods – experimental seawater

2.4.1 Chlorophyll *a*

Chlorophyll *a* (chl *a*) was measured in each incubation bottle. Triplicate samples (100 mL) from each replicate were filtered onto 25 mm GF/F filters (nominal pore size 0.7 μm), extracted in 90% acetone overnight at -20 °C and chl *a* was estimated on a Turner Trilogy ™ fluorometer using the non-acidified method of Welschmeyer (1994). The fluorometer was calibrated against a stock chl *a* standard (*Anacystis nidulans*, Sigma Aldrich, UK), the concentration of which was determined with a Perkin Elmer™ spectrophotometer. Absorbance at 663.89 nm provided the highest peak for Chl *a* concentration while absorbance at 750.11nm was used as a baseline. Absorbance at 663.89 nm was subtracted from the baseline value and divided by the extinction coefficient for Chl *a* (87.67) following the method described by (Jeffery, 1997).

2.4.2 Carbonate system

70 mL samples for total alkalinity (TA) and dissolved inorganic carbon (DIC) analysis were collected from experimental replicates, stored in amber borosilicate bottles with no head space and fixed with 40 μL of super-saturated $HgCl_2$ solution for later determination as per the method described in section 2.1.1.

2.4.3 Phytoplankton community analysis

Phytoplankton community analysis was performed by flow cytometry (Becton Dickinson Accuri ™ C6) for the 0.2 to 18 μm size fraction following Tarran *et al.*, (2006) (**Fig. 2.5**) and inverted light microscopy was used to enumerate cells > 18 μm (BS EN 15204,2006). For flow cytometry, 2 mL samples fixed with glutaraldehyde to a final concentration of 2% were flash frozen in liquid nitrogen and stored at -80 °C for later analysis. For inverted light microscopy, 140 ml samples were fixed with 2% (final concentration) acid Lugol's iodine solution and analysed by inverted light microscopy (Olympus™ IMT-2) using the Utermöhl counting technique (Utermöhl, 1958; Widdicombe *et al.*, 2010). Note: in the first experiment in the proceeding

chapter 3, FlowCAM™ (Fluid Imaging Technologies™) flow-through analysis was used for the 18-100 µm size fraction following the method described by Poulton & Martin, (2010). Use of this instrument was discontinued for the following experiments due the large range in cell sizes observed in the natural experimental communities. FlowCam analysis has one level of magnification per analysis which made taxonomic classification challenging.

2.4.4 Phytoplankton community biomass

The smaller size fraction (< 18 µm) identified and enumerated through flow cytometry included picophytoplankton, nanophytoplankton, *Synechoccocus*, coccolithophores, *Phaeocystis* and cryptophytes. Median cell diameters for the different groups were previously measured over an annual cycle to quantify group, species and seasonal variability (G. Tarran 2017, pers. comm.). At an approximate monthly frequency, samples of seawater from Station L4 were gravity-filtered through a series of membrane filters ranging from 10 µm down to 0.2 µm and the filtrate was analysed by flow cytometry. The cell numbers for different groups of algae were recorded and compared with counts from unfiltered seawater to assess what percentage of cells passed through each of the filters. The 'percentage of cells remaining' values were then plotted against pore size of the filters in µm. For each algal group, a line was drawn from the point at which 50 % of cells remained on the Y axis to each of the algal group plot lines and, at the intersection a vertical line was drawn down to the x axis. The point at which the line crossed the X axis was recorded as being the median cell diameter for whichever algal group was being measured. The median summaries provide information about changes in algal group median cell diameter variability throughout the year, where there were enough cells to calculate a median cell diameter. A spherical model was used to calculate mean cell volumes: $(\frac{4}{3} * \pi * r^3)$ Where r is the radius calculated from the mean cell diameter (Tarran et al., 2006). A carbon conversion factor of 0.22 pg C μm^{-3} was used for nano- and picophytoplankton, cryptophytes and *Synechococcus* (Booth, 1988). A conversion factor of 0.285 pg C μm^{-3} was used for

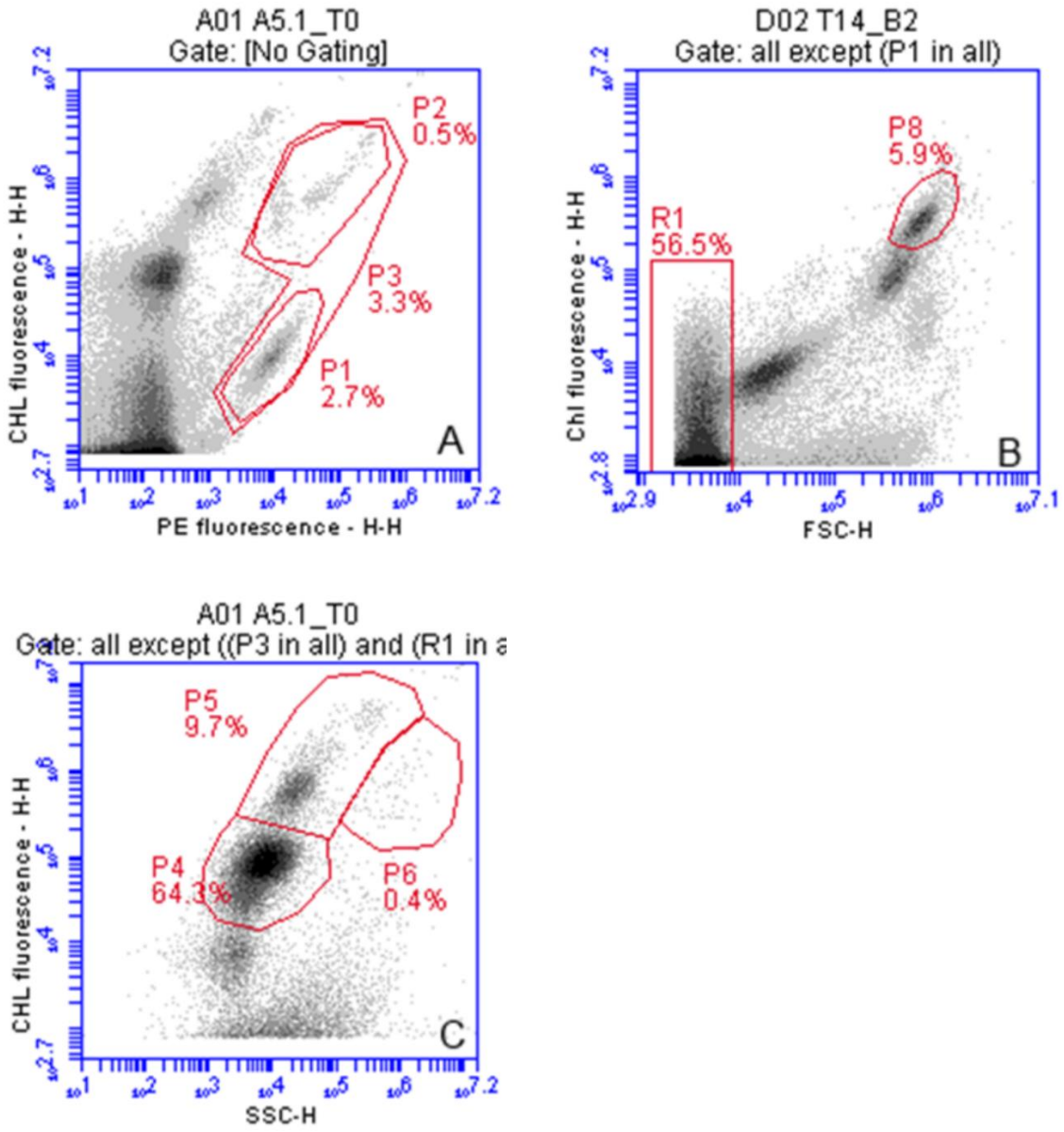

Fig. 2.5 Flow cytometric density plots using the BD Accuri CFlow Plus software for the analysis of phytoplankton. Regions for quantification of different phytoplankton groups are: (**A**) P1, *Synechococcus*; P2, cryptophytes, (**B**) P8, *Phaeocystis* spp., (**C**) P4, picoeukaryotes; P5, nanophytoplankton; P6, coccolithophores. *Synechococcus* and cryptophytes were quantified first. *Synechococcus* events (P1) were then excluded from the plot of FSC-H vs CHL fluorescence to clearly separate the remaining phytoplankton from non- fluorescent particles in region R1. Events in regions P3 (*Synechococcus* plus cryptophytes) and R1 were then excluded from the plot of SSC-H vs. CHL fluorescence so that picoeukaryotes, nanophytoplankton and coccolithophores could be quantified. *Phaeocystis* spp. were quantified in the plot of FSC-H vs CHL fluorescence (**B**) when their presence as colonies had first been confirmed by FlowCAM image capture or microscopy.

coccolithophores (Tarran et al., 2006) and a carbon cell^{-1} value of 18 pg applied for *Phaeocystis* spp. (Widdicombe *et al.*, 2010) . *Phaeocystis* spp. were identified and enumerated separately to the nanophytoplankton class due to high observed abundance in 2 experiments. Carbon was only attributed to the enumerated *Phaeocystis* cells as there was no accurate method to measure the colony mucus contribution. However, estimated biomass correlated with measured POC. Mean cell measurements of individual species/taxa were used to calculate cell bio-volume for the > 18 µm size fraction according to Kovala and Larrance (1966) and converted to biomass according to the equations of Menden-Deuer & Lessard, (2000).

2.4.5 POC and PON

150 ml samples were taken from each replicate and filtered under gentle vacum onto pre-ashed 25mm glass fibre filters (GF/F, nominal pore size 0.7 µm). Filters were stored in acid washed petri-slides at -20°C until further processing. Sample filters analysed for total particulate carbon (TPC) and total particulate nitrogen (TPN) were dried in a drying oven at 60°C for 24 hours. POC and PON sample filters were dried at 60°C for 24 hours, then acidified overnight in a desiccator (situated within a fume hood) with 37% concentration HCl, then re-dried for 24 hours at 60°C. All samples were then wrapped in aluminium foil pre-ashed at 450°C for 6 hours. Sample analysis was conducted using a Thermoquest Elemental Analyser (Flash 1112). Acetanilide standards over a range of ten concentrations (weighed at 205 µg to 1797 µg) were used to calibrate measurements of carbon and nitrogen and also during the analysis to account for any drift in analysis values. Calibration data and sample measurement calculations were rejected if R^2 calibration values fell below 0.99. Particulate inorganic carbon (PIC) and nitrogen (PIN) was calculated as the difference between TPC and POC, and TPN and PIN, respectively.

2.4.6 Chl fluorescence-based photophysiology

Photosystem II (PSII) variable chl fluorescence parameters were measured using a Fast Repetition Fate fluorometer (FRRf) (FastOcean sensor in combination with an Act2Run

laboratory system (Chelsea Technologies, West Molesey, UK)). The excitation wavelengths of the FRRf's light emitting diodes LEDs) were 450, 530 and 624 nm. The instrument was used in single turnover mode with a saturation phase comprising 100 flashlets on a 2 µs pitch and a relaxation phase comprising 40 flashlets on a 50 µs pitch. Measurements were conducted in a temperature-controlled chamber at 15 °C. The minimum (F_o) and maximum (F_m) chl fluorescences were estimated according to Kolber et al., (1998). Maximum quantum yields of PSII were calculated as:

$$F_v / F_m = (F_m - F_o) / F_m$$

PSII electron flux was calculated on a volume basis (JV_{PSII}; mol e^- m^{-3} d^{-1}) using the absorption algorithm (Oxborough et al., 2012) following spectral correction by normalising the FRRf LED emission to the white spectra using Fast^{PRO} 8 software. As a post processing step during the spectral correction of the FRRf data, mean literature values of the fluorescence excitation spectra (FES) for each phytoplankton group (and in some cases, individual species) enumerated after the experiments were used, since this parameter was not measured (**Fig. 2.6**). The FES values were calculated for each group proportionally based on their respective contribution to total estimated biomass, as representative values for the experimental samples. The JV_{PSII} rates were converted to chl- specific carbon fixation rates (g C (g chl *a*)$^{-1}$ h^{-1}), calculated as:

$$JV_{PSII} \times \varphi_{E:C} \times MW_C / \text{chl } a$$

where $\varphi_{E:C}$ is the electron requirement for carbon uptake (molecule CO_2 (mol electrons)$^{-1}$), MW_C is the molecular weight of carbon and chl a is the chl *a* measurement specific to each sample. Chl specific JV_{PSII} based photosynthesis-irradiance curves were conducted in replicate batches between 10:00 – 16:00 to account for variability over the photo-period at between 8 - 14 irradiance intensities. The maximum intensity applied was adjusted according to ambient natural irradiance on the days of sampling. Maximum photosynthetic rates of carbon fixation (P^B_m), the light limited slope (α^B) and the light saturation point of photosynthesis (E_k) were estimated by fitting the data to the model by Webb et al., (1974):

$P^B = (1\text{-}e \times (-\alpha \times I/P^B{}_m))$

Due to repeated instrument failure, the FRRf was unavailable to take measurements during experiment 1 (chapter 4) and only available to take measurements at the experiment end (T36) during experiment 2 (chapter 5) and the experiment start (T0) and end (T30) during experiment 3 (chapter 6).

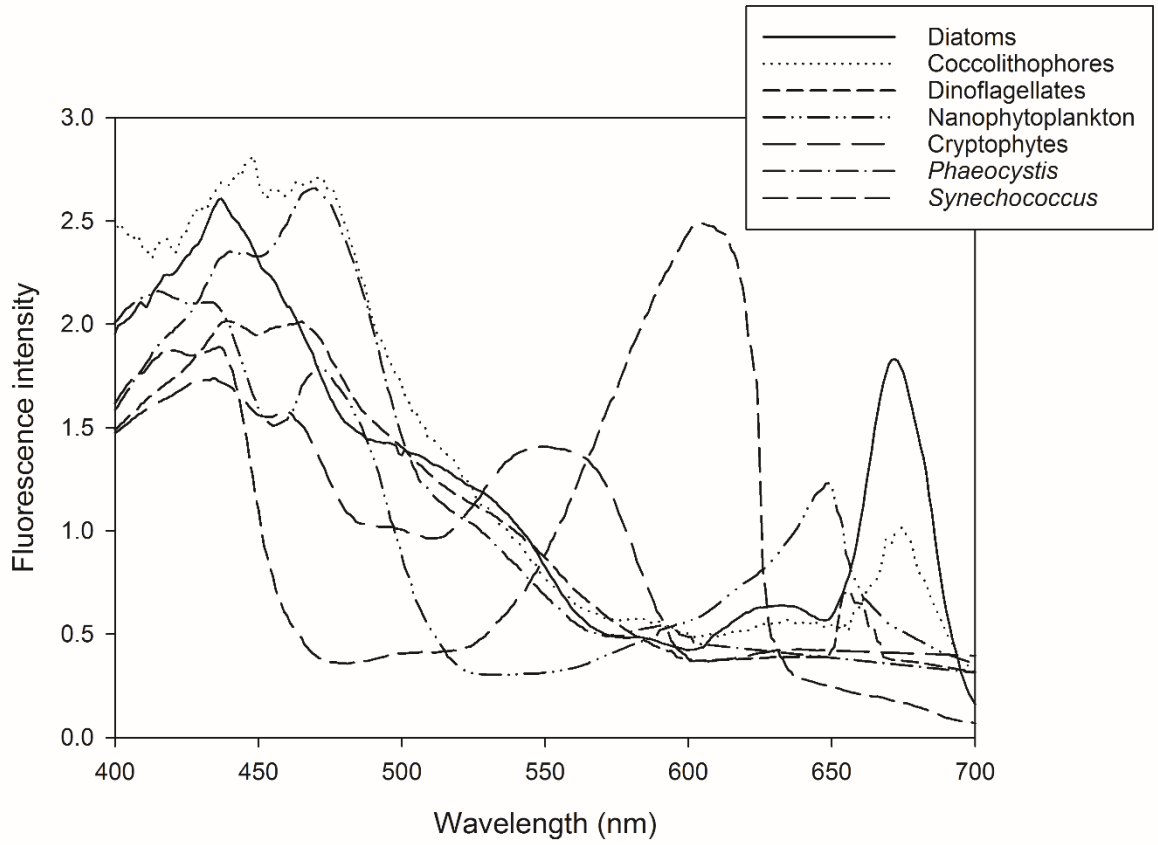

Fig. 2.6 Mean fluorescence excitation spectra literature values used for the spectral correction when post processing FRRf data

Chapter 3 – Determination of carbonate system manipulation and nutrient amendment.

Abstract

To investigate the most appropriate experimental protocols for carbonate system perturbations and L4 site-specific optimal nutrient regimes for natural phytoplankton incubations, a series of pilot studies were conducted. Performance of CO_2 enriched seawater addition on carbonate system control was evaluated against the more widely used approaches of acid/base manipulation and direct CO_2 gas bubbling. Addition of CO_2 enriched medium was found to be just as effective at controlling target carbonate system values as direct bubbling, with no significant difference between the two methods during natural phytoplankton incubations over 9 days. Furthermore, the acid/base manipulation method resulted in significantly lower carbonate system parameters and was the least effective method in maintaining target values. Since addition of CO_2 enriched seawater most closely replicates the natural system and avoids the effects of mechanical bubbling and chemical addition on phytoplankton, it was selected as the optimal protocol for further experiments. Three nutrient regimes were assessed to evaluate the most appropriate concentrations to apply experimentally during incubations of natural phytoplankton communities sampled from L4. Low nutrient concentrations maintained at in situ measured values of 0.07 µM nitrate (N), 0.03 µM phosphate (P) and 0.45 µM silicate (Si) resulted in rapid phytoplankton population crashes over 9 days. Addition of N according to an empirical ratio of 0.5 µM N:1 µg L^{-1} chl *a* also resulted in population crashes over 17 days of incubation (final concentrations: 1.125 µM N, 0.135 µM P and 2.0 µM Si). Analysis of the L4 nutrients time series (2000-2014) showed mean annual maximum N and P concentrations for the periods March to April and August to September to be ~8 µM N and ~0.5 µM P. Applying these concentrations resulted in a stimulation of phytoplankton biomass over 17 days, suggesting this nutrient addition sufficient to support natural communities over medium-term incubation experiments. Furthermore, the L4 nutrient amendments simulate in situ nutrient

pulse conditions regularly evidenced in the time series data set, making them environmentally relevant to the study site.

3.1 Experimental carbonate system manipulation method

3.1.1 Introduction

To study the effects of elevated pCO_2 on phytoplankton, experimental methods to manipulate seawater carbonate system parameters are required, either altering total alkalinity (TA) with constant dissolved inorganic carbon (DIC), vice versa, or both. This is commonly achieved through (1) acid, base, bicarbonate (HCO_3^-) and/ or carbonate (CO_3^{2-}) addition, (2) use of buffers or pH-stats, (3) bubbling CO_2 gas directly into culture vessels or (4) addition of CO_2-enriched medium (Riebesell et al., 2010). All methods may present potential 'bottle effects'. The addition of CO_2-enriched medium (method 4) is the most realistic simulation of environmental conditions and may minimise bottle effects through the lack of chemicals introduced to the medium and lack of directly bubbling culture vessels (method 3). The mechanical effects of direct-bubbling are known to inhibit some phytoplankton species (Riebesell et al., 2010; Shi et al., 2009) and may cause a reduction in growth rates and the formation of aggregates (Love et al., 2016). Three studies have compared the first three carbonate system manipulation methods (1, 2 and 3) on single phytoplankton species laboratory cultures (Hoppe et al., 2011; Schulz et al., 2009; Shi et al., 2009). However, to date these methods have not been compared with CO_2-enriched medium addition. To investigate the effectiveness of this potentially less invasive approach in bottle incubations, a pilot study comparison of seawater carbonate manipulation methods was conducted with a natural phytoplankton community sampled from L4 in the WEC.

3.1.2 Methods

Experimental seawater and medium were collected on 30th June 2014 as per the method described in section 2.2. Three manipulation treatments were applied as follows: (1) $NaHCO_3^-$/HCl adjusted medium transferred semi-continuously to 4 incubation replicates ($NaHCO_3^-$/HCl),

(2) medium pre-bubbled with CO_2 gas transferred semi-continuously to 4 incubation replicates (CO_2-enrichment), (3) medium pre-bubbled with CO_2 gas transferred semi continuously to incubation replicates also being directly bubbled at the same pCO_2 level (direct-bubbling). An ambient control medium was also used (filtered seawater) and transferred semi-continuously to 4 control incubation replicates. The experimental set up was as per **Fig. 3.1**. For the CO_2-enrichment and direct-bubbled treatments, the media was aerated with CO_2-free air and 5 % CO_2 in air, precisely mixed using a mass flow controller (Bronkhorst UK Limited). Medium transfer was facilitated by peristaltic pumps and dilution rates were set at 10% bottle volume per 24-hour period. Since the objective of this study was to examine differences in carbonate system manipulation methods, not the effects of elevated pCO_2 on phytoplankton, the target pCO_2 concentration was ambient. Initial day (T0) replicates were prepared for each of the treatments and control and samples were taken for TA and DIC analysis for the calculation of initial pCO_2 levels which were: 319.19 ± 0.95 µatm pCO_2 ($NaHCO_3$-/HCl), 319.48 ± 0.88 µatm pCO_2 (CO_2-enrichment), 319.27 ± 0.98 µatm pCO_2 (direct-bubbling) and 319.87 ± 0.79 µatm pCO_2 (control). The incubation bottles were temperature controlled in a flow-through bath at 15.7°C (temperature monitored twice daily) to match 10 m depth L4 temperature on the day of sampling. Light was supplied by a cool white LED light bank at irradiance of 300 µmol photons m^{-2} s^{-1} on a 16:8 hour light:dark cycle. Samples for TA and DIC analysis were subsequently taken from the experimental replicates on days T3, T5, T7 and T9. TA and DIC samples were analysed and pCO_2 was calculated as per the methods described in section 2.1.1.

3.1.3 Results

pCO_2 declined in all treatments over time due to biological uptake of DIC by the phytoplankton community (**Fig. 3.2**). Compared to initial T0 values, at T9 pCO_2 declined by ~ 12 µatm in the $NaHCO_3$-/HCl treatment, ~ 9 µatm in the CO_2-enrichment treatment, ~ 8 µatm in the direct-bubbling treatment and ~10 µatm in the control. A generalised linear mixed model (for

repeated measures) showed the $NaHCO_3$-/HCl treatment to be significantly different to the control and other treatments (**Table 3.1**).

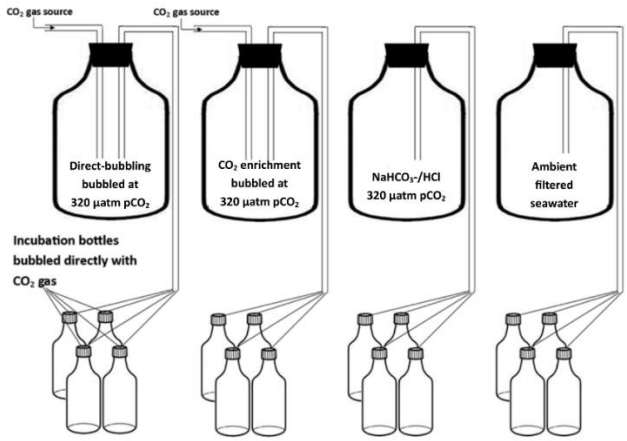

Fig. 3.1 Experimental set up for the pilot study investigating seawater carbonate system manipulation methods.

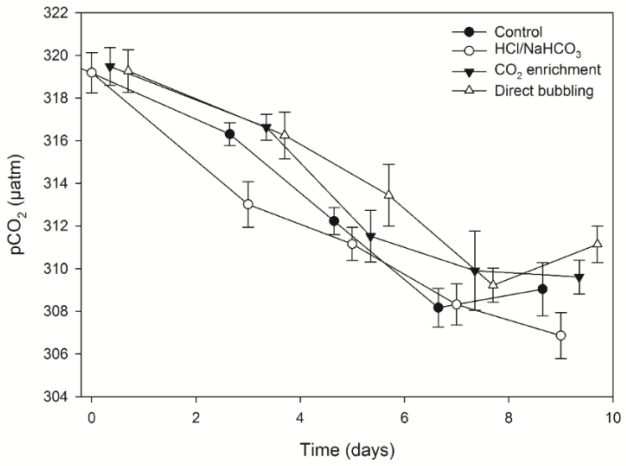

Fig. 3.2 Time course of pCO_2 values throughout the carbonate system manipulation methods comparison (mean ± standard deviation).

Pairwise comparisons showed this treatment's pCO_2 levels to be significantly lower than the CO_2-enrichment and direct-bubbling treatments as well as the control at T3 (t = -5.093, p < 0.01, t = -3.666, p < 0.05, t = -4.768, p < 0.01, respectively (n = 16)) and significantly lower than the CO_2-enrichment and direct-bubbling treatments at T9 (t = -3.558, p = 0.05, t = -5.335, p = 0.001, respectively (n = 16)).

Table 3.1 Results of generalised linear mixed model testing for differences in pCO_2 values between carbonate system manipulation methods.

Response variable	n	*df*	*z*-value	*p*
Control	80	74	0.1	0.843
HCl/$NaHCO_3$-	80	74	-0.3	<0.001
CO_2-enriched addition	80	74	0.1	0.956
Direct-bubbling	80	74	0.1	0.895

3.1.4 Conclusion

The results indicate that addition of CO_2-enriched medium is just as effective at maintaining experimental pCO_2 levels as the established methods of acid, base manipulation and direct bubbling of CO_2 gas. Further, the results indicate the $NaHCO_3$-/HCl method is the least effective at maintaining target pCO_2 concentration. Given the avoidance of potential bottle effects the CO_2-enrichment method offers, the results provide justification for the use of CO_2-enrichment as the carbonate system manipulation protocol throughout this thesis.

3.2 Determination of experimental nutrient concentrations, pilot experiment 1

3.2.1 Introduction

For phytoplankton culture, use of natural seawater is seldom acceptable. However, if large quantities of medium are required and natural communities are being cultured in the laboratory, natural seawater is the preferred medium, though nutrient additions must be made to enhance the biomass yield (Preisig and Andersen, 2005). In mesocosm field experiments, concentrations of nitrate (N) and phosphate (P) additions have been varied: 14 μM N, 1 μM P (Riebesell et al., 2007), 16 μM N, 0.8 μM P (Schulz et al., 2008), 17 μM N, 0.5 μM P (Delille et al., 2005) and 23 μM N, 0.9 μM P (Kim et al., 2006b). In bottle incubations using natural seawater and phytoplankton communities sampled from the field, additions of N and P are reduced relative to mesocosm field experiments but still vary: 5 μM N, 0.31 μM P (Feng et al., 2009), 4

µM N, 1 µM P (Hare et al., 2007a) and 8 µM N, 0.5 µM P (Calbet et al., 2014). Silicate (Si) is rarely added irrespective of initial Si concentration and no explanation has been offered to justify the nutrient regimes employed in these research papers. To determine an optimum nutrient regime in bottle incubations sufficient to support phytoplankton communities sampled from the WEC for periods of more than 21 days, two pilot studies were conducted.

3.2.2 Methods

The first assessment to determine the optimum nutrient regime was conducted during the pilot study on carbonate system manipulation methods at ambient pCO_2 (discussed in section 3.1) using the experimental set up detailed in **Fig. 3.1**. Experimental seawater and medium were collected as per the method described in section 2.2. on 30th June 2014. To assess if nutrient addition was required to support a natural phytoplankton community, no nutrients were added in this pilot experiment. The experimental seawater was sampled for initial (T0) nutrient concentrations and characterisation of the phytoplankton community as per the methods described in sections 2.1.2 and 2.4.3. Phytoplankton community samples were subsequently taken at T3, T5, T7 and T9.

3.2.3 Results

Nutrient concentrations in the collected seawater were low: 0.07 µM N, 0.03 µM P and 0.45 µM silicate (Si). The resulting biomass measured over 9 days demonstrated insufficient nutrient concentrations to support a natural community as the population crashed in all treatments over time (**Fig. 3.3**). The phytoplankton cell count data were used as a qualitative assessment of cell concentration response to low levels of nutrients and were not statistically analysed.

3.2.4 Conclusion

No nutrient additions resulted in population crashes in all treatments when ambient concentrations were low. Therefore, nutrient additions are required to sustain natural phytoplankton communities in manipulative experiments.

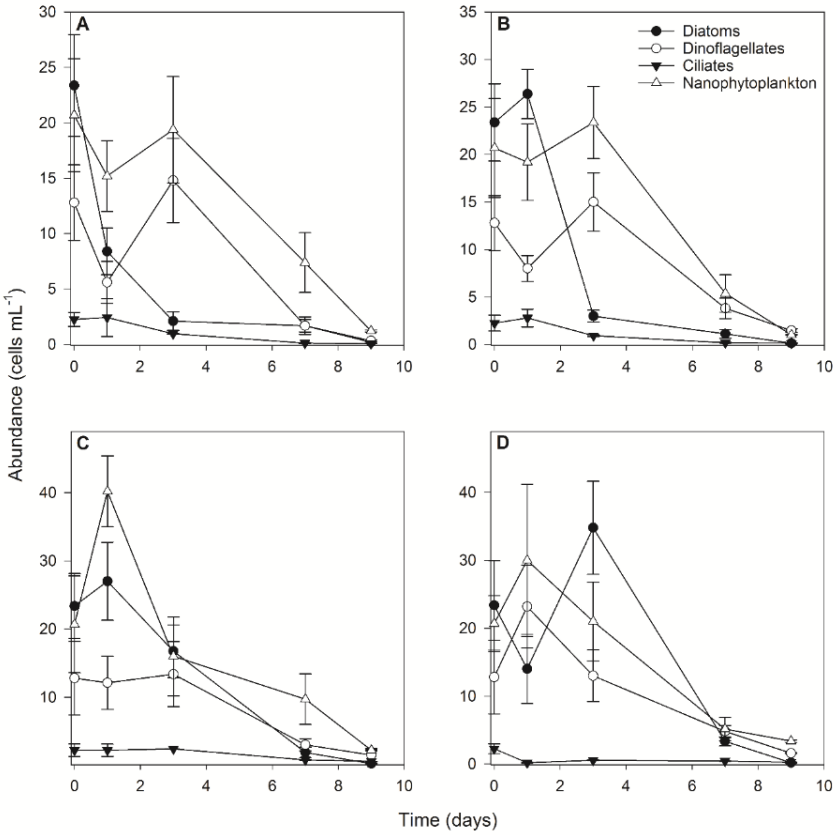

Fig. 3.3 Cell counts from a natural phytoplankton community incubated under ambient pCO_2 (~319 µatm) with no nutrient additions under low ambient nutrient concentrations. Each plot represents a different pCO_2 control method: (**A**) unaltered filtered seawater at ambient pCO_2, (**B**) pCO_2 adjusted by addition of $NaHCO_3$-/HCl medium, (**C**) pCO_2 adjusted by addition of CO_2-enriched medium and (**D**) pCO_2 adjusted by directly bubbling culture vessels with CO_2 gas.

3.3 Determination of experimental nutrient concentrations, pilot experiment 2

3.3.1 Introduction

To determine the optimum concentrations of nutrient addition to support natural phytoplankton communities sampled from L4, a second pilot study was conducted to investigate the effects of applying two nutrient regimes. Gilpin et al., (2004) showed that chlorophyll *a* (chl *a*) yield against cumulative N uptake of a typical phytoplankton community has an empirical ratio of 0.5 µM N:1 µg L^{-1} chl *a*, though this relationship was derived from phytoplankton communities in Trondheimsfjord, Norway and may not be applicable to

phytoplankton communities at station L4 in the WEC. Prior to the spring phytoplankton bloom at L4, nutrient concentrations can be high due to winter storm activity and associated water column mixing (Smyth et al., 2010). During late summer and early autumn, pulses of nutrient inputs frequently occur at L4 following heavy rainfall events and subsequent riverine inputs to the system, which act to stimulate phytoplankton productivity (Barnes et al., 2015). For example, localised flooding in the catchment around the WEC in the summer of 2007 led to an increase in Chl *a* of 8.46 µg L^{-1} at in-shore stations due to high nutrient loads from river run-off (Rees et al., 2009). The objectives of this second pilot experiment were therefore to assess the application of nutrient additions on an L4 phytoplankton community according to the N uptake:chl *a* ratio from (Gilpin et al., 2004) and mean maximum L4 nutrient concentrations.

3.3.2 Methods

3.3.2.1 Station L4 nutrients time series analysis

The L4 nutrients time series (2000 to 2014) was analysed to elucidate the mean maximum N and P concentrations during the periods March to April and August to September, coincident with high phytoplankton productivity at this time series station. This was achieved by identifying the years with the lowest maximum values and calculating the arithmetic mean of all data between the lowest and all other maximum values for N and P.

3.3.2.2 Nutrient addition experiment

Experimental seawater and medium were collected on 30th June 2014 as per the method described in section 2.2 on 26th August 2014. The objective of this pilot experiment was to evaluate effects of the different nutrient additions (denoted as Gilpin amended and L4 amended) on phytoplankton biomass under conditions for future planned elevated pCO_2 experiments, not the effects of elevated pCO_2 on phytoplankton biomass. Four manipulation treatments, each with 4 replicates were applied as follows: (1) Gilpin amended at ambient pCO_2, (2) L4 amended at ambient pCO_2, (3) Gilpin amended at high pCO_2 and (4) L4 amended at high pCO_2 (**Fig. 3.4**). The ambient and elevated pCO_2 levels were 380 µatm and 760 µatm

respectively and were achieved as per the method described in 3.1. Samples were taken for nutrients (N, P and Si), TA, DIC and phytoplankton community analysis on the day of seawater collection. Analysis of these samples was as per the methods described in 2.1.2, 2.1.1 and 2.4.3. Incubation bottles were swirled gently twice each day to keep phytoplankton cells in suspension and prior to sampling to ensure homogenous samples. Samples for phytoplankton community analysis were subsequently taken on days T4, T8, T12, T14 and T17.

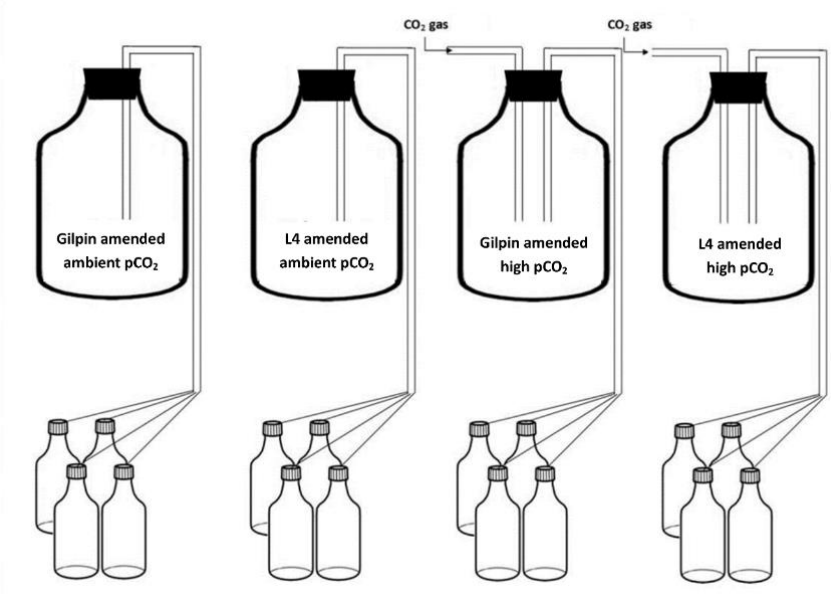

Fig 3.4 Experimental set up for the pilot study investigating the effects of two different nutrient regimes on natural phytoplankton communities sampled from L4 in WEC.

3.3.3 Results

3.3.3.1 Station L4 nutrients time series analysis

Analysis of the L4 nutrients time series (2000 – 2014) during March and April showed that N and P concentrations attained maximum values between 5.52 µM N (in 2000) and 11.17 µM N (in 2010) and 0.25 µM P (in 2000) and 1.05 µM P (in 2003) (**Fig. 3.5 A & B**). During August and September, N and P concentrations attained maximum values between 6.03 µM N (in 2011) and 11.68 µM N (in 2002) and 0.3 µM P (in 2004, 2013 and 2016) and 1.04 µM P (in 2003) (**Fig. 3.5 C & D**). In March and April, mean annual maximum N and P concentrations were 7.49 (± 1.37)

µM N (n = 48) and 0.48 (± 0.14) µM P (n = 70). In August and September mean annual maximum values were 8.05 (± 1.8) µM N (n = 18) and 0.42 (± 0.15) µM P (n = 146).

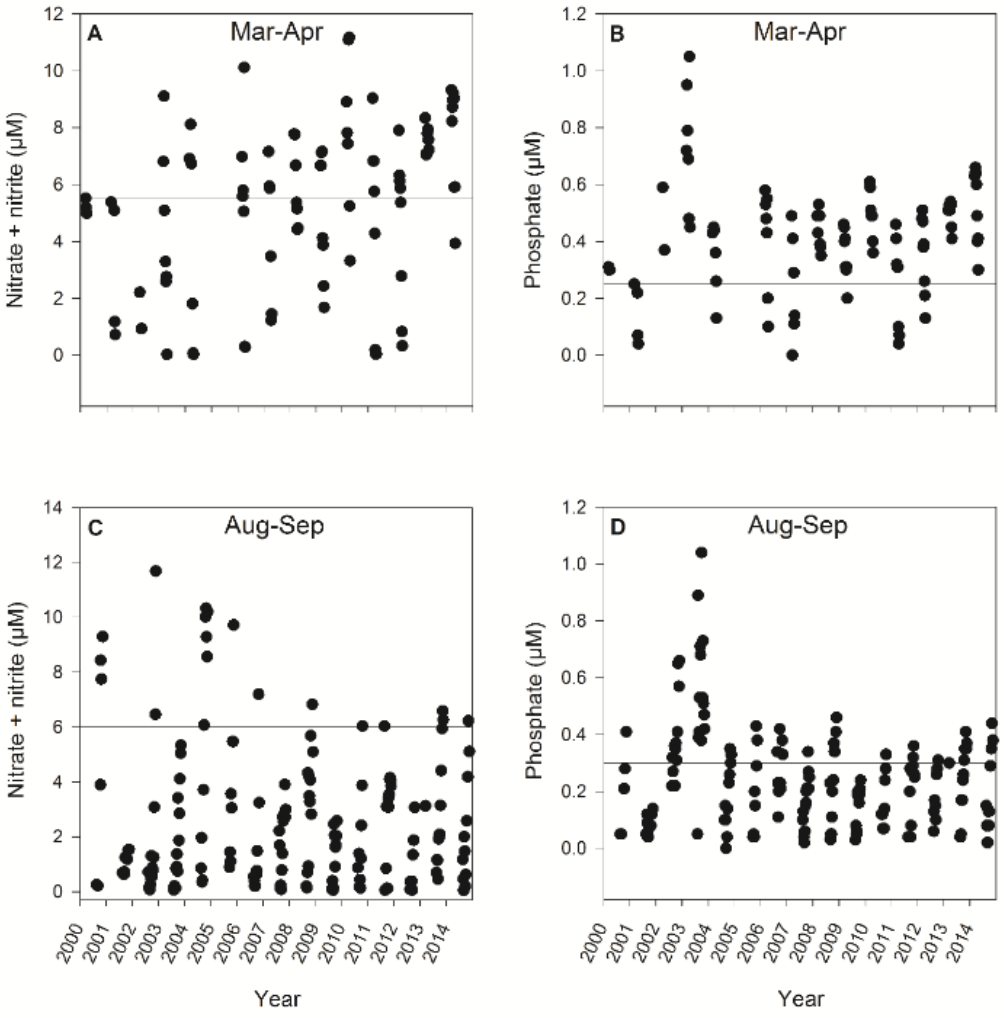

Fig. 3.5 L4 nutrient time series (2000 – 2014). During March – April nitrate + nitrite (N) maximum concentrations averaged 7.49 (± 1.37) µM (reference line shows lowest maximum value of 5.52 µM) (**A**) and phosphate (P) maximum concentrations averaged 0.48 (± 0.14) µM (reference line shows lowest maximum value of 0.25 µM) (**B**). During August – September

3.3.3.2 Initial (T0) nutrient concentrations and experimental amendments

Initial nutrient concentrations of the filtered seawater medium on the day of sampling were 1.125 µM N, 0.135 µM P and 2.0 µM Si. The initial Chl *a* concentration measured on the day of sampling was 3.115 µg L^{-1} showing a community requirement of 1.56 µM N according to the Gilpin amendment method (0.5 x 3.115). Therefore, for the Gilpin amended ambient and high

pCO_2 treatments, initial N was adjusted from the measured concentration (1.125 µM) to a final concentration of 1.56 µM. At this N concentration the Redfield P value would be 0.098 µM (1.56/16) and since the initial value was well above this, P in the Gilpin amended treatments was unaltered. Each set of mean annual maximum N and P values at L4 approximated the Redfield ratio (March and April N:P = 15.6, August and September N:P = 19.2). Since the values for both periods were very close and within the range used in previous bottle incubation experiments on natural communities (e.g. Calbet et al., 2014), L4 amended nutrient concentrations of 8 µM N and 0.5 µM P (Redfield ratio N:P 16:1) were tested. Therefore, for the L4 amended ambient and high pCO_2 treatments N and P were adjusted to final concentrations of 8 µM and 0.5 µM respectively. Egge and Aksnes, (1992) previously reported that diatoms dominate when Si concentration is ≥ 2 µM. In order not to pre-select diatoms in the experimental phytoplankton community, Si concentrations were not altered.

3.3.3.3 Nutrient amended phytoplankton incubations

pCO_2 levels were 380 µatm and 760 µatm respectively and carbonate system values remained stable throughout the pilot experiment (data not shown). Phytoplankton biomass in the L4 amended ambient and high pCO_2 treatments showed a positive response to media dilutions, increasing from the initial (T0) biomass value of 133.31 (± 10.23) mg C m^{-3} to 1021.20 (± 186) mg C m^{-3} (L4 amended ambient pCO_2) and ~760 (± 165) mg C m^{-3} (L4 amended high pCO_2) by T17 (**Fig. 3.6**). In contrast, biomass in both Gilpin amended treatments declined throughout the pilot experiment resulting in biomass on day 17 of 9.93 (± 4.66) mg C m^{-3} (Gilpin amended ambient pCO_2) and 18.53 (± 8.13) mg C m^{-3} (Gilpin amended high pCO_2) (**Fig. 3.6**). Since there were such obvious differences in the biomass response between the two nutrient concentrations applied, the biomass data were used as a qualitative assessment of community response to experimental treatments and were not statistically analysed.

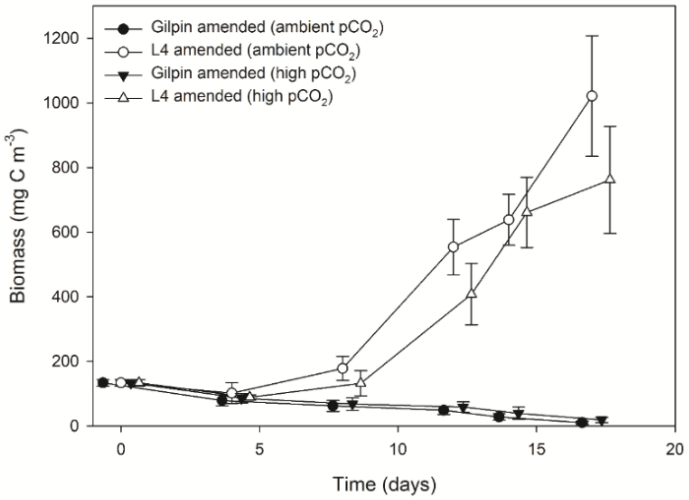

Fig. 3.6 The phytoplankton community biomass response to Gilpin amended (0.5 µM N:1 µg L^{-1} Chl *a*, with P adjusted as per the Redfield ratio) and L4 amended (8 µM N, 0.5 µM P) N and P concentrations.

3.3.4 Conclusion

To maintain natural phytoplankton communities for periods greater than 21 days, the results provide justification for the use of final concentrations of 8 µM N and 0.5 µM P as nutrient addition protocols sufficient to support natural phytoplankton communities in culture throughout the experiments presented in this thesis. Furthermore, the L4 nutrient amendments simulate in situ nutrient pulse conditions regularly evidenced in the time series data set, making them environmentally relevant to the study site. Si was not adjusted in this pilot experiment due to an initial concentration of 2.0 µM, beyond which a higher concentration may pre-select diatom dominated communities. In the experiments presented in this thesis, Si concentration was only adjusted if values significantly deviated below 2 µM. A limitation of this PhD thesis research was a lack of nutrient measurements beyond the first day of sampling phytoplankton communities and collecting seawater medium. This was unfortunately due to funding and logistical constraints. Therefore, only initial day (T0) nutrient data is presented as it was the very least nutrient data required for the necessary experimental concentration amendments.

Chapter 4 – Effects of elevated pCO_2 on spring bloom succession to *Phaeocystis* spp.

Abstract

The effect of elevated pCO_2 on the *Phaeocystis* spp. spring bloom was investigated during a fifteen-day semi-continuous microcosm experiment. The initial phytoplankton community biomass was estimated at ~160 mg carbon C m^{-3} and was dominated by nanophytoplankton (40%, excluding *Phaeocystis* spp.), *Phaeocystis* spp. (30%) and cryptophytes (12%). Picophytoplankton contributed ~9% of total biomass while the remaining 9% comprised diatoms, *Synechococcus*, coccolithophores, dinoflagellates and ciliates in low abundance. Over the experimental period, total biomass increased significantly by 90% to ~305 mg C m^{-3} in the high CO_2 treatment while the ambient pCO_2 control showed no net gains. *Phaeocystis* spp. exhibited the greatest response to the high CO_2 treatment, increasing by 330%, from ~50 mg C m^{-3} to over 200 mg C m^{-3} and contributing ~70% of the total biomass. A 21-year time series of phytoplankton community structure was analysed in relation to *Phaeocystis* spp. to elucidate its contribution to the annual carbon budget at station L4 in the western English Channel (WEC). Between 1993-2014 *Phaeocystis* spp. contributed ~4.6% of the annual phytoplankton carbon biomass at station L4. During the March – May spring bloom period, the mean *Phaeocystis* spp. biomass constituted 17% of total biomass with a maximum contribution of 47% in 2001. Maximal weekly *Phaeocystis* spp. biomass above the time series mean ranged from 63% – 82% of the total phytoplankton carbon (~42 – 137 mg C m^{-3}) with significant inter-annual variability. Maximal biomass usually occurred by the end of April, although in some cases as early as mid-April (2007) and as late as late May (2013). Taken together, the results of the microcosm experiment and analysis of the time series suggest that a future high CO_2 scenario may favour dominance of *Phaeocystis* spp. during the spring bloom. This has significant implications for the formation of hypoxic zones and the alteration of food web structure including inhibitory feeding effects and lowered fecundity in many copepod species.

4.1 Introduction

Marine phytoplankton have been shown to exhibit sensitivity to elevated pCO_2 in seawater in growth and photosynthetic rates, in both laboratory studies using model species in culture and on natural populations in the field (e.g. Endo et al., 2013; Eggers et al., 2013; Feng et al., 2009; Hare et al., 2007; Schulz et al., 2008; Tortell et al., 2002). For example, the response of diatoms under elevated pCO_2 is not linear and species-specific. Diatom-dominated natural communities exhibited no increase in growth under pCO_2 elevated to 800 µatm during shipboard incubations (Tortell et al., 2000). The diatom *Skeletonema costatum* also showed no increase in growth during laboratory studies at 800 µatm pCO_2 (Burkhardt and Riebesell, 1997), but increased growth rates at 750 µatm pCO_2 during a mesocosm experiment (Kim et al., 2006a). Feng et al., (2010) observed dominance of the large centric *Chaetoceros* spp. relative to the smaller pennate *Cylindrotheca closterium* during shipboard incubations under CO_2 elevated to 760 ppm. Conversely, Coello-Camba et al., (2014) observed significant increases in growth of smaller centric diatoms (≤ 7 µm) and a decline in growth rates of larger centric diatoms (≥ 11 µm) under CO_2 elevated to 1000 ppm. Coccolithophores exhibit no change in growth rates but increased particulate organic carbon content and decreased inorganic carbon content (calcification) (Barcelos e Ramos et al., 2010; Feng et al., 2008b) , whereas for the lesser-studied *Phaeocystis* spp. a decrease or no change in growth rates have been observed (Chen and Gao, 2011; Thoisen et al., 2015). The few studies on natural populations suggest that elevated pCO_2 may lead to a shift in community composition with consequences for overall rates of primary production through the pCO_2 influence on photosynthesis, elemental composition and calcification of marine phytoplankton (Riebesell, 2004). To investigate the natural community response to elevated pCO_2 alone, experimental communities were sampled from station L4 during the 2015 spring bloom transition from diatoms to nanophytoplankton when *Phaeocystis* spp. was present in the water column.

In spring, pCO_2 levels attain their time series minimum values in the Western English Channel (WEC) at station L4. Following the start of the spring phytoplankton bloom, pCO_2 levels ranged

between 390.56 (± 132.81) (n = 22) to 279.47 (± 24.50) (n = 27) µatm between April and May (2008 – 2015). This CO_2 undersaturation results from cooling in late winter followed by biological productivity in the spring (Kitidis et al., 2012). Predicted future ocean acidification is likely to show significant impacts over this period when the present upper limit of observed pCO_2 levels increases during this period of undersaturation and biological activity. The shift in dissolved inorganic carbon (DIC) equilibria associated with increased pCO_2 has wide-ranging implications for phytoplankton growth, carbon biomass and community composition (Riebesell, 2004).

From a biological perspective, the most pronounced shift in the phytoplankton community at L4 occurs between March and May. Increased day length and integrated daily irradiance lead to maximum growth rates of diatoms, typically *Chaetoceros* spp. and *Thalassiosira* spp., which regularly dominate the spring phytoplankton bloom at this time series site (Holligan and Harbour, 1977; Widdicombe et al., 2010a). Following the initial spring phytoplankton bloom, nano-flagellate biomass increases and *Phaeocystis* spp. co-occur or follow the spring diatom peak (Lebour, 1917; Widdicombe et al., 2010a).

Phaeocystis spp. are ubiquitous with a unique polymorphic life-cycle, alternating free-living solitary (~6µm in size) and colonial (~2mm in diameter) cells, a process that changes organism bio-volume by 6 to 9 orders of magnitude taking the colony and mucus matrix into account (Verity et al., 2007). As such *Phaeocystis* spp. can outcompete other phytoplankton and form massive blooms (up to 10 g C m^{-3}) with impacts on food webs, global biogeochemical cycles and climate regulation (Schoemann et al., 2005). Since *Phaeocystis* spp. produce dimethylsulfoniopropionate (DMSP) their blooms also provide an important source of dimethylsulphide (DMS) (Stefels et al., 1995) playing a key role in the transfer of carbon and sulphur between ocean and atmosphere and vice versa (Liss *et al.*, 1994). While not a toxic algal species, *Phaeocystis* spp. are considered a harmful algal species (HAB) when biomass reaches sufficient concentrations to cause anoxia and mucus foam which can clog the feeding apparatus

of zooplankton and fish (Eilertsen & Raa, 1995). Along the European coasts of the North Sea dense blooms of *Phaeocystis globosa* known to impact ecosystem function have been well documented as localised events for many years (Lancelot and Mathot, 1987). More recently, other locations with nutrient enriched waters have reported massive blooms such as the Arabian Gulf and southeast coastal waters of China (Lancelot et al., 2002; Schoemann et al., 2005). In these ecosystems, *P. globosa* bloom formation is predominantly a result of anthropogenic factors, i.e. nutrient inputs via riverine and land run-off routes (Cadée and Hegeman, 2002). Consequently, *Phaeocystis* spp. have been identified as key water disturbance indicator species (Tett et al., 2007) and recommendations for decreasing its abundance to that of non-problem areas been made in the scope of the OSPAR strategy (Ospar, 2005) and the Water Framework Directive of the European Union (2000/60/EC) (Lancelot et al., 2009). However, dense blooms of *Phaeocystis antarctica* colonies are also observed in naturally nutrient rich waters such as the Ross Sea (DiTullio et al., 2000), Greenland Sea and Barents Sea (Eilertsen et al., 1989; Wassmann et al., 1990). Given the ecological, global biogeochemical and climate regulation relevance, *Phaeocystis* spp. are a highly suitable and a significant model phytoplankton species to study in the context of OA.

The goals of the present study were to investigate: 1) the effects of elevated pCO_2 on phytoplankton community structure and the relative species contribution to community biomass during the spring bloom succession to *Phaeocystis* spp. and 2) assess the natural variability in phytoplankton community structure and the carbon biomass of *Phaeocystis* spp. at station L4 over two decades (1993-2014).

4.2 Sampling and experimental set-up

Experimental seawater and experimental medium were collected as per the method described in chapter 2, section 2.2 on 13th April 2015 from 10 m depth. The experimental seawater was gently and thoroughly mixed and transferred in equal parts from each carboy (to ensure homogeneity) to sixteen 2.5 L borosilicate incubation bottles (2 sets of 8 replicates). The

remaining experimental seawater was sampled for initial (T0) concentrations of nutrients, chlorophyll *a*, total alkalinity and dissolved inorganic carbon and was also used to characterise the starting experimental phytoplankton community (as per the methods described in chapter 2). A semi-continuous closed incubation culture system linked the replicate incubation bottles to two 22 L media reservoirs which were enriched with CO_2 gas as per the method described in chapter 3. This CO_2-enriched seawater media was then used for the microcosm dilutions, adjusted as per the following treatments: (1) Ambient pCO_2 (control at ~340 µatm, matching station L4 in situ values) and (2) elevated pCO_2 (high CO_2 at ~800 µatm, predicted for the end of this century assuming the IPCC business as usual scenario (Alley et al., 2007)).

Initial nutrient concentrations (measured at 1.4 µM nitrate + nitrite, 0.05 µM phosphate and 2.0 µM silicate on 13th April 2015) were amended to 8 µM nitrate+nitrite and 0.5 µM phosphate. CO_2-enriched seawater was added to the high CO_2 treatment replicates every 24 hrs, acclimating the natural phytoplankton population to increments of elevated pCO_2 from ambient to ~800 µatm over 8 days followed by maintenance at ~800 µatm. The incubation bottles were maintained at 11 °C in a flow-through seawater bath (temperature was monitored twice daily) to replicate in situ temperature on the day of sampling. Light was supplied by a cool white LED light bank at irradiance of ~200 µmol photons m^{-2} s^{-1} on a 16:8 hour light:dark cycle. The light level used approximated PAR at 10 m depth measured on the day of sampling with a daily light dose over 16 hours of 11.52 mol m^{-2} d^{-1}. Incubation bottles were inverted and gently agitated twice each day to maintain phytoplankton cells in suspension and also prior to sampling to ensure homogeneity. Sampling time points over the course of the experiment are prefixed by T for each sampling occasion.

4.2.1 Statistical analysis

In order to test for effects of high CO_2 and to account for possible time dependence of the measured response variables (chl *a*, C:chl *a*, total community biomass and biomass of individual species), a generalised linear model (glm) with the factors pCO_2 and time were applied to the

data following target pCO_2 equilibration between T9 and T14, since this was a relatively short experiment and equilibration to target pCO_2 occurred later in the second week. Where main effects were established, pairwise comparisons were performed using the method of Herberich *et al.*, (2010) for data with non-normality and/or heteroscedasticity. However, between treatment differences over the entire time course of the experiment were visualized using non-metric multidimensional scaling ordination (nMDS). The Bray-Curtis index was used to calculate the resemblance of biomass in the experimental treatments based on the community structure. The resulting resemblance matrix was then used to perform an ordination nMDS. Individual group and species vectors were then superimposed on the nMDS ordination and their resulting contribution to biomass was represented by the proximity to experimental treatments. Weekly biomass values from the L4 time-series were averaged over years to elucidate the variability and seasonal cycles of *Phaeocystis* spp. and total phytoplankton carbon biomass. A glm was used to test for differences in biomass between years. All time series sample sizes are given in the figure legends of the plotted data. All statistical data are reported as the arithmetic means with standard deviation describing the error term, unless otherwise stated. Analyses were conducted using the R statistical package (R Core Team (2014).

4.3 Results

4.3.1 Elevated pCO_2 perturbation experiment

Chl *a* concentration in the WEC and the Celtic Sea ranged between 0.4 – 6.0 mg m^3 from 8th – 14th April according to the MODIS weekly composite Chl *a* data (**Fig. 4.1 A**). Declining nitrate and silicate concentrations at station L4 from February coincided with a chl *a* peak in early March, indicating the presence of an early diatom bloom. A second chl *a* peak was evident during April, indicating that community sample timing coincided with the successional phase from diatoms to the nanophytoplankton functional group / *Phaeocystis* spp. (**Fig. 4.1 B**). A diverse diatom community dominated by *Cocinodiscus wailesii* was observed in routine qualitative time series net trawl samples (200 µm) from station L4 from late February into March and *Phaeocystis* spp. colonies were observed throughout April (data not shown).

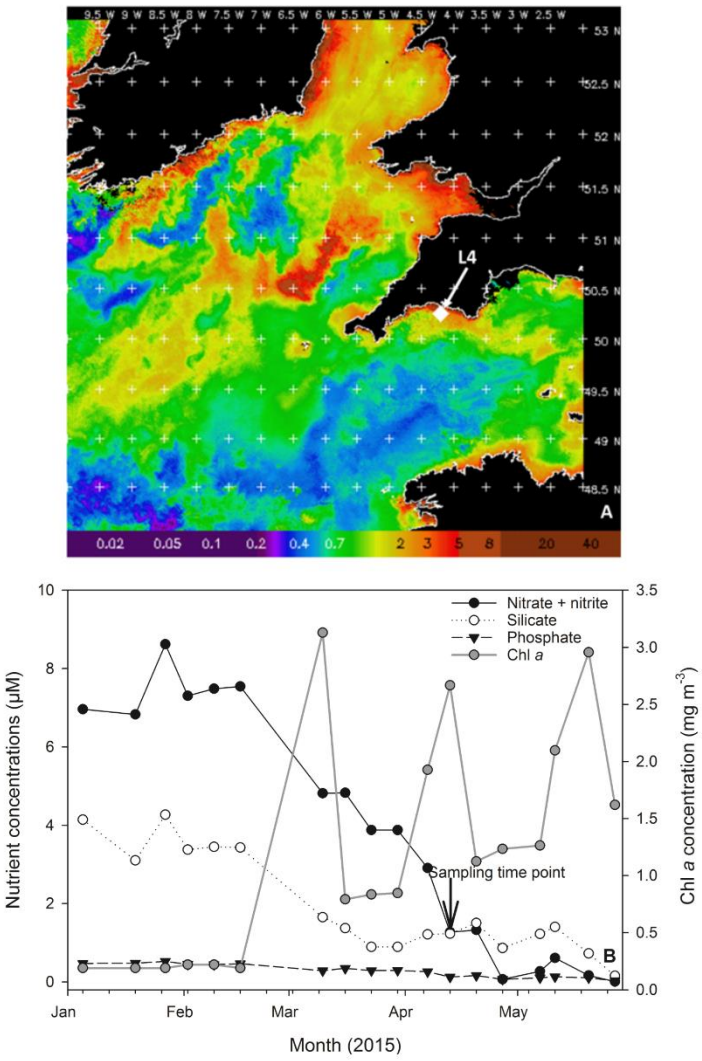

Fig. 4.1 A MODIS weekly composite chl *a* image of the western English Channel covering the period 8th – 14th April 2015 (coincident with the week of phytoplankton community sampling for the present study), processing courtesy of NEODAAS. The position of coastal station L4 is marked with a white diamond. **B.** Time series of weekly nutrient and Chl *a* measurements from station L4 at a depth of 10 m over the first half of 2015 in the months prior to experimental phytoplankton community sampling (indicated by black arrow and text).

4.3.2 Carbonate system

Mean pCO_2 values of media for the control and high CO_2 treatments were 361 (± 56) and 1006 (± 61) µatm respectively. Due to the dilution volume regime of the phytoplankton community incubations, full equilibration to the target pCO_2 value (800 µatm) within the high CO_2 treatment incubations was achieved at T8. The high pCO_2 treatment incubations were slowly acclimated to rising pCO_2 over 8 days while the ambient control pCO_2 incubations were acclimated at the

same ambient carbonate system values as that from station L4 on the day of sampling. Following equilibration, the mean pCO_2 values within the control and high CO_2 incubations were 350 (± 95) and 812 (± 39) µatm respectively (**Fig. 4.2 A–D**).

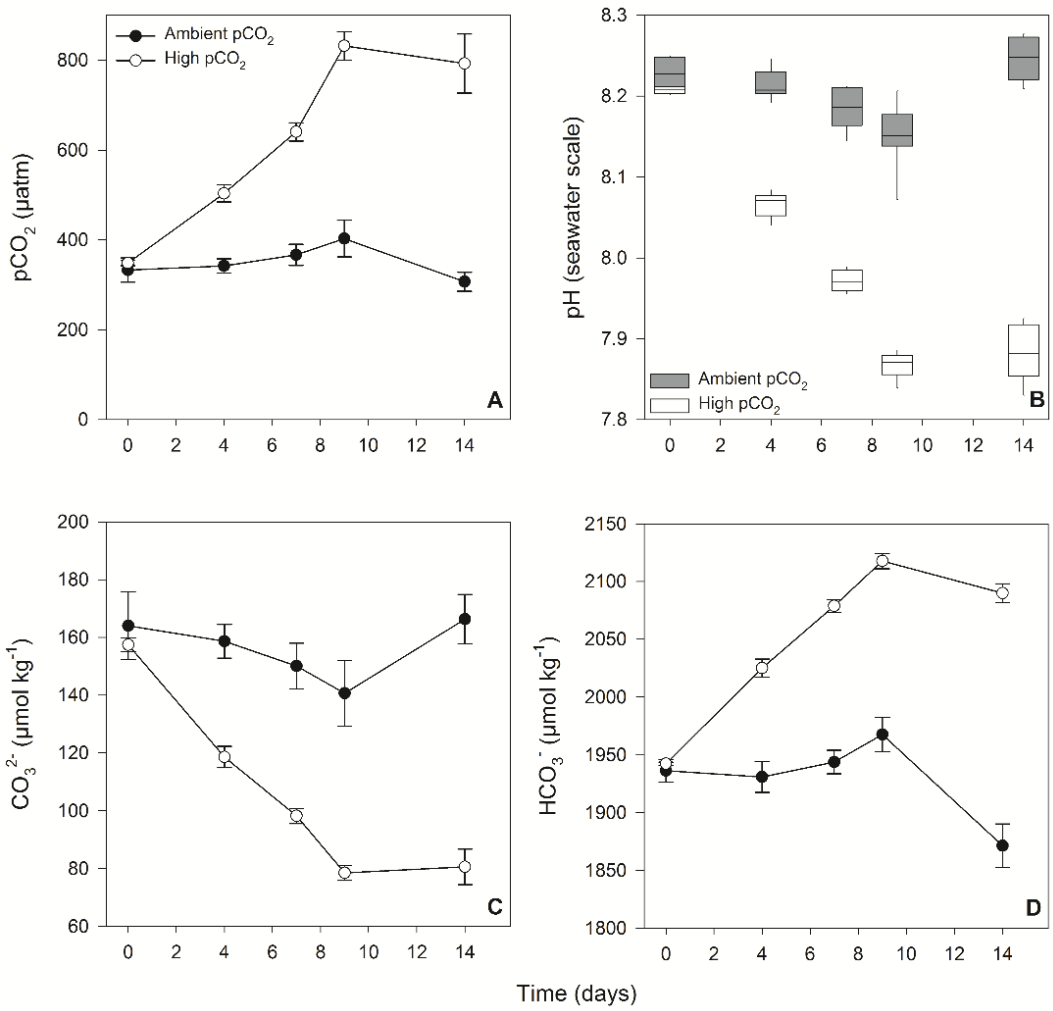

Fig. 4.2 Carbonate system values of the experimental phytoplankton incubations. **A.** pCO_2, **B.** pH on the seawater scale **C.** carbonate concentration (CO_3^{2-}) and **D.** bicarbonate concentration (HCO_3^-) were calculated from direct measurements of total alkalinity and dissolved inorganic carbon.

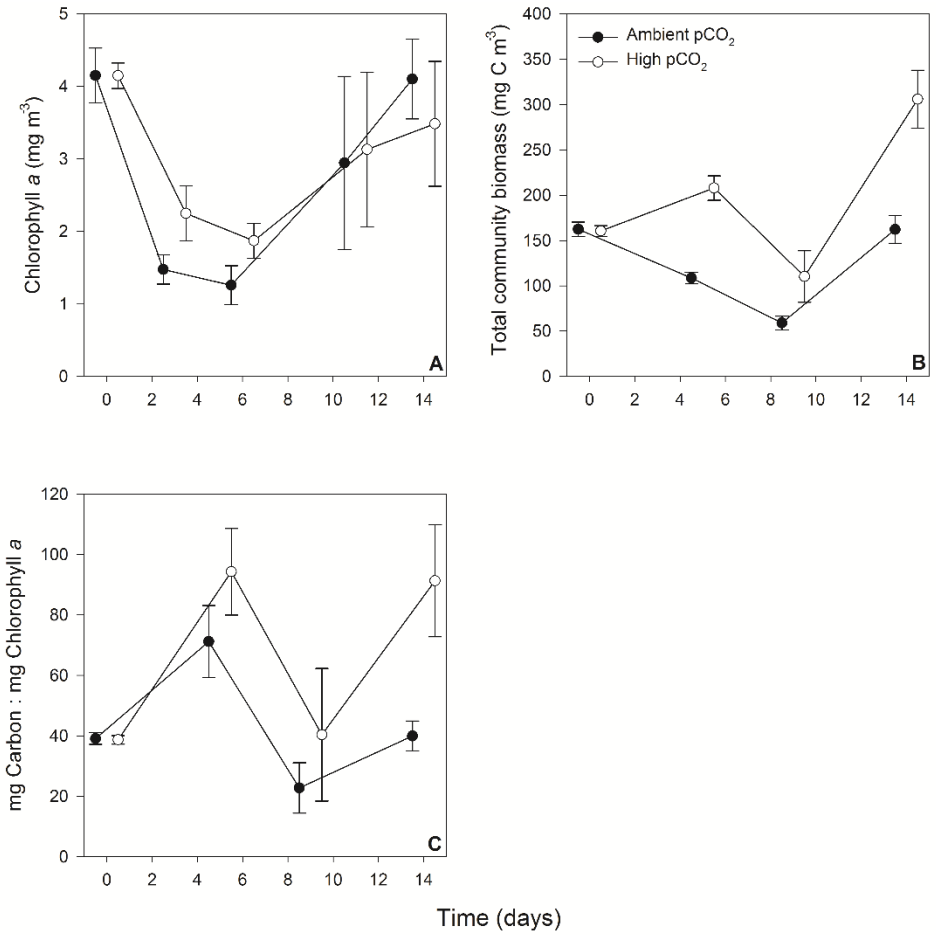

Fig. 4.3 A. Time series of chl *a*, **B.** total phytoplankton community biomass and **C.** carbon:chl *a* ratio. Following equilibration to experimental target pCO_2 (800 µatm), no significant response to elevated pCO_2 was observed in chl *a* between the ambient control and high CO_2 treatments, however both treatments showed a significant increase in chl *a* over time. A highly significant increase in total community biomass was observed in the elevated CO_2 treatment compared to that of the ambient control.

4.3.3 Chlorophyll *a*

Mean chl *a* concentration in the experimental seawater at T0 was 4.15 (± 0.38) mg m^{-3}. The concentration dropped between T0 and T6 which in the control was 1.2 (± 0.27) mg m^{-3} at T6 and in the high CO_2 treatment was 1.87 (± 0.24) mg m^{-3}. Both control and high CO_2 treatments showed a positive response to media dilutions from T6 onwards with no significant difference in increased chl *a* concentration following target pCO_2 equilibration at T8.

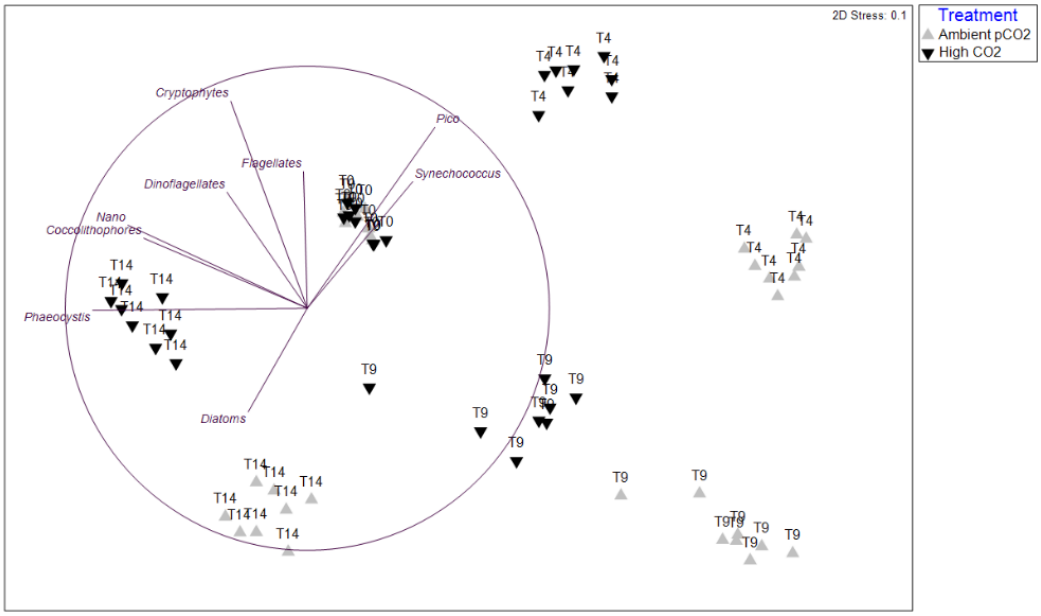

Fig 4.4 nMDS plot structure showing the ordination of differences in phytoplankton biomass over time by experimental treatment in 2 dimensions. The numbers on the treatment data points represent the time points of the samples during the experiment (T0, T4, T9, T14).

There was a significant increase in chl *a* concentration in both treatments over time (z = 2.437, p < 0.05) (**Table 4.1**). Mean chl *a* values on the final day of the experiment (T14) were 4.1 (± 0.55) and 3.5 (± 0.86) mg m^{-3} for the control and high CO_2 treatment respectively and pairwise comparisons showed no statistical difference between the high CO_2 treatment and ambient control Chl *a* at this final time point (t = -1.599, p = 0.132, (n = 16)) (**Fig. 4.3 A**).

4.3.4 Phytoplankton biomass

The starting biomass was estimated at ~160 mg C m^{-3} in both treatment groups. The community was dominated by nanophytoplankton (excluding *Phaeocystis* spp. ~40%), *Phaeocystis* spp. (~30%) and cryptophytes (~12%). Picophytoplankton contributed ~9% of total biomass while the remaining 10% comprised diatoms, phytoflagellates, *Synechococcus*, ciliates, coccolithophores and dinoflagellates in low abundance.

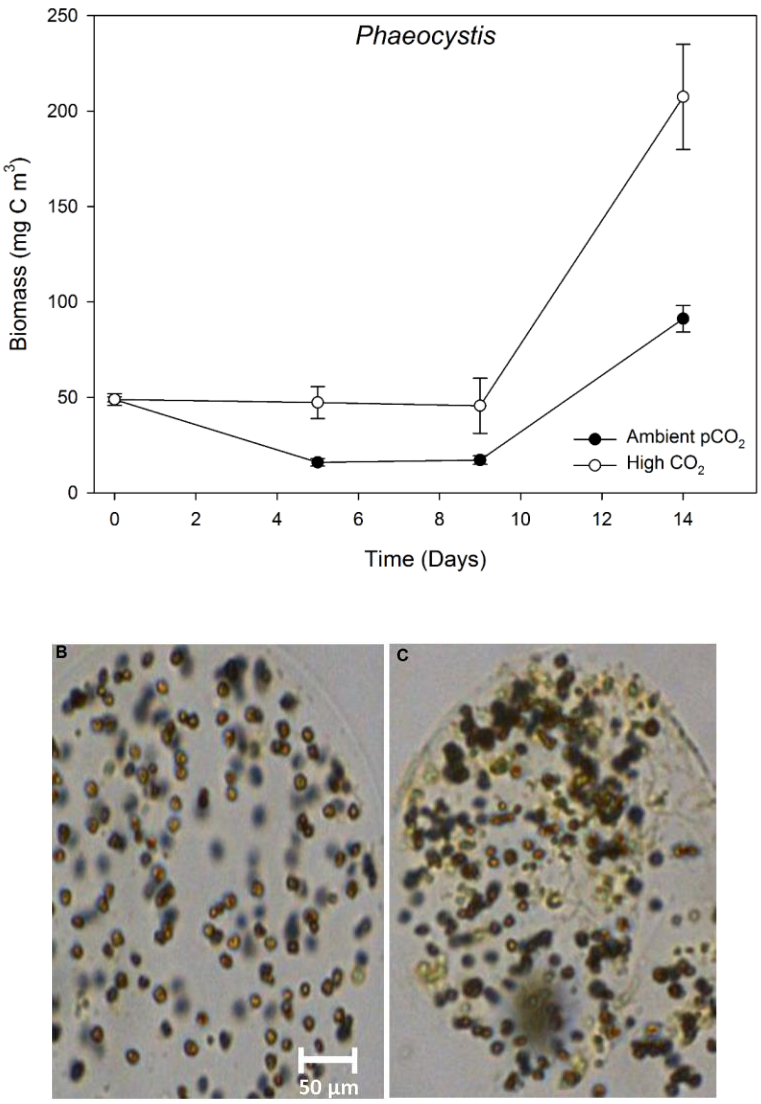

Fig. 4.5 A. The highly significant response of *Phaeocystis* spp. to elevated pCO_2 in comparison to the ambient pCO_2 control. Note, biomass is the sum of solitary and colonial cells. **B. & C.** Image capture from FlowCAM analysis at T9 and T14 established the presence of *Phaeocystis spp.* colonies bound into a gelatinous matrix.

While total community biomass in both treatments declined to T9, the biomass in the high CO_2 treatment increased significantly from 110 to 305 mg C m^{-3} between T9 and T14 ($z = 12.89$, $p < 0.0001$) (**Fig. 4.3 B, Table 4.1**) showing a 90% increase. The control community also increased between T9 and T14 and was restored to the initial starting value of 160 mg C m^{-3} showing no overall net gain over the experimental period. Pairwise comparisons between the treatments showed the high CO_2 treatment total biomass to be significantly greater than the control at T14

(t = 10.787, p < 0.001 (n = 16)). In both treatments there were significant differences in C:chl *a* (mg C:mg chl *a*) over time (z = 6.684, p <0.0001). For the control, the ratio was 22.75 at T9 and 39.97 at T14, whereas for the high CO_2 treatment the ratio significantly increased to 40.38 at T9 and 90.4 at T14, (z = 6.778, p < 0.0001, **Fig. 4.3 C, Table 4.1**). The high CO_2 treatment C:Chl a ratios were significantly greater than the control at both T9 (pairwise comparisons: t = 3.558, p < 0.05) and T14 (t = 12.43, p < 0.001 (n = 16)).

The nMDS showed a clear separation of biomass between the control and high CO_2 treatment over the time course of the experiment and the significant influence of *Phaeocystis* spp. in the high CO_2 treatment at T14 (**Fig 4.4**). Performance of the nMDS ordination was assessed using Kruskal's stress formula 1. The stress value of 0.1 showed that it adequately resolved the differences between treatments in 2 dimensions. Stress < 0.05 gives an excellent representation with no misinterpretation and stress < 0.1 corresponds to a good ordination with no real prospect of misleading interpretation (Clarke, K. R. and Warwick, 2001).

Phaeocystis spp. decreased in the control community from T0 to T5 followed by a sharp increase at T9 to T14, from 17 to 91 mg C m^{-3}. It dominated the control community, contributing 56% of overall biomass, more than any other group at T14 and increased by almost 90% compared to its initial T0 value. In the high CO_2 treatment however, there was a significant increase in *Phaeocystis* spp. relative to the control community at T9 to T14, from 45 to 207 mg C m^{-3} (**Fig. 4.5 A**), and it dominated the community within this treatment contributing ~70% of total community biomass, increasing by 330% compared to the T0 starting biomass (z = 3.707, p= <0.0001) (**Table 4.2**). Pairwise comparisons showed *Phaeocystis* spp. biomass in the high CO_2 treatment to be significantly higher than the control at T5 (t = 9.632, p < 0.001, (n = 16)), T9 (t = 5.139, p < 0.001, (n = 16)) and T14 (t = 10.811, p < 0.001, (n = 16)). Between T9 and T14, colonies of *Phaeocystis spp.* were observed in both treatments in the FlowCAM images, which provided a qualitative assessment of colony presence (**Fig. 4.5 B & C**).

Table 4.1 Results of generalized linear models testing for the effects of pCO_2 and time on measured phytoplankton community parameters. Significance results are given as: ∗ p < 0.05 and ∗∗∗ P < 0.0001

Response variable	n	*df*	*z*-value	*p*	sig
Chl *a* (mg m^{-3})					
pCO_2	32	29	1.032	0.52061	
Time	32	29	2.437	**< 0.05**	*
Carbon:Chl *a* (mg:mg)					
pCO_2	32	29	6.778	**< 0.0001**	***
Time	32	29	6.684	**<0.0001**	***
Total biomass (mg C m^{-3})					
pCO_2	32	29	12.890	**< 0.0001**	***
Time	32	29	20.48	**<0.0001**	***

Nanophytoplankton biomass (excluding *Phaeocystis* spp.) declined in both treatment groups from T0 to T5, which was greater in the control community, from ~65 to 15 mg C m^{-3} compared to ~65 to 23 mg C m^{-3} in the high CO_2 treatment. Biomass increased significantly in both treatments between T9 and T14 (z = 4.141, p = < 0.001) (**Fig. 4.6 A, Table 4.2**). Nanophytoplankton showed an overall net loss in biomass at T14 in the high CO_2 treatment (~46 mg C m^{-3} at T14 compared to a starting biomass of ~63 mg m^{-3} at T0, a decrease of 27%). A pairwise comparison however, showed nanophytoplankton biomass to be significantly greater in the high CO_2 treatment compared to the control at T14 (t = 5.297, p < 0.001, (n = 16)).

Following an initial (acclimation) response of increased biomass between T0 and T5, picophytoplankton and *Synechococcus* both declined over time. The high CO_2 treatment maintained significantly higher biomass of picophytoplankton relative to the control following target pCO_2 equilibration (T9 to T14, t = 5.470, p < 0.001, (n = 16)) and significantly greater biomass of *Synechococcus* which showed a net gain at T14 compared to its starting biomass value, an increase of ~60% (3.9 to 6.2 mg C m^{-3}, pairwise comparison, t = 5.239, p < 0.001, (n = 16) **Fig. 4.6 D & F, Table 4.2**). An initial short-term response of increased biomass was also observed with cryptophytes in the high CO_2 treatment (T0 to T5), followed by a decrease in both

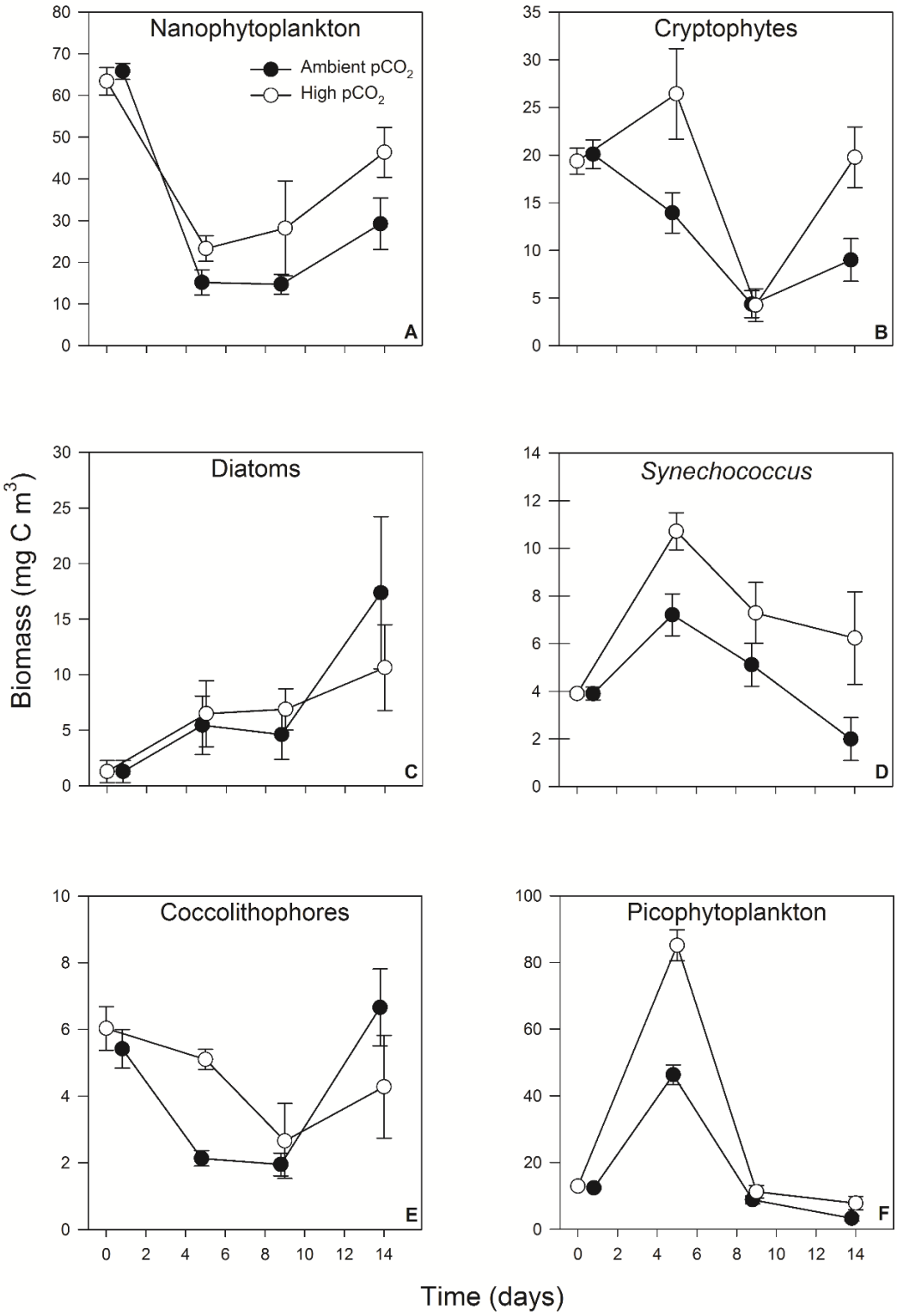

Fig. 4.6 Response of individual components of the experimental phytoplankton community to elevated pCO_2. Cells were enumerated and converted to carbon biomass.

Table 4.2. Results of generalized linear models testing for the effects of pCO_2 and time on individual phytoplankton species biomass, (n = 32). Significance results are given as: $*$ p < 0.05, and $***$ P < 0.0001.

Response variable	Parameter	*df*	*z*-value	*p*	sig
Ciliate biomass (mg C m^{-3})	pCO_2	29	2.532	0.17	
	Time	29	0.622	0.539	
Coccolithophore biomass (mg C m^{-3})	pCO_2	29	-1.723	0.095	
	Time	29	5.763	<0.0001	***
Cryptophyte biomass (mg C m^{-3})	pCO_2	29	-2.060	0.039	*
	Time	29	3.513	<0.0001	***
Diatom biomass (mg C m^{-3})	pCO_2	29	-1.068	0.286	
	Time	29	5.648	<0.001	***
Dinoflagellate biomass (mg C m^{-3})	pCO_2	29	1.567	0.117	
	Time	29	1.205	0.228	
Flagellate biomass (mg C m^{-3})	pCO_2	29	-0.342	0.732	
	Time	29	0.345	0.73	
Nanophytoplankton biomass (mg C m^3)	pCO_2	29	2.36	0.018	*
	Time	29	3.697	<0.0001	***
Phaeocystis biomass (mg C m^{-3})	pCO_2	29	3.707	<0.0001	***
	Time	29	15.636	<0.0001	***
Picophytoplankton biomass (mg C m^{-3})	pCO_2	29	-1.448	0.148	
	Time	29	-4.331	<0.0001	***
Synechococcus biomass (mg C m^{-3})	pCO_2	29	-2.334	0.027	*
	Time	29	-5.407	<0.0001	***

control and high CO_2 treatments (T5 to T9). Between T9 and T14 however, cryptophyte biomass increased significantly in both treatments although to a greater extent in the high CO_2 treatment

(pairwise comparison, $t = 7.332$, $p < 0.001$, (n = 16)) where it was restored to the starting value of ~20 mg C m^{-3} compared to 9 mg C m^3 in the control (**Fig. 4.6 B, Table 4.2**).

Dinoflagellate biomass was greater in the high CO_2 treatment compared to the control at T9, however by T14 there was no significant difference between treatments (**Table 4.2**). Flagellate biomass (not including *Phaeocystis* spp.) remained low and exhibited a decline in both the control and high CO_2 treatments, though the variability was high. With a mean of ~ 0.3 mg C m^{-3} throughout the experiment, flagellates were the lowest biomass contributor and showed no significant difference between treatments.

Ciliate biomass declined between T9 and T14 relative to the control. Both coccolithophore and diatom biomass increased between T9 and T14 in both treatments, however the increase in the high CO_2 treatment was lower compared to the control although not significantly for diatoms (**Fig. 4.6 C** & **E, Table 4.2**; pairwise comparisons for coccolithophores $t = -3.272$, $p < 0.02$; and diatoms $t = -2.266$, $p < 0.276$, (n = 16)). Diatom community biomass was dominated by the chain forming *Chaetoceros curvisetus* and pennates *Proboscia alata* and *P. truncata* species. Smaller biomass contributions were made by *Chaetoceros socialis, C. decipiens, C. eibenii, Leptocylindrus danicus, Pseudonitzschia spp. and Thalassiosira* spp. At T9 *Proboscia* spp. contributed 66% and 62% (~1.5 and 2.2 mg C m^{-3}) of total diatom biomass in the control and high CO_2 treatments while *C. curvisetus* contributed 32% and 30% (~0.5 and 0.7 mg C m^{-3}) respectively (mean values). At T14 *Proboscia spp*. contributed 32% and 30% (~2.85 and 1.6 mg C m^{-3}) of total diatom biomass respectively in the control and high CO_2 treatments, while *C. curvisetus* contributed 52% and 34% respectively (~4.6 and 1.8 mg C m^{-3}).

4.3.5 Station L4 time-series, *Phaeocystis* spp. biomass in the WEC

Over the time series from 1993 to 2014, the annual mean total phytoplankton biomass sampled at L4 was 1646 (± 521) mg C m^{-3}, with annual mean *Phaeocystis* spp. biomass of 72 (± 69) mg C m^{-3}. Maximum total annual phytoplankton biomass occurred in 1997 (3206 mg C m^{-3}) and minimum values were in 2007 (998 mg C m^3) when the associated annual *Phaeocystis* spp.

biomasses were 121 and 75 mg C m^{-3}, respectively (**Fig. 4.7 A**). *Phaeocystis* spp. contributed 4.6% of the total phytoplankton annual carbon budget, which peaked at ~16% in 2001 (~270 mg C m^3). **Fig. 4.7 B** shows the biomass trends over the March – May seasonal bloom period. *P. globosa* and *P. pouchetii* were both recorded at the L4 time-series site but were grouped as *Phaeocystis* spp. due to the inherent difficulties in distinguishing single cells using microscopy.

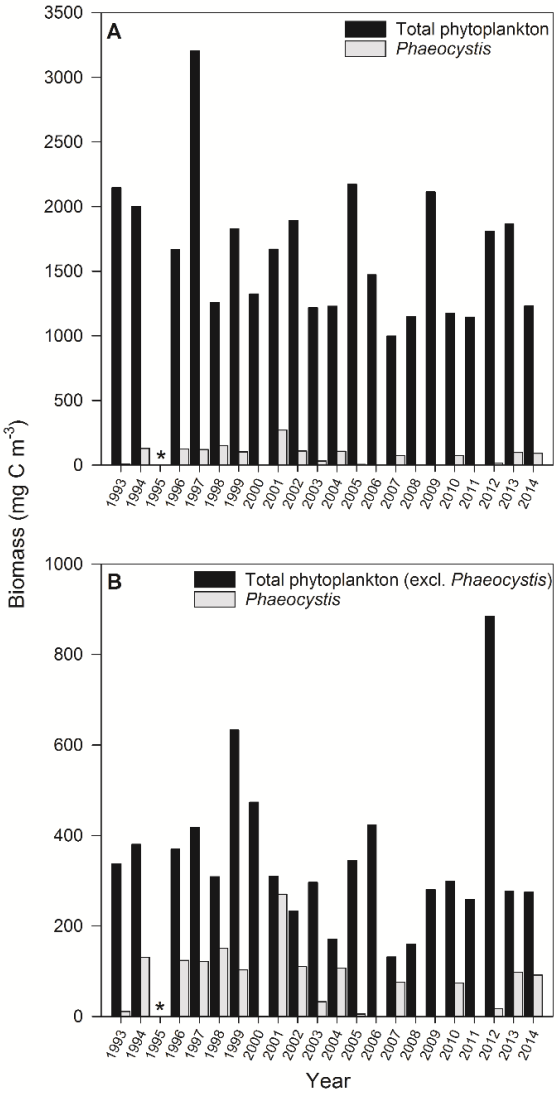

Fig. 4.7 A Total annual *Phaeocystis* spp. biomass (n = 158) and total annual phytoplankton biomass (n = 909) over the time series at station L4, **B**. Total *Phaeocystis* spp. biomass (n = 113) with total phytoplankton biomass (excluding *Phaeocystis* spp. biomass) over the spring bloom period (March – May).* Insifficient data for 1995.

Weekly *Phaeocystis* spp. biomass recorded from January to December throughout the time series ranged from undetectable to 137 mg C m^{-3} (**Fig. 4.8 A**). Bloom initiation occurred as early

as mid to late March (2007 and 2011). The bloom initiation (taken as an increase in biomass > 0.5 mg C m^{-3}) usually occurred by the end of April, though in 2007 it was mid-April and in 2013 it was late May. The mean yearly maximal biomass peak was 41.6 (± 39.3) mg C m^{-3} (**Fig. 4.8 B**). The generalised linear model highlighted significant inter-annual variability in *Phaeocystis* spp. biomass between 1993 and 2014 with biomass in 2001 significantly greater than any other year throughout the time series, when maximal biomass reached 137 mg C m^{-3} ($z = 3.355$, $p < 0.001$) (**Table 4.3**). Half of the 21 years analysed showed a maximal peak *Phaeocystis* spp. biomass range between 42 and 137 mg C m^{-3} (above the time series mean maximum of 41.6 mg C m^{-3}), significantly higher than all other years over the time-series, (indicated in **Table 4.3** with significance between $p < 0.05$* to $p < 0.001$***). Biomass as low as between 0.09 – 1.5 mg C m^{-3} however, was observed during the seasonal bloom in 6 out of the 21 years, denoted by the negative z scores in **Table 4.3**. Total phytoplankton biomass peaked during the spring bloom period, typically between March and May and was highest (215 mg C m^{-3}) when the associated *Phaeocystis* spp. biomass increased above the time series mean peak maxima (to 56 mg C m^{-3}). Throughout the time-series *Phaeocystis* spp. maximal biomass (above the mean maximum biomass) contributed between 26% (1994) – 82% (1998 and 2013) of phytoplankton carbon, while total *Phaeocystis* spp. biomass over the March – May bloom period contributed a mean value of 17% to total phytoplankton carbon, between 20%-47% during years of high biomass above the mean maximum (i.e. 2001 and 2010) and between 0.1% to 13.9% during years of low biomass (i.e. 2006, 2001 and 1999). Mean bloom duration, which was calculated when biomass values > 0.5 mg C m^{-3} over the time-series was 22 days with a range between 6 days (2000) and 44 days (1994).

4.4 Discussion

4.4.1 Elevated pCO_2 Perturbation experiment

Results from the microcosm experiments showed that pCO_2 elevated to ~800 µatm caused: 1) a significant increase in total community biomass by 90%, from ~160 to 305 mg C m^{-3}, 2)

significant changes in community structure from a nanophytoplankton (40%) and *Phaeocystis* spp. (30%) dominated community to a *Phaeocystis* spp. (~70%) dominated community and 3) either positive or negative responses in the rest of the phytoplankton community. Both diatoms and coccolithophores were the only other phytoplankton groups to show a constant increase in biomass in the control which was greater than that of the high CO_2 treatment, but only significant for coccolithophores.

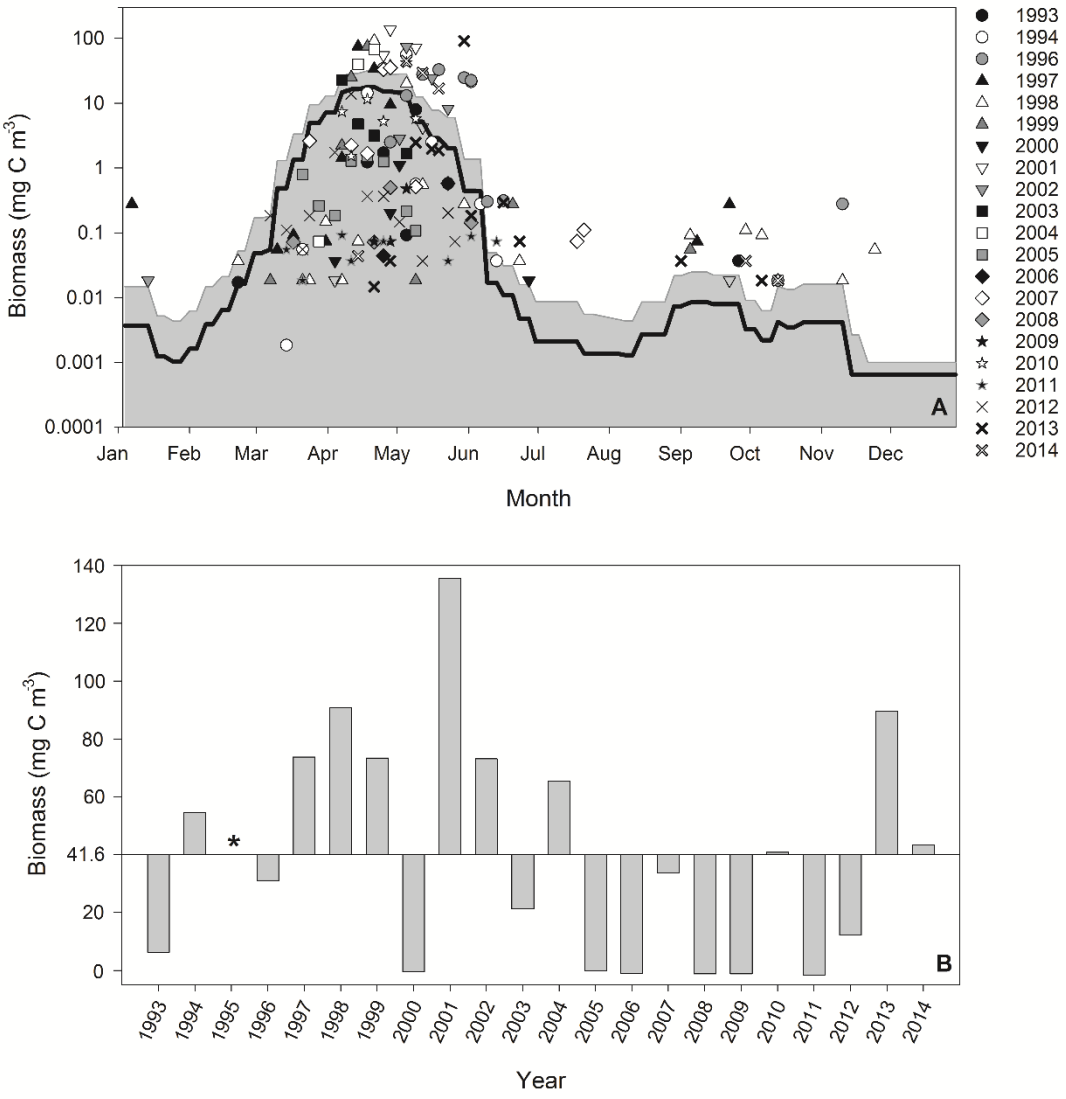

Fig 4.8 A. Seasonal profiles of *Phaeocystis* spp. carbon biomass (common log scale) between 1993 – 2014 (n = 158). Black line is smoothed running average over the time-series, grey area is the standard deviation and all symbols are observed data values by year. **B.** Annual anomalies of maximal *Phaeocystis spp.* carbon biomass above and below the time series mean maxima of 41.6 mg C m^{-3}. * Insufficient data 1995.

Table 4.3. Inter-annual differences in *Phaeocystis* spp. carbon biomass at station L4 between 1993 – 2014 tested with a generalised linear model. Significance results are given as: ∗ p < 0.05, ∗∗ p < 0.01 and ∗∗∗ p < 0.001 (n = 21).

Response variable (Year)	*df*	*z* value	*p*	sig
1993	20	1.458	0.144737	
1994	20	2.055	0.039883	*
1996	20	2.1	0.035769	*
1997	20	2.567	0.010258	*
1998	20	2.343	0.01915	*
1999	20	2.522	0.011669	*
2000	20	-1.009	0.313129	
2001	20	3.355	0.000794	***
2002	20	2.473	0.013411	*
2003	20	1.153	0.249038	
2004	20	2.649	0.008075	**
2005	20	-1.48	0.138741	
2006	20	-0.806	0.420182	
2007	20	1.764	0.077781	
2008	20	-0.847	0.39682	
2009	20	-0.86	0.389549	
2010	20	1.74	0.081802	
2011	20	-2.298	0.021548	*
2012	20	0.2	0.841177	
2013	20	2.34	0.019302	*
2014	20	2.405	0.016167	*

The overall increase in total community biomass followed the same trend as previous studies conducted on natural phytoplankton community CO_2 enrichments (Feng et al., 2009; Hare et al., 2007b; Riebesell et al., 2007; Tortell et al., 2008b). *Phaeocystis* spp., diatoms and *Synechococcus* were the only species/groups to show an overall net gain in biomass in the high CO_2 treatment, irrespective of significant increases (or decreases) relative to the control community following target pCO_2 equilibration. A number of other studies have shown that the growth rates of specific diatoms can increase by 5% to 33% following 20 generations acclimated at elevated pCO_2 between 750 – 1000 µatm (*Phaeodactylum tricornutum, Thalassiosira pseudonana, T. guillardi, T. weissflogii, T. punctigera and Cocinodiscus wailesii*) (Wu et al., 2010a, 2014) and that

the highest growth occurred in diatoms > 40 µm in diameter (*T. punctigera* and *C. wailesii*). Similarly in some natural phytoplankton communities exposed to elevated CO_2 (750 ppmv) diatoms and prymnesiophytes become dominant, making up 60% and 30% of the total biomass (Tortell *et al.*, 2002). Tortell *et al.*, (2008) also observed in Ross Sea phytoplankton, a shift in dominance from *Phaeocystis antarctica* (contributing > 90% community biomass) to large chain-forming diatoms (*Chaetoceros* spp.) within high CO_2 treatments (800 ppmv).

Solitary and colonial cells of *P. globosa* exposed to high CO_2 (750 ppm) have been shown to exhibit a differential response (Wang et al., 2010). During 14 day incubations, solitary cell biomass decreased by 46%, while the number of colonies increased by 26%. Maximum growth rates of colonies significantly increased by 30%, but no change in growth rate was observed in solitary cells. Wang et al., (2010) also observed increased particulate organic carbon (POC), nitrogen (PON) and cellular C:N ratios were also observed under elevated CO_2. This suggests that elevated CO_2 may enhance carbon export.

In a monoculture study using a *P. globosa* isolate from the South China Sea, Chen *et al*, (2014) recently showed that high CO_2 (1000 ppmv) caused a decrease in non-photochemical energy loss. Short term exposure to elevated pCO_2 in combination with low, medium and high light levels (25, 200 and 800 µmol photons m^2 s-1) resulted in reduced growth rates under high light conditions, however little effect was observed under low light conditions in short term incubations. This is in agreement with a similar study using a North Sea *P. globosa* isolate where Hoogstraten *et al*, (2012) demonstrated decreased growth rates and photosynthetic efficiency over a 6 day incubation period. However, following acclimation to experimental conditions after 9 and 14 generations, Chen *et al*, (2014) observed enhanced growth rates, increased cellular chl *a* and photosynthetic activity that had recovered to values equivalent of the control, which contradicts the findings of Hoogstraten *et al*, (2012). The authors concluded that effects of elevated CO_2 on *P. globosa* are strongly influenced not just by irradiance, but also the stage of acclimation to acidification. In the present study, no decline in *Phaeocystis* spp. biomass was

observed over the first 8 days under high CO_2 exposure, but biomass remained constant, followed by a significant increase to T14. The experimental irradiance was equal to that of the mid-light level applied by Chen *et al.*, (2014). In the present experiment, biomass declined between T0 and T9 in the ambient control and was constant in the high pCO_2 treatment before increasing from T9 to T14. This demonstrates effects of acclimation to bottle containment and experimental conditions. Had the experiment been terminated on or before T9, the significant response of *Phaeocystis* spp. to elevated pCO_2 would have gone unreported. Biomass was increasing at the point the experiment was terminated, demonstrating it could have been extended beyond 14 days. Results from the similar experiments discussed were obtained over shorter time-courses (7 days, 6 days and 8 days). They should be treated with some caution as the conclusions drawn may be based on short-term cellular stress and acclimation responses, rather than responses to experimental treatments. This is a critical observation that should be considered for all similar environmental perturbation experiments to ensure the response is a direct result of experimental treatments. Logistical, equipment and scheduling constraints may often determine the time-course of such experiments, however this needs to be prioritised in future studies.

For *P. antarctica* in the Southern Ocean exposed to high CO_2 (current ambient, 600 and 800 ppmv), +2°C temperature increments (i.e. 2, 4 and 6°C respectively) and +50 μmol photons m^2 s^{-1} irradiance increments (i.e. 50, 100 and 150 μmol photons m^2 s^{-1}) under both Fe replete and limited conditions, there was a 64% decrease in growth rates at 800 ppmv (Fe replete) and a 46% decrease under Fe limiting conditions (Xu *et al*, 2014). The Fe replete treatment increased the percentage of solitary cells by 136% compared to 258% in the Fe limited treatment. Cellular chl *a* decreased in the same treatments, but no influence was observed on cellular POC. The experiment also assessed the competition between *P. antarctica* and the diatom *Fragilariopsis cylindrus* and showed that the diatom dominated the population after day 8 at 800 ppmv CO_2. In the present study, the effects of macro or micro nutrients, temperature and irradiance were not investigated and N and P were maintained constantly replete (8 μM and 0.5 μM respectively),

though Si concentration was 2.0 μM with no further amendments. The findings of Xu *et al.*, (2014) contrast the present study results and probably reflect differences between monoclonal and two-species competition incubations compared to experiments on a natural phytoplankton community.

Monoclonal incubations of *Phaeocystis* spp. under different CO_2 treatments can produce variable responses related to species, strain or ecotype as well as due to differences in experimental approaches. Incubations of a natural Arctic phytoplankton community under four pH treatments (pH 8.0, 7.7, 7.4 and 7.1) showed that growth rates of *P. pouchetii* were unaffected by pH from 8.0 – 7.4. There was however, a 50% decrease in growth rates at pH 7.1 (Thoisen et al., 2015).

Accurate identification of *Phaeocystis* spp. relies on composite independent investigations combining light microscopy, transmission and scanning electron microscopy as well as flow cytometry for a complete identification of the morphotype (Rousseau et al., 2007). Such an investigation was beyond the scope and resources available for this study. Therefore, on the basis of the FlowCam image capture, current knowledge of global geographical distributions of the different *Phaeocystis* species (Verity et al., 2007) and records from station L4 phytoplankton community time-series (Widdicombe *et al.*, 2010), it is likely the *Phaeocystis* species observed in the microcosm exp. were a combination of *P. globosa* and *P. pouchetii*. The FlowCam image capture was not used to enumerate *Phaeocystis* spp. colonies since the samples were preserved with lugol's iodine which is known to cause colony disaggregation (Rutten et al., 2005) which can cause an underestimation in group biomass. Flow cytometric analysis causes cleavage of cell aggregations through the sheer force of sheath fluid (Dubelaar and van der Reijden, 1995), and thus provides more accurate enumeration of single cells disaggregated from colonies. This technique however, does not enable us to distinguish between colonial cells/colonies and free-living solitary cells.

From the present experimental results, the biomass range of *Phaeocystis* spp. in the control was within the range measured throughout the L4 time series (~48 - 91 mg C m^3 compared to in situ values of between 33 – 137 mg C m^3). The response of *Phaeocystis* spp. to the high CO_2 treatment (increase of 330% from initial starting value to ~207 mg C m^3) is above the maxima measured at L4. Schoemann *et al.*, (2005) illustrated the difficulties in estimating *Phaeocystis* spp. biomass due to the high carbon content of the polysaccharide matrix. The difference in carbon content between a solitary (without the mucus matrix carbon contribution) and colonial cell has been estimated to be 42.85 – 107.85 pg C $cell^{-1}$ based on empirical methods (Jahnke and Baumann, 1987). Since samples were fixed in Lugol's iodine, the C biomass could be underestimated. The steady state incubation conditions in the experiment; (irradiance, nutrients, temperature, dilution and mixing regime) may have preferentially selected for *Phaeocystis* spp. compared to the fluctuating conditions of the natural environment. Sommer, (1985) demonstrated that variability in resource supply controls the number and relative proportion of coexisting species and using monoclonal cultures subjected to carbonate system manipulation can result in significantly different growth rates of the same species (e.g. Shi *et al.*, 2009).

4. 4.2 Trends in *Phaeocystis* spp. biomass from time-series analysis

In agreement with the present study, previous analysis of the L4 *Phaeocystis* spp. time-series (1992-2007) elucidated: 1) significant inter-annual variability in biomass and 2) the occurrence of a spring peak in biomass between mid-April to late May which contributed on average 17% of phytoplankton biomass between March – May (Widdicombe et al., 2010).

On a global level, using 5057 observations from 1955-2009 Vogt *et al.*, (2013) showed that 64% of *Phaeocystis* spp. biomass, was recorded during spring (northern hemisphere) with more observations in the month of April compared to March and May, which was also observed in the present time-series analysis. Vogt *et al.*, (2013) also showed that the minimum and maximum *Phaeocystis* spp. biomass was between 2.9 x 10^{-5} mg C m^{-3} and 5.4 x 10^3 mg C m^{-3}, with a global

mean of 45.7 mg C m^{-3} for both northern and southern hemispheres (**Fig. 7**), which is similar to the mean at station L4 (41.6 mg C m^{-3}). Inclusion of the colony mucus matrix carbon caused a significant increase in the global mean to 183.8 mg C m^{-3}, highlighting the effect of colony mucus on the carbon budget.

4.5 Implications

Dense blooms of *Phaeocystis* spp. in some ecosystems can be responsible for fish and shell-fish mortality and alteration of fish taste (Levasseur et al, 1994; Peperzak & Poelman, 2008). *Phaeocystis* spp. colony mucous matrix can inhibit copepod grazing, and therefore affect food web structure through predator-prey size mis-match (Nejstgaard et al., 2007). Several studies have found consumption rates of *Phaeocystis* spp. by copepods to be significantly lower than consumption of co-occurring diatoms and heterotrophic protists during *Phaeocystis* spp. blooms, showing preferential feeding strategies towards more palatable and nutritious prey sources (e.g. Gasparini *et al.*, 2000; Rousseau *et al.*, 2000; Verity, 2000). Additionally, carbohydrates excreted by *Phaeocystis* spp. that coagulate to form transparent exopolymer particles (TEP) have strong inhibitory feeding effects on both nauplii and adult copepods (Dutz et al., 2005). *Phaeocystis* spp. can also be inadequate as a food source for some copepods (e.g. *Calanus helgolandicus*, *Temora stylifera* and *Acartia tonsa*), which can lead to negative effects on fecundity and egg production (Tang et al., 2001; Turner et al., 2002). Stabell *et al.*, (1999) extracted toxins from both *P. pouchetii* in culture and seawater samples collected during a *Phaeocystis* spp. bloom, which have anaesthetic properties and can be toxic to fish larvae. Exotoxins produced by *Phaeocystis* spp. during the spring bloom in the northern Norwegian coast can also induce stress in cod larvae (*Gadus morhua*) (Eilertsen and Raa, 1995). Additionally, mass fish mortalities have been linked to *Phaeocystis* spp. blooms in the Irish Sea (Rogers and Lockwood, 2009) and south-eastern Vietnamese coastal waters (Tang et al., 2004). The mass transport and sedimentation of a *P. globosa* bloom in 2001 in the Oosterschelde estuary (North Sea) caused anoxic conditions that led to the mass mortality of 10 million kg of *Mytilus edulis* with a market value of 15 to 20 million euro (Peperzak and Poelman, 2008).

Phaeocystis spp. are also known to produce and release the cytotoxic α, β, γ, δ-unsaturated aldehyde 2-trans-4-decadienal (DD), which can inhibit mitotic cell divisions. An increase in DD concentration can have a negative effect on the growth rates of the diatoms *Skeletonema costatum*, *Chaetoceros socialis* and *Thalassiosira antarctica* (Hansen and Eilertsen, 2007). In addition, the odorous foam produced by *Phaeocystis* spp. blooms can wash up on beaches and create anoxic conditions in the surface sediment which can lead to mortality of the intertidal benthic community (Desroy and Denis, 2004; Spilmont et al., 2009). These foam deposits also have a deleterious effect on coastal tourism (Lancelot and Mathot, 1987). The microcosm experiment suggests that future high CO_2 scenarios could increase *Phaeocystis* spp. blooms at station L4 in the WEC which could adversely affect ecosystem functioning, food web structure, fisheries and tourism.

4.6 Conclusion

Microcosm experiments showed that *Phaeocystis* spp. carbon biomass increased by 330% at elevated pCO_2 (~800 μatm) over a 15-day period. This study suggests that future high pCO_2 concentrations in the WEC may favour the dominance of *Phaeocystis* spp. biomass during the spring bloom, with associated negative impacts on ecosystem function and food web structure.

Chapter 5 – Effects of elevated pCO_2 and temperature on the autumn bloom

Abstract

The effects of elevated pCO_2 and temperature were investigated on the autumn phytoplankton bloom transition from diatoms and dinoflagellates to nanophytoplankton in the Western English Channel (WEC). A full factorial 36-day microcosm experiment was conducted under year 2100 predicted temperature (+4.5 °C) and pCO_2 levels (800 µatm). The starting phytoplankton community biomass was 110.2 (± 5.7) mg carbon C m^{-3} and was dominated by dinoflagellates (~50 %) with smaller contributions from nanophytoplankton (~13 %), cryptophytes (~11 %) and diatoms (~9 %). Over the experimental period total biomass was significantly increased by elevated pCO_2 (20-fold increase) and elevated temperature (15-fold increase). In contrast, the combined influence of these two factors had no effect on biomass relative to the ambient control. Chlorophyll *a* normalised maximum photosynthetic rates of carbon fixation (P^B_m) increased > 6-fold under elevated pCO_2 and > 3-fold under elevated temperature while no effect on P^B_m was observed when pCO_2 and temperature were elevated simultaneously. The phytoplankton community structure shifted from dinoflagellates to nanophytoplankton at the end of the experiment in all treatments. Under elevated pCO_2 nanophytoplankton contributed 90% of community biomass and was dominated by *Phaeocystis* spp. (mean cell diameter (MCD) 5.04 (± 0.03) µm), while under elevated temperature nanophytoplankton contributed 85% of the community biomass and was dominated by smaller nano-flagellates (MCD 3.61 (± 0.06) µm). Under ambient conditions larger nano-flagellates dominated (MCD 6.34 (± 0.30) µm) while the smallest nanophytoplankton contribution was observed under combined elevated pCO_2 and temperature (~40 %, MCD 4.28 (± 0.13) µm). Dinoflagellate biomass declined significantly under the individual influences of elevated pCO_2, temperature and ambient conditions while under the combined effects dinoflagellate biomass almost doubled from starting values. This was influenced by a 30-fold increase in the harmful algal bloom (HAB) species, *Prorocentrum cordatum*. The results suggest that increases in

temperature and pCO_2 do not appear to influence coastal phytoplankton productivity during autumn in the WEC, suggesting no change in feedbacks on atmospheric CO_2. However, the increase in HAB species observed may have further implications. The breakdown of high biomass from HABS may lead to episodes of oxygen depletion and anoxia. High biomass of HAB species in the upper water column can also create substantial shading, leading to light-limiting conditions for the phytoplankton communities below, reducing productivity. Toxicity can have detrimental effects on growth rates of other phytoplankton species and grazing rates of zooplankton which may also alter the flow of carbon.

5.1 Introduction

In autumn, sea surface temperature and pCO_2 start to decline following their respective time series maximal values in the Western English Channel (WEC) at station L4. During October, mean seawater temperatures at 10m decrease from 15.39 °C (± 0.49) (n = 18) to 14.37 °C (± 0.62) (n = 14) (1993-2015). The influence of warming on the density of seawater will cause much of the surface ocean to become more stratified, driving shifts in biological variables such as nutrient supplies and irradiance levels (Boyd et al., 2008; Cermeno et al., 2008; Sommer et al., 2012). Long-term data sets already suggest that ongoing changes in coastal phytoplankton communities are likely due to climate shifts and other anthropogenic influences (Edwards et al., 2006; Smetacek and Cloern, 2008; Widdicombe et al., 2010). Following a period of CO_2 oversaturation in late summer, pCO_2 returns to near-equilibrium at station L4 in October (Kitidis et al., 2012) when mean values decrease during this month from 455.32 µatm pCO_2 (± 63.92) (n = 5) to 404.06 µatm pCO_2 (± 38.55) (n = 6) (2008-2015). As is the case with seawater warming, predicted future ocean acidification is likely to impact coastal phytoplankton communities in autumn when the present upper limit of the pCO_2 threshold increases during this period of surface ocean-atmosphere equilibrium. The shift in dissolved inorganic carbon (DIC) equilibria associated with increased pCO_2 has wide ranging implications for

phytoplankton photosynthetic carbon fixation rates, growth and community composition (Riebesell, 2004).

From a biological perspective, the autumn period at station L4 is characterised by the decline of the late summer diatom and dinoflagellate blooms (Widdicombe et al., 2010) when biomass of these two groups approaches values close to the time series minima (diatom biomass range: 6.01 (± 6.88) – 2.85 (± 3.28) mg C m^{-3}; dinoflagellate biomass range: 1.75 (± 3.28) – 0.66 (± 1.08) mg C m^{-3}). Typically, over this period nanophytoplankton become numerically dominant when biomass of this group ranges from 20.94 (± 33.25) – 9.38 (± 3.31), though the time series shows high variability in this biomass.

Laboratory studies of phytoplankton species in culture and studies on natural populations in the field have shown most species to exhibit sensitivity in terms of growth and photosynthetic rates to elevated pCO_2 and temperature individually. In laboratory studies with the diatom *Thalassiosira weissflogii,* pCO_2 elevated to 1000 µatm and +5 °C temperature increase synergistically enhances growth, while the same conditions result in a reduction in growth for the diatom *Dactyliosolen fragilissimus* (Taucher et al., 2015). Although there have been fewer studies on dinoflagellates, similar variability in responses has been observed, e.g. (Errera et al., 2014; Fu et al., 2008). In natural populations, elevated pCO_2 stimulates growth in pico- and nanophytoplankton communities (Engel et al., 2008) while increased temperature has reduced biomass of these groups (Moustaka-Gouni et al., 2016). In a recent field study on natural phytoplankton communities, elevated temperature (+3°C above ambient) enhanced community biomass in natural populations but the combined influence of elevated temperature and pCO_2 caused a reduction (Gao et al., 2017).

The goals of the present study were to investigate: 1) the combined effects of elevated pCO_2 and temperature on phytoplankton community structure, biomass and photosynthetic carbon fixation rates during the autumn transition from diatoms and dinoflagellates to nanophytoplankton at station L4; 2) assess the natural variability in phytoplankton community

structure and the carbon biomass of the dominant species observed in the experimental community relative to long-term observations at station L4 over two decades (1993-2014); and 3) assess the distribution of biomass of the dominant species observed at the end of the experiment relative to the in-situ temporal gradients of temperature and pCO_2 observed at station L4. The effects of elevated pCO_2 and temperature on phytoplankton succession at L4 in autumn is presently unknown.

5.2 Sampling and experimental set-up

Experimental seawater and medium were collected and processed as per the method described in chapter 2, section 2.2 on 7th October 2015 from 10m depth. Upon return to the laboratory the experimental seawater was gently and thoroughly mixed and transferred in equal parts from each carboy (to ensure homogeneity) to sixteen 2.5 L borosilicate incubation bottles (4 sets of 4 replicates). The remaining experimental seawater was sampled for initial (T0) concentrations of nutrients, chlorophyll *a*, total alkalinity, dissolved inorganic carbon, particulate organic carbon (POC) and nitrogen (PON) and was also used to characterise the starting experimental phytoplankton community. The incubation bottles were placed in an outdoor simulated in-situ incubation culture system (see chapter 3 for detailed experimental set-up) and each set of replicates were linked to one of four 22 L media reservoirs filled with the filtered seawater media. The media was enriched with CO_2 gas as per the method described in chapter 3 and used for the microcosm dilutions as per the following experimental design: (1) control (390 µatm pCO_2, 14.5 °C matching station L4 in-situ values), (2) high temperature (390 µatm pCO_2, 18.5 °C), (3) high pCO_2 (800 µatm pCO_2, 14.5 °C) and (4) combination (800 µatm pCO_2, 18.5 °C).

Initial nutrient concentrations (measured at 0.24 µM nitrate + nitrite, 0.086 µM phosphate and 1.39 µM silicate on 7th October 2015) were amended to 8 µM nitrate+nitrite and 0.5 µM.

5.2.1 Experimental sampling

pH was monitored daily to adjust the pCO_2 of the experimental media (+/-) prior to dilutions to maintain target pCO_2 levels in the incubation bottles. Samples for Chl *a*, total alkalinity (TA) and dissolved inorganic carbon (DIC) were taken every 2-3 days. Samples for particulate organic carbon (POC) and particulate organic nitrogen (PON) were taken at T0, T15 and T36. Samples for the micro-phytoplankton community for microscopical analysis and the pico- and nanophytoplankton community for flow cytometric analysis were taken at days T0, T10, T17, T24 and T36. Samples for FRRf fluorescence-based light curves were taken at T30.

5.2.2 Statistical analysis

To test for effects of high pCO_2, high temperature and high pCO_2 x high temperature on the measured response variables (Chl *a*, total community biomass, C:chl *a* POC, PON, photosynthetic parameters and biomass of individual species), generalised linear mixed models (repeated measures) with the factors pCO_2, temperature and time (and all interactions) were applied to the data between T0 and T30. Where main effects were established, pairwise comparisons were performed using the method of Herberich *et al.*, (2010) for data with non-normality and/or heteroscedasticity. Between treatment differences over the time course of the experiment were visualized using non-metric multidimensional scaling ordination (nMDS). The Bray-Curtis index was used to calculate the resemblance of biomass in each experimental treatment based on the community structure. The resulting resemblance matrix was then used to perform an ordination nMDS. Individual group and species vectors were then superimposed on the nMDS ordination and their resulting contribution to biomass was represented by the proximity to experimental treatments. PE curve parameters modelled from the FRRf data were analysed by a generalised linear model as this data was just from one time point. Weekly biomass values from the L4 time-series were averaged over years to elucidate the variability and seasonal cycles of the dominant species observed in the experimental community at T36, relative to the time-series observations. The distribution of these species' biomass at station L4 was also analysed relative to the in-situ temporal gradients of temperature (1993-2014) and pCO_2 (2008-2014)

using frequency histograms. All time series sample sizes are given in the figure legends of the plotted data. Analyses were conducted using the R statistical package (R Core Team (2014). All statistical data are reported as the arithmetic means with standard deviation describing the error term, unless otherwise stated (R: A language and environment for statistical computing. R Foundation for Statistical Computing, Vienna, Austria).

5.3 Results

Chl *a* concentration in the WEC ranged between 0.02-~5 mg m^{-3} from 30 September - 6th October 2015 based on MODIS composite weekly satellite data, with a concentration of ~1.6 mg m^{-3} at station L4 (**Fig. 5.1 A**). Over the period leading up to phytoplankton community sampling, increasing nitrate and silicate concentrations coincided with a chl *a* peak on 23rd September (**Fig. 5.1 B**). Routine net trawl (20 µm) sample observations indicated a phytoplankton community dominated by the diatoms *Leptocylindrus danicus* and *L. minimus* with a lower presence of the dinoflagellates *Prorocentrum cordatum*, *Heterocapsa* spp. and *Oxytoxum gracile*. Following decreasing nitrate concentrations, this community transitioned to a *P. cordatum* bloom on 29th September, the week before experimental community sampling (data not shown).

5.3.1 Carbonate system

Equilibration to the target high pCO_2 values (800 µatm) within the high pCO_2 and combination treatments was achieved at T10 (**Fig. 5,2 A**). These treatments were slowly acclimated to increasing levels of pCO_2 over 7 days (from the initial dilution at T3) while the control and high temperature treatments were acclimated at the same ambient carbonate system values as that from station L4 on the day of sampling. Following equilibration, the mean pCO_2 values within the control and high temperature treatments were 394.9 (± 4.3) and 393.2 (± 4.8) µatm respectively, while in the high pCO_2 and combination treatments mean pCO_2 values were 822.6 (± 9.4) and 836.5 (± 15.6) µatm respectively. Carbonate system values remained stable throughout the experiment. **Fig. 5.2 B, C, D, E** and **F** show other carbonate system parameters.

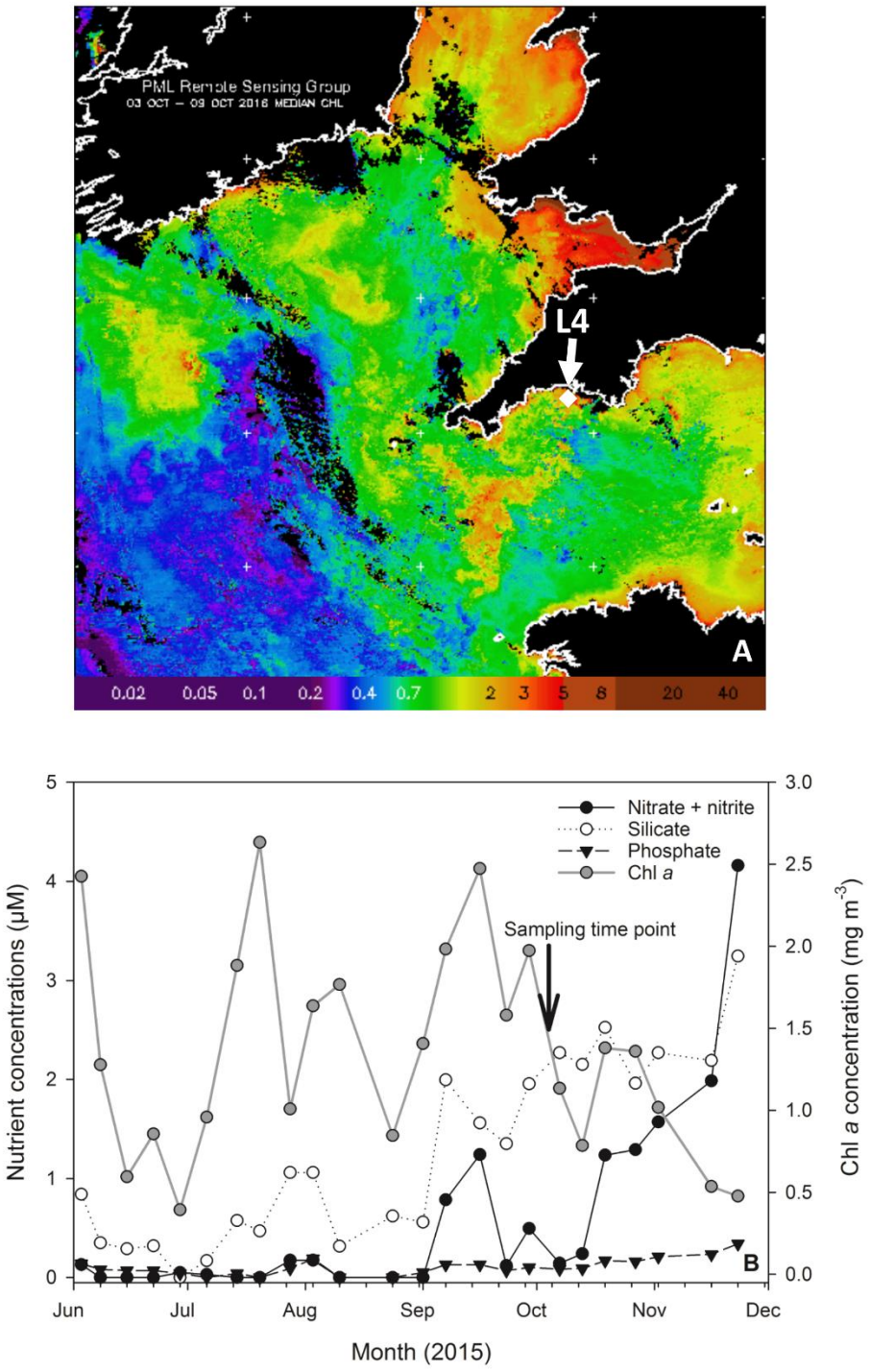

Fig. 5.1. (**A**). MODIS weekly composite chl *a* image of the western English Channel covering the period 30th September – 6th October 2015 (surface chl *a* data averaged over 7 days, coincident with the week of phytoplankton community sampling for the present study), processing courtesy of NEODAAS. The position of coastal station L4 is marked with a white diamond. (**B**). Time series of weekly nutrient and chl *a* concentration from station L4 at a depth of 10 m over the second half of 2015 in the months prior to phytoplankton community sampling (indicated by black arrow and text).

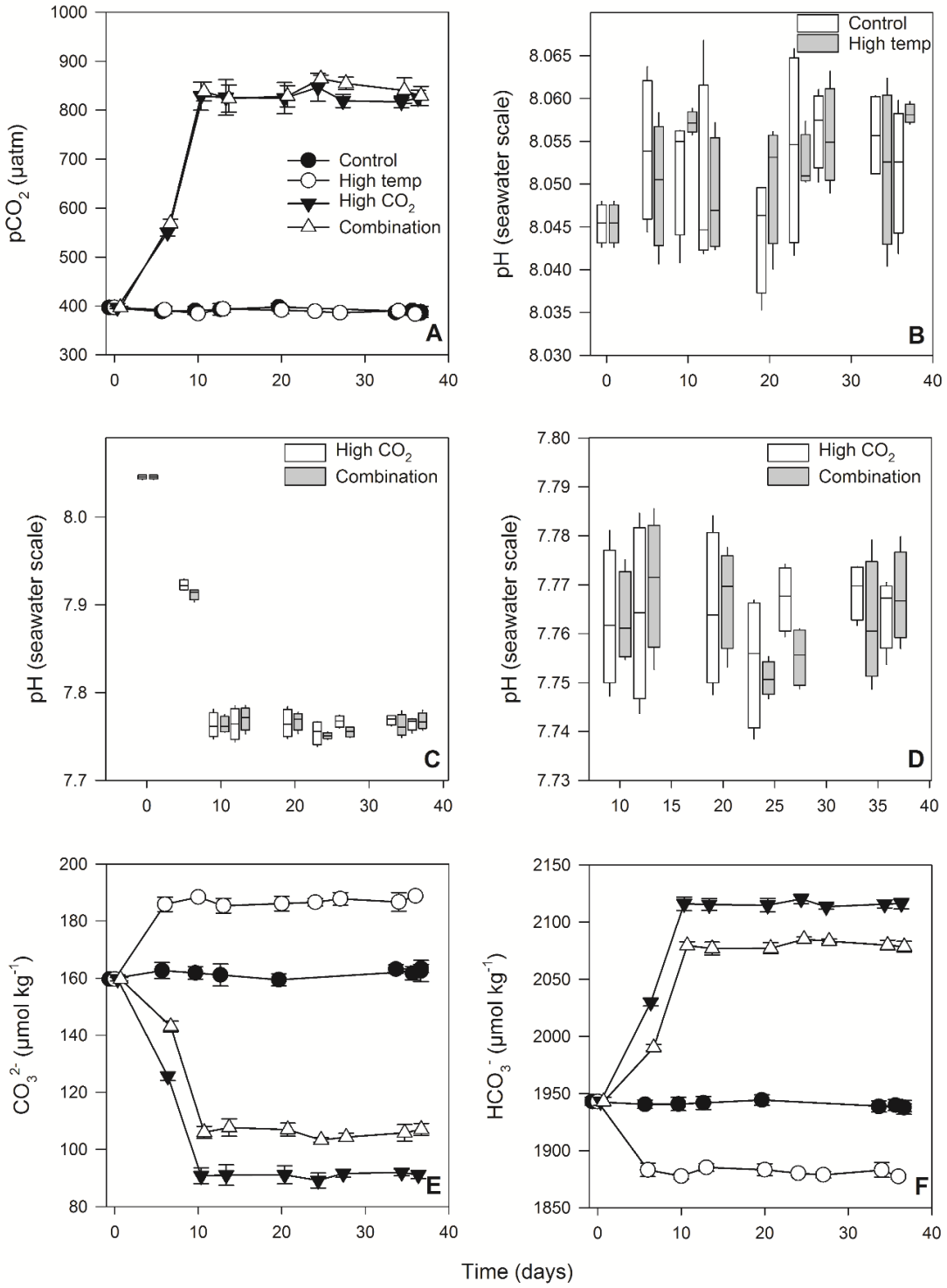

Fig.5. 2. Carbonate system values of the experimental phytoplankton incubations. (**A**)**.** partial pressure of CO_2 in seawater (pCO_2), (**B, C & D**)**.** pH on the seawater scale, (**E**)**.** carbonate concentration (CO_3^{2-}) and (**F**)**.** bicarbonate concentration (HCO_3^-) were estimated from direct measurements of total alkalinity and dissolved inorganic carbon. Note: pH for high CO_2 and combination treatments shown twice (in **C & D)** for finer scale at target concentration,

5.3.2 Experimental temperature treatments

Mean temperatures in the control and high pCO_2 treatments were 14.1 (± 0.35) °C (**Fig. 5.3 A**) and in the high temperature and combination treatments the mean temperatures were 18.6 (± 0.42) °C. This resulted in a mean temperature difference between the ambient and high temperature treatments of 4.46 (± 0.42) °C.

5.3.3 Chlorophyll *a*

Mean chl *a* in the experimental seawater at T0 was 1.64 (± 0.02) mg m^{-3} (**Fig. 5.4 A**) and was significantly influenced over time, independent of any treatment (**Table 5.1**).Chl *a* decreased in all treatments between T0 to T7 to ~0.1 (± 0.09, 0.035 and 0.035) mg m^{-3} in the control, high pCO_2 and combination treatments, respectively while in the high temperature treatment at T7 chl *a* was 0.46 mg m^{-3} (± 0.29). From T7 to T12 there was an increase in chl *a* in all treatments which was significantly higher in the combination (4.99 mg m^{-3} (± 0.69)) and high pCO_2 treatment (3.83 mg m^{-3} (± 0.43)) (pairwise comparisons: $t = 5.728$, $p < 0.001$, $t = 7.210$, $p < 0.001$ and $t = 3.794$, $p < 0.05$, $t = 5.403$, $p < 0.001$) when compared to the control and high temperature treatments, respectively, (n = 16). At T36 chl *a* concentration in the combination treatment was significantly higher than all other treatments at 6.87 (± 0.58) mg m^{-3} (pairwise comparisons: $t = 14.891$, $p < 0.001$, $t = 8.396$, = $p < 0.001$, $t = 12.188$, $p < 0.001$), compared to the control, high temperature and high CO_2 treatments, respectively (n = 16), while the high temperature treatment concentration was significantly higher than the control and high pCO_2 treatments at 4.77 (± 0.44) mg m^{-3} (pairwise comparisons: $t = 9.084$, $p < 0.001$, $t = 6.037$, $p < 0.001$, respectively (n = 16)). Mean concentrations for the control and high pCO_2 treatments at T36 were not significantly different at 3.30 (± 0.22) and 3.46 (± 0.35) mg m^{-3} respectively.

5.3.4 Phytoplankton biomass

The starting biomass in all treatments was 110.2 (± 5.7) mg C m^{-3} (**Fig. 5.4 B**) and the community biomass was dominated by dinoflagellates (~50%) with smaller contributions from

nanophytoplankton (~13%), cryptophytes (~11%), diatoms (~9%), coccolithophores (~8%), S*ynechococcus* (~6%) and picophytoplankton (~3%). Total biomass initially increased in all treatments and the control over time and was most significantly influenced by high CO_2 followed by high temperature (**Table 5.1**). At T10, biomass was significantly higher in the high temperature treatment when it reached 752 (± 106) mg C m^{-3} (pairwise comparisons: $t = 9.655$, $p < 0.001$, $t = 8.209$, $p < 0.001$, $t = 4.391$, $p < 0.01$) compared to the control, high CO_2 and combination treatments, respectively (n = 16). Biomass in the combination treatment declined from T17 followed by the control at T24 and overall showed no significant difference in the data relative to the control (Table 1). At T36 however, total biomass was significantly higher in the high pCO_2 treatment and reached 2481 (± 182.68) mg C m^{-3}, which increased more than 20-fold from T0 (pairwise comparisons: $t = 19.603$, $p = < 0.001$, $t = 5.191$, $p < 0.001$, $t = 18.329$, $p < 0.001$) compared to the control, high temperature and combination treatments, respectively (n = 16). Total biomass in the high temperature treatment increased more than 15-fold to 1735 (± 169.24) mg C m^{-3} at T36 and was significantly higher than the combination treatment and ambient control, which were 525 (± 28.02) mg C m^{-3} and 378 (± 33.95) mg C m^{-3}, respectively (pairwise comparisons: $t = 12.211$, $p < 0.001$, $t = 13.612$, $p < 0.001$, respectively, (n = 16)).

Measured POC followed the same trends as estimated biomass in all treatments between T0 and T36 (**Fig. 5.4 C, Table 5.1**) and despite some variability between the two measures, POC was within the range of estimates (R_2 0.914, **Fig. 5.4 D**). At T36, POC was significantly higher in the high pCO_2 treatment (2086 ± 155.19 mg m^{-3}) (pairwise comparisons: $t = 1697.42$, $p < 0.001$, $t = 3.795$, $p < 0.05$, $t = 15.590$, $p < 0.001$) compared to the control, high temperature and combination treatments, respectively (n = 16). This was followed by the high temperature treatment exhibiting the second highest POC value (1594 ± 162.24 mg m^{-3}) which was significantly higher than the control and combination treatment (pairwise comparison: $t = 11.534$, $p < 0.001$, $t = 10.200$, $p < 0.001$, respectively (n = 16)). PON followed the same trends as POC over the course of the experiment (**Fig. 5.4 E, Table 5.1**) when at T36 concentrations were 147 (± 12.99) and 133 (± 15.59) mg m^{-3} in the high pCO_2 and high temperature treatments

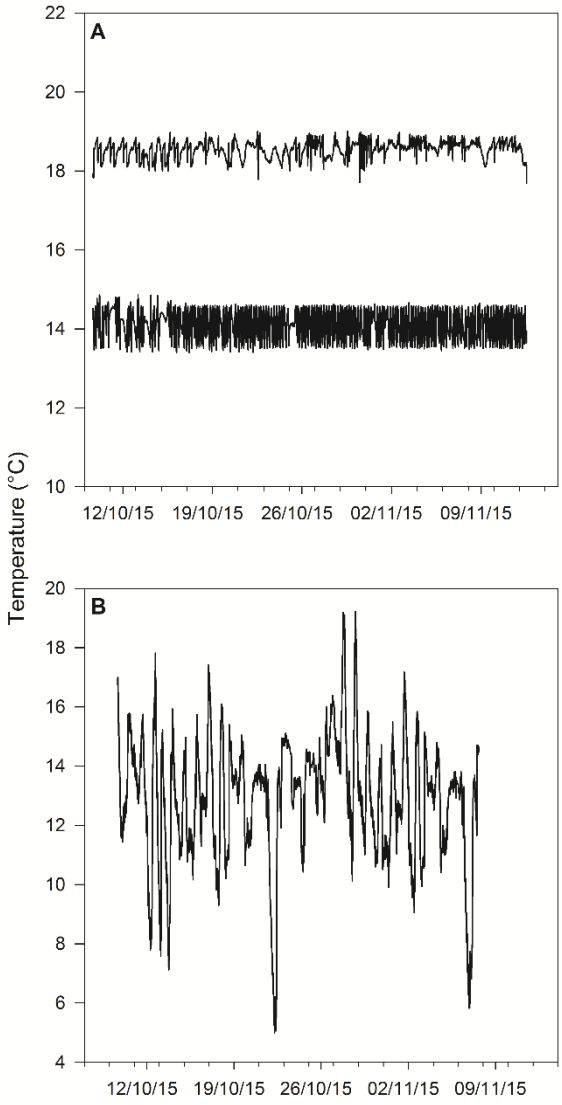

Fig. 5.3. Time course of temperature treatments throughout the experiment. Control and high CO_2 treatments maintained at a mean temperature of 14.1 °C (± 0.35 sd) and the high temperature and combination treatments maintained at a mean temperature of 18.6 °C (± 0.42 sd) (**A**). External ambient air temperature logged over the experimental period (**B**).

respectively, while PON was 57.75 (± 13.07) mg m^{-3} in the combination treatment and 47.18 (± 9.32) mg m^{-3} in the control. POC:PON ratios increased significantly over time, most notably in the high pCO_2 treatment (**Table 5.1**) in which it increased by 33%, from 10.72 to 14.26 mol C: mol N (± 1.73). The high temperature treatment ratio also increased significantly during the experiment by 17% to 12.09 (± 2.14) mol C:mol N (**Fig. 5.4 F, Table 5.1**). In contrast, the POC:PON ratios in the control and combination treatment were significantly lower than the high

temperature and high CO_2 treatments (pairwise comparisons: t = -10.668, p < 0.001, t = 16.207, p < 0.001, t = -9.320, p < 0.001, t = -14.859, p < 0.001, respectively, (n = 16)). POC:PON in the control declined by 20% from T0 to T36, from 10.33 to 8.26 (± 0.50) mol C:mol N, though it was not significantly lower than the combination treatment at T36.

5.3.5 Carbon:Chlorophyll *a*

The initial mean C:chl a was 67.2 (± 4.15) mg C:mg chl *a* across treatments and the control. Over the experimental period high pCO_2 had the greatest effect on C:chl *a* with a final value at T36 significantly higher than any other treatment (720.3 (± 74.7) mg C:mg Chl *a*, **Fig 5.5**, **Table 5.1**). The high temperature treatment also had a significant stimulating effect relative to the combination treatment and ambient control with a final value at T36 of 364.4 (± 39.4) mg C:mg chl *a* (**Table 5.1**). An initial high level of variability in C:chl *a* was observed in all treatments early in the experiment when at T10 values in the control and combination treatment were higher than in the high CO_2 and high temperature treatments. Pairwise comparisons showed the combination treatment to be significantly higher than the high CO_2 treatment at this time point (t = 3.598, p < 0.05, (n = 16)). Following this, C:chl *a* declined in the combination treatment and was significantly lower than the high temperature treatment at T17 (pairwise comparison: t = -3.061, p < 0.05, (n = 16)). This trend continued throughout the experiment when at T24 and T36 the combination treatment values were significantly lower than the control, high temperature and high CO_2 treatments (pairwise comparisons: T24; t = -5.070, p < 0.01, t = -2.744, p = 0.06 and t = -3.153, p < 0.05 respectively, (n = 16) and T36; t = -5.832, p < 0.001, t = -12.594, p < 0.001 and t = -14.913, p < 0.001 respectively, (n = 16)).

5.3.6 Community composition

At T36 diatoms dominated the phytoplankton community biomass in the ambient control with a substantial contribution from nanophytoplankton (**Fig. 5.6 A**), while the high temperature and high pCO_2 treatments exhibited near mono-specific dominance of nanophytoplankton (**Figs. 5.6**

B & C). The most diverse community was in the combination treatment where dinoflagellates and *Synechococcus* became more prominent (**Fig. 5.6 D**).

The nMDS analysis showed tight clustering of most treatments between T10 and T24 indicating little dissimilarity, other than the control at T10 and the combination treatment at T24. Between T24 and T36 the community diverged in experimental treatments (**Fig. 5.6 E**). The ordination performed well with a stress value of 0.1, adequately representing the biomass in two dimensions. Between T10 and T24 the community shifted to nanophytoplankton in all experimental treatments. This dominance was maintained through to T36 in the high temperature and high pCO_2 treatments whereas in the ambient control and combination treatment, a community shift was observed (**Fig. 5.7 A**). Nanophytoplankton was most significantly influenced by the high CO_2 and high temperature treatments (**Table 5.2**) and at T36 this biomass was significantly higher in the high pCO_2 treatment followed by the high temperature treatment (pairwise comparison: $t = 4.938$, $p < 0.01$ (n = 16), **Table 5.2**) when biomass attained 2216 (± 189.67) mg C m^{-3} and 1489 (± 170.32) mg C m^{-3}, respectively. In the combination treatment nanophytoplankton biomass was 238 (± 14.16) mg C m^{-3} at T36 which was significantly higher compared to the ambient control (162 (± 20.02)) mg C m^{-3} (pairwise comparison: $t = 5.336$, $p < 0.001$ (n = 16)). However, when considering all data, the combination treatment did not significantly influence nanophytoplankton biomass (**Table 5.2**).

In addition to significant differences in nanophytoplankton biomass amongst the experimental treatments, treatment-specific differences in cell size were observed. Larger nano-flagellates dominated the control (mean cell diameter of 6.34 (± 0.30) µm, **Fig. 5.7 B**), smaller nano-flagellates dominated the high temperature and combination treatments (mean cell diameters of 3.61 (± 0.06) µm and 4.28 (± 0.13) µm, **Fig. 5.7 C & E**) whereas *Phaeocystis* spp. dominated the high pCO_2 treatment (mean cell diameter 5.04 (± 0.03) µm, **Fig. 5.7 D**) and was not observed in any other treatment. The smaller nano-flagellates dominant the high temperature and combination treatments were both significantly smaller than in the control ($t = -13.61$, $p <$

Table 5.1. Results of generalised linear mixed model testing for effects of time, high temperature, high CO_2 and all interactions on chl *a*, phytoplankton biomass and particulate organic nitrogen. Significant results are in bold; * p < 0.05, ** p < 0.001, *** p < 0.0001.

Response variable	n	*df*	*z*-value	*p*	sig
Chla (mg m^{-3})					
High temp	684	674	0.353	0.724	
High pCO_2	684	674	1.618	0.106	
Combination	684	674	1.757	0.079	
Time	684	674	4.303	**<0.001**	***
Time x high temp	684	674	-0.097	0.923	
Time x high CO_2	684	674	-0.541	0.589	
Time x combination	684	674	0.373	0.709	
Estimated biomass (mg C m^{-3})					
High temp	80	70	0.118	0.9057	
High pCO_2	80	70	-2.295	**<0.05**	*
Combination	80	70	1.356	0.175	
Time	80	70	2.786	**<0.01**	**
Time x high temp	80	70	1.986	**<0.05**	*
Time x high CO_2	80	70	4.738	**<0.001**	***
Time x combination	80	70	-1.109	0.268	
mg C: mg Chla					
High temp	80	70	-1.778	0.075	
High pCO_2	80	70	-3.412	**<0.001**	***
Combination	80	70	0.912	0.362	
Time	80	70	0.406	0.684	
Time x high temp	80	70	2.402	**<0.05**	*
Time x high CO_2	80	70	4.646	**<0.001**	***
Time x combination	80	70	-1.642	0.101	
POC (mg m^{-3})					
High temp	48	38	-1.201	0.230	
High pCO_2	48	38	-1.085	0.278	
Combination	48	38	-0.365	0.715	
Time	48	38	-0.227	0.821	
Time x high temp	48	38	4.14	**<0.001**	***
Time x high CO_2	48	38	4.971	**<0.001**	***
Time x combination	48	38	1.04	0.299	
PON (mg m^{-3})					
High temp	48	38	-0.716	0.474	
High pCO_2	48	38	-0.716	0.474	
Combination	48	38	0.87	0.384	
Time	48	38	0.261	0.794	
Time x high temp	48	38	1.927	**<0.05**	*
Time x high CO_2	48	38	2.066	**<0.05**	*
Time x combination	48	38	-0.138	0.891	
mg POC: mg PON					
High temp	48	38	1.918	0.055	
High pCO_2	48	38	1.664	0.096	
Combination	48	38	1.115	0.265	
Time	48	38	0.443	0.658	
Time x high temp	48	38	8.484	**<0.001**	***
Time x high CO_2	48	38	10.142	**<0.001**	***
Time x combination	48	38	-2.835	**<0.05**	*

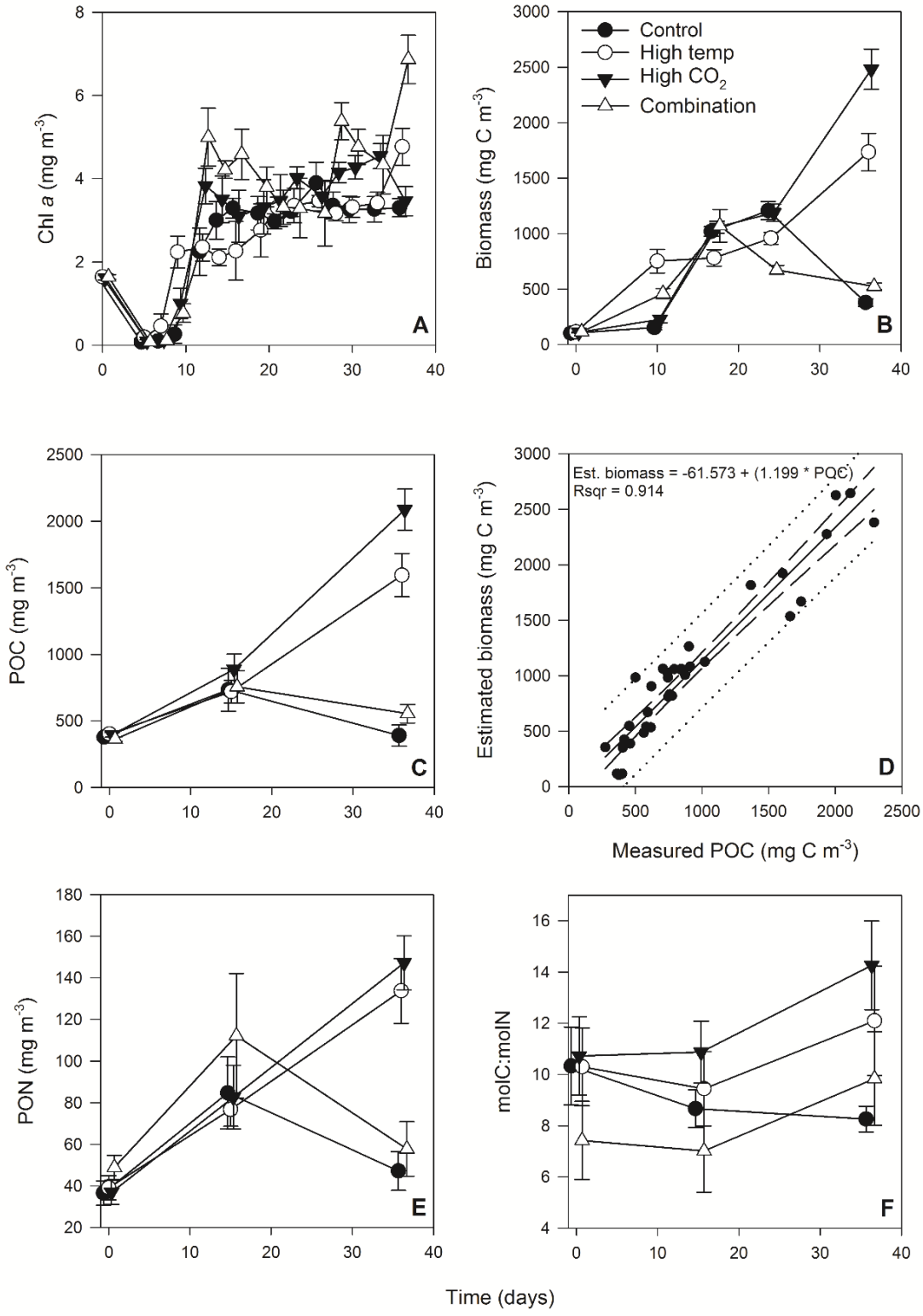

Fig. 5.4. Time course of chl *a* (**A**), phytoplankton biomass (**B**), POC (**C**), regression of calculated phytoplankton carbon vs measured POC (**D**), PON (**E**) and POC:PON (**F**).

0.001, t = -9.312, p < 0.001 respectively), similarly *Phaeocystis* spp. dominant in the high pCO_2 treatment was also significantly smaller than the control nanophytoplankton (t = -6.643, p < 0.001) but significantly larger than the nano-flagellates in the high temperature and combination treatments (t = 19.090, p < 0.001, t = 6.389, p < 0.001) (50 nanophytoplankton cells were randomly measured from each replicate at T36, n = 800). No small dinoflagellates or diatoms were detected within the nanophytoplankton, either quantitatively through flow cytometry of qualitatively through microscopy.

Low starting biomass of diatoms at T0 was dominated by *Coscinodiscus wailessi* (48%; 4.99 mg C m^{-3}), *Pleurosigma* (25%; 2.56 mg C m^{-3}) and *Thalassiosira subtilis* (19%; 1.94 mg C m^{-3}). Small biomass contributions were made by *Navicula distans*, undetermined pennate diatoms and *Cylindrotheca closterium*. Biomass in the diatom group was not significantly influenced by any of the experimental treatments when considering all data, but rather through time (**Table 5.2**) and remained low from T0 to T24. This biomass increased between T24 and T36 in all treatments and was significantly higher in the high pCO_2 treatment compared to the high temperature and combination treatments (235 (± 21.41) mg C m^{-3}, (pairwise comparisons: t = 6.091, p < 0.001, t = 6.700, p < 0.001, respectively (n = 16)), (**Fig. 5.8 A**). At T36 there was no significant difference in diatom biomass between the high CO_2 treatment and the control (pairwise comparison: t = 2.341, p = 0.140 (n = 16)). The highest diatom contribution to total community biomass at T36 was in the ambient control (52 % of biomass; 198 (± 17.28) mg C m^{-3}). In both the high temperature and combination treatments diatom biomass was significantly lower at T36 (151 (± 10.94) and 124 (± 19.16) mg C m^{-3}, respectively). In all treatments at T36, diatom biomass shifted away from dominance of the larger *C. Wailessii* to the comparatively smaller *C. closterium*, *N. distans*, *T. subtilis* and *Tropidoneis* spp., the relative contributions of which were treatment-specific. Overall *N. distans* dominated diatom biomass in all treatments at T36 (ambient control: 112 (± 24.86) mg C m^{-3}; 56 % of biomass, high temperature: 106 (± 17.75) mg C m^{-3}, 70 % of biomass, high pCO_2: 152 (± 19.09) mg C m^{-3}, 61 % of biomass and combination: 111 (± 20.97) mg C m^{-3}, 89 % of biomass (**Fig, 5.9**).

The starting dinoflagellate community was dominated by *Gyrodinium spirale* (91%; 49 mg C m^{-3}), with smaller contributions from *Katodinium glaucum* (5%; 2.76mg C m^{-3}), *Prorocentrum cordatum* (3%; 1.78 mg C m^{-3}) and undetermined *Gymnodiniales* (1%; 0.49 mg C m-3). Dinoflagellate biomass was most significantly influenced by the combination and high temperature treatments (**Table 5.2**) and at T36 this biomass was significantly higher in the combination treatment (90 (± 16.98) mg C m^{-3}) followed by the high temperature treatment (57 (± 6.87) mg C m^{-3}) (pairwise comparison: $t = 3.086$, $p < 0.05$, (n = 16)) (**Fig. 5.8 B**). There was no significant difference in dinoflagellate biomass between the high pCO_2 treatment and ambient control at T36 when biomass was low (pairwise comparison: $t = 1.805$, $p = 0.293$, (n = 16)). In the combination treatment, dinoflagellate biomass shifted away from the larger *G. spirale* and was dominated by *P. cordatum* which contributed 59 (± 12.95) mg C m^{-3} (66 % of biomass in this group).

Synechococcus biomass was significantly influenced by the combination and high temperature treatments with no significant influence from the high CO_2 treatment (**Fig. 5.8 C**, **Table 5.2**). This biomass was higher at T36 in the combination treatment (59.9 (± 4.30) mg C m^{-3} compared to the high temperature treatment (30 (± 5.98) mg C m^{-3}) (pairwise comparison: t = 6.813, p < 0.001, (n = 16)).

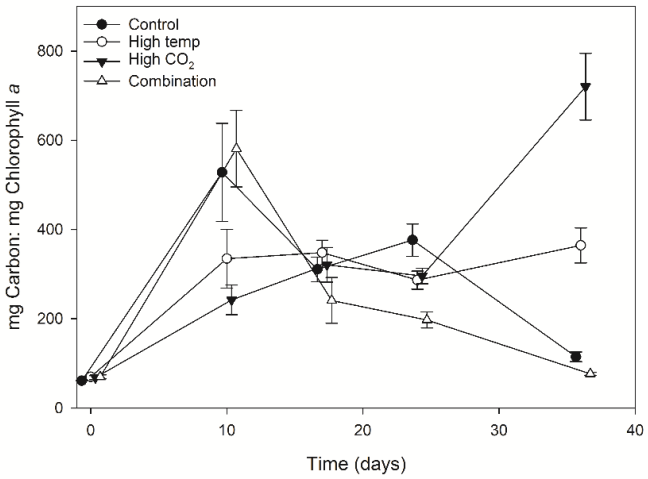

Fig 5.5. C:chl throughout the experiment.

In both the high pCO_2 treatment and ambient control, at T36 *Synechococcus* biomass was significantly lower (~7 mg C m^{-3} in both treatments) relative to the combination and high temperature treatments (pairwise comparisons: t = -21.062, p < 0.001, t = -6.874, p < 0.001, t = 19.825, p < 0.001, t = -6.618, p < 0.001, respectively, (n = 16)). Relative to the other phytoplankton groups, biomass of picophytoplankton (**Fig. 5.8 D**), cryptophytes (**Fig. 5.8 E**) and coccolithophores (**Fig. 5.8 F**) remained low in all treatments throughout the experiment. Picophytoplankton responded positively to the high pCO_2 and combination treatments at T36 (high pCO_2: 6.93 (± 0.63) mg C m^{-3}, combination: 11.26 (± 0.79) mg C m^{-3}), however, only the combination treatment was found to have a significant influence on picophytoplankton biomass (**Table 5.2**).

Microzooplankton was dominated by *Strombilidium* spp. in all treatments throughout the experiment, though biomass was low relative to the phytoplankton community (**Fig. 5.10**). Following a decline from T0 to T10, microzooplankton biomass increased in all but the high CO_2 treatment until T17 when biomass diverged. The biomass trajectory maintained an increase in the control and high temperature treatment when at T36 it was highest in the control at ~1.6 mg C m^{-3}, 90% higher than the high temperature treatment (0.83 mg C m^{-3}). Microzooplankton biomass was significantly lower in the high CO_2 treatment at T36 (z = -2.100, p = 0.036) and undetected in the combination treatment at this time point (**Table 5.2**).

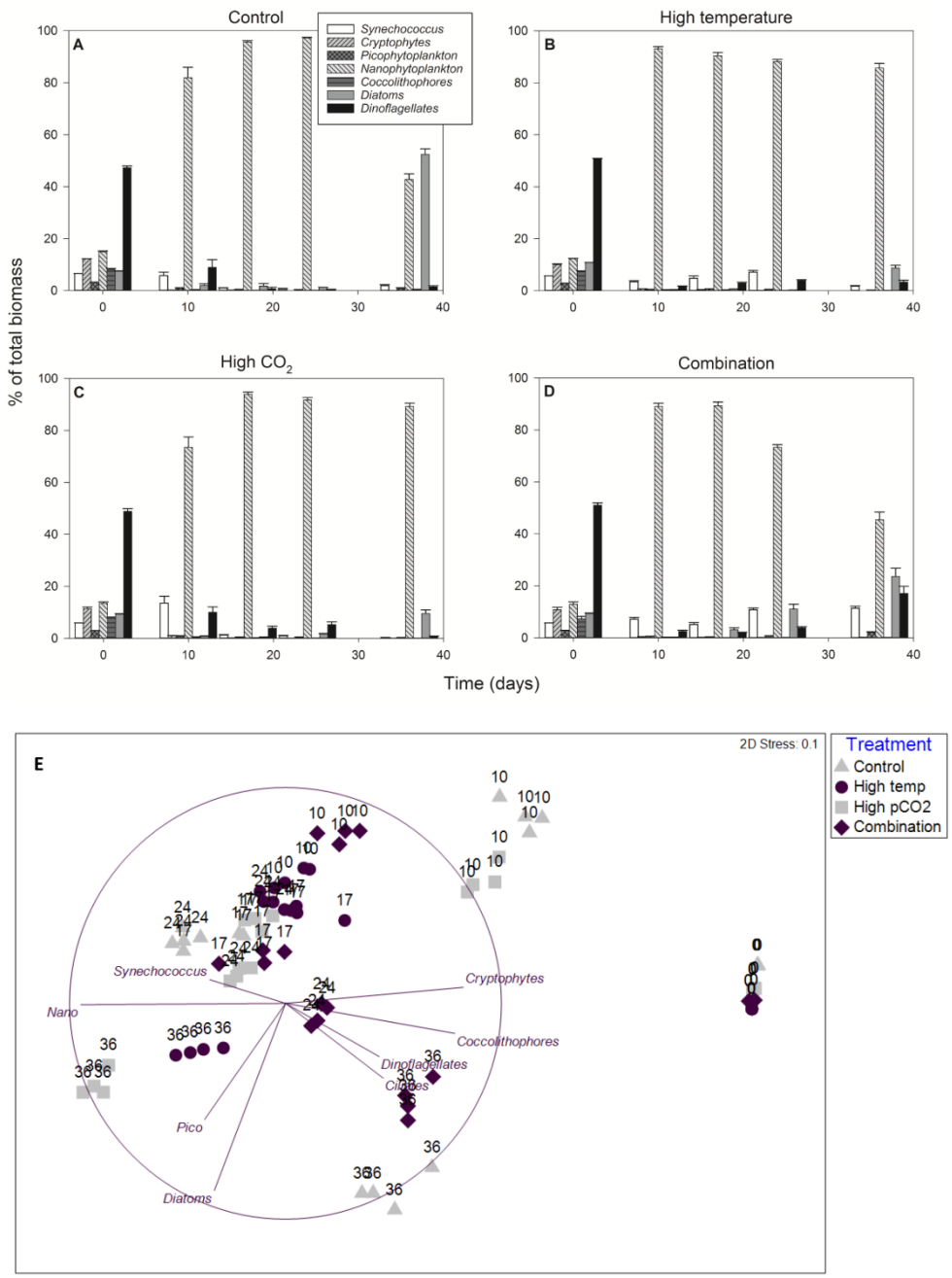

Fig. 5.6. Percentage contribution to community biomass by phytoplankton groups/species throughout the experiment in the control (**A**), high temperature (**B**), high CO_2 (**C**) and combination treatments. (**D**). nMDS plot structure showing the ordination of differences in phytoplankton biomass over time by experimental treatment in 2 dimensions.

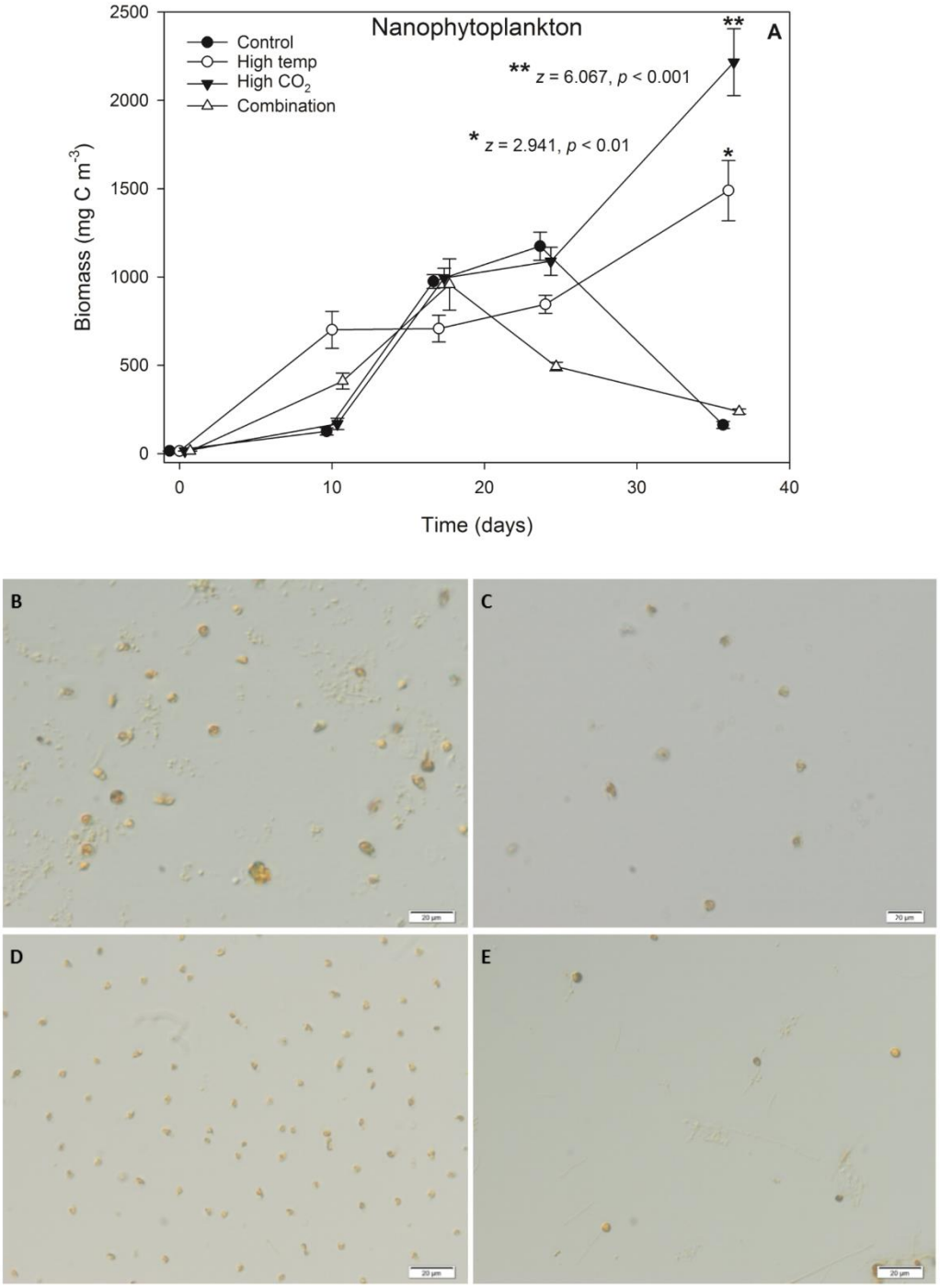

Fig. 5.7. Nanophytoplankton biomass progression throughout the experiment (**A**). Nanophytoplankton was the dominant group throughout the experiment between T10-T24 and remained dominant in the high temperature and high CO_2 treatments at T36. Large nano-flagellates observed in the control (**B**), smaller nano-flagellates observed in the high temperature and combination treatments (**C & E**) and *Phaeocystis* spp. observed in the high CO_2 treatment (**D**). Image magnification = x 300, scale bars = 20 µm, volume = 3 mL.

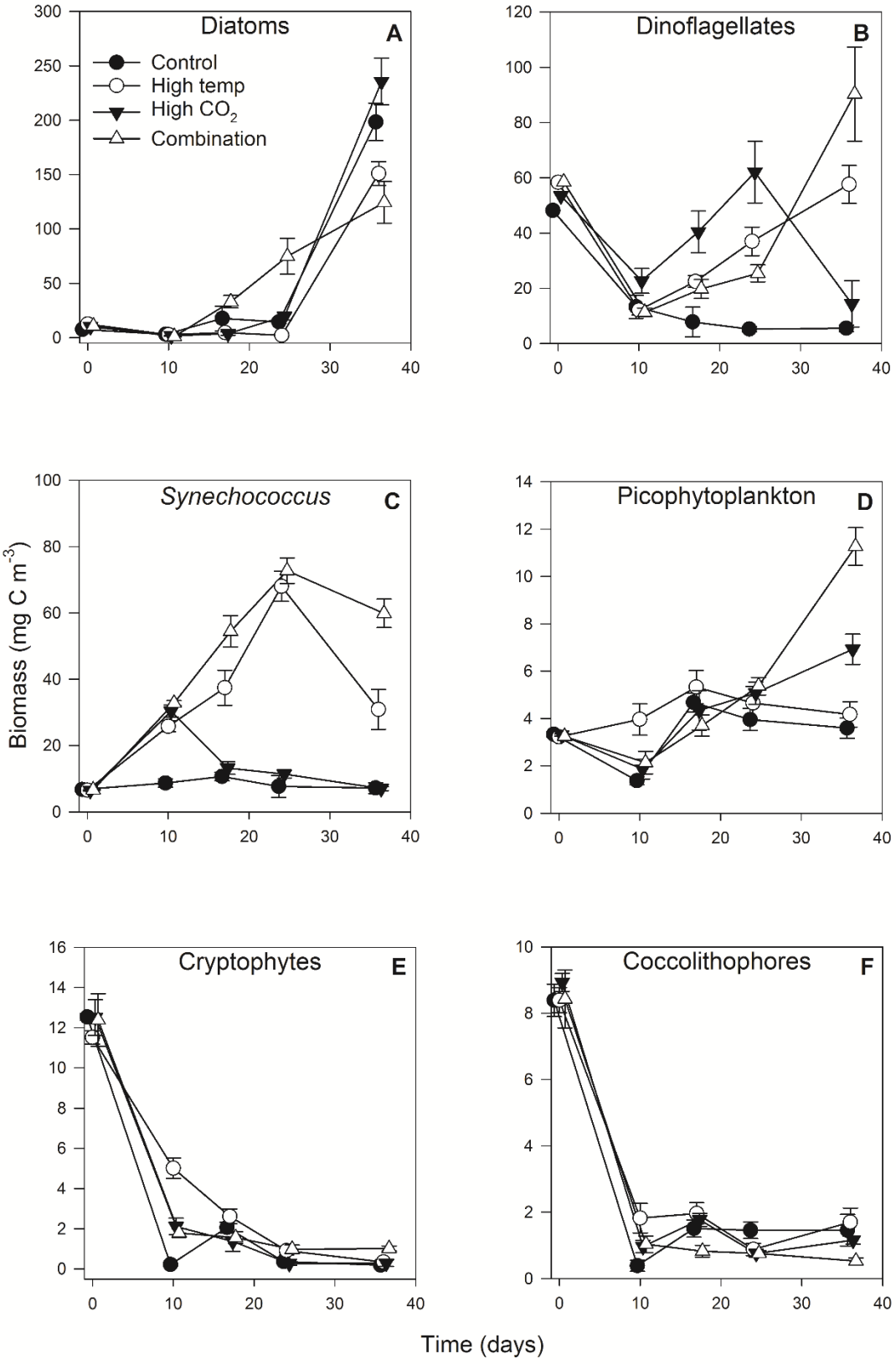

Fig. 5.8. Response of individual phytoplankton groups to experimental treatments.

Table 5.2. Results of generalised linear mixed model testing for effects of temperature, CO_2 and temperature x CO_2 on phytoplankton biomass over the time course of the experiment. Significant results are in bold; * p < 0.05, ** p < 0.001, *** p < 0.0001.

Response variable	n	*df*	*z*-value	*p*	sig
Diatoms (mg C m^{-3})					
High temp	80	70	-0.373	0.709	
High pCO_2	80	70	-0.711	0.477	
Combination	80	70	1.595	0.111	
Time	80	70	3.426	**<0.001**	***
Time x high temp	80	70	-0.419	0.675	
Time x high CO_2	80	70	0.719	0.472	
Time x combination	80	70	-1.241	0.215	
Dinoflagellates (mg C m^{-3})					
High temp	80	70	-0.34	0.734	
High pCO_2	80	70	0.941	0.347	
Combination	80	70	-0.794	0.427	
Time	80	70	-2.759	**<0.01**	**
Time x high temp	80	70	3.243	**<0.01**	**
Time x high CO_2	80	70	2.012	**<0.05**	*
Time x combination	80	70	3.746	**<0.001**	***
Nanophytoplankton (mg C m^{-3})					
High temp	80	70	-0.895	0.371	
High pCO_2	80	70	-3.72	**<0.001**	***
Combination	80	70	1.299	0.194	
Time	80	70	2.081	**<0.05**	*
Time x high temp	80	70	2.941	**<0.01**	**
Time x high CO_2	80	70	6.067	**<0.001**	***
Time x combination	80	70	-1.475	0.140	
***Synechococcus* (mg C m^{-3})**					
High temp	80	70	1.351	0.1765	
High pCO_2	80	70	1.696	0.090	
Combination	80	70	1.463	0.143	
Time	80	70	-0.032	0.975	
Time x high temp	80	70	1.897	**<0.05**	*
Time x high CO_2	80	70	-0.571	0.5682	
Time x combination	80	70	2.52	**<0.05**	*
Picophytoplankton (mg C m^{-3})					
High temp	80	70	1.232	0.218	
High pCO_2	80	70	-0.646	0.518	
Combination	80	70	-1.474	0.140	
Time	80	70	1.083	0.279	
Time x high temp	80	70	-0.259	0.796	
Time x high CO_2	80	70	1.75	0.080	
Time x combination	80	70	3.286	**<0.01**	**

Table 5.2 contd.

Coccolithophores (mg C m^{-3})					
High temp	80	70	0.459	0.646163	
High pCO_2	80	70	0.586	0.558081	
Combination	80	70	0.456	0.648393	
Time	80	70	-1.904	0.050	
Time x high temp	80	70	0.071	0.943751	
Time x high CO_2	80	70	-0.701	0.483376	
Time x combination	80	70	-1.605	0.108438	
Cryptophytes (mg C m^{-3})					
High temp	80	70	0.475	0.634944	
High pCO_2	80	70	0.307	0.75876	
Combination	80	70	-0.077	0.938884	
Time	80	70	-3.334	**<0.001**	***
Time x high temp	80	70	0.55	0.583	
Time x high CO_2	80	70	-0.035	0.972178	
Time x combination	80	70	0.901	0.367	
Microzooplankton (mg C m^{-3})					
High temp	80	70	0.135	0.892	
High pCO_2	80	70	-0.136	0.892	
Combination	80	70	0.307	0.759	
Time	80	70	0.378	0.706	
Time x high temp	80	70	-0.919	0.358	
Time x high CO_2	80	70	-2.073	**<0.05**	*
Time x combination	80	70	-1.977	**<0.05**	*

5.3.7 Chl fluorescence-based photophysiology

At T36 the fitted parameters of FRRf-based PI curves were strongly influenced by the experimental treatments (**Fig. 5.11, Tables 5.3 & 5.4**). Chl *a* normalised maximum photosynthetic rates (P^B_m) were significantly higher in the high pCO_2 treatment (0.0189 g C (g chl *a*)$^{-1}$ h^{-1}), followed by the high temperature treatment (0.0096 g C (g chl *a*)$^{-1}$ h^{-1}), (**Fig. 8, Tables 5.3 & 5.4**) (pairwise comparison: $t = 9.398$, $p < 0.001$, $t = 6.234$, $p < 0.001$, respectively, (n = 16)). There was no significant difference in P^B_m between the ambient control and combination treatment (0.0028 and 0.0030 g C (g chl *a*)$^{-1}$ h^{-1}) (**Table 5.4**). The light limited slope of photosynthesis (α^B) also followed the same trend and was significantly higher in the high pCO_2 treatment (1.32 x10^{-4} g C (mol photons)$^{-1}$ m^{-2} (g chl)$^{-1}$ followed by the high temperature treatment (8.60 x10^{-5} g C (mol photons)$^{-1}$ m^{-2} (g chl)$^{-1}$ (**Tables 5.3 & 5.4**) (pairwise

comparisons: t = 6.116, p < 0.001, t = 5.564, p < 0.001, respectively, (n = 16)). α^B was low in both the control and combination treatment with no significant difference (3.30 x10^{-5} and 3.58 x10^{-5} g C (mol photons)$^{-1}$ m^{-2} (g chl)$^{-1}$, respectively) (**Table 5.4**). The light saturation point of photosynthesis (E_k) was significantly higher in the high pCO_2 treatment relative to all treatments and the control (144.13 µmol photon m^{-2} s^{-1}, **Tables 5.3 & 5.4**).

Table 5.3. FRRf-based photosynthesis-irradiance curve parameters for the experimental treatments on the final day (T36). P^B_m (maximum photosynthetic rates, g C (g chl *a*)$^{-1}$ h^{-1}), α (light limited slope, g C (mol photons)$^{-1}$ m^{-2} (g chl)$^{-1}$) and E_k (light saturated photosynthesis, µmol photon m^{-2} s^{-1}).

	Control	sd	High temp	sd	High CO_2	sd	Combination	sd
P^B_m	0.0028	0.0016	0.0096	0.0019	0.0189	0.0026	0.0030	0.0010
α	3.30 x10^{-5}	6.63 x10^{-6}	8.60 x10^{-5}	1.27 x10^{-5}	1.32 x10^{-4}	1.10 x10^{-5}	3.58 x10^{-5}	3.82 x10^{-6}
E_k	85.33	45.47	110.93	6.09	144.13	17.91	86.38	33.06

Table 5.4. Results of generalised linear model testing for significant effects of temperature, CO_2 and temperature x CO_2 on phytoplankton photophysiology; P^B_m (maximum photosynthetic rates, g C (g chl *a*)$^{-1}$ h^{-1}), α (light limited slope, g C (mol photons)$^{-1}$ m^{-2} (g chl)$^{-1}$) and E_k (light saturated photosynthesis, µmol photon m^{-2} s^{-1}). Significant results are in bold; * p < 0.05, ** p < 0.001, *** p < 0.0001.

Response variable	n	*df*	*t*-value	*p*	sig
P^B_m					
High temp	16	12	6.234	**<0.001**	***
High pCO_2	16	12	9.398	**<0.001**	***
Combination	16	12	0.691	0.503	
α					
High temp	16	12	5.564	**<0.001**	***
High pCO_2	16	12	6.116	**<0.001**	***
Combination	16	12	0.39	0.70346	
E_k					
High temp	16	12	1.474	0.1661	
High pCO_2	16	12	2.809	**<0.05**	*
Combination	16	12	0.159	0.8765	

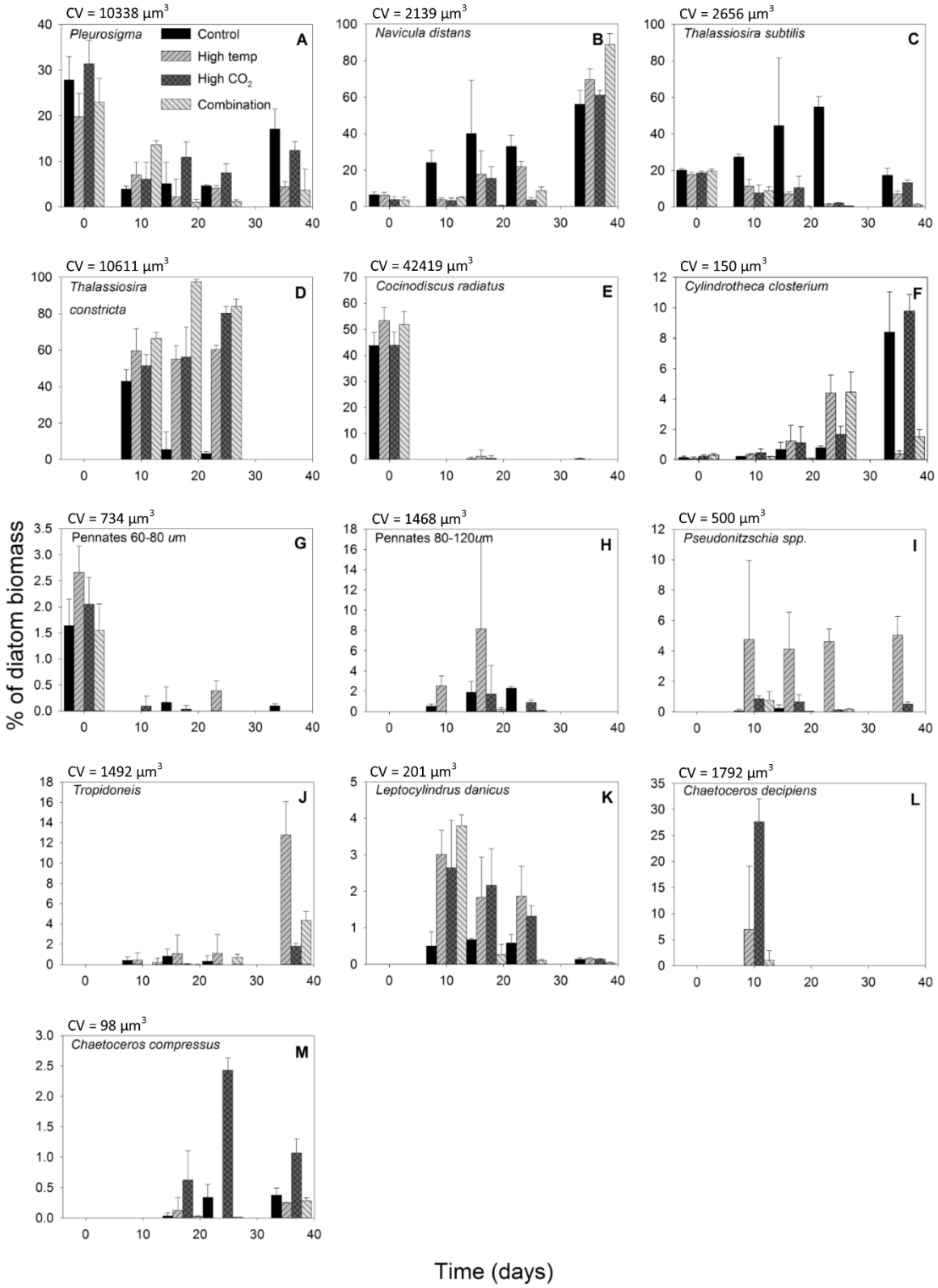

Fig. 5.9. Panels A to M show the shift in diatom species and size range from T0 to T36. The mean cell volume (CV) of each species is shown.

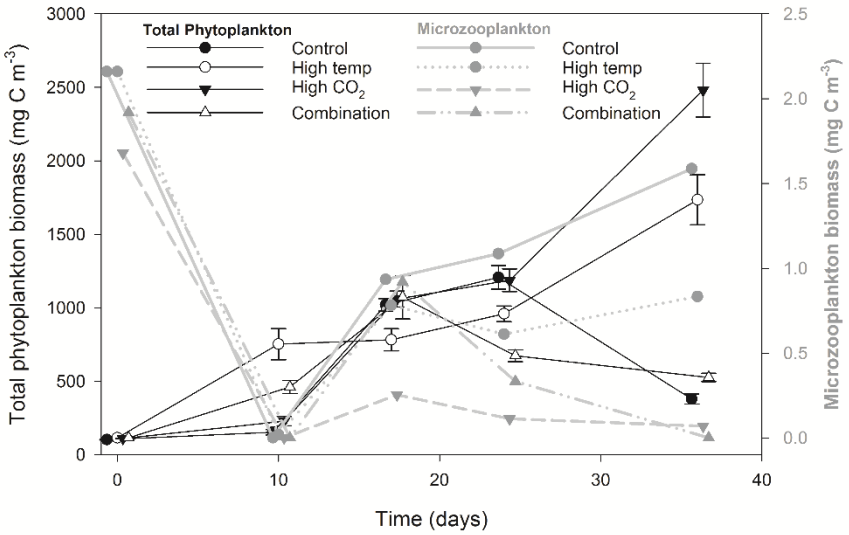

Fig. 5.10. Microzooplankton biomass relative to total phytoplankton biomass.

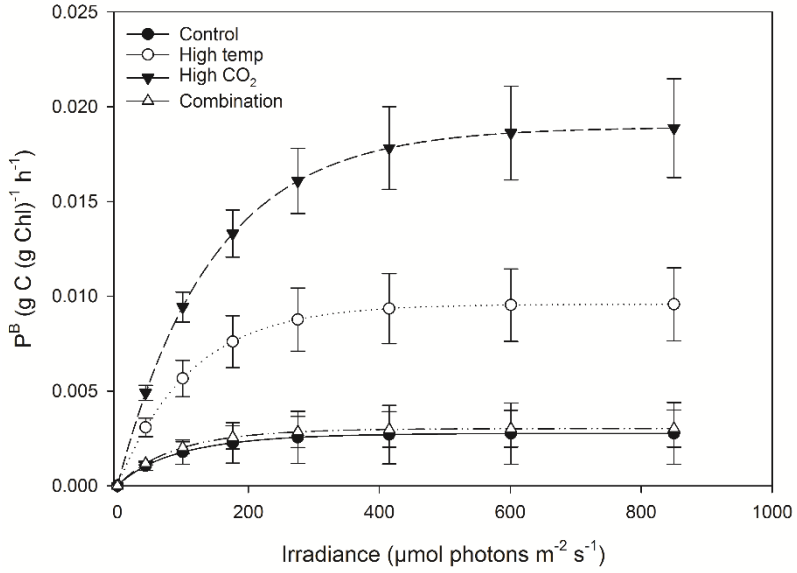

Fig. 5.11. Fitted parameters of FRRf-based photosynthesis-irradiance curves for the experimental treatments on the final experimental day (T36)

5.3.8 Natural variability of biomass in the WEC, station L4 time series.

Focussing on nanophytoplankton, which dominated the experimental treatments, analysis of the time series demonstrated this important group to be a critical component of the station L4 carbon budget. The mean annual total nanophytoplankton biomass over the time series (1993-2014) was 586 (± 16.54) mg C m^{-3} with maximum annual biomass of 1182 mg C m^{-3} in 2002 (62 % of total annual phytoplankton biomass) and minimum annual biomass of 262 mg C m^{-3} in 2008 (23 % of total annual phytoplankton biomass). In 8 of the 21 years of time series observations nanophytoplankton contributed more than 40 % of the station L4 carbon budget. Consistently throughout the time-series over a seasonal cycle, mean nanophytoplankton biomass > 10 mg C m^{-3} occurred from early April until the end of October, exhibiting sustained long-term seasonality relative to other phytoplankton groups, though maximal biomass was constrained between April – 3rd week of June with one exception (**Fig. 5.12 A**). *N. distans* dominated diatom biomass in the experimental communities though was found to be a very minor component of the diatom carbon budget at station L4 (0.04% of total annual diatom biomass). Weekly *N. distans* biomass averaged over the time series was very low and ranged from below the limit of detection to ~0.2 mg C m^{-3} with maximum total annual biomass of ~0.5 mg C m^{-3} in 2005 (**Fig. 5.12 B**). Seasonality of maximal *N. distans* biomass was constrained between September-October when the mean maximal biomass was 0.03 mg C m^{-3}. *P. cordatum* dominated dinoflagellate biomass in the experimental communities, making a significant contribution to total biomass in the combination treatment. Weekly *P. cordatum* biomass averaged over the time series ranged from 0.004 to 107 mg C m^{-3} and exhibited strong seasonality. Mean total annual *P. cordatum* biomass was 25.5 mg C m^{-3} with maximum annual biomass of 233 mg C m^{-3} in 2006 (minimum annual biomass of 0.004 mg C m^{-3} in 1994). The bloom peak (taken as an increase in biomass > 1.0 mg C m^{-3}) usually occurred in September although as early as mid-June (2001 and 2013) in some cases (**Fig. 5.12 C**). Mean maximal biomass was 12.7 mg C m^{-3} with positive anomalies occurring in 5 out of 21 years throughout the time-series (ranging from 15 to 107 mg C m^{-3}). *P. cordatum* contributed on average, 9.2 % of

the total annual dinoflagellate biomass throughout the time-series (maximum contribution of ~55 % in 2006; 12 % and 63 % when averaged over the bloom period, mid-June to end-September). *P. cordatum* contributed 3.4 % of total phytoplankton biomass during the bloom period and ~32 % of total phytoplankton biomass in 2006 during an unprecedented bloom when biomass attained 107 mg C m^{-3} in 2006 (**Fig 5.12 D**).

Nanophytoplankton, *N. distans* and *P. cordatum* optimal temperature ranges were found when considering how the dominant experimental species were temporally distributed relative to in-situ temperatures: nanophytoplankton exhibited a bi-modal distribution with 31 % biomass between 9-11 °C and 30 % between 15-16.5 °C, with 6 % above 16.5 °C (**Fig. 5.13 A**). ~60 % of *N. distans* biomass occurred between 14-16 °C and 2 % biomass above 16 °C (**Fig. 5.13 B**). In contrast, 66 % of *P. cordatum* biomass occurred between 14-16 °C and 24 % above 16 °C (**Fig. 5.13 C**). Biomass distribution relative to station L4 in-situ pCO_2 levels (2008-2014) also demonstrated group/species-specific optimal ranges. 71 % nanophytoplankton biomass occurred at a pCO_2 range of 245-410 µatm, 24 % 410-515 µatm and 7 % between 515-680 µatm (**Fig. 5.13 D**). *N. distans* followed a similar trend with 72% biomass between a pCO_2 range of 245-410 µatm, 26% between 410-515 µatm and < 2% beyond 515 µatm (**Fig. 5.13 E**). By contrast, *P. cordatum* exhibited greater sensitivity to higher in-situ pCO_2 values with 67% biomass between 245-350 µatm, 30% between 350-410 µatm and 3% biomass occurring beyond 410 µatm (**Fig. 5.13 F**).

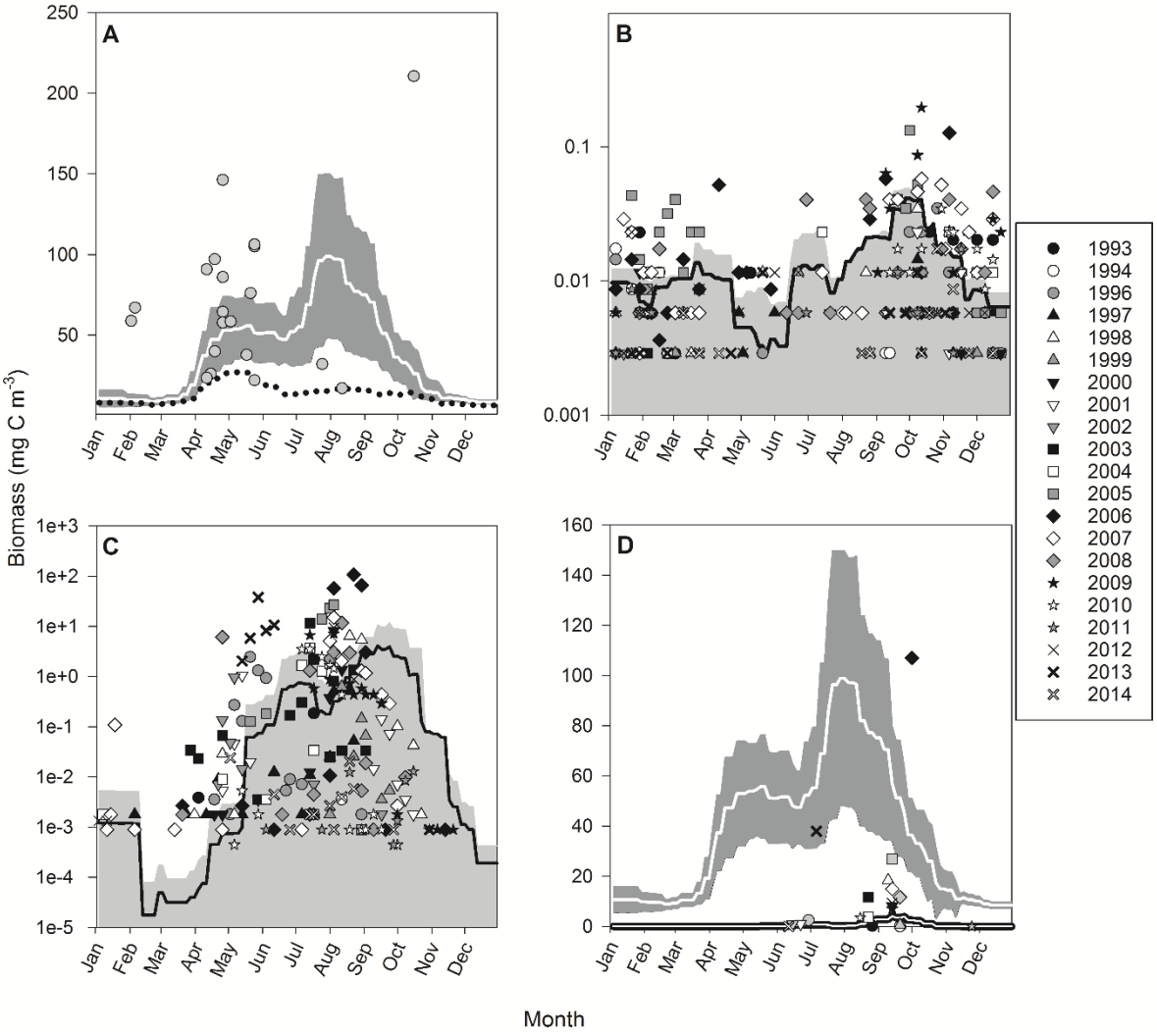

Fig. 5.12. (**A**) Temporal weekly profile of total phytoplankton carbon biomass at station L4 between 1993-2014 (n = 909). White line is smoothed running average of total phytoplankton, grey area is standard deviation, dotted line is smoothed running average of total nanophytoplankton biomass (n = 909) and grey circles are maximal nanophytoplankton biomass from weekly observations (mean maxima of 70 mg C m^{-3}) (n = 20). (**B**) Seasonal profiles of *Navicula distans* (common log scale) between 1993-2014 (n = 244). Black line is smoothed running average over the time series, grey area is standard deviation and all symbols are observed data values by year. (**C**) Seasonal profiles of *Prorocentrum cordatum* (common log scale) between 1993-2014 (n = 209). Black line is smoothed running average over the time series, grey area is standard deviation and all symbols are observed data values by year. (**D**)Maximal *P. cordatum* biomass values relative to total phytoplankton biomass. White line is smoothed running average of total phytoplankton biomass, grey area is standard deviation, inverse white line is mean *P. cordatum* biomass and symbols are maximal *P. cordatum* biomass from weekly observations by year (n = 21).

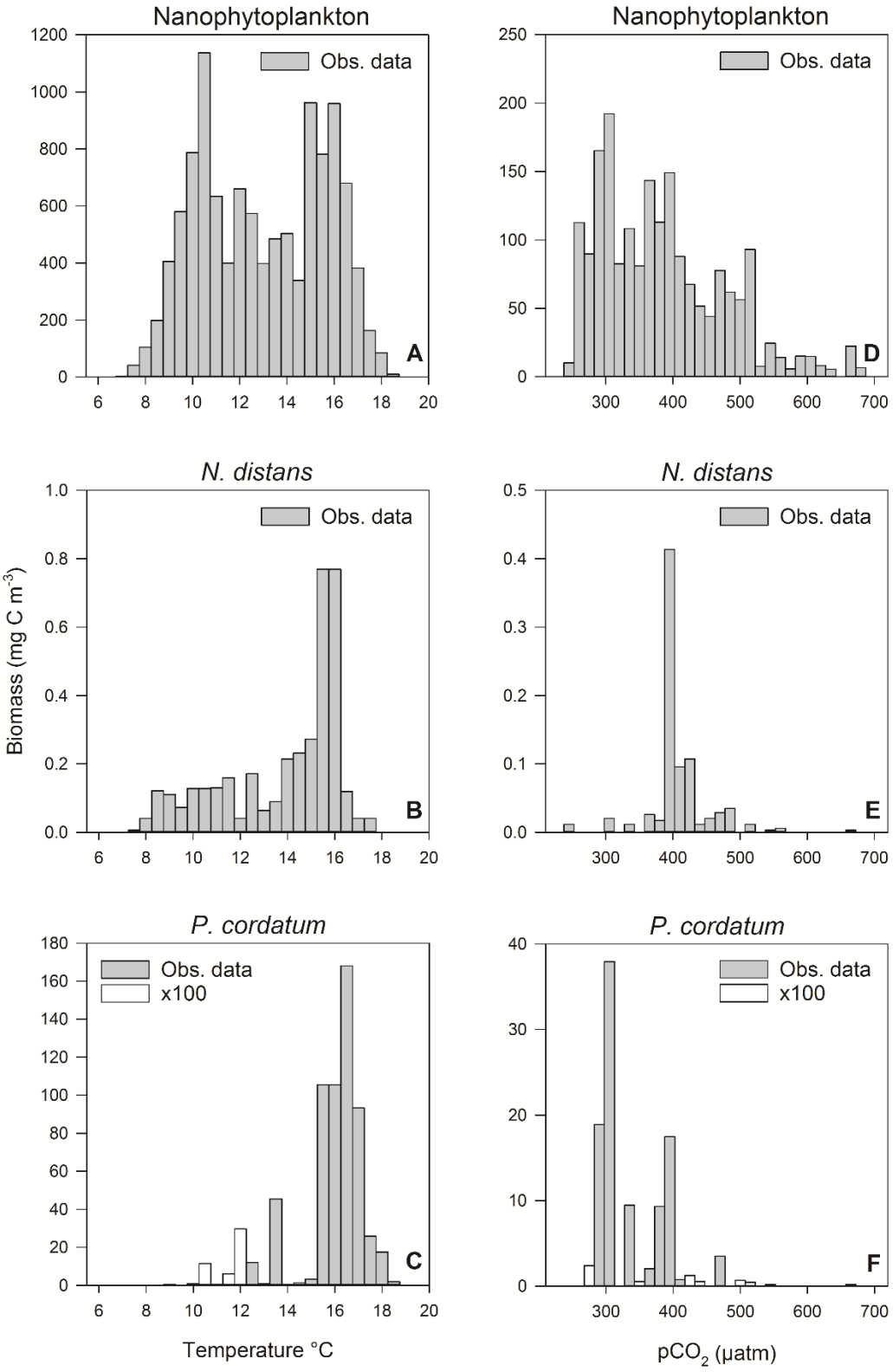

Fig. 5.13. Frequency distribution of biomass at station L4 along the in situ temporal gradients of temperature (1993-2014) and pCO_2 (2008-2014) for nanophytoplankton (**A & D**) *N. distans* (**B & E**) and *P. cordatum* (**C & F**).

5.4 Discussion

Individually, elevated temperature and pCO_2 resulted in the highest biomass and light saturated photosynthetic carbon fixation rates (P^B_m) together with significant shifts in community composition, exhibiting near mono-specific dominance of nanophytoplankton. The interactive effects of these two factors had no effect on total biomass with values close to the ambient control, and no effect on P^B_m. However, the combination treatment exhibited the greatest diversity of phytoplankton functional groups with increased dinoflagellates and *Synechococcus* biomass relative to the other treatments and control.

Elevated pCO_2 has been shown to enhance phytoplankton growth and photosynthesis since some phytoplankton species have active uptake systems for inorganic carbon (Giordano et al., 2005; Reinfelder, 2011). Elevated pCO_2 may therefore lead to lowered energetic costs of carbon assimilation in some species and a redistribution of the cellular energy budget to other processes (Tortell et al., 2002). Under elevated pCO_2 where the dominant group was nanophytoplankton, the community was dominated by the bloom-forming haptophyte *Phaeocystis* spp. Photosynthetic carbon fixation in *Phaeocystis* spp. is presently near saturation with respect to current levels of pCO_2 (Rost et al., 2003). Inorganic carbon acquisition in this species has been shown to be equal to or more efficient as that in diatoms and extracellular carbonic anhydrase is regulated by CO_2 (aq), while HCO_3^- is utilized as a carbon source in photosynthesis, indicating more efficient use of CO_2 in *Phaeocystis* spp. (Elzenga et al., 2000; Rost et al., 2003). Its relatively small size could make the extensive operation of active CO_2 and HCO_3^- uptake unnecessary, as the diffusive boundary layer is relatively small. Therefore it is possible that DIC supply and demand may be met by diffusion (Schulz et al., 2013). Dominance of *Phaeocystis* spp.. under elevated pCO_2 may also be due to lowered grazing pressure, since microzooplankton biomass was significantly low in the high CO_2 treatment throughout the experiment. The increased biomass in the high temperature treatment (where microzooplankton biomass remained stable between T17 to T36, though lower than the

control) may be attributed to group- and species-specific temperature optima, since algal growth commonly increases with temperature until after an optimal range (Boyd et al., 2013; Goldman and Carpenter, 1974; Savage et al., 2004). Optimum growth temperatures for marine phytoplankton are often several degrees higher than environmental temperatures (Eppley, 1972; Thomas et al., 2012). Increasing temperature will increase the substrate-saturated reaction rate of RUBISCO and thus the potential growth rates of phytoplankton, if growth is not limited by inorganic carbon or other factors (Beardal and Raven, 2004). Nanophytoplankton also dominated in this treatment and while *Phaeocystis* spp. was not discriminated, no further classification was made at a group/species level. Reduced biomass in the control from T24 onwards may be due to increased grazing pressure given the highest concentrations of microzooplankton biomass were observed in the control. Conversely, microzooplankton biomass declined significantly from T17 in the combination treatment, indicating reduced grazing pressure while phytoplankton biomass also declined from this time point, indicating a direct response to the experimental treatment. Nutrient concentrations were not measured beyond T0 and the possibility that differences in nutrient availability may have contributed to observed differences between the control and experimental treatments cannot be excluded.

5.4.1 Chl *a*

Biomass in the control peaked at T25 followed by a decline to T36. Correlated with this, Chl *a* also peaked at T25 in the control and declined to 3.3 mg m^{-3} by T27, remaining close to this value until T36. Biomass in the combination treatment peaked at T20 followed by decline to T36 whereas Chl *a* in this treatment declined from T20 to T25 followed by an increase at T27 before further decline, similar to the biomass. Chl *a* peaked in this treatment again at T36 (6.8 mg m^{-3}). The increase in Chl *a* between T25 – T27 (coincident with an overall biomass decrease) may be attributed to lower species specific carbon:Chl *a* ratios as a result of the increase in dinoflagellates, *Synechococcus* and picophytoplankton biomass from T25. The increased Chl *a* during a decline in biomass under nutrient replete conditions in the combination treatment may

have been due to slower species-specific growth rates when diatoms and dinoflagellates became more prominent in this treatment. Carbon:Chl *a* in diatoms and dinoflagellates have previously been demonstrated to be lower than nano- and picophytoplankton (Sathyendranath et al., 2009). This contrasts the results reported in comparable studies as Chl *a* is generally highly correlated with biomass, (e.g. Feng et al., 2009). Similar results were reported however by Hare et al., (2007) which indicates that Chl *a* may not always be a reliable proxy for biomass in mixed communities.

5.4.2 Biomass

This study shows that the phytoplankton community response to elevated temperature and pCO_2 is highly variable. pCO_2 elevated to ~800 µatm induced higher community biomass in agreement with Kim et al., (2006) and Riebesell et al., (2007) whereas in other natural community studies, no CO_2 effect on biomass has been observed (Delille et al., 2005; Maugendre et al., 2017; Paul et al., 2015b). A ~4.5 °C temperature increase also resulted in higher biomass, similar to the findings of Feng et al., (2009) and Hare et al., (2007) though elevated temperature has previously reduced biomass of natural nanophytoplankton communities in the Western Baltic Sea and Arctic Ocean (Coello-Camba et al., 2014; Moustaka-Gouni et al., 2016). When elevated temperature and pCO_2 were combined community biomass exhibited little response, similar to the findings of Gao et al., (2017), while an increase in biomass has also been reported (Calbet et al., 2014; Feng et al., 2009). Geographic location and season also play an important role in structuring the community and its response in terms of biomass to elevated temperature and pCO_2, (e.g. Li et al., 2009; Morán et al., 2010).

5.4.3 Carbon:Nitrogen

In agreement with others, the results of this experiment showed highest increases in C:N under elevated pCO_2 alone (Riebesell et al., 2007). C:N also increased under high temperature, consistent with the findings of Lomas and Glibert, (1999) and Taucher et al., (2015) and was stimulated to a lesser degree when pCO_2 and temperature were elevated simultaneously, which

was also observed in the study of (Calbet et al., 2014). In contrast, previous studies have observed C:N to be unaffected by the combined influence of elevated pCO_2 and temperature, (e.g. Deppeler and Davidson, 2017; Kim et al., 2006a; Paul et al., 2015b). In the present experiment nitrate was held constantly replete (though not measured throughout). The increased C:N ratios under elevated pCO_2, elevated temperature and the combination of both factors may indicate the potential for nitrate over-consumption under future elevated pCO_2 and temperature scenarios in natural systems. Nitrate can be rapidly depleted during natural blooms which has been reported in field populations in the northeast Atlantic Ocean (Körtzinger et al., 2001). Stoichiometry of cellular C and N in phytoplankton are emerging as important factors of marine biogeochemistry. Variability in elemental requirements can influence nutrient limitation patterns and stress (Bonachela et al., 2013), nitrogen fixation rates (Mills and Arrigo, 2010) and the link between nutrient supply and C export which ultimately feedback to atmospheric CO_2 (Teng et al., 2014). The significant increase in C:N under elevated pCO_2, elevated temperature and to a lesser degree the combination of both factors indicate shifts in biogeochemistry in more acidified, warmer oceans. C:N is a strong indicator of cellular protein content (Woods and Harrison, 2003) and increases under elevated pCO_2 and warming may likely lead to lowered nutritional value of phytoplankton with consequences for zooplankton reproduction and biogeochemical cycles.

5.4.4 Photosynthetic carbon fixation rates

The highest light saturated photosynthetic carbon fixation rates (P^B_m) at T36 under elevated pCO_2 was 6-fold higher than the ambient control. This has also been reported by Riebesell et al., (2007) and Tortell et al., (2008). Studies on laboratory cultures have shown that increased temperatures increase phytoplankton photosynthetic parameters (Feng et al., 2008; Fu et al., 2007; Hutchins et al., 2007) which was also observed in the present study (more than 3-fold higher than the ambient control). However, this increase in P^B_m was lower relative to the high pCO_2 treatment, contrasting observations from other natural population studies (Feng et al.,

2009; Hare et al., 2007) where the effect of elevated pCO_2 alone was found to reduce P^B_m. The present results showed no effect on P^B_m under the combined treatment which has also been observed in natural population experiments (Coello-Camba and Agustí, 2016; Gao et al., 2017). This strongly contrasts the findings of Feng et al., (2009) and Hare et al., (2007) who observed the highest P^B_m when temperature and pCO_2 were elevated simultaneously. The increased light limited photosynthetic efficiency (α^B) and maximum light saturation level (E_k) under elevated pCO_2, which decreased when elevated pCO_2 and temperature were combined in the present study also showed opposite trends to observations by (Feng et al., 2009).

P^B_m, α^B and temperature are tightly coupled (Uitz et al., 2008) and different phytoplankton species are adapted to a narrow temperature band with a sharp decrease in photosynthetic rates beyond their thermal optima (Eppley, 1972; Raven and Geider, 1988) which can be modified through the synthesis of photo-protecting rather than photosynthetic pigments (Kiefer and Mitchell, 1983). This may explain the difference in P^B_m between the high pCO_2 and high temperature treatments (in addition to differences in nanophytoplankton community composition in relation to *Phaeocystis* spp. discussed above), as the experimental high temperature treatment in the present study was ~4.5 ° C higher than ambient.

There was no significant effect of combined elevated pCO_2 and temperature on P^B_m which was strongly influenced by taxonomic differences between the experimental treatments. Warming has been shown to lead to smaller cell sizes in nanophytoplankton (Atkinson et al., 2003; Peter and Sommer, 2012) which was observed in the combined treatment together with decreased nanophytoplankton biomass. Diatoms also shifted to smaller species with reduced biomass observed by a reduction of the larger species in both the high temperature and combination treatments (which were *Pleurosigma* and *T. constricta*) (**Fig 5.9**), while dinoflagellate and *Synechococcus* biomass increased at T36. Dinoflagellates are the only photoautotrophs with form II RuBisCO (Morse et al., 1995) which has the lowest carboxylation:oxygenation specificity factor among eukaryotic phytoplankton (Badger et al., 1998), giving dinoflagellates a

disadvantage in carbon fixation under present ambient pCO_2 levels. This generalisation is not the case with every dinoflagellate spp. as demonstrated by Hu et al., (2017) with the dinoflagellate *Karenia mikimotoi*. Down-regulation of CCMs was observed by *K. mikimotoi* under elevated pCO_2 resulting in a stimulation of photosynthetic rates and growth. Dinoflagellates generally grow at slower rates in surface waters with high pH (≥9) resulting from photosynthetic removal of CO_2 by previous blooms (Hansen, 2002; Hinga, 2002). Though growth under high pH provides indirect evidence that dinoflagellates possess CCMs, direct evidence is limited and points to the efficiency of CCMs in dinoflagellates as moderate in comparison to diatoms and some haptophytes (Reinfelder, 2011 and references therein). This may explain the lower P^B_m in the combined treatment compared to elevated pCO_2 and temperature individually. Given that dinoflagellates accounted for ~20% of biomass in the combination treatment, exerting a minor influence on community photosynthetic rates, further work is required to explain the lower P^B_m under the combined influence of elevated pCO_2 and temperature compared to the individual treatment influences. The same electron requirement parameter was applied for carbon uptake across all treatments, though in nature and between species, there can be considerable variation in this parameter (e.g. 1.15 to 54.2 mol e^- $(mol\ C)^{-1}$; Lawrenz et al., 2013) which can co-vary with temperature, nutrients, Chl *a*, irradiance and community structure. Better measurement techniques at quantifying this variability are necessary in the future.

5.4.5 Community composition

Phytoplankton community structure changes were observed, with a shift from dinoflagellates to nanophytoplankton which was most pronounced under single treatments of elevated temperature and pCO_2. Amongst the nanophytoplankton, a distinct size shift to smaller cells was observed in the high temperature and combination treatments and in the high pCO_2 treatment *Phaeocystis* spp. dominated. Under combined pCO_2 and temperature at T36 however, dinoflagellate and *Synechococcus* biomass increased at the expense of nanophytoplankton.

An increase in pico- and nanophytoplankton has previously been reported in natural communities under elevated pCO_2 (Bermúdez et al., 2016; Boras et al., 2016; Brussaard et al., 2013; Engel et al., 2008) while no effect on these size classes has been observed in other studies (Calbet et al., 2014; Paulino et al., 2007). Moustaka-Gouni et al., (2016) also found no CO_2 effect on natural nanophytoplankton communities but increased temperature reduced the biomass of this group. Kim et al., (2006) observed a shift from nanophytoplankton to diatoms under elevated pCO_2 alone while a shift from diatoms to nanophytoplankton under combined elevated pCO_2 and temperature has been reported (Hare et al., 2007). A variable response in *Phaeocystis* spp. to elevated pCO_2 has also been reported with increased growth (Chen et al., 2014; Keys et al., 2017), no effect (Thoisen et al., 2015) and decreased growth (Hoogstraten et al., 2012) observed. *Phaeocystis* spp. can outcompete other phytoplankton and form massive blooms (up to 10 g C m^{-3}) with impacts on food webs, global biogeochemical cycles and climate regulation (Schoemann et al., 2005). While not a highly toxic algal species, *Phaeocystis* spp. are considered a harmful algal species (HAB) when biomass reaches sufficient concentrations to cause anoxia through the production of mucus foam which can clog the feeding apparatus of zooplankton and fish (Eilertsen & Raa, 1995).

The response of diatoms to elevated pCO_2 and temperature has been variable. For example, *Thalassiosira weissflogii* incubated at 1000 µatm pCO_2 increased growth by 8 % while for *Dactyliosolen fragilissimus*, growth increased by 39%. Temperature elevated by +5°C also had a stimulating effect on *T. weissflogii* but inhibited the growth rate of *D. fragilissimus* (Taucher et al., 2015). When the treatments were combined growth was enhanced in *T. weissflogii* but reduced in *D. fragilissimus*. In partial agreement, the results of the present experiment show that elevated pCO_2 increased biomass in diatoms but elevated temperature and the combination of these factors reduced biomass. A distinct size-shift in diatom species was observed in all treatments, from the larger *Coscinodiscus* spp., *Pleurosigma* and *Thalassiosira subtilis* to the smaller *Navicula distans*. This was most pronounced in the combination treatment where *N. distans* contributed 89% of diatom biomass. *Navicula* spp. have exhibited a differential response

to both elevated temperature and pCO_2. At +4.5 °C and 960ppm CO_2 Torstensson et al., (2012) observed no synergistic effects on the benthic *Navicula directa*. Elevated temperature increased growth rates by 43% while a reduction of 5% was observed under elevated CO_2. No effects on growth were detected at pH ranging from 8 – 7.4 units on *Navicula* spp. (Thoisen et al., 2015), while growth in *N. distans* was significantly stimulated along a CO_2 gradient at a shallow cold-water vent system (Baragi et al., 2015).

Synechococcus grown under pCO_2 elevated to 750 ppm and temperature elevated by 4 °C resulted in increased growth and a 4-fold increase in P^B_m (Fu et al., 2007) which was similar to the present study results.

The combination of elevated temperature and pCO_2 significantly increased dinoflagellate biomass which almost doubled, accounting for 17% of total biomass. This was due to *P. cordatum* which increased biomass by more than 30-fold between T0 and T30 (66% of dinoflagellate biomass in this treatment). Despite of the global increase in the frequency of HABS few studies have focussed on the response of dinoflagellates to elevated pCO_2 and temperature. In laboratory studies at 1000 ppm CO_2, growth rates of the HAB species *Karenia brevis* increased by 46%, at 1000 ppm CO_2 and +5 °C temperature it's growth increased by 30% but was reduced under elevated temperature alone (Errera et al., 2014). A combined increase in pCO_2 and temperature enhanced both the growth and P^B_m in the dinoflagellate *Heterosigma akashiwo*, whereas in contrast to the present findings, only pCO_2 alone enhanced these parameters in *P. cordatum* (Fu et al., 2008).

Among harmful algal bloom (HAB) species, *P. cordatum* is widely distributed geographically in temperate and subtropical waters, has detrimental effects at the organismal and environmental levels and is potentially harmful to humans via shellfish poisoning (Heil et al., 2005). Recent increases in the frequency, magnitude and distribution of harmful phytoplankton species has focussed attention on the unique physiological, ecological and toxicological aspects of the species involved (Andeson et al., 2002; Hallegraeff, 1993). Ocean acidification in combination

with warming could potentially affect the growth and toxicity of harmful algal species (Fu et al., 2012). Recent studies with several diatom and dinoflagellate species suggest that ocean acidification combined with elevated temperature may dramatically increase the toxicity of some harmful groups, e.g. (Flores-Moya et al., 2012; Fu et al., 2010; Sun et al., 2011; Tatters et al., 2012). The ecology and bloom dynamics of *P. cordatum* have been well documented in selected environments, e.g. (Chesapeake Bay, Baltic Sea), however there has been recent reports of apparent spreading to previously unreported areas via a variety of possible mechanisms, e.g. (ballast water transport, aquaculture development and increasing eutrophication) (Heil et al., 2005). In Chesapeake Bay *P. cordatum* 'mahogany tides' have been associated with anoxic/hypoxic events, fish kills, aquaculture shellfish kills and aquatic vegetation losses (Tango et al., 2005).

5.4.6 Natural variability of biomass in the WEC, station L4 time series.

Comparative analyses of the WEC time series and the dominant species from the experimental treatments showed the nanophytoplankton group to be a significant contributor to the station L4 carbon budget. The in-situ bimodal distribution of nanophytoplankton biomass at cold and warm temperature ranges indicates a potential tolerance to temperature increase. Most nanophytoplankton biomass occurred at an in-situ pCO_2 range between 245-410 µatm but almost 10% of biomass was distributed between 515-680 µatm, indicating some tolerance to elevated pCO_2 during periods of CO_2 oversaturation at station L4. The dominant diatom species in the experimental communities, *N. distans*, was a very minor contributor to diatom biomass over the time series with most biomass constrained to very narrow in-situ temperature and pCO_2 ranges of 14-16 ° C and 245-410 µatm. *P. cordatum* dominated dinoflagellate biomass in the combination treatment but was generally a low biomass contributor to dinoflagellate biomass over the time series, with the exception of one unprecedented bloom in 2006. *P. cordatum* biomass exhibited higher thermal in-situ optima with most biomass observed between 14-16 ° C and almost a quarter of biomass above 16 °C, indicating tolerance to

temperature increase, though the majority of biomass at station L4 occurred at times of low in-situ pCO_2 (245-350 µatm) with just 3% beyond 410 µatm. These trends suggest conditions of warming may favour nanophytoplankton and *P. cordatum*, elevated pCO_2 may favour nanophytoplankton and both factors combined may favour both species. These observations are consistent with the experimental results.

5.5 Implications

Increased biomass, P^B_m and a community shift to nanophytoplankton under individual increases in temperature and pCO_2 suggests a potential positive feedback on atmospheric CO_2, though selection of *Phaeocystis* spp. under elevated pCO_2 indicates the potential for negative impacts on ecosystem function and food web structure associated with this species (Schoemann et al., 2005; Verity et al., 2007). Selection for nanophytoplankton in both of these treatments indicates the potential for reduced carbon sequestration due to slower sinking rates of smaller phytoplankton cells (Bopp et al., 2001; Laws et al., 2000b). Particle flux is controlled by rates of particle aggregation and sinking and annual variability in carbon export to deep waters correlates strongly with the size of the dominant primary producing species (Boyd and Newton, 1995). Minerals such as calcium carbonate (produced by coccolithophores as coccoliths) and opal (produced by diatoms as silica frustules) may drive the sedimentation of particulate organic matter by adding density or "ballast" to organic aggregates (Armstrong et al., 2001). Sinking velocities of phytoplankton cells are only about a meter day^{-1} and require more than a year to reach the benthos. Given the rapid rates of microbial decomposition of organic material and zooplankton grazing it is virtually impossible for such slowly sinking particles to reach the seabed (Smayda, 1971). In contrast, sinking velocities of large (> 0.5 mm) particles are > 100 m day^{-1} (Shanks and Trent, 1980) and transit time to the deep in this case is days to weeks (Asper et al., 1992). Therefore, increased photosynthesis by a regime shift to nanophytoplankton may be off-set by reduced carbon export.

When temperature and pCO_2 were elevated simultaneously, community biomass showed no response and no effects on P^B_m were observed suggesting a negative feedback on atmospheric CO_2 and climate warming in future warmer high CO_2 oceans. Additionally, combined elevated pCO_2 and temperature significantly modified taxonomic composition, reducing diatom biomass relative to the ambient control with increased dinoflagellate biomass dominated by the potential HAB species, *P. cordatum* which has implications for fisheries, ecosystem function and human health.

5.6 Conclusion

These experimental results provide new evidence that increases in pCO_2 coupled with rising sea surface temperatures may have antagonistic effects on the autumn phytoplankton community in the WEC. Under future global change scenarios, the size range and biomass of diatoms may be reduced and negatively impact carbon export to deeper layers. Increased dinoflagellate biomass and the selection of potential HAB species may have negative consequences for fisheries and ecosystem function. The experimental simulations of year 2100 temperature and pCO_2 demonstrate that the effects of warming may be offset by elevated pCO_2, maintaining current levels of coastal phytoplankton productivity while significantly altering the community structure, and in turn these shifts will have consequences for carbon biogeochemical cycling in the WEC.

Chapter 6 – Effects of elevated pCO_2 and temperature on the late summer bloom

Abstract

The effects of elevated pCO_2 and temperature were investigated on the late summer phytoplankton bloom succession from diatoms to dinoflagellates in the Western English Channel (WEC). A full factorial 30-day microcosm experiment was conducted under year 2100 predicted temperature and pCO_2. The starting phytoplankton community biomass was ~140 mg c m^{-3} and was dominated by dinoflagellates (~46%), diatoms (~16%) and nanophytoplankton (~15%). Over the experimental period total biomass was significantly stimulated by elevated temperature (14-fold increase) and pCO_2 (11-fold increase). In contrast, the combined influence of these two factors significantly reduced total biomass relative to the ambient control, high pCO_2 and high temperature treatments individually. Chlorophyll *a* normalised maximum photosynthetic rates of carbon fixation (P^B_m) increased by 83% under elevated pCO_2 and 50% under elevated temperature while a significant reduction in P^B_m was observed when temperature and pCO_2 were elevated simultaneously. The phytoplankton community structure shifted from dinoflagellates to diatoms at the end of the experiment in all treatments. Under elevated temperature diatoms contributed 84% of community biomass and were dominated by *Leptocylindrus danicus* while under elevated pCO_2 diatoms contributed 90% of community biomass and were dominated by the smaller *L. minimus*. Under ambient conditions the diatom *C. closterium* dominated. The smallest diatom contribution to community biomass (60%) was observed under combined elevated temperature and pCO_2. Dinoflagellate biomass declined significantly under the individual influences of elevated temperature, elevated pCO_2 and ambient conditions while under the combined effects a significant 2-fold increase was observed where *Gymnodinium* spp. contributed 98% of dinoflagellate biomass. The results suggest that under future global change, further increases in temperature and pCO_2 may negatively influence coastal phytoplankton productivity during the late summer in the WEC which has implications for carbon biogeochemistry and a positive feedback on atmospheric CO_2.

6.1 Introduction

In late summer, sea surface temperature and pCO_2 attain their respective time series maximal values in the Western English Channel (WEC) at station L4. During late August to mid-September, mean seawater temperatures at 10m range from 15.46 °C (± 0.53) (n = 52) to 16.19 °C (± 0.58) (n = 44) (1993-2015) with maximal temperatures ranging from 17.02 to 18.07 °C (± 0.38) (n = 7), typically in September. Warming effects of climate change are thus likely to show greater impacts in late summer when the present upper limit of the temperature threshold increases over this period (Hegerl and Bindoff, 2005). The response of phytoplankton is likely to be species-specific, for example Edwards and Richardson., (2004) showed that dinoflagellates have greater phenological sensitivity to temperature change than diatoms. The seasonal cycles for the dinoflagellates *Ceratium*, *Protoperidinium* and *Dinophysis* now occur 1 month earlier compared to 1958 in the central North Sea. Similar trends have also been identified for the genus *Ceratium* at the ocean basin scale in the NE Atlantic (Beaugrand et al., 2010). Increases in seawater temperature are also predicted to lead to increased stratification which may negatively impact upon primary production due to nutrient limitation and higher integrated irradiance (Sarmiento et al., 2004). Mean pCO_2 values at station L4 in late summer range from 420.32 µatm (± 78.17) (n = 6) pCO_2 to 564.95 µatm (± 39.95) (n = 4) pCO_2 with maximal annual values between 615.0 to 661.9 (± 51.96) µatm pCO_2 (n = 5). This pCO_2 oversaturation is driven by the breakdown of stratification and mixing with high pCO_2 deeper waters (Kitidis et al., 2012). As is the case with increased seawater temperature, predicted future ocean acidification is likely to show greater impacts in late summer when the present upper limit of the pCO_2 threshold increases during this period of oversaturation. The shift in dissolved inorganic carbon (DIC) equilibria associated with increased pCO_2 has wide-ranging implications for phytoplankton photosynthetic carbon fixation rates, growth and community composition (Riebesell, 2004).

From a biological perspective, the late summer at station L4 is characterised by the second of two annual diatom blooms, more intense in late summer compared to spring with higher mean biomass. Over this period, diatom communities are typically dominated by pennate and centric species such as *Pseudonitzschia* spp. and *Leptocylindrus* spp. (Widdicombe et al., 2010a). Concurrently, as seawater temperatures increase, dinoflagellate biomass increases resulting in intense but brief blooms in late summer, typically dominated by *Karenia mikimotoi* and *Prorocentrum* spp. (Widdicombe et al., 2010a). Diatoms and dinoflagellates are critical components to the L4 phytoplankton carbon budget, and together they form 60% (± 11.68) of the total biomass.

Laboratory studies of phytoplankton species in culture and studies on natural populations in the field have shown that the growth and photosynthetic rates of most species are sensitive to either elevated pCO_2 or temperature. In the diatom *Thalassiosira weissflogii* in culture, 1000 µatm pCO_2 (+ 600 µatm above ambient) resulted in an 8% increase in growth and DIC uptake, while for the diatom *Dactyliosolen fragilissimus*, growth and DIC uptake increased by 39%. Temperature elevated to 20°C (+5°C above ambient) also had a stimulating effect on *T. weissflogii* but inhibited the growth rate of *D. fragilissimus* (Taucher et al., 2015). When the treatments were combined, elevated pCO_2 and temperature synergistically enhanced the growth of *T. weissflogii* but reduced the growth in *D. fragilissimus*. Although there have been fewer studies on dinoflagellates, similar variability in responses has been observed, e.g. (Errera et al., 2014; Fu et al., 2008). In a recent field study on natural phytoplankton communities, elevated temperature (+3°C above ambient) enhanced community biomass at both an off-shore and near-shore site (Gao et al., 2017). When combined with elevated pCO_2 (+610 µatm above ambient), no affect was observed in the near-shore community but there was a reduction in biomass in the off-shore community, demonstrating that seawater warming effects can be offset by elevated pCO_2 in mixed communities.

The goals of this study were to investigate: 1) the combined effects of elevated pCO_2 and temperature on phytoplankton community structure, biomass and photosynthetic carbon fixation rates during the late summer bloom succession from diatoms to dinoflagellates at station L4; 2) assess the natural variability in phytoplankton community structure and the carbon biomass of the dominant species observed in the experimental community relative to long-term observations at station L4 over two decades (1993-2014); and 3) assess the distribution of biomass of the dominant species observed at the end of the experiment relative to the in-situ temporal gradients of temperature and pCO_2 observed at station L4. The effects of elevated pCO_2 and temperature on succession from diatoms to dinoflagellates in late summer at L4 is presently unknown.

6.2 Sampling and experimental set-up

Experimental seawater containing a natural phytoplankton and seawater medium was collected on 5th September 2016 as per the methods described in chapter 2, section 2.2. The experimental seawater was gently and thoroughly mixed and transferred in equal parts from each carboy (to ensure homogeneity) to sixteen 2.5 L borosilicate incubation bottles (4 sets of 4 replicates). The remaining experimental seawater was sampled for initial (T0) concentrations of nutrients, chlorophyll *a*, total alkalinity, dissolved inorganic carbon, particulate organic carbon (POC) and nitrogen (PON) and was also used to characterise the starting experimental phytoplankton community. The incubation bottles were placed in an outdoor simulated in-situ incubation culture system (see chapter 3 for detailed experimental set-up) and each set of replicates were linked to one of four 22 L media reservoirs filled with the filtered seawater media. The media was enriched with CO_2 gas as per the method described in chapter 3 and used for the microcosm dilutions as per the following experimental design: 1) control (400 µatm pCO_2, 15.8 °C matching station L4 in-situ values), 2) high temperature (400 µatm pCO_2, 19.8 °C), 3) high pCO_2 (800 µatm pCO_2, 15.8 °C) and 4) combination (800 µatm pCO_2, 19.8 °C).

Initial nutrient concentrations (measured at 0.26 µM nitrate + nitrite and 0.09 µM phosphate and 1.35 µM silicate on 5th September 2016) were amended to 8 µM nitrate+nitrite and 0.5 µM phosphate.

6.2.1 Experimental sampling

pH was monitored daily to adjust the pCO_2 of the experimental media (+/-) prior to dilutions to maintain target pCO_2 levels in the incubation bottles. Samples for Chl *a*, total alkalinity (TA) and dissolved inorganic carbon (DIC) were taken every 2-3 days. Samples for particulate organic carbon (POC), particulate and organic nitrogen (PON) were taken at T0 and T30.Samples for community analysis were taken at T8, T17, T22 and T30. Samples for FRRf fluorescence-based light curves were taken at T0 and T30.

6.2.2 Statistical analysis

To test for effects of high pCO_2, high temperature and high pCO_2 x high temperature on the measured response variables (Chl *a*, total community biomass, POC, PON, photosynthetic parameters and biomass of individual species), generalised linear mixed models were applied to the data (repeated measures) with the factors pCO_2, temperature and time (and all interactions) Where main effects were established, pairwise comparisons were performed using the method of Herberich *et al.*, (2010) for data with non-normality and/or heteroscedasticity. Between treatment differences over the time course of the experiment were visualized using non-metric multidimensional scaling ordination (nMDS). The Bray-Curtis index was used to calculate the resemblance of biomass in each experimental treatment based on the community structure. The resulting resemblance matrix was then used to perform an ordination nMDS. Individual group and species vectors were then superimposed on the nMDS ordination and their resulting contribution to biomass was represented by the proximity to experimental treatments. Weekly biomass values from the L4 time-series were averaged over years to elucidate the variability and seasonal cycles of the dominant species observed in the experimental community at T30, relative to the time-series observations. All time series sample sizes are given in the figure

legends of the plotted data. The distribution of these species' biomass at station L4 was also analysed relative to the in-situ temporal gradients of temperature (1993-2014) and pCO_2 (2008-2014) using frequency histograms. All statistical data are reported as the arithmetic means with standard deviation describing the error term, unless otherwise stated. Analyses were conducted using the R statistical package (R Core Team (2014). R: A language and environment for statistical computing. R Foundation for Statistical Computing, Vienna, Austria).

6.3 Results

Chl *a* concentration in the WEC ranged between 0.7 and ~4 mg m^{-3} from 30th August – 5th September 2016 based on MODIS weekly composite satellite data with a concentration of 1.5 mg m^{-3} at station L4 on 5th September 2016 (**Fig. 6.1 A**). Over the period leading up to phytoplankton community sampling, increasing silicate concentrations coincided with a chl *a* peak between 15th-22nd August (**Fig. 6.1 B**). Routine time series net trawl (20µm) sample observations indicated a dinoflagellate bloom dominated by *Ceratium* and *Dinophysis* spp.. This was followed by decreasing silicate and increasing nitrate+nitrite concentrations coincident with a smaller secondary chl *a* peak on 5th September where dinoflagellates remained dominant and net trawl observations also indicated a diverse diatom community dominated by *Pseudonitzschia* spp. (data not shown).

6.3.1 Experimental carbonate system

Equilibration to the target high pCO_2 value (800 µatm) in the high pCO_2 and combination treatments was achieved by T4 (**Fig. 6.2. A.**). Mean pCO_2 values within the control and high temperature treatments were 392.9 (± 4.4) and 401.4 (± 3.7) µatm respectively, while in the high pCO_2 and combination treatments (following equilibration) mean pCO_2 values were 827.7 (± 30.2) and 847.4 (± 22.2) µatm respectively. Carbonate system values remained stable throughout the experiment, though pCO_2 was higher than the experimental target in the high pCO_2 and combination treatments. However, there were no significant differences between the

respective high pCO_2 treatments. **Fig. 6.2 B, C, D, E** and **F** show other carbonate system parameter values.

6.3.2 Experimental temperature treatments

Mean temperatures in the control and high pCO_2 treatments were 15.9 °C (± 0.2), (**Fig. 6.3 A**). In the high temperature and combination treatments mean temperatures were 19.6 °C (± 0.2) resulting in a mean difference between the ambient and high temperature treatments of 3.8 °C (± 0.3).

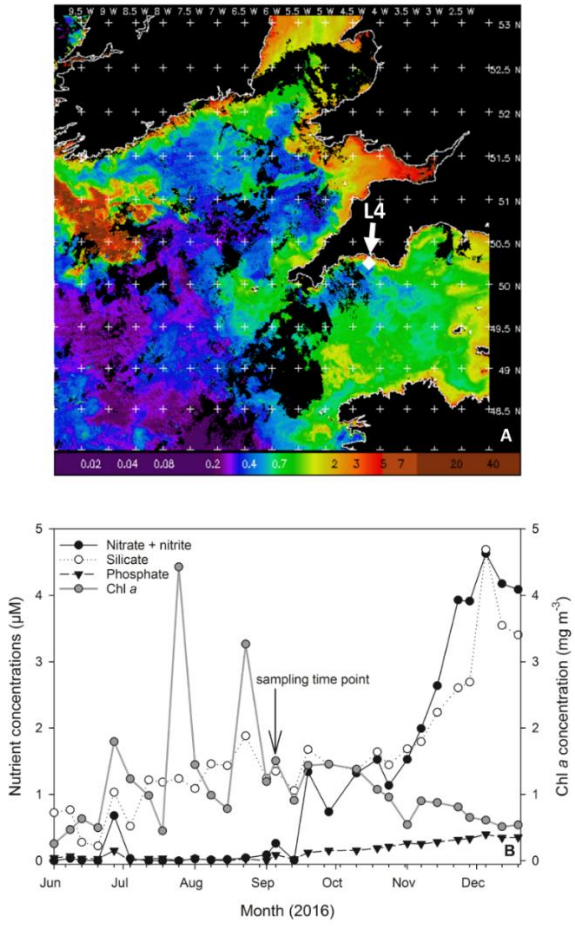

Fig. 6.1. MODIS weekly composite chl *a* image of the western English Channel over the period 30th August – 5th September 2016 (surface chl a averaged over the week coincident with phytoplankton community sampling for the present study), processing courtesy of NEODAAS. The position of coastal station L4 is marked with a white diamond (**A**). Time-series of weekly nutrient and chl *a* concentrations from station L4 at a depth of 10 m over the second half of 2016 in the months prior to phytoplankton community sampling (indicated by black arrow and text) (**B**).

6.3.3 Chlorophyll *a*

Mean chl *a* in the experimental seawater at T0 was 1.38 (± 0.04) mg m^{-3} (**Fig. 6.4 A**). This decreased in all treatments between T0 and T3 with mean concentrations of 0.36 (± 0.21), 1.22 (± 0.43), 0.56 (± 0.18) and 0.97 (± 0.33) mg m^{-3} in the control, high temperature, high pCO_2 and combination treatments, respectively. When considering all data, chl *a* was not significantly influenced by the high pCO_2 or high temperature treatments, but rather through time. It was however, significantly negatively influenced by the combination treatment (**Table 6.1**). Between T3 and T7 the high pCO_2 and combination treatments increased chl *a* concentration relative to the control and high temperature treatments, though not significantly due to high variability within the control replicates. Overall, chl *a* concentration increased in all treatments over time with the highest concentration at T30 in the control (5.44(± 0.11) mg m^{-3}). At T30 the concentrations in the high temperature, high pCO_2 and combination treatments were 3.94 (± 0.20), 3.60 (± 0.18) and 2.95 (± 0.54) mg m^{-3}, respectively, which were all significantly lower than the control (pairwise comparisons: t = -18.894, p < 0.001, t = -22.543, p < 0.001, t = -8.346, p < 0.001, respectively (n = 16)). Additionally, pairwise comparisons showed the high pCO_2 and combination treatments chl *a* concentration to be significantly lower than the high temperature treatment at T30 (t = -3.431, p = 0.007; t = -4.797, p < 0.001, (n = 16)).

6.3.4 Phytoplankton biomass

The initial biomass was 140.1 (± 2.78), 129.5 (± 0.37), 121.4 (± 0.91) and 125.2 (± 2.92) mg C m^{-3} in the control, high temperature, high pCO_2 and combination treatments, respectively. The community was dominated by dinoflagellates (~46%) with smaller contributions from diatoms (~16%), nanophytoplankton (~15%), ciliates (~11%), cryptophytes (~5%), *Synechococcus* (~4%), picophytoplankton (~2%) and coccolithophores (~1%). Total biomass increased significantly in all treatments over time between T0 and T30, though significant treatment influences were only detected for the high temperature and combination treatments which showed a positive and negative response, respectively (**Fig. 6.4 B, Table 6.1**). At T30 biomass

was significantly higher in the high temperature treatment compared to the control, with a 14-fold increase from T0 to 1973 (± 114.21) mg C m^{-3} (pairwise comparison: $t = 12.330$, $p < 0.001$, (n = 16)).

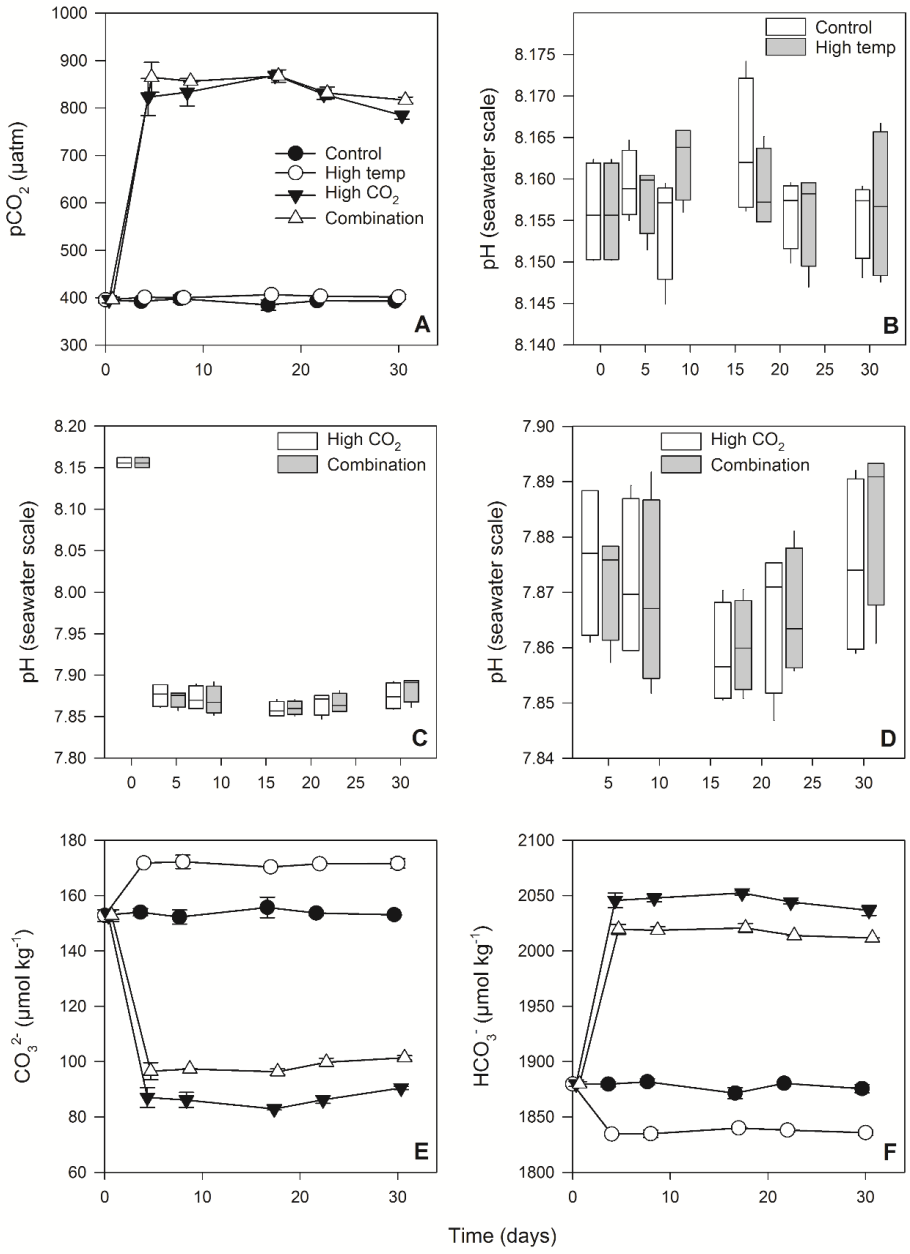

Fig. 6.2. Carbonate system values of the experimental phytoplankton incubations. (**A**)**.** partial pressure of CO_2 in seawater (pCO_2), (**B, C & D**)**.** pH on the seawater scale, (**E**)**.** carbonate concentration (CO_3^{2-}) and (**F**)**.** bicarbonate concentration (HCO_3^-) were calculated from direct measurements of total alkalinity and dissolved inorganic carbon. Note: pH for high CO_2 and combination treatments shown twice (in **C & D)** for finer scale at target concentration.

Total biomass in the high pCO_2 treatment increased more than 11-fold from T0 to T30 (1504 ± 12.99) mg C m^{-3} and was significantly higher than the control and combination treatments (pairwise comparisons: $t = 10.574$, $p < 0.001$, $t = -21.665$, $p < 0.001$, respectively, (n = 16)). The lowest biomass at T30 was measured in the combination treatment which was significantly lower when compared to the control (1045 (± 43.06) compared to 1249 (± 49.60) mg C m^{-3} (pairwise comparison: t = -6.582, p < 0.001, (n = 16)).

Measured POC at T0 and T30 corresponded well with estimated total phytoplankton biomass (R^2 0.996) and followed the same trends between T0 and T30 as biomass estimates (**Figs. 6.4 C & D, Table 6.1**). PON showed different responses than POC at T30 and was significantly higher in the high pCO_2 treatment (121.67 (± 7.74) mg m^{-3}) compared to the control and combination treatment (pairwise comparisons: $t = 4.014$, $p < 0.01$, $t = 7.352$, $p < 0.0001$, respectively (n = 16)). (**Fig. 6.4 E, Table 6.1**). PON was lowest in the combination treatment (89.79 (± 7.23) mg m^{-3}) which was significantly lower than the control (103.08 (± 5.23 mg m^{-3}), pairwise comparison: $t = -4.241$, $p < 0.01$, (n = 16)). POC:PON ratios were consequently, significantly higher in the high temperature treatment compared to all other treatments (**Fig. 6.4 F, Table 6.1**) and were 36%, 33% and 50% higher than the control, high pCO_2 and combination treatments (17.29 compared to 12.68, 12.99 and 11.48 mg m^{-3} respectively). There was no significant difference between the control and high pCO_2 treatment POC:PON ratio whereas the combination treatment ratio was significantly lower than all other treatments (**Table 6.1**).

6.3.5 Carbon:Chlorophyll *a*

The initial mean C:Chl *a* was 94.70 (± 6.12) mg C:mg Chl *a* across all treatments and the control. Significant differences in C:Chl *a* were time-dependent and variable when considering all of the data (**Fig 6.5**, **Table 6.1**). Early in the experiment the highest ratio at T8 was in the control

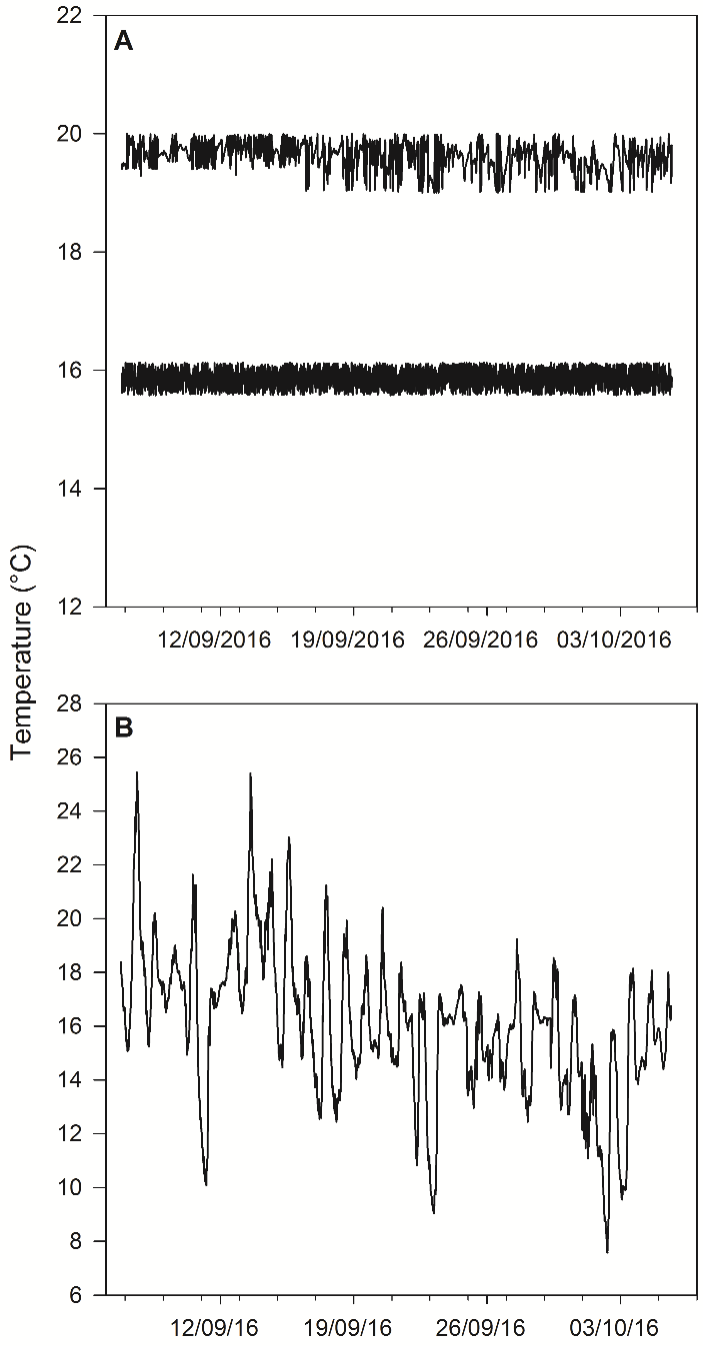

Fig. 6.3. Time course of temperature treatments throughout the experiment. Control and high CO_2 treatments maintained at a mean temperature of 15.85 °C and the high temperature and combination treatments maintained at a mean temperature of 19.62 °C (**A**). External ambient air temperature (**B**).

(247.88 (± 34.61) mg C:mg Chl *a*) followed by the high temperature treatment (158.06 (± 11.13) mg C:mg Chl *a*) which was significantly lower than the control (pairwise comparison: t = -5.241, $p < 0.001$, (n = 16)). At this time point, C:Chl *a* values in the high CO_2 and combination treatments were significantly lower than the high temperature treatment and control (pairwise comparisons: high CO_2; t = -8.559, $p < 0.001$ and t = -8.598, $p < 0.001$ respectively, combination; t = -9.790, p = < 0.001 and t = -8.864, $p < 0.001$ respectively, (n = 16)). At T17 the high temperature and combination treatment C:Chl *a* were significantly higher than in the control (pairwise comparison: t = 10.511, $p < 0.001$ and t = 3.075, $p < 0.05$ respectively, (n = 16)) while the ratio in the high CO_2 treatment remained significantly lower than the high temperature treatment (pairwise comparison: t = -3.165, $p < 0.05$, (n = 16)). Ratios in the high temperature and high CO_2 treatments increased sharply between T17 until T30 when they were 501.42 (± 24.33) and 417.82 (± 14.39) mg C:mg Chl *a* respectively while C:Chl *a* in the combination treatment increased sharply from T24 to T30 attaining a ratio of 364.34 (± 74.79) mg C:mg Chl *a*. At T30 all experimental treatment ratios were significantly higher than the control (pairwise comparisons: high temperature; t = 21.908, $p < 0.001$, high CO_2; t = 21.540, $p < 0.001$ and combination; t = 3.788, $p < 0.01$, (n = 16)), while the high CO_2 and combination treatment ratios were significantly lower compared to the high temperature treatment (Pairwise comparisons: high CO_2; t = -6.274, $p < 0.001$, combination; t = -3.697, $p < 0.05$, (n = 16)).

6.3.6 Community composition

Diatoms dominated biomass in all treatments at T30 followed by nanophytoplankton which exhibited the highest contribution in the ambient control (**Fig. 6.6A**). The least diverse communities were the in the high temperature and high pCO_2 treatments (**Fig. 6.6 B & C**) and the most diverse community was in the combination treatment, where dinoflagellates and *Synechococcus* became increasingly prominent (**Fig. 6.6 D**).

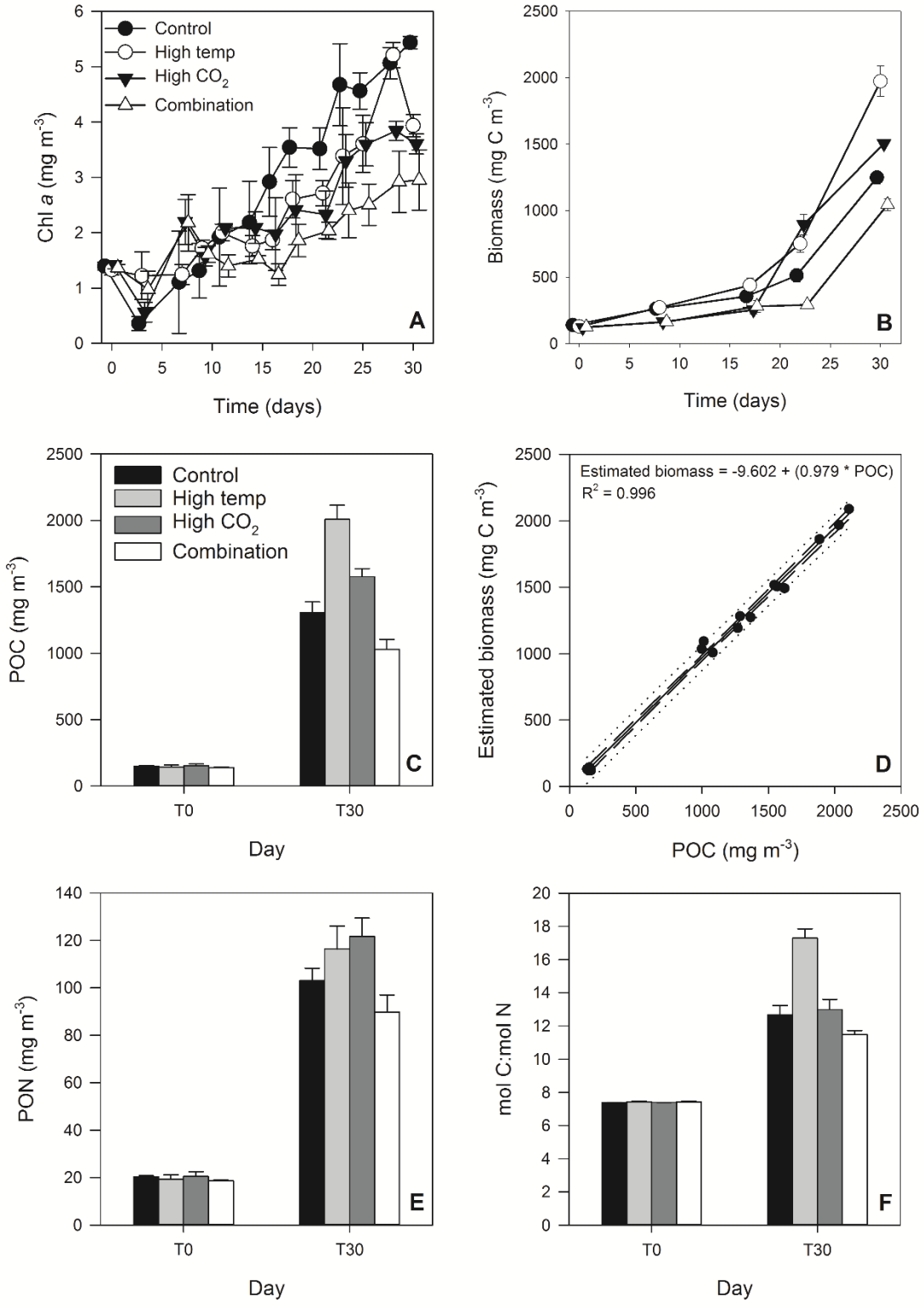

Fig. 6.4 Time course of chl *a* (**A**), phytoplankton biomass (**B**), POC (**C**), regression of calculated phytoplankton carbon vs measured POC (**D**), PON (**E**) and POC:PON (**F**).

Table 6.1. Results of generalised linear mixed model testing for effects of all variables and interactions on chl a, phytoplankton biomass POC and PON. Significant results are in bold; * p < 0.05, ** p < 0.001, *** p < 0.0001.

Response variable	n	*df*	z-value	*p*	sig
Chla (mg m^{-3})					
High temp	588	578	0.843	0.3991	
High CO_2	588	578	0.951	0.3416	
Combination	588	578	1.05	0.2936	
Time	588	578	4.85	**<0.001**	***
Time x high CO_2	588	578	-1.132	0.2576	
Time x high temp	588	578	-1.382	0.167	
Time x combination	588	578	-1.962	**<0.05**	*
Estimated biomass (mg C m^{-3})					
High temp	80	70	-0.347	0.729	
High CO_2	80	70	-1.244	0.214	
Combination	80	70	-1.05	0.294	
Time	80	70	6.466	**<0.001**	***
Time x high CO_2	80	70	0.499	0.618	
Time x high temp	80	70	2.140	**<0.05**	*
Time x combination	80	70	-2.180	**< 0.05**	*
mg C: mg Chla					
High temp	80	70	-0.245	0.807	
High CO_2	80	70	-0.451	0.652	
Combination	80	70	-0.377	0.706	
Time	80	70	1.028	**<0.01**	**
Time x high CO_2	80	70	0.562	0.574	
Time x high temp	80	70	0.64	0.522	
Time x combination	80	70	0.452	0.652	
POC (mg m^{-3})					
High temp	32	26	-0.435	0.664	
High CO_2	32	26	-0.233	0.816	
Combination	32	26	-0.276	0.782	
Time	32	26	6.438	**<0.001**	***
Time x high CO_2	32	26	0.898	0.369	
Time x high temp	32	26	2.137	**< 0.05**	*
Time x combination	32	26	-2.291	**< 0.05**	*
PON (mg m^{-3})					
High temp	32	26	-0.082	0.93433	
High CO_2	32	26	0.001	0.9996	
Combination	32	26	-0.113	0.90993	
Time	32	26	2.888	**< 0.001**	**
Time x high CO_2	32	26	2.081	**<0.05**	*
Time x high temp	32	26	1.397	0.162	
Time x combination	32	26	-2.318	**< 0.05**	*
mg POC: mgPON					
High temp	32	26	-0.019	0.9845	
High CO_2	32	26	0.005	0.9963	
Combination	32	26	0.032	0.9743	
Time	32	26	2.324	**<0.05**	*
Time x high CO_2	32	26	0.120	0.904	
Time x high temp	32	26	1.897	**<0.05**	*
Time x combination	32	26	-1.767	**<0.05**	*

The nMDS analysis showed similarities in the biomass between treatments between T0 and T8. At T17 the biomass of the control and high pCO_2 treatment diverged away from the high temperature and combination treatments. Dissimilarity of all treatments was most notable at T30 (**Fig. 6.6 E**). The analysis performed an excellent representation of the biomass with a stress value of 0.07 in two dimensions.

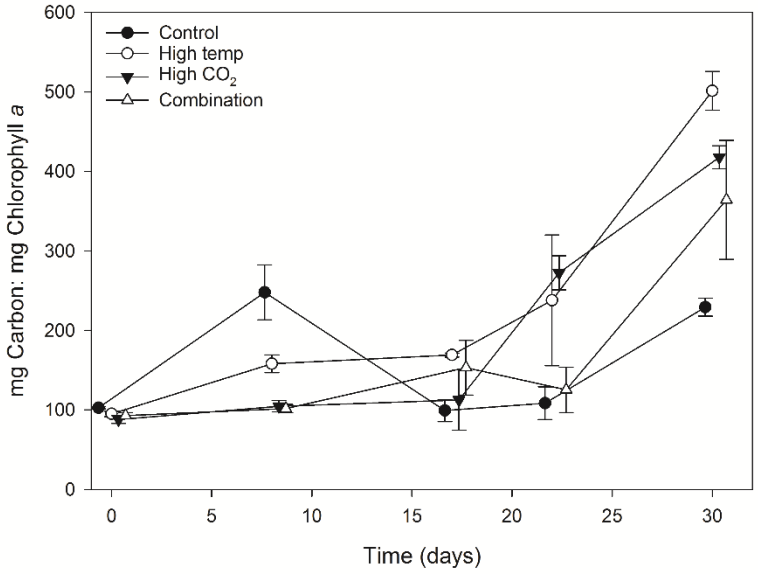

Fig 6.5. Carbon:chlorophyll *a* ratios throughout the experiment.

Diatom biomass was significantly influenced by the high temperature and high pCO_2 treatments positively, while it was significantly negatively influenced by the combination treatment (**Fig. 6.7 A, Table 6.2**). At T30 diatom biomass was significantly higher in the high temperature treatment relative to all other treatments, increasing more than 90-fold from T0 with biomass attaining 1661 (± 103.38) mg C m^{-3} (pairwise comparisons: $t = 15.609$, $p < 0.001$, $t = 6.380$, $p < 0.001$, $t = 18.866$, $p < 0.001$, when compared to the control, high pCO_2 and combination treatments, respectively, (n = 16))). Diatom biomass in the high pCO_2 treatment was significantly higher than the control and combination treatments at 1349 (± 10.54) mg C m^{-3} (pairwise comparisons: $t = 11.907$, $p < 0.001$, $t = 14.063$, $p < 0.001$, respectively, (n = 16)), whereas the combination treatment attained significantly lower diatom biomass compared to

all other treatments (630 (± 52.57) mg C m^{-3} compared to 878 (± 25.41) mg C m^{-3} in the control(pairwise comparison: t = -9.016, p < 0.001 (n = 16)).. In addition to significant differences in diatom biomass amongst the experimental treatments at T30, a shift in species dominance was observed between T0 and T30 and the response in each treatment was species-specific. The T0 starting diatom community biomass was dominated by *Guinardia* spp. (33%), *Thalassiosira* spp. (24%), *Stephanopyxis palmeriana* (9%), *Pseudonitzschia* spp. (10%) and *Proboscia alata* (7%). A diverse diatom community was observed at T0 with the remaining 17% of this biomass comprising a further 20 spp. At T30, the control diatom biomass was dominated by *Cylindrotheca closterium* with smaller contributions from *Leptocylindrus danicus* and *Pseudonitzschia* spp.; the high temperature and combination treatments had biomass dominated by *L. danicus*; whereas in the high pCO_2 treatment *Leptocylindrus minimus* dominated with smaller contributions from *L. danicus* and *C. closterium*.

Nanophytoplankton was not significantly influenced by any of the experimental treatments (**Fig. 6.7 B, Table 6. 2**) and its biomass remained low throughout the experiment until T24 when a sharp increase was observed in all treatments and the control. The highest nanophytoplankton biomass at T30 was attained in the control (364 (± 48.52) mg C m^{-3}) where biomass increased 20-fold from T0 (**Fig. 6.7 B, Table 6.2**). Significantly lower nanophytoplankton biomass was observed in the high pCO_2 treatment (150 (± 8.47) mg C m^{-3} followed by 237 (± 17.99) mg C m^{-3} in the high temperature treatment and 189 (± 22.11) mg C m^{-3} in the combination treatment (pairwise comparisons: t = -9.219, p < 0.001, t = -5.192, p < 0.001, t = -6.945, p < 0.001, respectively, (n = 16)).

Dinoflagellate biomass showed a differential response to the experimental treatments and was significantly influenced by the combination and high temperature treatments (**Fig. 6.7 C, Table 6.2**). Pairwise comparisons showed significantly higher dinoflagellate biomass in the combination treatment compared to the high temperature treatment at T17 (t = 8.252, p < 0.001), T22 (t = 10.89, p < 0.001, (n = 16)) and T30 (t = 17.53, p < 0.001, (n = 16)). At T30

dinoflagellate biomass in the combination treatment was 132 (± 8.05) mg C m^{-3} compared to 49 (± 5.87) mg C m^{-3} in the high temperature treatment and was almost absent in the control (0.54 (± 0.06) mg C m^{-3}) and entirely absent in the high pCO_2 treatment. A shift in dinoflagellate species dominance was observed in the high temperature and combination treatments between T0 and T30. The T0 dinoflagellate community was dominated by the large heterotrophic *Gyrodinium spirale* (63%) with smaller contributions from *Karenia mikimotoi* (11%), *Ceratium* spp. (8%), undetermined (undet.) *Gymnodiniales* (7%), *Azidinium* spp. (5%) and *Katodinium glaucum* (2%). The remaining 4% of dinoflagellate biomass at T0 comprised *Dinophysis acuta*, *Protoperidinium* spp. and *Prorocentrum cordatum*. At T30 undet. *Gymnodinium* spp. became dominant in the high temperature and combination treatments, accounting for 92% and 98% of dinoflagellate biomass, respectively. The exact taxonomic identification of the *Gymnodinium* species present was undetermined through microscopy and to maintain consistency with the station L4 phytoplankton species composition time series, this dinoflagellate genus was collectively classified as undet. *Gymnodiniales*.

Synechococcus and picophytoplankton biomass also exhibited a differential response to the experimental treatments. *Synechococcus* was significantly influenced by the combination and high temperature treatments, but only from T22, while picophytoplankton was significantly influenced only by the combination treatment, also from T22 (**Fig, 6.7 D & E, Table 6.2**). At T30 biomass of *Synechococcus* in the combination treatment (77 (± 6.18) mg C m^{-3}) was significantly higher compared to the high temperature treatment (17.0 (± 2.51) mg C m^{-3}), high pCO_2 treatment (3.4 (± 0.56) mg C m^{-3}) and control (2.4 (± 0.38) mg C m^{-3}), (pairwise comparison: t = 18.928, p = 0.001, t = 25.515, $p < 0.001$, t = 25.107, $p < 0.001$, respectively, (n = 16)). This biomass in the high temperature treatment was significantly higher than the high pCO_2 treatment and control (pairwise comparison: t = 12.480, $p < 0.001$, t = 11.471, $p < 0.001$, (n = 16).

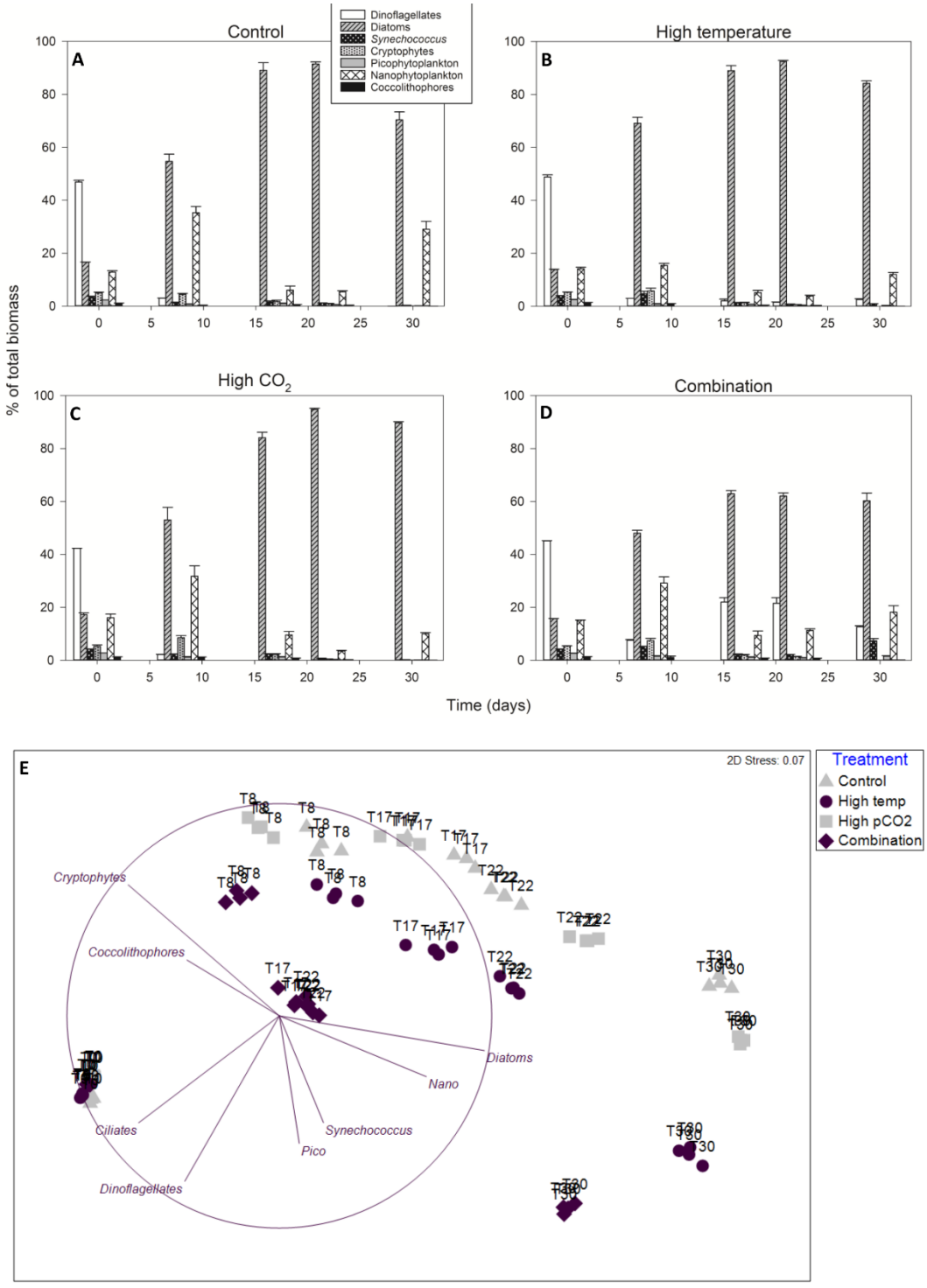

Fig. 6.6. Percentage contribution to community biomass by phytoplankton groups/species in the control (**A**), high temperature (**B**), high CO_2 (**C**) and combination treatments (**D**). nMDS plot structure showing the ordination of differences in phytoplankton biomass over time by experimental treatment in 2 dimensions (numbers are sampling days of the experiment (**E**)

Table 6.2. Results of generalised linear mixed model testing all variables and interactions on individual species biomass. Significant results are in bold; * p < 0.05, ** p < 0.001, *** p < 0.0001.

Response variable	n	*df*	*z*-value	*p*	sig
Diatoms (mg C m^{-3})					
High temp	80	70	-0.087	0.930	
High pCO_2	80	70	-0.353	0.724	
Combination	80	70	-0.392	0.695	
Time	80	70	2.038	**<0.05**	*
Time x high temp	80	70	3.128	**<0.01**	**
Time x high CO_2	80	70	2.148	**<0.05**	*
Time x combination	80	70	-3.467	**<0 .001**	***
Dinoflagellates (mg C m^{-3})					
High temp	80	70	-1.387	0.165	
High pCO_2	80	70	0.017	0.987	
Combination	80	70	-1.127	0.260	
Time	80	70	-4.854	**<0.001**	***
Time x high temp	80	70	4.85	**<0.001**	***
Time x high CO_2	80	70	-1.592	0.111	
Time x combination	80	70	5.843	**<0.001**	***
Nanophytoplankton (mg C m^{-3})					
High temp	80	70	-0.654	0.513	
High pCO_2	80	70	0.017	0.987	
Combination	80	70	-0.22	0.826	
Time	80	70	2.165	**<0.05**	*
Time x high temp	80	70	-0.023	0.982	
Time x high CO_2	80	70	-1.07	0.285	
Time x combination	80	70	-0.587	0.557	
***Synechococcus* (mg C m^{-3})**					
High temp	80	70	0.861	0.3891	
High pCO_2	80	70	0.18	0.857	
Combination	80	70	-1.853	0.064	
Time	80	70	-0.253	0.800	
Time x high temp	80	70	2.733	**<0.01**	**
Time x high CO_2	80	70	-0.306	0.7598	
Time x combination	80	70	6.316	**<0.001**	***
Picophytoplankton (mg C m^{-3})					
High temp	80	70	-0.604	0.546	
High pCO_2	80	70	0.08	0.937	
Combination	80	70	-2.138	<0.05	*
Time	80	70	-0.696	0.486	
Time x high temp	80	70	1.714	0.087	
Time x high CO_2	80	70	-0.368	0.713	
Time x combination	80	70	4.795	**<0.001**	***

Table 6.2 contd.

Coccolithophores (mg C m^{-3})					
High temp	80	70	0.291	0.771	
High pCO_2	80	70	0.199	0.842	
Combination	80	70	0.26	0.795	
Time	80	70	-0.41	0.682	
Time x high temp	80	70	0.197	0.844	
Time x high CO_2	80	70	0.014	0.989	
Time x combination	80	70	-0.016	0.987	
Cryptophytes (mg C m^{-3})					
High temp	80	70	1.027	0.3046	
High pCO_2	80	70	0.58	0.5621	
Combination	80	70	0.359	0.7199	
Time	80	70	-2.341	**<0.05**	*
Time x high temp	80	70	-0.772	0.440	
Time x high CO_2	80	70	-0.709	0.4783	
Time x combination	80	70	-0.817	0.414	
Microzooplankton (mg C m^{-3})					
High temp	80	70	-0.308	0.758	
High pCO_2	80	70	-0.525	0.600	
Combination	80	70	-0.278	0.781	
Time	80	70	-1.918	**<0.05**	*
Time x high temp	80	70	0.143	0.886	
Time x high CO_2	80	70	1.133	0.257	
Time x combination	80	70	0.129	0.8973	

Picophytoplankton biomass at T30 was significantly higher in the combination treatment (16 (± 1.90) mg C m^{-3}) compared to the high temperature treatment (5.5 (± 0.46) mg C m^{-3}), high pCO_2 treatment (1.8 (± 0.06) mg C m^{-3}) and the control (1.26 (± 0.14) mg C m^{-3}), (pairwise comparisons: $t = 11.710$, $p < 0.001$, $t = 16.736$, $p < 0.001$, $t = 16.169$, $p < 0.001$, respectively (n = 16). Biomass in the high CO_2 treatment and control was significantly lower than picophytoplankton biomass in the high temperature treatment (pairwise comparisons: $t = -18.685$, $p < 0.001$, $t = -16.866$, $p < 0.001$, respectively, (n = 16).

Cryptophyte and coccolithophore biomasses were not influenced by experimental treatments (**Fig. 6.7 F & G, Table 6.2**) and low biomasses declined throughout the experiment, collectively contributing less than one percent of community biomass at T30.

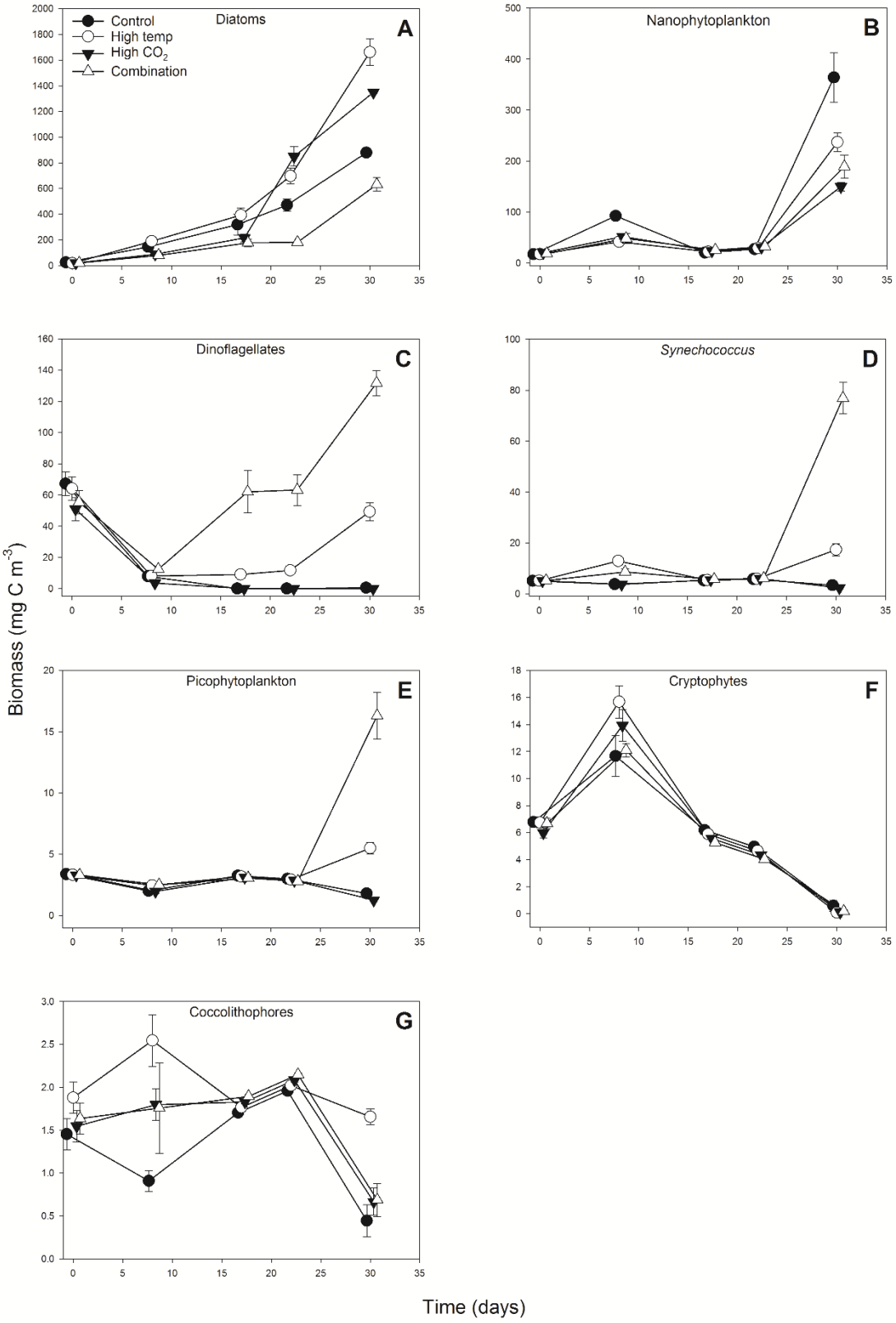

Fig. 6.7 Biomass of individual phytoplankton groups (and *Synechococcus*) in response to experimental treatments.

Initial microzooplankton biomass accounted for ~11% of total biomass (13.81 (± 1.97) mg C m^{-3} and was dominated by *Lohmaniella* spp. with smaller contributions from *Strombilidium* spp. and *Mesodinium* spp.. Beyond T0, the microzooplankton community significantly declined (**Table 6.2**) and was undetected in all treatments and the control except for the high CO_2 treatment, when biomass of *Strombilidium* spp. was 1.18 (± 0.97) mg C m^{-3} at T30 (**Fig. 6.9**).

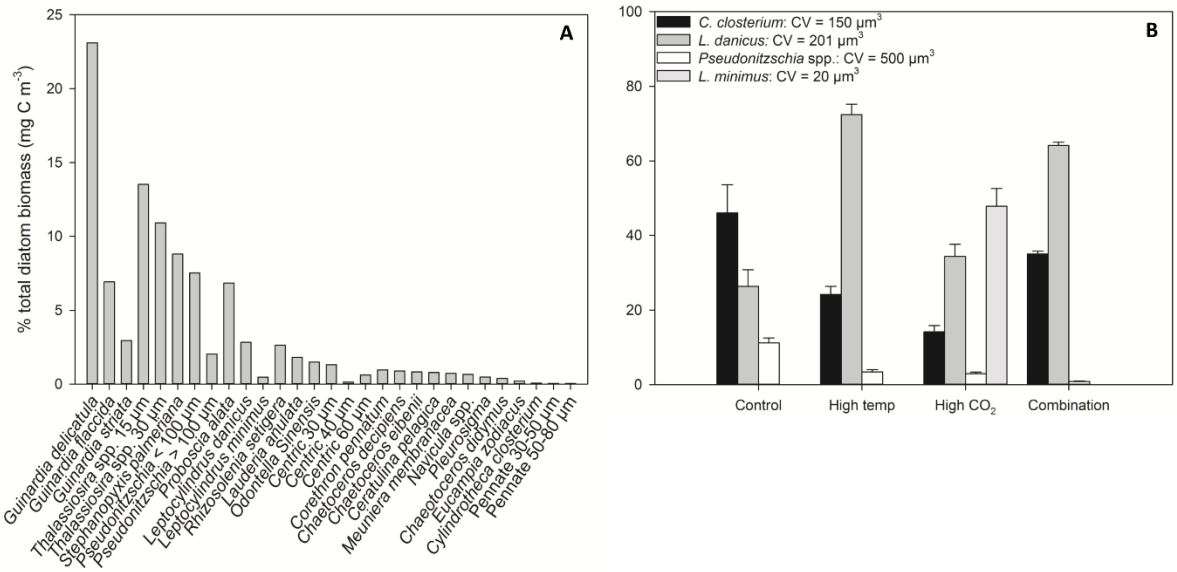

Fig. 6.8 Species contributing to diatom biomass in the initial community at T0 (**A**). This community shifted both in diversity and size range and was dominated by smaller diatoms at T30 (**B**).

6.3.7 Chl fluorescence-based photophysiology

The mean chl *a* normalised maximum photosynthetic rate (P^B_m) among all treatments at T0 was 0.001 (± 0.0005) g C (g chl *a*)$^{-1}$ h^{-1} (**Fig. 6.10 A**), with no significant difference between treatments in any FRRf-based PE curve fitted parameters (**Table 6.3**). The T0 mean light limited photosynthetic efficiency (α slope) among all treatments was 6.79 x10^{-5} (± 2.02 x 10^{-6}) g C (mol photons)$^{-1}$ m^{-2}(chl *a*)$^{-1}$ resulting in a mean light saturation point (E_k) of 145.37 (± 5.63) µmol photons m^{-2} s^{-1}. At T30 PE curve fitted parameters were strongly influenced by the high pCO_2 and high temperature treatments (**Fig. 6.10 B & C, Tables 6.3 & 6.4**).

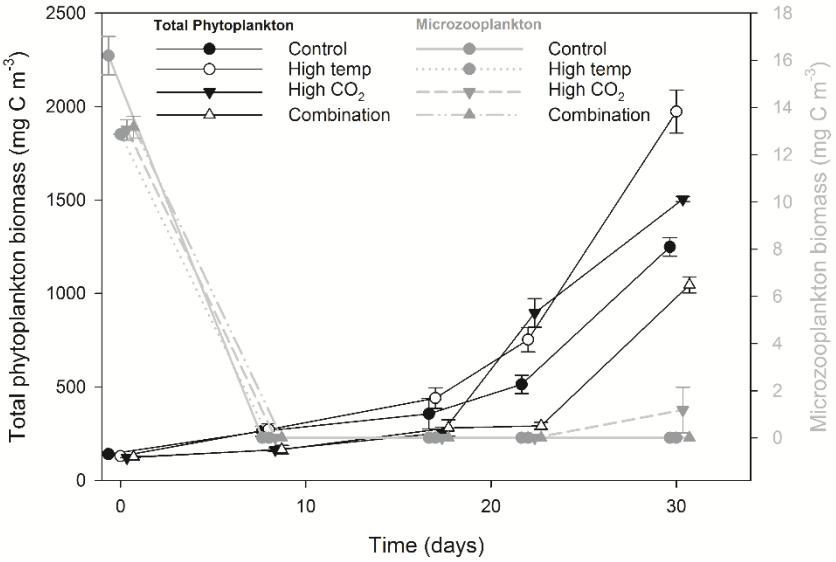

Fig 6.9. Microzooplankton relative to zooplankton throughout the experiment.

P^B_m significantly increased by 83 % from T0 to T30 in the high pCO_2 treatment to 0.018 g C (g chl *a*)$^{-1}$ h^{-1}, **Fig. 6.10 C, Tables 6.3 & 6.4**) and was significantly higher than in the high temperature treatment which increased 50 % from T0 to T30 to 0.0148 g C (g chl *a*)$^{-1}$ h^{-1}) (pairwise comparison: $t = 10.832$, $p < 0.001$, (n = 16)). P^B_m in the high temperature treatment was significantly higher than in the combination treatment and control (pairwise comparisons: $t = 6.912$, $p < 0.001$, $t = 5.332$, $p < 0.001$, respectively, n = (16)), while P^B_m was lower in the combination treatment at T30 compared to the control, although not significantly. Trends in α values were different to P^B_m at T30 (**Fig. 6.10 D, Tables 6.3 & 6.4**) when in the high pCO_2 and high temperature treatments α was 7.56 x10^{-5}(± 3.57 x 10^{-6}) and 6.85 x10^{-5} (± 6.35 x 10^{-6}) g C (mol photons)$^{-1}$ m^{-2} h^{-1} (chl)$^{-1}$, respectively. While pairwise comparisons showed no significant difference between these treatments, they were both significantly higher than in the combination treatment and control (high pCO_2: $t = 8.568$, $p < 0.001$, $t = 10.732$, $p < 0.001$, respectively; high temperature: $t = 3.193$, $p < 0.05$, $t = 4.695$, $p < 0.01$, respectively (n = 16)), while the combination treatment α value was significantly higher than in the control (pairwise comparison: $t = 3.017$, $p < 0.05$, (n = 16)).

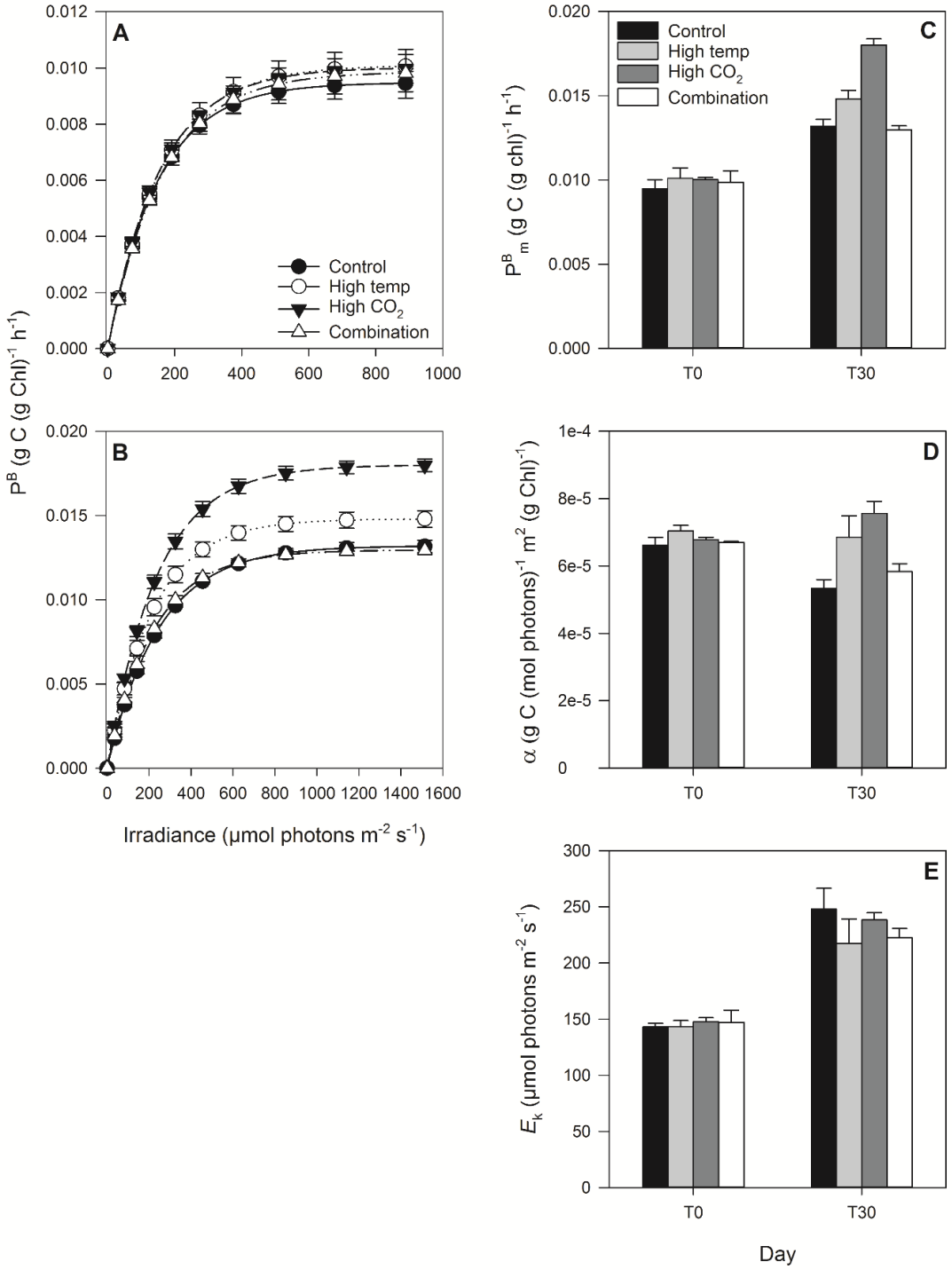

Fig. 6.10. Fitted parameters of FRRf-based photosynthesis-irradiance (PE) curves for the experimental treatments at T0 (**A**) and T30 (**B**). PE parameters for P^B_m (**C**), α (**D**) and E_k (**E**).

There was no significant difference in E_k between the high pCO_2 treatment and control (238.28 (± 6.37) and 248.01 (± 18.42) µmol photons m^{-2} s^{-1}, respectively), whereas the high temperature

treatment and combination treatments exhibited significantly lower E_k values relative to the control, with no significant difference between the high temperature and high pCO_2 treatments (**Fig. 6.10 E, Table 6. 4**).

Table 6.3. FRRf-based photosynthesis-irradiance curve parameters for the experimental treatments at T0 and T30. P^B_m (maximum photosynthetic rates, g C (g chl *a*)$^{-1}$ h^{-1}), α (light limited slope, g C (mol photons)$^{-1}$ m^{-2} h^{-1} (chl)$^{-1}$) and E_k (light saturated point of photosynthesis, µmol photons m^{-2} s^{-1})

Day		Control	sd	High temp	sd	High CO_2	sd	Combination	sd
T0	P^B_m	0.0095	5.35 x10^{-4}	0.0101	6.14 x10^{-4}	0.0100	1.25 x 10^{-4}	0.0099	6.77 x10^{-4}
	α	6.62 x10^{-5}	2.26 x10^{-6}	7.04 x10^{-5}	1.70 x10^{-6}	6.78 x10^{-5}	7.07 x10^{-7}	6.70 x10^{-5}	3.00 x10^{-7}
	E_k	143.12	3.18	143.36	5.26	147.82	3.38	147.19	10.7
T30	P^B_m	0.0132	3.87 x10^{-4}	0.0148	5.08 x10^{-4}	0.0180	3.65 x10^{-4}	0.0130	2.56 x10^{-4}
	α	5.34 x10^{-5}	2.57 x10^{-6}	6.85 x10^{-5}	6.35 x10^{-6}	7.56 x10^{-5}	3.57 x10^{-6}	5.83 x10^{-5}	2.36 x10^{-6}
	E_k	248.01	18.42	217.34	21.79	238.28	6.37	222.28	8.37

Table 6.4. Results of generalised linear mixed model testing for effects of all variables and interactions on phytoplankton photophysiology; P^B_m (maximum photosynthetic rates, g C (g chl *a*)$^{-1}$ h^{-1}), α (light limited slope, g C (mol photons)$^{-1}$ m^{-2} h^{-1} (chl)$^{-1}$) and E_k (light saturated point photosynthesis, µmol photons m^{-2} s^{-1}) at T30. Significant results are in bold; * p < 0.05, ** p < 0.001, *** p < 0.0001.

Response variable	n	*df*	z-value	*p*	sig
P^B_m					
High temp	32	26	5.048	**<0.001**	**
High pCO_2	32	26	15.098	**<0.0001**	***
Combination	32	26	-0.783	0.455	
α					
High temp	32	26	4.802	**< 0.001**	**
High pCO_2	32	26	6.836	**<0.0001**	***
Combination	32	26	1.646	0.138	
E_k					
High temp	32	26	-2.461	**< 0.05**	*
High pCO_2	32	26	-0.764	0.445	
Combination	32	26	-2.054	**<0.05**	*

6.3.8 Natural variability of biomass in the WEC, station L4 time series.

Focussing on diatoms, as they dominated the experimental treatments, the mean annual total diatom biomass over the time series (1993-2014) was 528 (± 199.55) mg C m^{-3} with range of 1150 mg C m^{-3} (occurring in 2012) to 301 mg C m^{-3} (occurring in 2002). Consistently throughout the time-series over a seasonal cycle, mean diatom biomass > 10 mg C m^{-3} was sustained from April until mid-September. In the experimental communities, the dominant diatom species across all treatments at T30 were *L. danicus*, *L. minimus*, *C. closterium* and *Pseudonitzschia* spp. Analysis of these dominant species from the experimental communities relative to their natural variability at station L4 indicates these species to be minor contributors to the L4 diatom carbon budget (**Fig. 6.11**). *L. danicus* was observed to contribute a maximum of ~7 % of total diatom biomass (year 2014: 21.5 mg C m^{-3}), however a larger bloom was observed in 2012 (62.3 mg C m^{-3}), but this only contributed ~5 % of total diatom biomass (~ 3.5 % of total phytoplankton biomass). The maximum *L. minimus* contribution to total diatom biomass was 2 % (year 2000: ~12 mg C m^{-3}, 1 % of total phytoplankton biomass) while the maximum biomass of *C. closterium* was 2.1 mg C m^{-3} in 2010 (0.6% of total diatom biomass). *Pseudonitzschia* spp. was observed to contribute maximal biomass of 6.5% (year 2014: ~6 mg C m^{-3}), though a larger bloom in 1999 resulted in ~49 mg C m^{-3} which was 6.4% of total diatom biomass (2.7% of total phytoplankton biomass).

Temporal trends of *L. danicus* and *L. minimus* over the time series demonstrate biomass to be constrained to between late April to November for both species. Maximal biomass was constrained to between June to mid-September for *L. danicus* (**Fig. 6.12 A**) and June to the 3rd week of August for *L. minimus* (**Fig. 6.12 B**). The mean total annual biomass for *L. danicus* was 14.51 (± 14.53) mg C m^{-3}, whereas for *L. minimus* this was 2.64 (± 3.21) mg C m^{-3}, both species exhibiting high inter-annual variability. *C. closterium* and *Pseudonitzschia* spp. biomass was distributed throughout the year for both species with maximal biomass constrained to between mid-April to the 3rd week of August for *C. closterium* (**Fig. 6.12 C**) and only in the month of June

for *Pseudonitzschia* spp. (**Fig. 6.12 D**). The mean total annual biomass for *C. closterium* was 1.13 (± 0.58) mg C m^{-3} whereas for *Pseudonitzschia* spp. this was 17.59 (± 12.32) mg C m^{-3}, exhibiting high inter-annual variability.

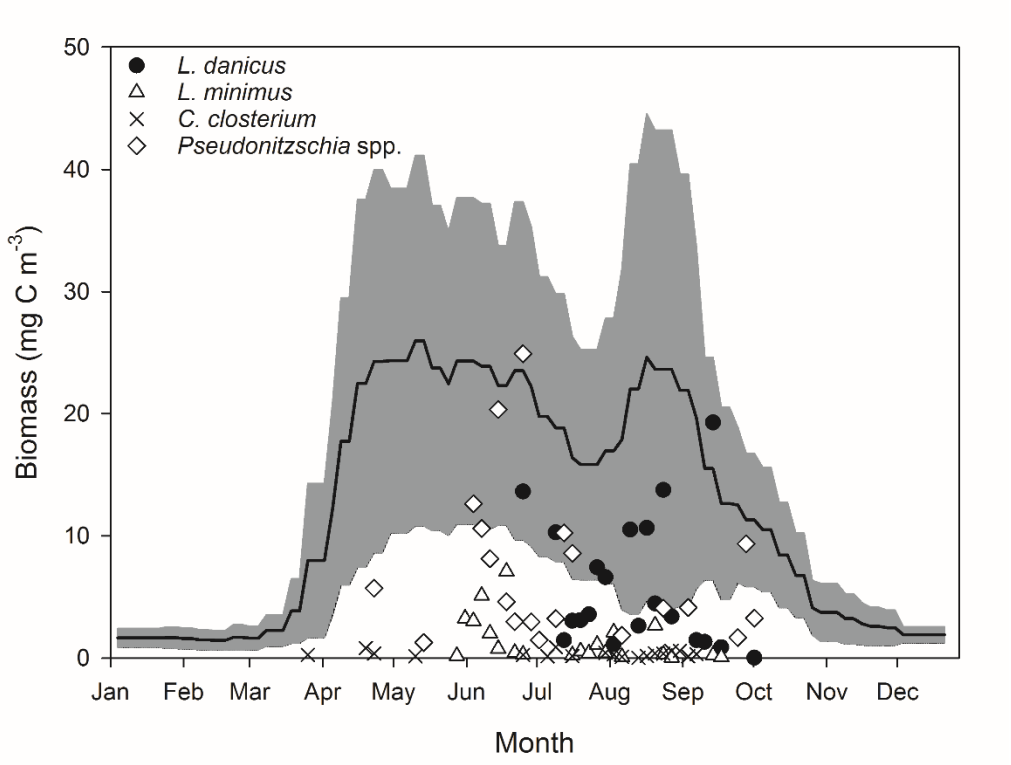

Fig. 6.11. Temporal weekly profile of total diatom carbon biomass at station L4 between 1993-2014 (n = 909). Black line is smoothed running average, grey area is standard deviation. Black circles are maximal L. danicus biomass above the time series mean maxima of 6.43 mg C m-3 (n = 20), open triangles are maximal L. minimus biomass above the time series mean maxima of 1.43 mg C m-3 (n = 21), black crosses are maximal C. closterium biomass above the time series mean maxima of 0.32 mg C m-3 (n = 19) and open diamonds are maximal Pseudinitzschia spp. biomass above the time series mean maxima of 7.19 mg C m-3 (n = 20).

Species-specific optimal temperature ranges were found when considering how the dominant experimental species were temporally distributed relative to in-situ temperatures: For *L. danicus* 68 % of biomass occurred between 14-16 °C, 9 % between 13-14 °C, and 22 % between 16-17.5 °C (**Fig. 6.13 A**). For *L. minimus*, 61 % of biomass occurred between 14-16 °C ,23 % between 13-14 °C, and 6 % between 16-17.5 °C (**Fig. 6.13 B**).

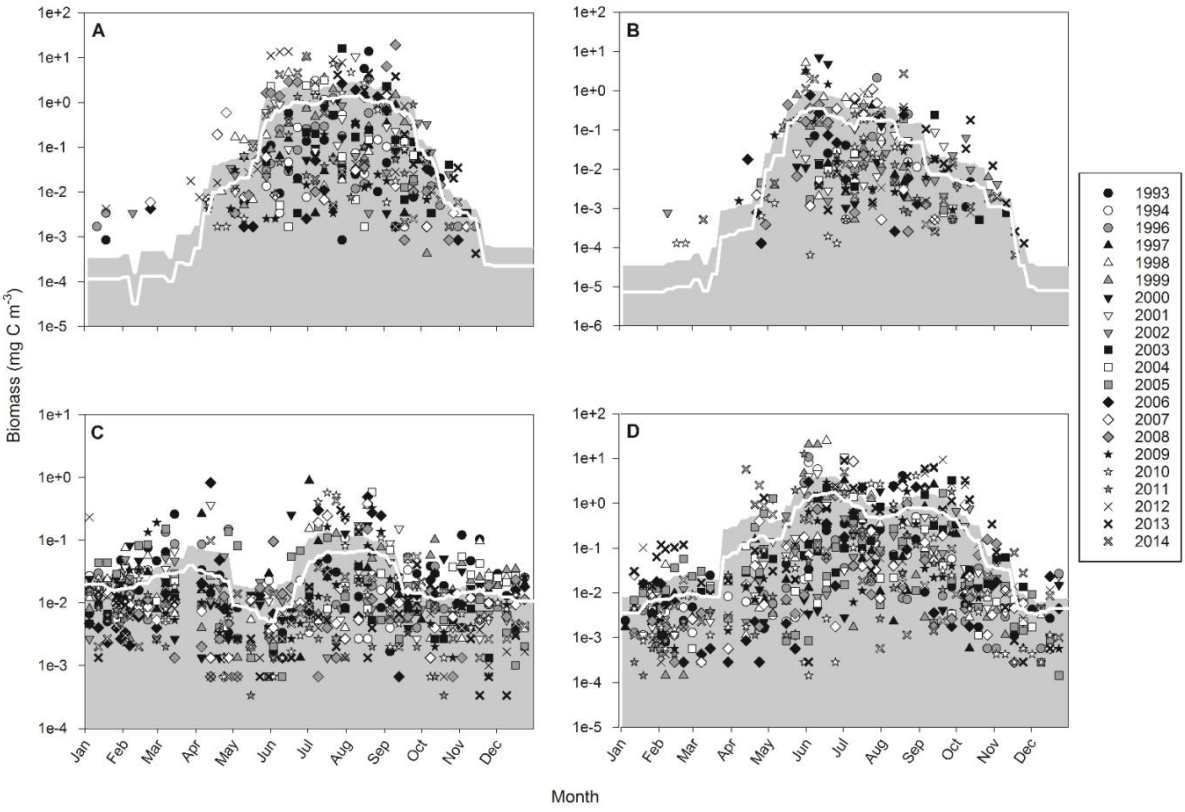

Fig. 6.12. Seasonal profiles of the dominant diatom spp. from the experimental community (common log scale) at station L4 between 1993-2014. White line is smoothed running average, grey area is standard deviation and all symbols are observed data values by year for *L. danicus* (n = 363) (**A**), *L. minimus* (n = 252) (**B**), *C. closterium* (n = 772) (**C**) and *Pseudonitzschia* spp. (n = 927) (**D**).

C. closterium exhibited a much wider temperature optimum with ~50 % of biomass occurring between 8-14 °C, 40 % between 14-16 °C, and only 8 % occurring between 16-17.5 °C (**Fig. 6.13 C**). Similarly, 45 % of *Pseudonitzschia* spp. biomass occurred between 8-14 °C with 35 % and 19 % between 14-16 °C and 16-17.5 °C, respectively (**Fig. 6.13 D**). Biomass distribution relative to station L4 in-situ pCO_2 levels (2008-2014) also demonstrated species-specific optimal ranges. 59 % of *L. danicus* biomass occurred at a pCO_2 range of 245-350 µatm, with 16 % between 350-410 µatm, 10 % between 410-485 µatm and 11 % between 560-680 µatm (**Fig. 6.13 E**). *L. minimus* exhibited a lower pCO_2 optimum range with 92 % of biomass at 245-410 µatm, 2 % between 410-485 µatm, 3 % between 485-560 µatm and 1 % between 560-680 µatm (**Fig. 6.13 F**). *C. closterium* exhibited a wider pCO_2 optimum with 45 % biomass between 245-410 µatm, 25

% between 410-485 µatm, 17 % between 485-560 µatm and 12 % between 560-680 µatm (**Fig. 6.13 G**). Similarly, *Pseudonitzschia* spp. followed a similar trend with 43 % of biomass occurring between 245-410 µatm, 13 % between 410-485 µatm, 9 % between 485-560 and 15 % between 560-680 µatm (**Fig. 6.13 H**).

The dinoflagellate group of undet. *Gymnodiniales* made a significant contribution to total biomass in the combination treatment at T30. The mean annual total dinoflagellate biomass over the time series was 490 mg C m^{-3} with range of 1866 mg C m^{-3} (in 1997) and 83 mg C m^{-3} (in 2011). Mean dinoflagellate biomass > 10 mg C m^{-3} was consistently sustained from July until the first week of October. Analysis of undet. *Gymnodiniales* biomass relative to the natural variability at station L4 indicates this group is a minor contributor to the L4 dinoflagellate biomass carbon budget (**Fig. 6.14 A**). Undet. *Gymnodiniales* were observed to contribute a maximum of 16 % to dinoflagellate biomass (year 2000: 27.55 mg C m^{-3}) which was ~3.5 % of total phytoplankton biomass. However, a maxima of 29.01 mg C m^{-3} was observed in 2001, but this only contributed ~7 % of total dinoflagellate biomass (~1.74 % of total phytoplankton biomass). Temporal trends of undet. *Gymnodiniales* over the time series demonstrate low biomass throughout the year, with maximal biomass tightly constrained to between mid-July to mid-September (**Fig. 6.14 B**). The mean total annual biomass for this group was 6.81 (± 14.92) mg C m^{-3}. Biomass distribution across in-situ temperatures at L4 showed undet. *Gymnodiniales* to have a specific optimum temperature range with 60 % of biomass between 16-17.5 °C, 31 % between 14-16 °C and ~7 % between 13-14 °C (**Fig. 6.14 C**). 52 % of biomass occurred within a pCO_2 range of 350-410 µatm, 12 % between410-485 µatm, 17 % between 485-560 µatm and 14 % between 560-680 µatm (**Fig. 6.14 D**).

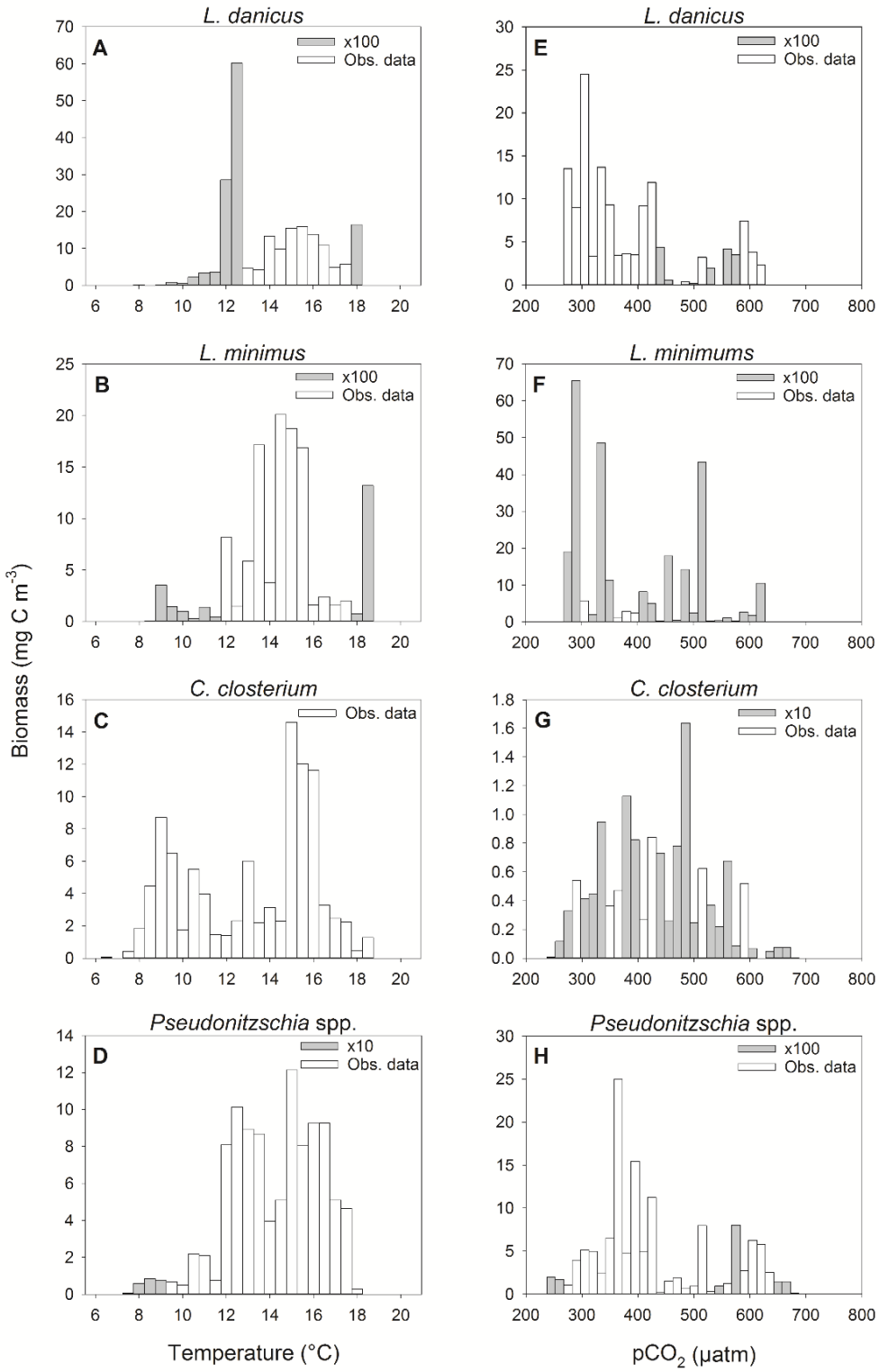

Fig 6.13. Frequency distribution of diatom species biomass at station L4 along the in-situ temporal gradients of temperature (1993-2014) and pCO_2 (2008-2014) for *L. danicus* (**A. & E.**), *L. minimus* (**B. & F.**), *C. closterium* (**C. & G.**) and *Pseudonotzschia* spp. (**D. & H.**).

6.4 Discussion

Individually, elevated temperature and pCO_2 resulted in the highest biomass and light saturated photosynthetic carbon fixation rates (P^B_m) together with significant shifts in community composition, exhibiting near mono-specific dominance of diatoms. The interactive effects of these two factors significantly reduced total biomass and photosynthetic rates to values below the ambient control. However, the combination treatment exhibited the greatest diversity of phytoplankton functional groups.

Temperature exerts a substantial influence on most cellular processes. Consequently, growth and metabolic rates are enhanced by increasing temperatures until a species' optimum is reached. A further increase in temperature beyond this optimum is detrimental, leading to reduced growth rates, cellular damage, and eventually cell death (Boyd et al., 2010; Finkel et al., 2009; Raven and Geider, 1988). Increasing temperature increases the substrate-saturated reaction rate of RUBISCO and thus the potential growth rates of phytoplankton, if growth is not limited by inorganic carbon or other factors (Beardal and Raven, 2004). Elevated pCO_2 has been shown to enhance phytoplankton growth and photosynthesis since many phytoplankton species have active uptake systems for inorganic carbon, rendering carbon assimilation saturated under present day pCO_2 levels (Giordano et al., 2005). Elevated pCO_2 may therefore lead to lowered energetic costs of carbon assimilation in some species and a redistribution of the cellular energy budget to other processes (Tortell et al., 2002, 2008b) such as growth and photosynthesis (Gao, 2017).

6.4.1 Chl *a*

Chl *a* concentration was significantly higher in the ambient control at T30 where total biomass was lower relative to the high pCO_2 and high temperature treatments. This result contrasts most pCO_2 enrichment and elevated temperature studies where chl *a* concentration is generally highly correlated with phytoplankton biomass, e.g. (Feng et al., 2009). However, Hare et al., (2007) reported higher chl *a* concentrations within ambient control replicates compared to

elevated pCO_2 and temperature treatments when biomass was enhanced during shipboard bottle incubations. As the control replicates in the present study exhibited the greatest contribution of nanophytoplankton biomass amongst all treatments, the likely explanation for differences in chl *a* concentration may be attributed to differences in community composition, which highlights that chl *a* may not always be a reliable proxy for biomass in mixed communities. However, in the high pCO_2, high temperature and combination treatments, chl *a* concentration was proportional to total biomass.

6.4.2 Biomass

The present study shows that the natural phytoplankton community biomass response to elevated temperature and pCO_2 is variable, and in accordance with a growing body of literature, demonstrates that community composition plays an important role in determining these responses. A ~4 °C increase in temperature caused higher biomass of micro-phytoplankton, which is similar to the findings of Feng et al., (2009) and Hare et al., (2007). Under elevated temperature however, some studies in the Western Baltic Sea and Arctic Ocean observed a decrease in nanophytoplankton biomass (Coello-Camba et al., 2014; Moustaka-Gouni et al., 2016). pCO_2 elevated to 800 μatm also caused an increase in biomass, which has also been observed by Kim et al., (2006) and Riebesell et al., (2007). By contrast, other studies observed no pCO_2 effect on biomass (Delille et al., 2005; Paul et al., 2015b). When elevated temperature and pCO_2 were combined, the biomass decreased which has also previously been observed by Gao et al., (2017), but the opposite was reported by Calbet et al., (2014) and Feng et al., (2009). Geographic location and season also play an important role in structuring the community and its response in terms of biomass to elevated temperature and pCO_2, (e.g. Li et al., 2009; Morán et al., 2010). Microzooplankton biomass crashed in all treatments at the start of the experiment and was undetected in all treatments and the control other than very low biomass in the high CO_2 treatment at the experiment end. This implies an almost complete lack of top-down grazing pressure leading to a clearer response of the phytoplankton biomass to experimental

treatments, while in natural systems grazers play an important role in regulating phytoplankton community structure (e.g. Strom, 2002).

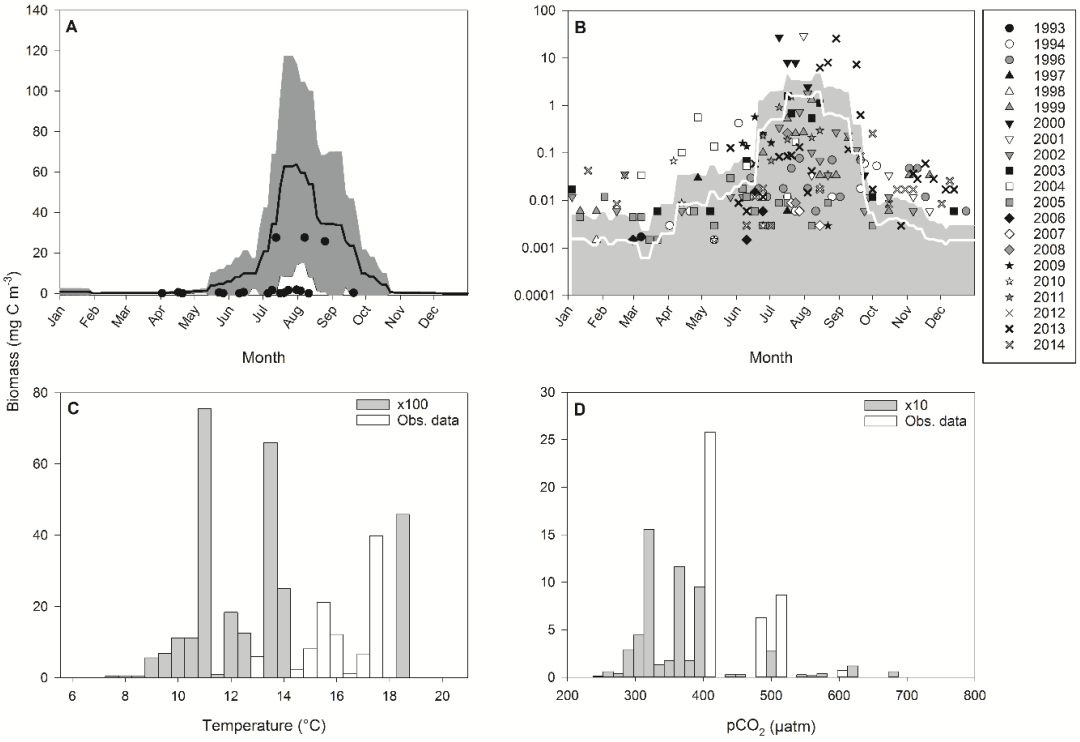

Fig 6.14. Temporal weekly profile of total dinoflagellate carbon biomass at station L4 between 1993-2014 (n = 090). Black line is smoothed running average, grey area is standard deviation and black circles are maximal undet. *Gymnodiniales* biomass above the time series mean maxima of 4.33 mg C m^{-3} (n = 20) (**A**). Seasonal profiles of undet. *Gymnodiniales* (common log scale) at station L4 between 1993-2014 (n = 183). White line is smoothed running average, grey area is standard deviation and all symbols are observed data values by year (**B**). Frequency distribution of *Gymnodiniales* biomass at station L4 along the in-situ temporal gradients of temperature (1994-2014) (**C**) and pCO_2 (2008-2014) (**D**).

6.4.3 Carbon:Chlorophyll *a*

C:Chl *a* was significantly higher under individual treatments of warming and elevated pCO_2, particularly from T24 to T30. Chl *a* in both treatments was not significantly different between T18 and T25, though diatom biomass increased more rapidly under warming over this period, explaining the higher C:Chl *a* ratios under warming. While significantly lower in the control and when warming and elevated pCO_2 were combined, C:Chl *a* increased to a lesser degree between

T24 and T30. During this period, when total community biomass was significantly lower relative to the individual warming and elevated pCO_2 treatments, nanophytoplankton biomass increased in the control and pico- and nanophytoplankton as well as *Synechococcus* biomass increased under the combined effects of elevated pCO_2 and warming. The increase in ratios at T30 in the control and combined treatment may be explained by higher C:Chl *a* of pico- and nanophytoplankton compared to diatoms (Sathyendranath et al., 2009) and thus the observed C:Chl *a* appeared tightly coupled to community composition as well as total community biomass in all treatments and the control.

6.4.4 Carbon:Nitrogen

The experimental results showed a reduction in C:N under elevated pCO_2 alone and further reductions in combined treatments which has also been reported by Fu et al., (2007). Stoichiometry of cellular C and N in phytoplankton are emerging as important factors of marine biogeochemistry. Variability in elemental requirements can influence nutrient limitation patterns and stress (Bonachela et al., 2013), nitrogen fixation rates (Mills and Arrigo, 2010) and the link between nutrient supply and C export which ultimately feedback to atmospheric CO_2 (Teng et al., 2014). However C:N increased under elevated temperature alone, similar to Lomas and Glibert, (1999) in diatom communities, which indicates shifts in biogeochemistry in warmer oceans. By contrast, other studies have found an increase in C:N in response to combined elevated temperature and pCO_2 (Calbet et al., 2014) or no significant response (Kim et al., 2006b; Paul et al., 2015a). Increased C:N under warming could lead to lowered nutritional value of phytoplankton which may affect the efficiency of zooplankton reproduction. This has implications for ecosystem dynamics, processes and biogeochemical cycles. Lowered C:N under combined elevated temperature and pCO_2 however, may enhance these processes.

6.4.5 Photosynthetic carbon fixation rates

Studies on laboratory cultures have shown that increased temperatures can increase photosynthetic rates (Feng et al., 2008b; Fu et al., 2007b; Hutchins et al., 2007). The same trend

was also observed in the present study (**Fig. 7 B**), but the increase in photosynthetic carbon fixation rates (P^B_m) was lower compared to the high pCO_2 treatment, which contrasts observations in other natural population studies which found a reduction in P^B_m (Feng et al., 2009; Hare et al., 2007b). The highest P^B_m under elevated pCO_2 alone observed in the present study is consistent with the findings of Riebesell et al., (2007) and Tortell et al., (2008). The most striking result in the present study was the significant reduction in P^B_m under the combined treatment which has also been observed in similar experiments on natural populations (Coello-Camba and Agustí, 2016; Gao et al., 2017). Feng et al., (2009) and Hare et al., (2007), however found the opposite effect with the highest P^B_m when temperature and pCO_2 were both elevated. The increased light limited photosynthetic efficiency (α^B) and maximum light saturation level (E_k) under elevated pCO_2, decreased in the combined pCO_2 and temperature treatment which also contrasts the findings of (Feng et al., 2009).

Both pH- and temperature-dependent enzymatic reactions through the Calvin-Benson cycle mediate photosynthetic carbon fixation (Giordano et al., 2005; Portis and Parry, 2007). Consequently, future increases in pCO_2 and temperature are predicted to affect the uptake of dissolved inorganic carbon (DIC) differently amongst phytoplankton groups (Badger et al., 1998). P^B_m and α^B show a strong relationship with temperature (Uitz et al., 2008) and the distribution of the dominant phytoplankton species observed in the present experiment, relative to their thermal niches at station L4 (**Figs. 10 A-D & 11 C**), demonstrate species-specific adaptation to narrow ranges in temperature (Xie et al., 2015). Furthermore, Ribulose Bisphosphate Carboxylase (RuBisCO) is the primary enzyme responsible for photosynthetic carbon fixation, though it has a low affinity for CO_2 (Giordano et al., 2005). Consequently, phytoplankton have evolved adaptive strategies to enhance RuBisCO performance by either altering the affinity of RuBisCO for CO_2 by upregulating RuBisCO activity, or through CCMs (Raven, 2011; Tortell et al., 2000). Through both strategies most phytoplankton achieve photosynthetic saturation under present ambient pCO_2 assuming light and nutrients are not limiting factors (Raven and Johnston, 1991). Therefore, the effect of elevated pCO_2 and

temperature individually and simultaneously, may favour phytoplankton species based on the efficiency of RuBisCO or CCM. The differences in photosynthetic parameters in the present study were therefore likely driven by differences in treatment-specific community composition and largely influenced by diatoms which dominated biomass to a greater extent in the high CO_2 and high temperature treatments. Previous studies have suggested that the photosynthetic carbon fixation rate of diatoms at the present day pCO_2 is close to rate saturation (Burkhardt et al., 2001; Rost et al., 2003). Ratios of CO_2:HCO_3^- uptake in diatoms decrease under conditions of lowered pCO_2 with the opposite relationship when pCO_2 is elevated (Giordano et al., 2005). Additionally, CO_2 in the form of DIC is responsible for regulating CCM gene expression in diatoms (Matsuda et al., 2002). Growth and photosynthetic rates in most diatoms therefore increase under CCM down-regulation when cellular energy switches away from CO_2 acquisition and altered metabolic pathways result in up-regulating photorespiration and heat dissipating processes (Gao, 2017).

6.4.6 Community composition

Phytoplankton community structure changes were observed, with a shift from dinoflagellates to diatoms which was most pronounced under single treatments of elevated temperature and pCO_2. Amongst the diatoms, a distinct size shift to smaller species was observed, the relative ratios of which were treatment-specific. The biomass of nanophytoplankton also increased but was not as high as the diatoms. Previous studies have shown variability in natural community taxonomic shifts though few have considered elevated pCO_2 and temperature in combination. By comparison, under elevated pCO_2, Kim et al., (2006) observed a shift from flagellates to diatoms. A shift in size from small to large diatoms has also been observed by Feng et al., (2010), while a shift from nano- to picophytoplankton has also been reported (Brussaard et al., 2013). Under combined elevated pCO_2 and temperature a shift from a mixed coccolithophore and diatom community to coccolithophore dominance has been observed (Feng et al., 2009), whereas Hare et al., (2007b) observed a shift from diatoms to nanophytoplankton.

Laboratory studies on diatoms have shown varying responses to elevated pCO_2 and temperature. For example, *Thalassiosira pseudonana* incubated at 760 µatm pCO_2 exhibited no effects on growth and photosynthetic efficiency (Crawfurd et al., 2011) whereas at 1000 ppm CO_2 *Phaeodactylum tricornutum* growth increased by 5% and P^B_m by 12% (Wu et al., 2010a). An increase in growth rates by 5 % - 30 % at 750 µatm pCO_2 has also been recorded in *T. pseudonana*, *T. guillardii*, *T. weissflogii*, *T. punctigera* and *Coscinodiscus wailesii* where growth increased linearly with cell volume (Wu et al., 2014). By contrast, in the present experiment elevated pCO_2 favoured dominance of smaller diatoms. Increases in temperature of 5 °C have decreased the growth rate of *Skeletonema costatum* but *Chaetoceros debilis* exhibited enhanced growth (Hyun et al., 2014b). In contrast, *Chaetoceros didymus* and *Thalassiosira nordenskioeldii* exhibited similar growth rates under ambient and elevated temperature (Hyun et al., 2014b). In natural phytoplankton communities, elevated pCO_2 alone favoured *Pseudonitzschia* spp. over *Cylindrotheca* spp. (Feng et al., 2009) and the larger centric *Chaetoceros lineola* but not *C. closterium* (Feng et al., 2010). However, Tortell et al., (2000) reported no change in diatom community structure under elevated pCO_2. The results of these studies highlight the variability in the response of diatoms to elevated pCO_2 and temperature with species-specific growth responses in culture and differential selection in natural populations. In the current study, a shift to smaller species was a feature of all experimental treatments and the control, with subtle size differences between treatments. The initial diatom community biomass was dominated by the large *Guinardia delicatula* (6176 µm^3 mean cell volume (MCV), *G. flaccida* (294539 µm^3 MCV), *Thalassiosira* spp. (10611 µm^3 MCV), *Stephanopyxis palmeriana* (104743 µm^3 MCV), *Proboscia alata* (33937 µm^3 MCV) and *Pseudonitzschia* spp. (500 µm^3 MCV). At the end of the experiment, the control was dominated by *Cylindrotheca closterium* (150 µm^3 MCV), the high temperature and the combination treatments were dominated by *Leptocylindrus danicus* (201 µm^3 MCV) while the high CO_2 treatment was dominated *by Leptocylindrus minimus* (20 µm^3 MCV). The observations of this experiment demonstrate a trend of larger diatom cell size under warming and a decrease under elevated pCO_2 relative to the control. This contrasts some

previous studies and emphasizes differences in responses between culture studies and natural populations as well as differences between natural populations from different oceanic provinces.

The biomass of nanophytoplankton can decrease under high temperatures (Moustaka-Gouni et al., 2016), whereas the nano-flagellate *Phaeocystis* spp. biomass can increase 3-fold at 800 µatm pCO_2 (Keys et al., 2017).

In this study, the combined increase in temperature and pCO_2 significantly increased the dinoflagellate biomass by 2-fold which was due to *Gymnodiniales* that accounted for 13% of the total biomass. Few studies have focussed on the response of dinoflagellates to elevated pCO_2 and temperature despite of the global increase in the frequency of harmful algal blooms (HABS). Dinoflagellates possess Form II RuBisCO which has low kinetic properties (Morse et al., 1995). Relative to diatoms, dinoflagellates possess less efficient CCMs, exhibit a lower affinity for CO_2 and are consequently limited in terms of growth and photosynthesis under current ambient pCO_2 (Ratti et al., 2007; Reinfelder, 2011). In laboratory studies at 1000 ppm CO_2, growth rates of the HAB species *Karenia brevis* increased by 46%, at 1000 ppm CO_2 and +5 °C temperature it's growth increased by 30% but was reduced under elevated temperature (Errera et al., 2014). A combined increase in pCO_2 and temperature increased both the growth and P^B_m in the dinoflagellate *Heterosigma akashiwo* whereas only pCO_2 alone enhanced these parameters in *Prorocentrum cordatum* (Fu et al., 2008). Less is known of the dinoflagellate response to high pCO_2 levels in natural populations. A North Atlantic sub-tropical gyre dinoflagellate dominated community responded significantly to 760 µatm pCO_2 over short-term (48 hour) incubations (Tilstone et al., 2016), when biomass, P^B_m and α^B were higher compared to ambient conditions. These trends are similar to observations under combined elevated temperature and pCO_2 in the present experiment.

6.4.7 Natural variability of biomass in the WEC, station L4 time series.

Comparative analyses of the WEC time series and the experimental treatments showed that the dominant diatom and dinoflagellate species in the experiments comprise minor contributors to the annual carbon budget at station L4. Species-specific variability of seasonality, in-situ temperature and pCO_2 optima was observed. These trends suggest conditions of warming may favour *L. danicus*, *Pseudonitzschia* spp. and undet. *Gymnodiniales*. Elevated pCO_2 may favour *C. closterium*, *Pseudonitzschia* spp. and undet. *Gymnodiniales*, while simultaneous warming and elevated pCO_2 may favour *Pseudonitzschia* spp. and undet. *Gymnodiniales*. Consistent with observations, from the experimental treatments, *L. danicus* biomass dominated under warming and for the undet. *Gymnodiniales*, biomass significantly increased under combined warming and elevated pCO_2. The response of *C. closterium*, *L. minimus* and *Pseudonitzschia* spp. in the experiments was not evident at L4. The results indicate that trends in individual species biomass distribution along present day in-situ temporal temperature and pCO_2 gradients are not reliable predictors for the direction of species-specific response to future warming and elevated pCO_2 conditions for coastal phytoplankton communities in the WEC.

6.5 Implications

Increased biomass, P^B_m and a community shift to diatoms under individual increases in temperature and pCO_2 suggests a potential negative feedback on atmospheric CO_2. Though selection of different dominant diatom species in these experimental treatments indicates the potential for differential carbon export rates. The high temperature treatment caused a significant increase in *L. danicus* and high pCO_2 caused a significant increase in the smaller *L. minimus*. Cellular biovolume and carbon values for these two species are significantly different; 201 μm^{-3} and 21 pg C $cell^{-1}$ for *L. danicus* compared to 20 μm^{-3} and 3 pg C $cell^{-1}$ for *L. minimus*. This suggests that warmer temperatures select for larger diatoms and organic carbon sinking rates may be lower under higher temperatures due to a shift to smaller species/cells (Bopp et al., 2001; Laws et al., 2000a) which was not observed in the phytoplankton community from the

WEC. Phytoplankton community composition determines the build-up of organic matter and its export to deeper layers. Larger cells (e.g., diatoms) account for a large proportion of export production compared to smaller cells (e.g., pico- and nanophytoplankton) (Armstrong et al., 2001). Taucher et al., (2015) observed greater DIC uptake and biomass accumulation with the larger diatom, *Dactyliosolen fragilissimus* compared to the smaller diatom, *Thalassiosira weissflogii* under elevated pCO_2 (1000 µatm), citing species-specific and cell size differences as the driving factor in the response. Conversely, a +5 °C temperature increase had a stimulating effect *on T. weissflogii* but acted as a stressor on *D. fragilissimus*. Sommer and Lengfellner, (2008) also found a decline in cell size and numbers of large diatoms in response to warming during a mesocosm experiment with a natural community. The size difference in the dominant diatom species in the present experiment was an order of magnitude greater in the high temperature and combination treatments compared to the high CO_2 treatment, demonstrating an opposite response compared to the studies discussed. It is however important to emphasize that in all experimental treatments, selection of smaller diatoms occurred from the initial community compared to the diatom community composition at the end of the experiment. *L. danicus*, which dominated the high temperature and combination treatments diatom community, showed a higher percentage of biomass (22%) between a temperature range of 16 – 17.5 °C over the L4 time series. In contrast, only 6% of *L. minimus* biomass, which dominated the high CO_2 treatment diatom community, occurred at a temperature range of 16 – 17.5 °C over the time series. This indicates that *L. danicus* may have a higher thermal optimum which could explain the difference in diatom species dominance between the experimental treatments. It is important to note however that photosynthesis may be limited by other factors in the natural environment such as nutrients and light which are also predicted to change as a result of intensified stratification in future climate warming scenarios (Sarmiento et al., 2004). When temperature and pCO_2 were elevated simultaneously in the present experiment, community biomass and P^B_m were significantly reduced relative to the other treatments and lower than the control (though not significantly). In addition, the diatom biomass was also significantly

reduced whereas smaller dinoflagellates, nano- and picophytoplankton, and *Synechococcus*, increased. The significant reduction in carbon fixation would suggest no change in feedback on atmospheric CO_2 and climate warming.

6.6 Conclusion

These experimental results provide new evidence that increases in pCO_2 coupled with rising sea surface temperatures may have contrasting effects on the late summer phytoplankton community in the WEC. Under future global change scenarios, the biomass of diatoms may be reduced during the late summer seasonal bloom relative to dinoflagellates. The experimental simulations of year 2100 temperature and pCO_2 demonstrate that the positive effects of warming may be offset by elevated pCO_2 which may negatively influence coastal phytoplankton productivity, community structure and carbon biogeochemistry in the WEC.

Chapter 7 – General discussion

7.1 Introduction

CO_2 storage in the oceans is strongly affected by biological processes (Raven., Caldeira, and Elderfield, 2005). Production of organic matter through photosynthesis drives CO_2 sequestration and therefore feeds back to atmospheric CO_2 and global climate. The ongoing increases in atmospheric CO_2 and temperature are strongly associated with changes in ocean chemistry and sea surface temperatures. The resulting changes in phytoplankton community structure are expected to have cascading effects on primary production, food web dynamics and carbon biogeochemistry (Finkel et al., 2009). Consequently, over the past two decades there has been a concerted research effort to quantify the effect of these changes on phytoplankton. Due to many constraints, the growing body of evidence has mainly focussed on individual phytoplankton species in culture. While much in the way of physiological responses to global change stressors is learned from tightly controlled single species laboratory studies, extrapolating to the natural environment is challenging. These studies lack the high genetic diversity and competitive interactions observed in natural populations.

Supporting an estimated 10–15 % of global ocean net annual primary production, coastal regions are responsible for more than 40 % of oceanic carbon sequestration (Muller-Karger, 2005). The coastal station L4 study site, together with its associated time series observations on phytoplankton community structure and biomass has provided a unique opportunity to test for the effects of elevated pCO_2 and temperature on coastal phytoplankton communities in the WEC. Results of three natural phytoplankton community experiments testing for the response to elevated temperature and pCO_2 are discussed below.

7.2 Quantifying trends in biomass across experiments

Principal components analysis (PCA) reduces the dimensionality of data sets in which there are many interrelated variables, while retaining the variation present. This reduction is achieved by

transforming to a new set of variables, the principal components, which are uncorrelated and ordered so that the first few retain most of the variation present in all of the original variables (Jolliffe, 2002). For graphical interpretation, component scores can be ordinated (usually in two or three dimensions) to reflect dissimilarities in structure (Clarke, K. R. and Warwick, 2001). PCA is therefore a powerful tool to ordinate differences in biological communities and the influencing factors. A standardized (PCA) was conducted on biomass observed on the final sampling day of all 3 experiments presented in this thesis (**Fig. 7.1 A & B**). The PCA explained ~64 % of variation in the data: The first principal component (PCA-1) explained ~43 % of the variation and the second (PCA-2) explained 21 %. PCA-1 was highly positively correlated with 6 of the variables and increased with elevated temperature and biomass of dinoflagellates, *Synechococcus*, total community biomass, diatoms and nanophytoplankton. PCA-1 was also highly negatively correlated with 2 of the variables and decreased with low biomass of cryptophytes and coccolithophores. PCA-2 was highly positively correlated with 3 of the variables and increased with elevated pCO_2 and biomass of picophytoplankton and *Phaeocystis* spp., while it was also strongly negatively correlated with ciliate biomass.

The component scores (**Fig. 7.1 A**) generally exhibited consistent clustering. There is a clear separation between Ambient-1 and high CO_2-1 (see **Fig. 7.1** caption for label descriptions) relative to the other experimental treatments. This is explained by a lower ambient temperature (11 °C) as this experiment was conducted during spring when associated in situ temperature was lower and only pCO_2 was manipulated as a single factor (chapter 4). The two high pCO_2 treatments from the multivariate experiments also exhibited separation (high CO_2-2 and high CO_2-3). This can be explained by significantly higher community biomass favoured under elevated pCO_2 in the second experiment (chapter 5) while elevated temperature promoted the highest community biomass in the third experiment (chapter 6). Following this, the ambient control, high temperature and combination treatments from the multivariate experiments exhibit very similar trends.

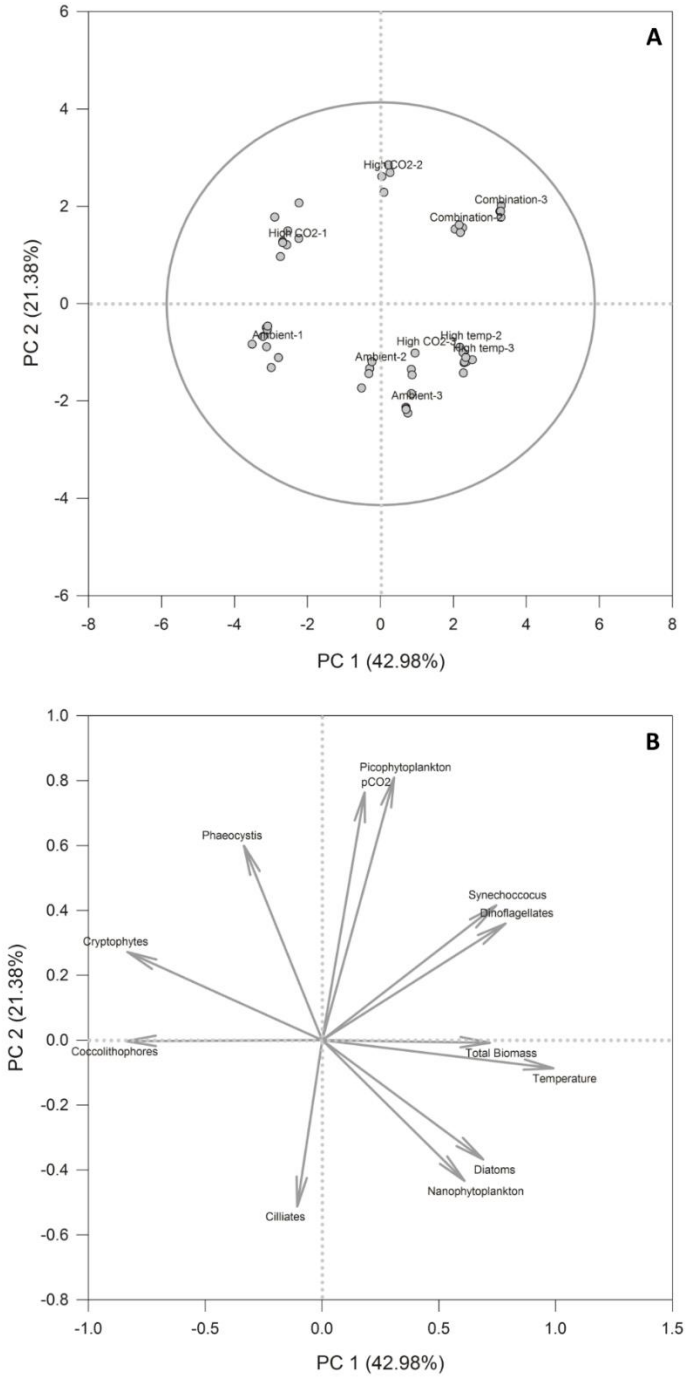

Fig. 7.1 (**A**) Component scores from the principal components analysis on biomass on the final day of sampling from all 3 experiments. The component scores are labelled relative to each experiment: Ambient-1, High CO_2-1 (chapter 3); Ambient-2, high CO_2-2, high temp-2 and combination-2 (chapter 4); Ambient-3, high CO_2-3, high temp-3 and combination-3 (chapter 5). (**B**) Component loadings from the principal components analysis.

The component loadings (**Fig. 7.1 B**) show that overall, total community biomass was influenced by elevated pCO_2 and elevated temperature. This aspect of the PCA analysis may be confounded as a result of the first experiment in chapter 4 being univariate and attaining comparatively lower biomass accumulation due to the shorter experimental period compared to experiments 2 and 3 (chapters 5 and 6). The lower biomass accumulation in experiment 1 may have resulted in reduced influence in the PCA. Biomass of dinoflagellates and *Synechococcus* positively covaried when elevated temperature and pCO_2 were combined, but the PCA-1 scores demonstrate that elevated temperature was more influential in this response. *Phaeocystis* spp. biomass was strongly influenced by elevated pCO_2 alone but was only observed in two of the three experiments (chapters 4 and 5).

Diatoms exhibited variable responses, with biomass stimulated more by ambient conditions in the first experiment (chapter 4), elevated pCO_2 in the second experiment (chapter 5) and elevated temperature in the third experiment (chapter 6), but overall, was most highly correlated to elevated temperature. Again, lower biomass accumulation in diatoms in experiments 1 and 2 compared to experiment 3 may have resulted in reduced influence in the PCA. Nanophytoplankton biomass also showed variability with biomass positively influenced by elevated pCO_2 in two experiments (chapters 4 and 5) while ambient conditions promoted the highest biomass (chapter 6) when diatoms were dominant in the community. Picophytoplankton biomass was highly correlated to elevated pCO_2 alone, though also showed a weaker correlation to the combined influence of elevated pCO_2 and temperature. Biomass of coccolithophores and cryptophytes was highly negatively correlated with elevated temperature though cryptophytes showed a weak correlation to elevated pCO_2 alone. Ciliate biomass (microzooplankton) was weakly negatively correlated to elevated temperature and showed a more highly negative correlation to elevated pCO_2. In all three experiments, coccolithophore, cryptophyte and ciliate biomass was very low.

At the taxonomic level, the results indicate that under future conditions of combined warming and elevated pCO_2, an increase in dinoflagellates and *Synechococcus* may occur at the expense of diatoms, nano- and picophytoplankton, which have been demonstrated to be critical components of the carbon budget at station L4. The response of coccolithophores, cryptophytes and ciliates is less clear and most likely a product of the very low biomass of these species in the initial experimental communities. The results of all experiments in this thesis are summarised in **Fig. 7.2**.

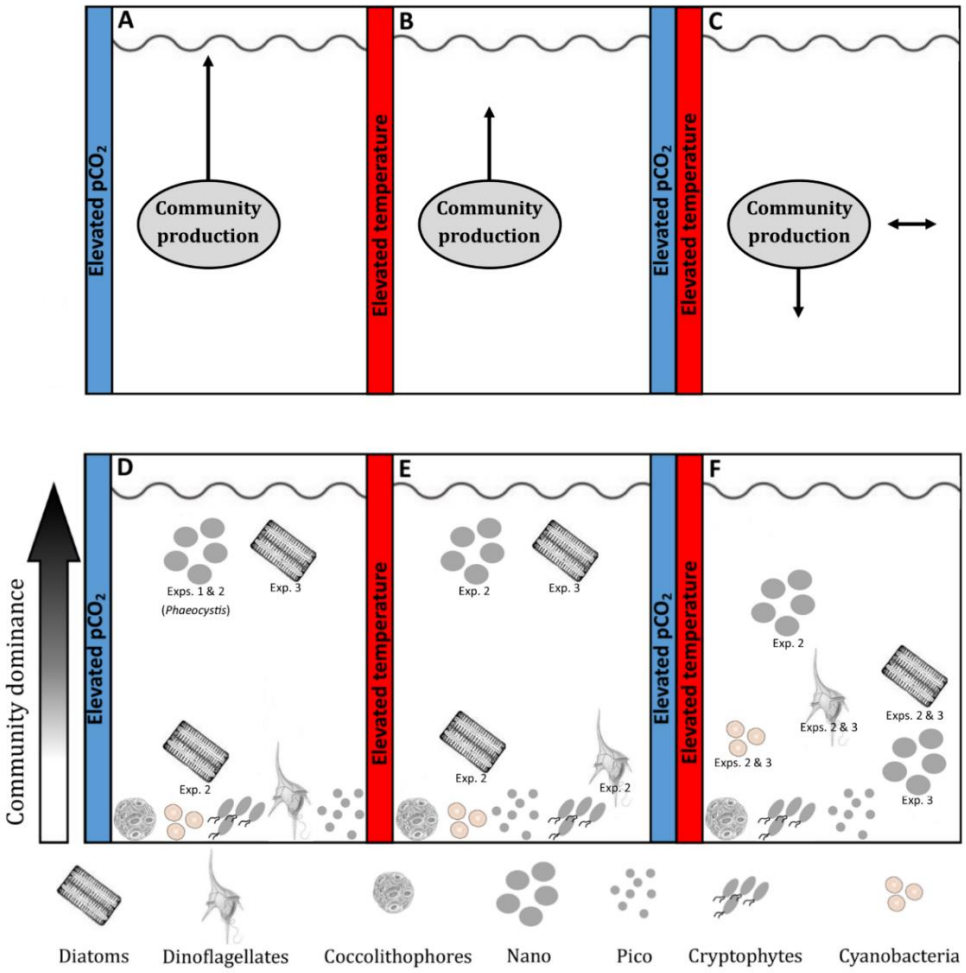

Fig. 7.2. Schematic representation of the relative differences in the magnitude of the community production response and the relative contributions of phytoplankton groups and species to total biomass from all 3 experiments, to elevated pCO_2 (**A** & **D**), elevated temperature (**B** & **E**) and the combined influence of both factors (**C** & **F**). Vertical (↕) error bars in panels A, B and C represent the relative number of experiments reporting either increased or decreased production and the horizontal (↔) error bars represent the relative number of experiments to report no change in production.

In chapters 4, 5 and 6, the response in total community biomass to elevated temperature and pCO_2 individually, demonstrated significant increases. Under elevated pCO_2 the results showed an almost doubling to 20-fold increase in community biomass (**Fig 7.2 A**), while under elevated temperature the biomass increase was 11 – 14-fold (**Fig 7.2 B**). When these treatments were combined however a reduction in biomass was observed in the late summer community (chapter 6) while no significant response was observed in the autumn community (chapter 5) (**Fig. 7.2 C)**. The results under the combined treatments contrast much of the present literature, (e.g. Calbet et al., 2014; Feng et al., 2009; Hare et al., 2007b). In all experiments the trends in the total community response were driven by significant modifications to taxonomic composition which were treatment-specific (**Fig. 7.2 D**, **E** & **F**).

7.3 Comparing results to hypotheses

Returning to the summary figure of trends in the natural phytoplankton community response to changes in pCO_2 and temperature, presented in the introduction of this thesis, the results of the thesis experiments presented can be evaluated (**Fig 7.3**) The hypotheses set out in the introduction, relative to community production (biomass accumulation and photosynthetic rates) were based on the summary figure. The hypotheses were:

1. Elevated pCO_2 alone will have the greatest influence, increasing total community production and photosynthetic rates significantly, relative to elevated temperature treatments, combined elevated pCO_2 and temperature treatments and ambient controls.

2. Elevated temperature and combined elevated pCO_2 and temperature will increase total community production and photosynthetic rates with equal weight significantly, relative to ambient controls but will be significantly lower than production under elevated pCO_2 alone.

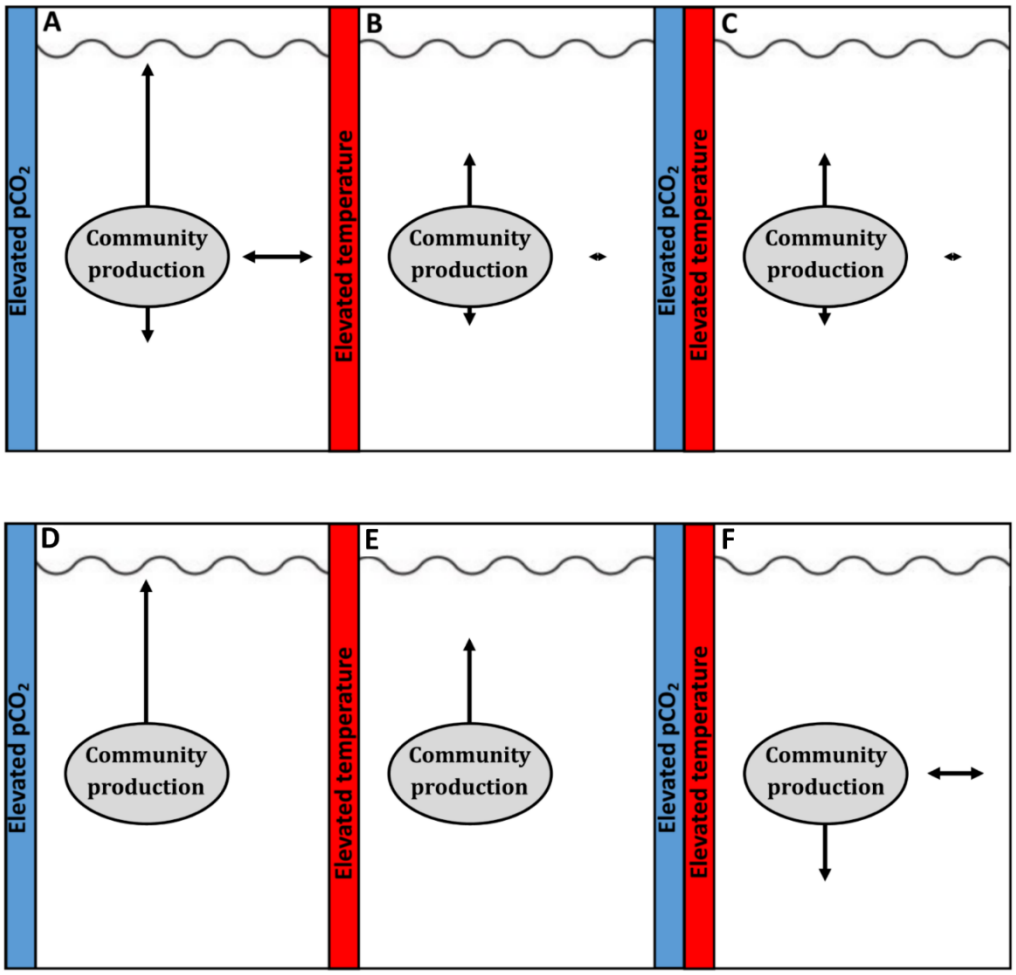

Fig. 7.3. Schematic representation of the relative differences in the magnitude of the phytoplankton community production response to elevated pCO_2 (**A**), elevated temperature (**B**) and the combined influence of both factors (**C**) from previous experiments conducted on natural phytoplankton communities over the last 20 years. Vertical (↕) error bars represent the relative number of published studies reporting either increased or decreased production and the horizontal (↔) error bars represent the relative number of studies to report no change in production. These experimental results formed the basis of the working hypotheses formulated in this thesis research. Trends in the results from all three experiments presented in this thesis are presented for comparative purposes (**D**, **E** & **F,** vertical and horizontal error bars not to scale with panels A, B and C)

When considering the experimental results, hypothesis 1. must be rejected. While elevated pCO_2 alone resulted in the highest biomass accumulation in experiments 1 and 2 (chapters 4 and 5) and the highest maximum photosynthetic rates in experiments 2 and 3 (chapters 5 and 6),

biomass accumulation in experiment 3 was significantly lower under the elevated pCO_2 compared to elevated temperature treatment (**Fig. 7.3 D** & **E**).

Hypothesis 2. must also be rejected. Elevated temperature alone stimulated significantly higher biomass accumulation and maximum photosynthetic rates compared to the simultaneous effects of elevated pCO_2 and temperature in experiments 2 and 3. As mentioned above, elevated temperature also resulted in the highest biomass accumulation of all treatments in experiment 3 (**Fig. 7.3 E**). The combined influence of elevated pCO_2 and temperature was not only significantly lower than the individual influence of elevated temperature alone, in experiment 2 biomass accumulation showed no significant difference relative to the control and in experiment 3, it was significantly lower than the control. Maximum photosynthetic rates were not significantly altered relative to the control in either experiments 2 and 3 (**Fig. 7.3 F**).

The hypotheses relative to treatment-specific shifts in taxonomic composition were also based on the summary figure (**Fig. 7.4**). The hypotheses were:

3. Elevated pCO_2 will select for picophytoplankton dominated communities with significant contributions from diatoms and cyanobacteria, dependent on the relative abundance in the initial experimental communities.

4. Elevated temperature will select for picophytoplankton and/or coccolithophore dominated communities with minor contributions from cryptophytes, dependent on the relative abundance in the initial experimental communities.

5. Combined elevated pCO_2 and temperature will select for diatom, nanophytoplankton or coccolithophore dominated communities, dependent on the relative abundance in the initial experimental communities.

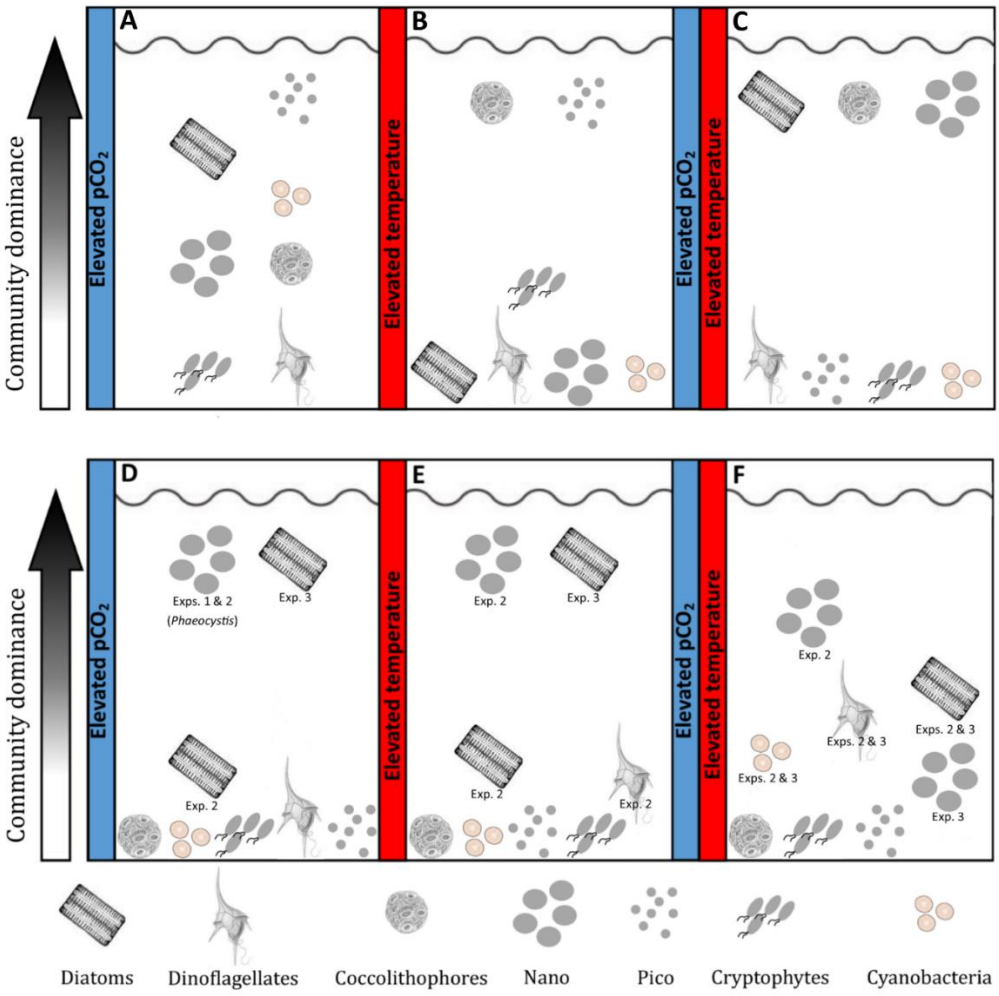

Fig. 7.4. Schematic representation of the relative contributions of phytoplankton groups and species to total biomass in response to elevated pCO_2 (**A**), elevated temperature (**B**) and the combined influence of both factors (**C**) from previous experiments conducted on natural phytoplankton communities over the last 20 years. These experimental results formed the basis of the working hypotheses formulated for shifts in community composition in this thesis research. Trends in the results from all three experiments presented in this thesis are presented for comparative purposes (**D**, **E** & **F**).

When considering the experimental results in relation to changes in community structure, accepting or rejecting the hypotheses is more ambiguous since previous experiments have found that the initial experimental community exerts significant impacts on the direction of the group- and species-specific response. Eggers et al., (2014) demonstrated that initial ratios between cyanobacteria, diatoms and dinoflagellates strongly influenced experimental outcomes under elevated pCO_2, independent of experimental treatments.

Hypothesis 3. stated that picophytoplankton will dominate community biomass in elevated pCO_2 treatments, as has been the trend in previous elevated pCO_2 studies (**Fig. 7.4 A**). Yet this group comprised very low fractions of the total biomass in the initial experimental communities (nine percent in experiment 1, three percent in experiment 2 and two percent in experiment 3). Hypothesis 3. also stated that significant contributions will be made by diatoms and cyanobacteria in elevated pCO_2 treatments. While diatoms dominated the elevated pCO_2 community biomass in experiment 3 (**Fig. 7.4 D**), biomass of cyanobacteria in these treatments was very low and it was *Phaeocystis* spp. that dominated high pCO_2 treatments in experiments 1 and 2. Therefore, hypothesis 3. must be rejected.

Hypothesis 4. stated that community biomass would be dominated by picophytoplankton and/or coccolithophores under elevated temperature treatments (**Fig. 7.4 B**). The fraction of picophytoplankton to total biomass was very low in initial experimental communities as discussed above, as was also the case with coccolithophores (eight percent in experiment 2 and just one percent in experiment 3). Since nanophytoplankton dominated community biomass in elevated temperature treatments in experiment 2 and diatoms dominated in this treatment in experiment 3 (**Fig. 7.4 E**), hypothesis 4. must also be rejected.

Hypothesis 5. stated that elevating pCO_2 and temperature simultaneously would select diatom, nanophytoplankton or coccolithophore dominated communities (**Fig. 7.4 C**). Since the communities in the combined treatments were the most diverse, dominance of any single group or species was supressed. While nanophytoplankton and diatoms accounted for more biomass than any other group, the biomass was significantly lower compared to the other experimental treatments and the control. Dinoflagellates and *Synechococcus* made significant contributions to community biomass which was a unique feature of response in the combined treatments (**Fig. 7.4 F**). Therefore hypothesis 5. must also be rejected.

Results among studies, particularly when performed on natural communities, are highly variable. The rejection of the hypotheses due to contrasting results that do not conform to

previous experimental trends emphasize the challenge of repeatability in this complex area of research. Taken individually, single experiments presented in this thesis were in close agreement with both previous experimental trends and the thesis hypotheses in some, but not all cases. Taken as a whole, variability in responses that diverged from trends of previous experiments may have been influenced by different initial experimental community composition, season, site- and environment-specific responses (Richier et al., 2014). Geographic location and seasonality play an important role in structuring phytoplankton communities (Li et al., 2009; Morán et al., 2010), which may also act as a bias when comparing results with studies which differ spatially and temporally.

7.4 L4 Time series: natural variability of the dominant experimental groups and species

Analysis of the species found to be dominant in the experimental treatments, over the L4 phytoplankton biomass time series provided insight to potential shifts in community and size structure under future environmental conditions. Elevated pCO_2 alone suggested that the nanophytoplankton group, a significant contributor to the annual carbon budget at L4, may shift to dominance of the nuisance HAB species *Phaeocystis* in spring and autumn, which was found to have a low but variable biomass over the past two decades at the time series station. Species-specific response to elevated pCO_2 also indicated a shift to smaller diatoms, thus potentially reducing diatom biomass at L4. Elevated temperature showed the potential for a shift to smaller nanophytoplankton and diatoms which may reduce the biomass of these groups in the future and an increase in the HAB dinoflagellate *Prorocentrum cordatum* and the dinoflagellate *Gymnodiniales* spp., which were both demonstrated to have low biomass over the time series. The combined influence of elevated pCO_2 and temperature indicated overall decreases in the abundance and biomass of nanophytoplankton and diatoms, both significant contributors to the L4 carbon budget, as well as a shift to smaller species in these groups, further holding the potential to reduce the cycling of carbon at L4 under future climate scenarios. The combined influence of elevated pCO_2 and temperature also indicated a stronger shift in the dinoflagellate

species community compared to elevated temperature alone, to the HAB species *P. cordatum* and the dinoflagellate *Gymnodiniales* spp..

7.5 Mechanisms for changes in community composition

Although inorganic carbon is abundant in the sea, 90 % of it is in the form of bicarbonate ions (HCO_3^-). Less than 1 % is present as CO_2, the form required by Ribulose Bisphosphate Carboxylase (RuBisCO), the primary enzyme responsible for photosynthetic carbon fixation (Riebesell and Jones, 2002). The low affinity of RuBisCO for CO_2 poses limitations on photosynthetic carbon fixation and hence the adaptive strategies of phytoplankton; upregulating RuBisCO activity or employing CO_2 concentrating mechanisms (CCMs) are species specific (Giordano et al., 2005; Raven, 2011; Tortell et al., 2000). Concurrently, photosynthetic rates may be limited by temperature. Maximum photosynthetic rates (P^B_m), the light limited slope of photosynthesis (α^B) and temperature are tightly coupled (Uitz et al., 2008). Different phytoplankton species are adapted to a narrow temperature band with a sharp decrease in photosynthetic rates beyond their thermal optima (Eppley, 1972; Raven and Geider, 1988). Hence increases in pCO_2 and temperature have been predicted to differentially affect uptake rates of dissolved inorganic carbon (Badger et al., 1998). The results of the three experiments in this thesis highlight these species-specific differences in terms of the competitive interactions, and how changing environmental conditions of elevated pCO_2 and temperature may change community composition.

7.6 Experimental considerations

A critical goal of this thesis research was to understand how phytoplankton species succession is affected by increased pCO_2 and temperature seasonally. There are important considerations when testing for the effects of climate change on natural phytoplankton communities using a bottle incubation approach. Methodological concerns include the community sampling protocol, addition of macro-nutrients, acclimation to experimentally manipulated factors, bottle effects and incubation time.

The considered approach to community sampling was to gently pre-filter seawater containing natural phytoplankton communities through a 200 µm Nitex mesh to remove mesozooplankton grazers. While grazers play an important role in regulating phytoplankton community structure (e.g. Strom, 2002), the experimental goals considered only the effects of elevated temperature and pCO_2, not the additional top down grazing effects, though the mesh size used does not remove microzooplankton. This is a common approach in similar studies (e.g. Coello-Camba et al., 2014; Feng et al., 2009) and was also applied to the sampling protocol presented in this thesis for purposes of comparability. The results therefore lack the influence of grazing regulation on communities which would have acted as an additional factor when relating responses to the natural environment as well as when comparing results to other studies that did not exclude zooplankton grazers.

Pilot studies (presented in the methods section, chapter 3) were conducted to determine the optimum nutrient regimes required to sustain a natural community in bottle incubations. No addition of nutrients (nitrate (N) and phosphate (P)) under low nutrient concentrations resulted in population crashes. This was also the case with the addition of low levels of nutrients according to empirical N:Chl *a* relationships for cumulative N uptake in natural phytoplankton communities (Gilpin et al., 2004). Analysis of the L4 nutrients time series showed maximum mean annual N and P concentrations to be close to Redfield ratios at 8 µM N and 0.5 µM P during the periods when community sampling was conducted. Addition at these concentrations was tested and found to be sufficient to support the natural community. These high concentrations simulated the pulsed supply of nutrients at L4 due to winter mixing in the spring period and high rainfall events during late summer, making them environmentally relevant to the study site. However, maintaining the nutrients constant at these concentrations is not realistic of a natural system, but was required to sustain the natural phytoplankton community. Similar (and much higher) concentrations have also been applied in previous similar studies (e.g. Calbet et al., 2014; Feng et al., 2009). Schulz et al., (2013) observed that addition of high levels of nutrients amplified the CO_2 response of phytoplankton communities

rather than acted as an additional driver. Similarly, Richier et al., (2014) found that physiological responses of natural communities were consistent in repeated experiments, irrespective of natural or manipulated nutrient status. The decision to not add silicate (Si) when in situ concentrations were between ~1 µM and 2 µM was based on the observation of Egge and Aksnes., (1992), that Si concentrations ≥ 2 µM and pre-select diatom communities. Si addition may therefore have biased the experimental results and the lower concentration in the experiments was clearly sufficient to sustain diatoms as this group was prominent in the biomass in experiment 2 (chapter 5) and dominated the biomass in experiment 3 (chapter 6) when the Si concentration was 1.35 µM. Semi- qualitative microscopical assessment of diatom health was performed during routine microscopy and there was no evidence to suggest weakly silicified diatoms as a result of the nutrient regime. A limitation of this thesis research was the absence of nutrient measurements beyond the days of community sampling. This was unfortunately due to funding and logistical reasons and as a result, the time course of nutrient concentrations and subsequent uptake rates during experiments was not possible.

A pilot study to determine the optimum CO_2 enrichment method (chapter 3) showed that addition of CO_2 enriched filtered seawater bubbled with CO_2 gas was just as effective at maintaining experimental pCO_2 levels as the established methods of acid, base manipulation and direct bubbling of CO_2 gas. The level of carbonate system control and avoidance of potential bottle effects this method offers justified the use of this method for the carbonate system manipulation protocol throughout this thesis. Most similar studies increase elevated pCO_2 levels to the maximum target value at the experiment start. This is not realistic of the natural environment as pCO_2 levels are predicted to increase gradually over time. A slow acclimation protocol to gradually increasing pCO_2 levels was maintained in the experiments in this thesis research to better replicate what is predicted to occur in the natural environment in the future (albeit over a much shorter time scale, but relative the experimental time-scales). A feature of all 3 experiments was a decline in chl *a* and community biomass over the first 7 to 10 days, likely a result of acclimation to bottle containment. It is therefore unlikely that this approach

selected for specific groups or species dominance early in the experiments, though this would be a challenging factor to analyse.

Microbial growth on bottle walls may occur over long incubation periods which may impact the communities being experimentally incubated (Marra, 2009). Incubation bottles were visually inspected throughout the experiments and no microbial build-up was observed. Several recent studies found no evidence of significant bottle effects due to microbial growth on bottle walls (e.g. Hammes et al., 2010).

Experimental results can be ambiguous when interpreting short-term acclimation responses from incubation periods of hours to days, (e.g. Chen et al., 2014) which motivated the current research to extend experimental testing over multiple weeks. In experiment 1 (chapter 4) which lasted fourteen days, a significant response between treatments was not observed until day nine. In experiments 2 and 3 (chapters 5 and 6), significant responses were not observed between treatments until days 22 and 24. This indicates the existence of a tipping point when testing for the direction of response to climate change experiments on natural phytoplankton communities. It is therefore possible that some observations in the literature may in fact be reporting cellular stress and/or acclimation responses to experimental treatments if conducted over short time periods (hours to days). Three studies have attempted to address the question of differentiating short-term physiological plasticity and adaptive evolution through long-term exposure to elevated pCO_2. The coccolithophore *Emiliania huxleyi* was grown in a high pCO_2 selection experiment for 500 generations (Lohbeck et al., 2012). When compared with populations grown at elevated pCO_2 over short time scales, higher growth rates were observed, and calcification was 50 % higher. By contrast, the coccolithophore *Gephrocapsa oceanica* exhibited reduced growth and POC production following 2000 generations at elevated pCO_2 (Jin and Gao, 2016). *Trichodesmium* grown at 750 ppm CO_2 for 4.5 years exhibited significant increases in nitrogen fixation that were observed to be irreversible, even following transferral back to ambient pCO_2 for hundreds of generations, demonstrating an unprecedented

evolutionary response (Hutchins et al., 2015). These mixed results however, demonstrate that even in long term evolutionary studies, the response can be variable but critically, highlight the need to consider longer experimental time periods.

7.7 Key findings

1. Individually, elevated temperature and pCO_2 resulted in the highest biomass and light saturated photosynthetic carbon fixation rates. For elevated pCO_2 this occurred in spring and autumn while for elevated temperature this occurred in late summer (note: only elevated pCO_2 was tested during spring).

2. The combined effects of elevated temperature and pCO_2 reduced biomass in the late summer community and had no effect on biomass in the autumn community.

3. No significant effects on P^B_m were observed under the combined treatments, independent of season.

4. Individual treatments of elevated pCO_2 and temperature resulted in near mono-specific communities: diatoms in late summer and nanophytoplankton in autumn.

5. Combined effects of both factors resulted in the most diverse phytoplankton communities and promoted increased dinoflagellate and *Synechococcus* biomass at the expense of diatoms in late summer and nanophytoplankton in autumn.

6. Elevated pCO_2 alone promoted dominance of the HAB species, *Phaeocystis* during spring and autumn.

7. The combined treatment promoted dominance of the HAB species, *Prorocentrum minimum* in autumn.

7.8 Further work

This thesis has tested the combined effects of two of the most prominent global stressors predicted to impact phytoplankton productivity and community structure. As such, it is one of a

limited number of studies. To date just one study has presented results on the cumulative effect of five global change stressors predicted to impact phytoplankton physiology and productivity: light, nutrients, CO_2, temperature and iron (Boyd et al., 2015). These types of experiments are labour intense, costly and logistically challenging. The traditional factorial experimental approach employed in this thesis limits the feasibility of more than 2 to 3 interactive experimental treatments. The study of Boyd et al., (2015) employed a new collapsed factorial design which requires accurate identification of the dominant physiological control factors before grouping sets of them together. Further focus is also needed on the top down controls of microzoo- and zooplankton grazing as an additional treatment factor in the context of global change stressors, a factor that has been largely overlooked in OA studies on phytoplankton response. A simplistic approach would be to statistically analyse the ratio of meso- and microzooplankton to natural phytoplankton communities in perturbation experiments that do not screen grazers when sampling. This would, at the very least, allow for inferences in the response of top down grazing controls under conditions of elevated pCO_2 and temperature. Following this approach, Thomson et al., (2016) concluded reduced grazing pressure on picophytoplankton by heterotrophic nano-flagellates under conditions of elevated pCO_2, though the exact mechanism was not confirmed. A more valid approach (experimentally and statistically) is to include grazing experiments in phytoplankton OA and elevated temperature experimental design. Studies that have adopted this experimental design have reported variable results, including no evidence of alterations to grazing rates (Brussaard et al., 2013) and copepods exhibiting a stronger preference for dinoflagellates under elevated pCO_2 (Tarling et al., 2016). Since changes in food quality and altered grazing selectivity may be a major consequence of elevated pCO_2, more experimental data is required in the future.

7.9 Conclusions

The experimental results provide new evidence that ongoing increases in pCO_2 coupled with rising sea surface temperatures may have contrasting effects on the phytoplankton community

structure in the WEC. Under future global change scenarios in the WEC, the biomass of *Phaeocystis* spp. may be increased in spring, diatom biomass may be reduced during late summer with increased dinoflagellate biomass, while in autumn biomass of the HAB species *Prorocentrum cordatum* may increase at the expense of nanophytoplankton. The experimental simulations of year 2100 temperature and pCO_2 demonstrate that the positive effects of warming may be offset by elevated pCO_2.

Bibliography

Alley, D., Berntsen T, Bindoff NL, Chen ZL, Chidthaisong A, Friedlingstein P, Gregory J G, Hegerl Heimann M, Hewitson B, Hoskins B, Joos F, Jouzel, Kattsov V, Lohmann U, Manning M, Matsuno T, Molina M, Nicholls N, Verpeck J, Qin DH, Raga G, Ramaswamy V, Ren JW, Rusticucci M, Solomon S, Somerville R, Stocker TF, Stott P, Stouffer RJ, Whetton P, Wood RA and Wratt D. (2007). *Climate Change 2007*. The Physical Science basis: Summary for policymakers. Contribution of Working Group I to the Fourth Assessment Report of the Intergovernmental Panel on Climate Change.

Anderson, T. R.: Plankton functional type modelling: running before we can walk?, J. Plankton Res., 27(3), 1073–1081, doi:10.1093/plankt/fbi076, 2005.

Andeson, D., Gilbert, P. and Burkholder, J.: Harmful Algal Blooms and Eutrophication : Nutrient Sources , Composition , and Consequences, Estuaries, 25(4), 704–726, 2002.

Armstrong, R. A., Lee, C., Hedges, J. I., Honjo, S. and Wakeham, S. G.: A new, mechanistic model for organic carbon fluxes in the ocean based on the quantitative association of POC with ballast minerals, Deep Sea Res. Part II Top. Stud. Oceanogr., 49(1), 219–236, doi:https://doi.org/10.1016/S0967-0645(01)00101-1, 2001.

Arnold, H. E., Kerrison, P. and Steinke, M.: Interacting effects of ocean acidification and warming on growth and DMS-production in the haptophyte coccolithophore *Emiliania huxleyi*, Glob.

Chang. Biol., 19(4), 1007–1016, doi:10.1111/gcb.12105, 2013.

Asper, V. L., Deuser, W. G., Knauer, G. A. and Lohrenz, S. E.: Rapid coupling of sinking particle fluxes between surface and deep ocean waters, Nature, 357, 670 [online] Available from: http://dx.doi.org/10.1038/357670a0, 1992.

Atkinson, D., Ciotti, B. J. and Montagnes, D. J. S.: Protists decrease in size linearly with temperature: ca. 2.5% °C^{-1}, Proc. R. Soc. B Biol. Sci., 270(1533), 2605–2611, doi:10.1098/rspb.2003.2538, 2003.

Bach, L. T., Riebesell, U., Gutowska, M. A., Federwisch, L. and Schulz, K. G.: A unifying concept of coccolithophore sensitivity to changing carbonate chemistry embedded in an ecological framework, Prog. Oceanogr., 135, 125–138, doi:10.1016/j.pocean.2015.04.012, 2015.

Badger, M. R., Andrews, T. J., Whitney, S. M., Ludwig, M., Yellowlees, D. C., Leggat, W. and Price, G. D.: The diversity and coevolution of Rubisco , plastids , pyrenoids , and chloroplast-based CO_2-concentrating mechanisms in algae, Can. J. Bot., (76), 1052–1071, 1998.

Baragi, L. V., Khandeparker, L. and Anil, A. C.: Influence of elevated temperature and pCO_2 on the marine periphytic diatom *Navicula distans* and its associated organisms in culture, Hydrobiologia, 762, (1), 127–142, doi:10.1007/s10750-015-2343-9, 2015.

Barcelos e Ramos, J., Biswas, H., Schulz, K. G., LaRoche, J. and Riebesell, U.: Effect of rising atmospheric carbon dioxide on the marine nitrogen fixer *Trichodesmium*, Global Biogeochem. Cycles, 21(2), doi:10.1029/2006GB002898, 2007.

Barcelos e Ramos, J., Müller, M. N. and Riebesell, U.: Short-term response of the coccolithophore *Emiliania huxleyi* to an abrupt change in seawater carbon dioxide concentrations, Biogeosciences, 7, (1), 177–186, doi:10.5194/bg-7-177-2010, 2010.

Beardal, J. and Raven, J.: The potential effects of global climate change in microalgal photosynthesis, growth and ecology, Phycologia , 43, 26–40, 2004.

Beardall., J., Stojkovic., S. and Larsen., S.: Living in a high CO_2 world: impacts of global climate change on marine phytoplankton, Plant Ecol. Divers., 2, (2), 191–205, doi:10.1080/17550870903271363, 2009.

Beardall, J. and Stojkovic, S.: Microalgae under Global Environmental Change : Implications for Growth and Productivity , Populations and Trophic Flow, Sci. Asia, 1, 1–10, doi:10.2306/scienceasia1513-1874.2006.32(s1).001, 2006.

Beardall, J., Ihnken, S. and Quigg, A. Gross and net primary production: closing the gap between concepts and measurements, Aquat. Microb. Ecol., 56, 113–122, doi:10.3354/ame01305, 2009.

Beaugrand, G., Edwards, M. and Legendre, L.: Marine biodiversity, ecosystem functioning, and carbon cycles, PNAS, 107, (22), 10120–10124, doi:10.1073/pnas.0913855107/-/DCSupplemental.www.pnas.org/cgi/doi/10.1073/pnas.0913855107, 2010.

Behrenfeld, M. J., O'Malley, R. T., Siegel, D. A, McClain, C. R., Sarmiento, J. L., Feldman, G. C., Milligan, A. J., Falkowski, P. G., Letelier, R. M. and Boss, E. S.: Climate-driven trends in contemporary ocean productivity., Nature, 444, (7120), 752–5, doi:10.1038/nature05317, 2006.

Bermúdez, J. R., Riebesell, U., Larsen, A. and Winder, M.: Ocean acidification reduces transfer of essential biomolecules in a natural plankton community, Sci. Rep., 6, (1), 27749, doi:10.1038/srep27749, 2016.

Biswas, H. Cros, A. Yadav, K. Ramana, V. Prasad, R. Acharyya, T and RaghunadhBabu, P. J.: Response of a natural phytoplankton community from the Qingdao coast (Yellow Sea, China) to variable CO_2 levels over a short-term incubation experiment Exp. Mar. Biol. Ecol, 407, 284–293, 2011.

De Bodt, C., Van Oostende, N., Harlay, J., Sabbe, K. and Chou, L.: Individual and interacting effects of pCO_2 and temperature on *Emiliania huxleyi* calcification: study of the calcite production, the

coccolith morphology and the coccosphere size, Biogeosciences, 7, (5), 1401–1412, doi:10.5194/bg-7-1401-2010, 2010.

Bonachela, J. A., Allison, S. D., Martiny, A. C. and Levin, S. A.: A model for variable phytoplankton stoichiometry based on cell protein regulation, Biogeosciences, 10, (6), 4341–4356, doi:10.5194/bg-10-4341-2013, 2013.

Booth, B. C.: Size classes and major taxonomic groups of phytoplankton at two locations in the subarctic pacific ocean in May and August, 1984, Mar. Biol., 97, (2), 275–286, doi:10.1007/BF00391313, 1988.

Bopp, L. ., Monfray, P. ., Aumont, O. ., Dufresne, J.-L. ., Le Treut, H. ., Madec, G. ., Terray, L. . and Orr, J. C. .: Potential impact of climate change on marine export production, Global Biogeochem. Cycles, 15, (1), 81–99, doi:10.1029/1999GB001256, 2001.

Boras, J. A., Borrull, E., Cardelu, C., Cros, L., Gomes, A., Sala, M. M., Aparicio, F. L., Balague, V., Mestre, M., Movilla, J., Sarmento, H., Va, E. and Lo, A.: Contrasting effects of ocean acidification on the microbial food web under different trophic conditions, ICES J. Mar. Sci., 73, (3), 670–679, 2016.

Boyd, P. and Newton, P.: Evidence of the potential influence of planktonic community structure on the interannual variability of particulate organic carbon flux, Deep Sea Res. Part I Oceanogr. Res. Pap., 42, (5), 619–639, doi:https://doi.org/10.1016/0967-0637(95)00017-Z, 1995.

Boyd, P. W. and Doney, S. C.: Modelling regional responses by marine pelagic ecosystems to global climate change, Geophys. Res. Lett., 29, (16), 1–4, 2002.

Boyd, P. W., Doney, S. C., Strzepek, R., Dusenberry, J., Lindsay, K. and Fung, I.: Climate-mediated changes to mixed-layer properties in the Southern Ocean: assessing the phytoplankton response, Biogeosciences, 5, 847–864, doi:10.5194/bgd-4-4283-2007, 2008.

Boyd, P. W., Strzepek, R., Fu, F. and Hutchins, D. A.: Environmental control of open-ocean

phytoplankton groups: Now and in the future, Limnol. Oceanogr., 55, (3), 1353–1376, doi:10.4319/lo.2010.55.3.1353, 2010.

Boyd, P. W., Rynearson, T. A., Armstrong, E. A., Fu, F., Hayashi, K., Hu, Z., Hutchins, D. A., Kudela, R. M., Litchman, E., Mulholland, M. R., Passow, U., Strzepek, R. F., Whittaker, K. A., Yu, E. and Thomas, M. K.: Marine Phytoplankton Temperature versus Growth Responses from Polar to Tropical Waters - Outcome of a Scientific Community-Wide Study, PLoS One, 8, (5), doi:10.1371/journal.pone.0063091, 2013.

Boyd, P. W., Dillingham, P. W., McGraw, C. M., Armstrong, E. A., Cornwall, C. E., Feng, Y. -y., Hurd, C. L., Gault-Ringold, M., Roleda, M. Y., Timmins-Schiffman, E. and Nunn, B. L.: Physiological responses of a Southern Ocean diatom to complex future ocean conditions, Nat. Clim. Chang., (October), doi:10.1038/nclimate2811, 2015.

Brading, P., Warner, M. E., Davey, P., Smith, D. J., Achterberg, E. P. and Suggett, D. J.: Differential effects of ocean acidification on growth and photosynthesis among phylotypes of *Symbiodinium* (Dinophyceae), Limnol. Oceanogr., 56, (3), 927–938, doi:10.4319/lo.2011.56.3.0927, 2011.

Brownlee, C. and Taylor, A.: Algal Calcification and Silification, Encycloped., Nature Publishing Group., 2002.

Brussaard, C. P. D., Noordeloos, A. A. M., Witte, H., Collenteur, M. C. J., Schulz, K., Ludwig, A. and Riebesell, U.: Arctic microbial community dynamics influenced by elevated CO_2 levels, Biogeosciences, 10, (2), 719–731, doi:10.5194/bg-10-719-2013, 2013.

Buitenhuis, E. T., de Baar, H. J. W. and Veldhuis, M. J. W.: Photosynthesis and Calcification By *Emiliania Huxleyi* (Prymnesiophyceae) As a Function of Inorganic Carbon Species, J. Phycol., 35, (5), 949–959, doi:10.1046/j.1529-8817.1999.3550949.x, 1999.

Burkhardt, S. and Riebesell, U.: CO_2 availability affects elemental composition (C : N : P) of the marine diatom S*keletonema costatum*, Mar. Biotechnol. (NY)., 155, 67–76, 1997.

Burkhardt, S., Zondervan, I. and Riebesell, U.: Effect of CO_2 concentration on the C:N:P ratio in marine phytoplankton: A species comparison, Limnol. Oceanogr., 44, (3), 683–690, doi:10.4319/lo.1999.44.3.0683, 1999.

Burkhardt, S., Amoroso, G. and Su, D.: CO_2 and HCO_3^- uptake in marine diatoms acclimated to different CO_2 concentrations, Limnol. Oceanogr., 46, (6), 1378–1391, 2001.

Burns, R. A., MacDonald, C. D., McGinn, P. J. and Campbell, D. A.: Inorganic Carbon Repletion Disrupts Photosynthetic Acclimation To Low Temperature in the Cyanobacterium *Synechococcus Elongatus*, J. Phycol., 41, (2), 322–334, doi:10.1111/j.1529-8817.2005.04101.x, 2005.

Cadée, G. C. and Hegeman, J.: Phytoplankton in the Marsdiep at the end of the 20th century; 30 years monitoring biomass, primary production, and *Phaeocystis* blooms, J. Sea Res., 48, (2), 97–110, doi:10.1016/S1385-1101(02)00161-2, 2002.

Calbet, A., Sazhin, A. F., Nejstgaard, J. C., Berger, S. A, Tait, Z. S., Olmos, L., Sousoni, D., Isari, S., Martínez, R. A, Bouquet, J.-M., Thompson, E. M., Båmstedt, U. and Jakobsen, H. H.: Future climate scenarios for a coastal productive planktonic food web resulting in microplankton phenology changes and decreased trophic transfer efficiency., PLoS One, 9, (4), e94388, doi:10.1371/journal.pone.0094388, 2014.

Van Cappellen, P.: Biomineralization and Global Biogeochemical Cycles, Rev. Mineral. Geochemistry, 54, (1), 357–381, doi:10.2113/0540357, 2003.

Cermeno, P., Dutkiewicz, S., Harris, R. P., Follows, M., Schofield, O. and Falkowski, P. G.: The role of nutricline depth in regulating the ocean, PNAS, 105, 51, 2008.

Chen, S. and Gao, K.: Solar ultraviolet radiation and CO_2-induced ocean acidification interacts to influence the photosynthetic performance of the red tide alga *Phaeocystis globosa* (Prymnesiophyceae), Hydrobiologia, 675, (1), 105–117, doi:10.1007/s10750-011-0807-0,

2011.

Chen, S., Beardall, J. and Gao, K.: A red tide alga grown under ocean acidification upregulates its tolerance to lower pH by increasing its photophysiological functions, Biogeosciences, 11, 4829–4837, doi:10.5194/bg-11-4829-2014, 2014.

Clarke, K. R. and Warwick, R. M.: Change In Marine Communities: An approach to statistical analysis and interpretation. Primer statistical analysis, 2nd ed., Primer-E Ltd, Plymouth., 2001.

Coello-Camba, A. and Agustí, S.: Acidification counteracts negative effects of warming on diatom silicification, Biogeosciences Discuss., 30, 1–19, doi:10.5194/bg-2016-424, 2016.

Coello-Camba, A., AgustÃ-, S., Holding, J., Arrieta, J. M. and Duarte, C. M.: Interactive effect of temperature and CO_2 increase in Arctic phytoplankton, Front. Mar. Sci., 1, 1–10, doi:10.3389/fmars.2014.00049, 2014.

Colman, B., Huertas, I. E., Bhatti, S. and Dason, J. S.: The diversity of inorganic carbon acquisition mechanisms in eukaryotic microalgae, Funct. Plant Biol., 29, (3), 261–270 [online] Available from: http://www.publish.csiro.au/paper/PP01184, 2002.

Crawfurd, K. J., Raven, J. A, Wheeler, G. L., Baxter, E. J. and Joint, I.: The response of *Thalassiosira pseudonana* to long-term exposure to increased CO_2 and decreased pH., PLoS One, 6, (10), e26695, doi:10.1371/journal.pone.0026695, 2011.

Crawley, A., Kline, D. I., Dunn, S., Anthony, K. and Dove, S.: The effect of ocean acidification on symbiont photorespiration and productivity in *Acropora formosa*, Glob. Chang. Biol., 16, (2), 851–863, doi:10.1111/j.1365-2486.2009.01943.x, 2010.

Czerny, J., Barcelos e Ramos, J. and Riebesell, U.: Influence of elevated CO_2 concentrations on cell division and nitrogen fixation rates in the bloom-forming cyanobacterium *Nodularia spumigena*, Biogeosciences, 6, (9), 1865–1875, doi:10.5194/bg-6-1865-2009, 2009.

Dason, J. S., Emma Huertas, I. and Colman, B.: Source of Inorganic Carbon for Photosynthesis in

Two Marine Dinoflagellates1, J. Phycol., 40, (2), 285–292, doi:10.1111/j.1529-8817.2004.03123.x, 2004.

Delille, B., Harlay, J., Zondervan, I., Jacquet, S., Chou, L., Wollast, R., Bellerby, R. G. J., Frankignoulle, M., Borges, A. V., Riebesell, U. and Gattuso, J.-P.: Response of primary production and calcification to changes of pCO_2 during experimental blooms of the coccolithophorid *Emiliania huxleyi*, Global Biogeochem. Cycles, 19, (2), doi:10.1029/2004GB002318, 2005.

Deppeler, S. L. and Davidson, A. T.: Southern Ocean Phytoplankton in a Changing Climate, Front. Mar. Sci., 4, (February), doi:10.3389/fmars.2017.00040, 2017.

Desroy, N. and Denis, L.: Influence of spring phytodetritus sedimentation on intertidal macrozoobenthos in the eastern English Channel, Mar. Ecol. Prog. Ser., 270, 41–53, doi:10.3354/meps270041, 2004.

Dickson, A. G. and Millero, F. J.: A comparison of the equilibrium constants for the dissociation of carbonic acid in seawater media, Deep Sea Res. Part I Oceanogr. Res. Pap., 34, (111), 1733–1743, 1987.

DiTullio, G. R., Grebmeier, J. M., Arrigo, K. R., Lizotte, M. P., Robinson, D. H., Leventer, A., Barry, J. P., VanWoert, M. L. and Dunbar, R. B.: Rapid and early export of *Phaeocystis antarctica* blooms in the Ross Sea, Antarctica, Nature, 404, (6778), 595–598 [online] Available from: http://dx.doi.org/10.1038/35007061, 2000.

Dubelaar, G. B. J. and van der Reijden, C. S.: Size distributions of *Microcystis aeruginosa* colonies: a flow cytometric approach, Water Sci. Technol., 32, (4), 171–176 [online] Available from: http://wst.iwaponline.com/content/32/4/171.abstract, 1995.

Dutz, J., Klein Breteler, W. C. M. and Kramer, G.: Inhibition of copepod feeding by exudates and transparent exopolymer particles (TEP) derived from a *Phaeocystis globosa* dominated phytoplankton community, Harmful Algae, 4, (5), 929–940, doi:10.1016/j.hal.2004.12.003,

2005.

Edwards, M. and Richardson, A. J.: Impact of climate change on marine pelagic phenology and trophic mismatch, Nature, 430, (7002), 881–884, doi:10.1038/nature02808, 2004.

Edwards, M., Johns, D., Leterme, S. C., Svendsen, E. and Richardson, A. J.: Regional climate change and harmful algal blooms in the northeast Atlantic, Limnol. Oceanogr., 51, (2), 820–829, doi:10.4319/lo.2006.51.2.0820, 2006.

Egge, J. K., Aksnes, D. L.: Silicate as a regulating nutrient in phytoplankton competition, Mar. Ecol. Prog. Ser., 83, 281–289, 1992.

Egge, J. K., Thingstad, T. F., Larsen, A., Engel, A., Wohlers, J., Bellerby, R. G. J. and Riebesell, U.: Primary production during nutrient-induced blooms at elevated CO_2 concentrations, Biogeosciences, 6, (5), 877–885, doi:10.5194/bg-6-877-2009, 2009.

Eggers, S. L., Lewandowska, A. M., Barcelos e Ramos, J., Blanco-Ameijeiras, S., Gallo, F. and Matthiessen, B.: Community composition has greater impact on the functioning of marine phytoplankton communities than ocean acidification., Glob. Chang. Biol., 20, (3), 713–723, doi:10.1111/gcb.12421, 2014.

Eilertsen, H. and Raa, J.: Toxins in seawater produced by a common phytoplankter : *Phaeocystis pouchetii*, J. Mar. Biotechnol., 3(1), 115–119 [online] Available from: http://ci.nii.ac.jp/naid/10002209414/en/ (Accessed 28 January 2016), 1995.

Eilertsen, H. C., Taasen, J. P. and WesIawski, J. M.: Phytoplankton studies in the fjords of West Spitzbergen: physical environment and production in spring and summer, J. Plankt. Res. , 11, (6), 1245–1260, doi:10.1093/plankt/11.6.1245, 1989.

Elzenga, J. T. M., Prins, H. B. A. and Stefels, J.: The role of extracellular carbonic anhydrase activity in inorganic carbon utilization of *Phaeocystis globosa* (Prymnesiophyceae): A comparison with other marine algae using the isotopic disequilibrium technique, , 45, (2), 372–

380, 2000.

Endo, H., Yoshimura, T., Kataoka, T. and Suzuki, K.: Effects of CO_2 and iron availability on phytoplankton and eubacterial community compositions in the northwest subarctic Pacific, J. Exp. Mar. Bio. Ecol., 439, 160–175, doi:10.1016/j.jembe.2012.11.003, 2013.

Engel, A., Schulz, K. G., Riebesell, U., Bellerby, R., Delille, B. and Schartau, M.: Effects of CO_2 on particle size distribution and phytoplankton abundance during a mesocosm bloom experiment (PeECE II), Biogeosciences, 5, 509–521, doi:10.5194/bgd-4-4101-2007, 2008.

Eppley, R. W.: Temperature and phytoplankton growth in the sea, Fish. Bull., 70(4), 1063–1085, 1972.

Errera, R. M., Yvon-Lewis, S., Kessler, J. D. and Campbell, L.: Reponses of the dinoflagellate *Karenia brevis* to climate change: pCO_2 and sea surface temperatures, Harmful Algae, 37, 110–116, doi:10.1016/j.hal.2014.05.012, 2014.

Falkowski, P. G. and Raven, J. A.: Aquatic Photosynthesis: Second Edition, Princeton University Press., 2007.

Feng, Y., Warner, M. E., Zhang, Y., Sun, J., Fu, F.-X., Rose, J. M. and Hutchins, D. A.: Interactive effects of increased pCO_2 , temperature and irradiance on the marine coccolithophore *Emiliania huxleyi* (Prymnesiophyceae), Eur. J. Phycol., 43, (1), 87–98, doi:10.1080/09670260701664674, 2008.

Feng, Y., Hare, C., Leblanc, K., Rose, J., Zhang, Y., DiTullio, G., Lee, P., Wilhelm, S., Rowe, J., Sun, J., Nemcek, N., Gueguen, C., Passow, U., Benner, I., Brown, C. and Hutchins, D. A: Effects of increased pCO_2 and temperature on the North Atlantic spring bloom. I. The phytoplankton community and biogeochemical response, Mar. Ecol. Prog. Ser., 388, 13–25, doi:10.3354/meps08133, 2009.

Feng, Y., Hare, C. E., Rose, J. M., Handy, S. M., DiTullio, G. R., Lee, P. a., Smith, W. O., Peloquin, J., Tozzi, S., Sun, J., Zhang, Y., Dunbar, R. B., Long, M. C., Sohst, B., Lohan, M. and Hutchins, D. A.:

Interactive effects of iron, irradiance and CO_2 on Ross Sea phytoplankton, Deep Sea Res. Part I Oceanogr. Res. Pap., 57, (3), 368–383, doi:10.1016/j.dsr.2009.10.013, 2010.

Findlay, H. S., Calosi, P. and Crawfurd, K. J.: Determinants of the PIC:POC response in the coccolithophore *Emiliania huxleyi* under future ocean acidification scenarios, Limnol. Oceanogr., 56, (3), 1168–1178, doi:10.4319/lo.2011.56.3.1168, 2011.

Finkel, Z. V., Beardall, J., Flynn, K. J., Quigg, A., Rees, T. A. V. and Raven, J. A.: Phytoplankton in a changing world: cell size and elemental stoichiometry, J. Plankton Res., 32, (1), 119–137, doi:10.1093/plankt/fbp098, 2009.

Finkel, Z. V, Katz, M. E., Wright, J. D., Schofield, O. M. E. and Falkowski, P. G.: Climatically driven macroevolutionary patterns in the size of marine diatoms over the Cenozoic., Proc. Natl. Acad. Sci. U. S. A., 102, (25), 8927–32, doi:10.1073/pnas.0409907102, 2005.

Flores-Moya, A., Rouco, M. Nica, García-Sánchez, M. J. S, García-Balboa, C., González, R., Costas, E. and López-Rodas, V.: Effects of adaptation, chance, and history on the evolution of the toxic dinoflagellate *Alexandrium minutum* under selection of increased temperature and acidification, Ecol. Evol., 2, (6), 1251–1259, doi:10.1002/ece3.198, 2012.

Fu, F.-X., Warner, M. E., Zhang, Y., Feng, Y. and Hutchins, D. A.: Effects of Increased Temperature and CO_2 on Photosynthesis, Growth, and Elemental Ratios in Marine *Synechococcus* and *Prochlorococcus* (Cyanobacteria), J. Phycol., 43, (3), 485–496, doi:10.1111/j.1529-8817.2007.00355.x, 2007.

Fu, F.-X., Zhang, Y., Warner, M. E., Feng, Y., Sun, J. and Hutchins, D. A.: A comparison of future increased CO_2 and temperature effects on sympatric *Heterosigma akashiwo* and *Prorocentrum minimum,* Harmful Algae, 7, (1), 76–90, doi:10.1016/j.hal.2007.05.006, 2008.

Fu, F., Tatters, A. and Hutchins, D. A.: Global change and the future of harmful algal blooms in the ocean, Mar. Ecol. Prog. Ser., 470, 207–233, doi:10.3354/meps10047, 2012.

Fu, F. X., Place, A. R., Garcia, N. S. and Hutchins, D. A.: CO_2 and phosphate availability control the toxicity of the harmful bloom dinoflagellate *Karlodinium veneficum*, Aquat. Microb. Ecol., 59, (1), 55–65, doi:10.3354/ame01396, 2010.

Gail, F. W.: Hydrogen ion concentration and other factors affecting the distribution of Fucus, California, Puget Sound Biol. Stn. Publ., 2, 287–306, doi:10.1149/1.4705483, 1919.

Gao, G., Jin, P., Liu, N., Li, F., Tong, S., Hutchins, D. A. and Gao, K.: Combined effects of elevated pCO_2 and temperature on biomass and carbon fixation of phytoplankton assemblages in the northern South China Sea, Biogeosciences Discuss., 1–29, doi:10.5194/bg-2016-403, 2016.

Gao, G., Jin, P., Liu, N., Li, F., Tong, S., Hutchins, D. A. and Gao, K.: The acclimation process of phytoplankton biomass, carbon fixation and respiration to the combined effects of elevated temperature and pCO_2 in the northern South China Sea, Mar. Pollut. Bull., 118, (1–2), 213–220, doi:10.1016/j.marpolbul.2017.02.063, 2017.

Gao, K.: Changes in Bioenergetics Associated with Ocean Acidification and Climate Changes, Bioenerg. Open Access, 06, (01), 8–9, doi:10.4172/2167-7662.1000147, 2017.

Gao, K., Xu, J., Gao, G., Li, Y., Hutchins, D. A., Huang, B., Wang, L., Zheng, Y., Jin, P., Cai, X., Häder, D.-P., Li, W., Xu, K., Liu, N. and Riebesell, U.: Rising CO_2 and increased light exposure synergistically reduce marine primary productivity, Nat. Clim. Chang., 2, (5), 519–523, doi:10.1038/nclimate1507, 2012.

Gasparini, S., Daro, M. H., Antajan, E., Tackx, M., Rousseau, V., Parent, J. Y. and Lancelot, C.: Mesozooplankton grazing during the *Phaeocystis globosa* bloom in the southern bight of the North Sea, J. Sea Res., 43(3–4), 345–356, doi:10.1016/S1385-1101(00)00016-2, 2000.

Geider, R. and MacIntyre, H.: Physiology and Biochemistry of photosynthesis and Algal Carbon Acquisition: Phytoplankton Productivity: Carbon Assimilation in Marine and Freshwater Ecosystems, John Wiley & Sons, 2008.

Gervais, F. and Riebesell, U.: Effect of phosphorus limitation on elemental composition and stable carbon isotope fractionation in a marine diatom growing under different CO_2 concentrations, Limnol. Oceanogr., 46, (3), 497–504, doi:10.4319/lo.2001.46.3.0497, 2001.

Gilpin, L. C., Davidson, K. and Roberts, E.: The influence of changes in nitrogen: silicon ratios on diatom growth dynamics, J. Sea Res., 51, (1), 21–35, doi:10.1016/j.seares.2003.05.005, 2004.

Giordano, M., Beardall, J. and Raven, J. A: CO_2 concentrating mechanisms in algae: mechanisms, environmental modulation, and evolution., Annu. Rev. Plant Biol., 56, 99–131, doi:10.1146/annurev.arplant.56.032604.144052, 2005.

Goldman, J. and Carpenter, E.: A kinetic approach to the effect of temperature on algal growth, Limnol. Oceanogr., 19, (5), 756–766, doi:10.4319/lo.1974.19.5.0756, 1974.

Gruber, N. and Sarmiento, J. L.: Global patterns or marine nitrogen fixation and denitrification, Global Biogeochem. Cycles, 11, (2), 235–266, 1997.

Gunawan, A. and Ng, K. M.: Solving the teacher assignment problem by two metaheuristics.: Intl j. Info, Mngnt Sci, 22, 1, 73-86, 2011.

Hallegraeff, G. M.: A review of harmful algal blooms and their apparent global increase, Phycologia, 32, (2), 79–99, doi:10.2216/i0031-8884-32-2-79.1, 1993.

Hammes, F., Vital, M. and Egli, T.: Critical evaluation of the volumetric “bottle effect” on microbial batch growth, Appl. Environ. Microbiol., 76, (4), 1278–1281, doi:10.1128/AEM.01914-09, 2010.

Hansen, E. and Eilertsen, H. C.: Do the polyunsaturated aldehydes produced by *Phaeocystis pouchetii* (Hariot) Lagerheim influence diatom growth during the spring bloom in Northern Norway?, J. Plankt. Res. , 29, (1), 87–96, doi:10.1093/plankt/fbl065, 2007.

Hansen, P.: Effect of high pH on the growth and survival of marine phytoplankton: implications for species succession, Aquat. Microb. Ecol., 28, 279–288, doi:10.3354/ame028279, 2002.

Hare, C., Leblanc, K., DiTullio, G., Kudela, R., Zhang, Y., Lee, P., Riseman, S. and Hutchins, D. A.: Consequences of increased temperature and CO_2 for phytoplankton community structure in the Bering Sea, Mar. Ecol. Prog. Ser., 352, 9–16, doi:10.3354/meps07182, 2007.

Harris, R.: The L4 time-series: the first 20 years, J. Plankton Res., 32, (5), 577–583, doi:10.1093/plankt/fbq021, 2010.

Hegerl, G. C. and Bindoff, N. L.: Ocean science. Warming the world's oceans., Science, 309, (5732), 254–5, doi:10.1126/science.1114456, 2005.

Heil, C. A., Glibert, P. M. and Fan, C.: *Prorocentrum minimum* (Pavillard) Schiller: A review of a harmful algal bloom species of growing worldwide importance, Harmful Algae, 4, (3), 449–470, doi:10.1016/j.hal.2004.08.003, 2005.

Hein, M. and Sand-Jensen, K.: CO_2 increases oceanic primary production, Nature, 388, (6642), 526–527, 1997.

Herberich, E., Sikorski, J. and Hothorn, T.: A Robust Procedure for Comparing Multiple Means under Heteroscedasticity in Unbalanced Designs, PLoS One, 5, (3), e9788, doi:10.1371/journal.pone.0009788, 2010.

Hinga, K. R.: Effects of pH on coastal marine phytoplankton, Mar. Ecol. Prog. Ser., 238, 281–300, 2002.

Holligan, P. M. and Harbour, D. S.: The vertical distribution and succession of phytoplankton in the western English Channel in 1975 and 1976, J. Mar. Biol. Assoc. United Kingdom, 57, (04), 1075–1093, 1977.

Hoogstraten, A., Peters, M., Timmermans, K. R. and De Baar, H. J. W.: Combined effects of inorganic carbon and light on *Phaeocystis globosa* Scherffel (Prymnesiophyceae), Biogeosciences, 9, (5), 1885–1896, doi:10.5194/bg-9-1885-2012, 2012.

Hoppe, C. J. M., Langer, G. and Rost, B.: *Emiliania huxleyi* shows identical responses to elevated

pCO_2 in TA and DIC manipulations, J. Exp. Mar. Bio. Ecol., 406, (1–2), 54–62, doi:10.1016/j.jembe.2011.06.008, 2011.

Hoppe, C. J. M., Holtz, L. and Trimborn, S.: Ocean acidification decreases the light-use efficiency in an Antarctic diatom under dynamic but not constant light, New Phytol., 2015.

Hu, S., Zhou, B., Wang, Y., Wang, Y., Zhang, X., Zhao, Y., Zhao, X. and Tang, X.: Effect of CO_2-induced seawater acidification on growth, photosynthesis and inorganic carbon acquisition of the harmful bloom-forming marine microalga, *Karenia mikimotoi*, PLoS One, 12, (8), 1–19, doi:10.1371/journal.pone.0183289, 2017.

Hutchins, D. A., Fu, F.-X., Zhang, Y., Warner, M. E., Feng, Y., Portune, K., Bernhardt, P. W. and Mulholland, M. R.: CO_2 control of *Trichodesmium* N_2 fixation, photosynthesis, growth rates, and elemental ratios: Implications for past, present, and future ocean biogeochemistry, Limnol. Oceanogr., 52, (4), 1293–1304, doi:10.4319/lo.2007.52.4.1293, 2007.

Hutchins, D. A., Walworth, N. G., Webb, E. A., Saito, M. A., Moran, D., McIlvin, M. R., Gale, J. and Fu, F.-X.: Irreversibly increased nitrogen fixation in *Trichodesmium* experimentally adapted to elevated carbon dioxide, Nat. Commun., 6, 8155, doi:10.1038/ncomms9155, 2015.

Hutchins, D. A., Mulholland, M. R. and Fu, F.: Nutrient Cycles and Marine Microbes in a CO_2 -Enriched Ocean, Oceanograpgy, 22, (4), 128–145, 2009.

Hyun, B., Choi, K., Jang, P., Jang, M. and Lee, W.: Effects of Increased CO_2 and Temperature on the Growth of Four Diatom Species (*Chaetoceros debilis , Chaetoceros didymus , Skeletonema costatum and Thalassiosira nordenskioeldii*) in Laboratory Experiments, J. Environ. Sci. Int., 2014.

Iglesias-Prieto, R., Beltrán, V. H., LaJeunesse, T. C., Reyes-Bonilla, H. and Thomé, P. E.: Different algal symbionts explain the vertical distribution of dominant reef corals in the eastern Pacific., Proc. Biol. Sci., 271, (1549), 1757–63, doi:10.1098/rspb.2004.2757, 2004.

Iglesias-rodriguez, M. D., World, H., Halloran, P. R., Rickaby, R. E. M., Hall, I. R., Colmenero-hidalgo, E., Gittins, J. R., Green, D. R. H., Tyrrell, T., Gibbs, S. J., Dassow, P. Von, Rehm, E., Armbrust, E. V. and Boessenkool, K. P.: Phytoplankton Calcification in a high CO_2 world, Science, (80)., 336, 336–340, doi:10.1126/science.1154122, 2008.

Ihnken, S., Roberts, S. and Beardall, J.: Differential responses of growth and photosynthesis in the marine diatom *Chaetoceros muelleri* to CO_2 and light availability, Phycologia, 50, (2), 182–193, doi:10.2216/10-11.1, 2011.

Jahnke, J. and Baumann, M. E. M.: Differentiation between *Phaeocystis pouchetii* (Har.) Lagerheim and *Phaeocystis globosa* Scherffel, Hydrobiol. Bull., 21, (2), 141–147, doi:10.1007/BF02255439, 1987.

Jeffery, S. W.: Phytoplankton Pigments in Oceanography: Guidelines to Modern Methods, 10th ed., edited by S. Jefferey, R. Mantoura, and S. Wright, UNESCO, Paris., 1997.

Jin, P. and Gao, K.: Reduced resilience of a globally distributed coccolithophore to ocean acidification: Confirmed up to 2000 generations, Mar. Pollut. Bull., 103, (1–2), 101–108, doi:10.1016/j.marpolbul.2015.12.039, 2016.

Joint, I., Doney, S. C. and Karl, D. M.: Will ocean acidification affect marine microbes?, ISME J., 5, (1), 1–7, doi:10.1038/ismej.2010.79, 2011.

Jolliffe, I. T.: Principal Component Analysis, Second Edition, Encycl. Stat. Behav. Sci., 30, (3), 487, doi:10.2307/1270093, 2002.

Keys, M., Tilstone, G., Findlay, H. S., Widdicombe, C. E. and Lawson, T.: Effects of elevated CO_2 on phytoplankton community biomass and species composition during a spring *Phaeocystis* spp. bloom in the western English Channel, Harmful Algae, 67, 92–106, doi:10.1016/j.hal.2017.06.005, 2017.

Kim, J.-M., Lee, K., Shin, K., Kang, J.-H., Lee, H.-W., Kim, M., Jang, P.-G. and Jang, M.-C.: The effect of

seawater CO_2 concentration on growth of a natural phytoplankton assemblage in a controlled mesocosm experiment, Limnol. Oceanogr., 51, (4), 1629–1636, doi:10.4319/lo.2006.51.4.1629, 2006.

Kitidis, V., Hardman-mountford, N. J., Litt, E., Brown, I., Cummings, D., Hartman, S., Hydes, D., Fishwick, J. R., Harris, C., Martinez-vicente, V., Woodward, E. M. S. and Smyth, T. J.: Seasonal dynamics of the carbonate system in the Western English Channel, Cont. Shelf Res., 42, 2–12, 2012.

Kolber, Z. S., Prášil, O. and Falkowski, P. G.: Measurements of variable chlorophyll fluorescence using fast repetition rate techniques: Defining methodology and experimental protocols, Biochim. Biophys. Acta - Bioenerg., 1367,(1–3), 88–106, doi:10.1016/S0005-2728(98)00135-2, 1998.

Körtzinger, A., Koeve, W., Kähler, P. and Mintrop, L.: C:N ratios in the mixed layer during the productive season in the northeast Atlantic Ocean, Deep Sea Res. Part I Oceanogr. Res. Pap., 48, (3), 661–688, doi:https://doi.org/10.1016/S0967-0637(00)00051-0, 2001.

Kovala, P. E. and Larrance, J. D.: Computation of phytoplankton cell numbers, cell volume, cell surface and plasma volume per liter, from microscopical counts., DTIC Document., 1966.

Kranz, S. A., Sultemeyer, D., Richter, K.-U. and Rost, B.: Carbon acquisition by *Trichodesmium* : The effect of pCO_2 and diurnal changes, Limnol. Oceanogr., 54, (2), 548–559, 2009.

Lancelot, C. and Mathot, S.: Dynamics of a *Phaeocystis*-dominated spring bloom in Belgian coastal waters. I. Phytoplanktonic activities and related parameters, Mar. Ecol. Prog. Ser., 37, 249–257, doi:10.3354/meps037249, 1987.

Lancelot, C., Rousseau, V., Schoemann, V., Becquevort, S., Garcés, E., Zingone, A., Montresor, M., Reguera, B. and Dalle, B.: On the ecological role of the different life forms of *Phaeocystis*, Proc. EC Work. LIFEHAB Life Hist. microalgal species causing harmful Bloom., 214, 2002.

Lancelot, C., Rousseau, V. and Gypens, N.: Ecologically based indicators for *Phaeocystis* disturbance in eutrophied Belgian coastal waters (Southern North Sea) based on field observations and ecological modelling, J. Sea Res., 61, 44–49, doi:10.1016/j.seares20088055010, 2009.

Langer, G., Geisen, M., Baumann, K.-H., Kläs, J., Riebesell, U., Thoms, S. and Young, J. R.: Species-specific responses of calcifying algae to changing seawater carbonate chemistry, Geochemistry, Geophys. Geosystems, 7, (9), doi:10.1029/2005GC001227, 2006.

Langer, G., Nehrke, G., Probert, I., Ly, J. and Ziveri, P.: Strain-specific responses of *Emiliania huxleyi* to changing seawater carbonate chemistry, Biogeosciences, 6, (11), 2637–2646, doi:10.5194/bg-6-2637-2009, 2009.

Lawrenz, E., Silsbe, G., Capuzzo, E., Ylöstalo, P., Forster, R. M., Simis, S. G. H., Prášil, O., Kromkamp, J. C., Hickman, A. E., Moore, C. M., Forget, M. H., Geider, R. J. and Suggett, D. J.: Predicting the Electron Requirement for Carbon Fixation in Seas and Oceans, PLoS One, 8, (3), doi:10.1371/journal.pone.0058137, 2013.

Laws, A., Falkowski, G., Smith, O., Hugh, J. and Mccarthy, J.: Temperature effects on export production in the open ocean, Global Biogeochem. Cycles, 14, (4), 1231–1246, 2000.

Lebour, M. V.: The microplankton of Plymouth Sound from the region beyond the Breakwater, J. Mar. Biol. Assoc. United Kingdom, 11, (2), 135–182, doi:http://dx.doi.org/10.1017/S0025315400047949, 1917.

Lefebvre, S. C., Benner, I., Stillman, J. H., Parker, A. E., Drake, M. K., Rossignol, P. E., Okimura, K. M., Komada, T. and Carpenter, E. J.: Nitrogen source and pCO_2 synergistically affect carbon allocation, growth and morphology of the coccolithophore *Emiliania huxleyi*: potential implications of ocean acidification for the carbon cycle, Glob. Chang. Biol., 18, (2), 493–503, doi:10.1111/j.1365-2486.2011.02575.x, 2012.

Leonardos, N. and Geider, R. J.: Elevated Atmospheric Carbon Dioxide Increases Organic Carbon Fixation By *Emiliania Huxleyi* (Haptophyta), Under Nutrient-Limited High-Light Conditions, J. Phycol., 41, (6), 1196–1203, doi:10.1111/j.1529-8817.2005.00152.x, 2005.

Levitan, O., Rosenberg, G., Setlik, I., Setlikova, E., Grigel, J., Klepetar, J., Prasil, O. and Berman-Frank, I.: Elevated CO_2 enhances nitrogen fixation and growth in the marine cyanobacterium *Trichodesmium*, Glob. Chang. Biol., 13, (2), 531–538, doi:10.1111/j.1365-2486.2006.01314.x, 2007.

Li, W. K. W., McLaughlin, F. A., Lovejoy, C. and Carmack, E. C.: Smallest Algae Thrive As the Arctic Ocean Freshens, Science, (80)., 326(5952), 539–539, doi:10.1126/science.1179798, 2009.

Liss, P., Malin, G., Turner, S. and Holligan, P.: Dimethyl sulphide and *Phaeocystis*: A review, J. Mar. Syst., 5, 41–53 [online] Available from: http://www.sciencedirect.com/science/article/pii/0924796394900159, 1994.

Lohbeck, K. T., Riebesell, U. and Reusch, T. B. H.: Adaptive evolution of a key phytoplankton species to ocean acidification, Nat. Geosci., 5, (5), 346–351, doi:10.1038/ngeo1441, 2012.

Lomas, M. W. and Glibert, P. M.: Interactions between NH_4^+ and NO_3^- uptake and assimilation: Comparison of diatoms and dinoflagellates at several growth temperatures, Mar. Biol., 133, (3), 541–551, doi:10.1007/s002270050494, 1999.

Mackinder, L., Wheeler, G., Schroeder, D., Riebesell, U. and Brownlee, C.: Molecular Mechanisms Underlying Calcification in Coccolithophores, Geomicrobiol. J., 27, (6–7), 585–595, doi:10.1080/01490451003703014, 2010.

Manning, M. M. and Gates, R. D.: Diversity in populations of free-living *Symbiodinium* from a Caribbean and Pacific reef, Limnol. Oceanogr., 53, (5), 1853–1861, doi:10.4319/lo.2008.53.5.1853, 2008.

Marinov, I., Doney, S. C. and Lima, I. D.: Response of ocean phytoplankton community structure

to climate change over the 21st century: partitioning the effects of nutrients, temperature and light, Biogeosciences, 7, (12), 3941–3959, doi:10.5194/bg-7-3941-2010, 2010.

Marra, J.: Net and gross productivity: weighing in with ^{14}C, Aquat. Microb. Ecol., 56, 123–131, doi:10.3354/ame01306, 2009.

Matsuda, Y., Satoh, K., Harada, H., Satoh, D., Hiraoka, Y. and Hara, T.: Regulation of the expressions of HCO^{3-} uptake and intracellular carbonic anhydrase in response to CO_2 concentration in the diatom *Phaeodactylum* sp., Funct. Plant Biol., 29, (3), 279–287 [online] Available from: https://doi.org/10.1071/PP01186, 2002.

Maugendre, L., Gattuso, J. P., Poulton, A. J., Dellisanti, W., Gaubert, M., Guieu, C. and Gazeau, F.: No detectable effect of ocean acidification on plankton metabolism in the NW oligotrophic Mediterranean Sea: Results from two mesocosm studies, Estuar. Coast. Shelf Sci., 186, 89–99, doi:10.1016/j.ecss.2015.03.009, 2017.

McClendon, J. F.: On changes in the sea, Pap. from Tortugas Lab. Carnegie Inst. Washingt., (102–103), 213, 1918.

Mehrbach, C., Culberson, C. H., Hawley, J. E. and Pytkowicz, R. M.: Measurement of the Apparent Dissociation Constants of Carbonic Acid in Seawater at Atmospheric Pressure, Limnol. Oceanogr., 18, (1932), 897–907, 1973.

Menden-Deuer, S. and Lessard, E. J.: Carbon to volume relationships for dinoflagellates, diatoms, and other protist plankton, Limnol. Oceanogr., 45, (3), 569–579, doi:10.4319/lo.2000.45.3.0569, 2000.

Milligan, A. J., Varela, D. E., Brzezinski, M. A. and Morel, F. M. M.: Dynamics of silicon metabolism and silicon isotopic discrimination in a marine diatom as a function of pCO_2, Limnol. Oceanogr., 49, (2), 322–329, doi:10.4319/lo.2004.49.2.0322, 2004.

Milliman, J. D.: Production and accumulation of calcium carbonate in the ocean: Budget of a

nonsteady state, Global Biogeochem. Cycles, 7, (4), 927–957, doi:10.1029/93GB02524, 1993.

Mills, M. M. and Arrigo, K. R.: Magnitude of oceanic nitrogen fixation influenced by the nutrient uptake ratio of phytoplankton, Nat. Geosci., 3, (6), 412–416, doi:10.1038/ngeo856, 2010.

Morán, X. A. G., López-Urrutia, Á., Calvo-Díaz, A. and Li, W. K. W.: Increasing importance of small phytoplankton in a warmer ocean, Glob. Chang. Biol., 16, (3), 1137–1144, doi:10.1111/j.1365-2486.2009.01960.x, 2010.

Morse, D., Salois, P., Markovic, P. and Hastings, J. W.: A nuclear-encoded form II RuBisCO in dinoflagellates., Science, 268, (5217), 1622–1624, doi:10.1126/science.7777861, 1995.

Moustaka-Gouni, M., Kormas, K. A., Scotti, M., Vardaka, E. and Sommer, U.: Warming and Acidification Effects on Planktonic Heterotrophic Pico- and Nanoflagellates in a Mesocosm Experiment, Protist, 167, (4), 389–410, doi:10.1016/j.protis.2016.06.004, 2016.

Muller-Karger, F. E.: The importance of continental margins in the global carbon cycle, Geophys. Res. Lett., 32, (1), L01602, doi:10.1029/2004GL021346, 2005.

Müller, M. N., Schulz, K. G. and Riebesell, U.: Effects of long-term high CO_2 exposure on two species of coccolithophores, Biogeosciences, 7, (3), 1109–1116, doi:10.5194/bg-7-1109-2010, 2010.

Nejstgaard, J. C., Tang, K. W., Steinke, M., Dutz, J., Koski, M., Antajan, E. and Long, J. D.: Zooplankton grazing on *Phaeocystis*: A quantitative review and future challenges, Biogeochemistry, 83, (1–3), 147–172, doi:10.1007/s10533-007-9098-y, 2007.

Ospar, S. and Report, I.: Eutrophication Status of the OSPAR Maritime Area Second OSPAR Integrated Report Eutrophication Series, 2009.

Oxborough, K., Moore, C. M., Suggett, D. J., Lawson, T., Chan, H. G. and Geider, R. J.: Direct estimation of functional PSII reaction center concentration and PSII electron flux on a volume basis: a new approach to the analysis of Fast Repetition Rate fluorometry (FRRf) data, Limnol.

Oceanogr. Methods, 10, 142–154, doi:10.4319/lom.2012.10.142, 2012.

Partensky, F., Blanchot, J. and Vaulot, D.: Differential distribution and ecology of *Prochlorococcus* and *Synechococcus* in oceanic waters: a review, Marine Cyanobacteria., edited by L. Charpy and A. W. D. Larkum, Institute of Oceanography, Monaco., 1999.

Paul, A. J., Bach, L. T., Schulz, K.-G., Boxhammer, T., Czerny, J., Achterberg, E. P., Hellemann, D., Trense, Y., Nausch, M., Sswat, M. and Riebesell, U.: Effect of elevated CO_2 on organic matter pools and fluxes in a summer, post spring-bloom Baltic Sea plankton community, Biogeosciences Discuss., 12, 6863–6927, doi:10.5194/bgd-12-6863-2015, 2015a.

Paul, C., Matthiessen, B. and Sommer, U.: Warming, but not enhanced CO_2 concentration, quantitatively and qualitatively affects phytoplankton biomass, Mar. Ecol. Prog. Ser., 528, 39–51, doi:10.3354/meps11264, 2015b.

Paulino, A. I., Egge, J. K. and Larsen, a.: Effects of increased atmospheric CO_2 on small and intermediate sized osmotrophs during a nutrient induced phytoplankton bloom, Biogeosciences Discuss., 4, (6), 4173–4195, doi:10.5194/bgd-4-4173-2007, 2007.

Peperzak, L. and Poelman, M.: Mass mussel mortality in The Netherlands after a bloom of *Phaeocystis globosa* (prymnesiophyceae), J. Sea Res., 60, (3), 220–222, doi:10.1016/j.seares.2008.06.001, 2008.

Peter, K. H. and Sommer, U.: Phytoplankton Cell Size: Intra- and Interspecific Effects of Warming and Grazing, PLoS One, 7, (11), doi:10.1371/journal.pone.0049632, 2012.

Pierrot, D., Lewis, E. and Wallace, D. W. R.: MS Excel program developed for CO_2 system calculations, ORNL/CDIAC-105a. Carbon Dioxide Inf. Anal. Center, Oak Ridge Natl. Lab. US Dep. Energy, Oak Ridge, Tennessee, 2006.

Portis, A. R. and Parry, M. A. J.: Discoveries in Rubisco (Ribulose 1,5-bisphosphate carboxylase/oxygenase): A historical perspective, Photosynth. Res., 94, (1), 121–143,

doi:10.1007/s11120-007-9225-6, 2007.

Poulton, N. J. and Martin, J. L.: Imaging flow cytometry for quantitative phytoplankton analysis - FlowCAM, Microsc. Mol. methods Quant. Phytoplankt. Anal., 47–54, doi:10.1016/j.resp.2011.02.009, 2010.

Preisig, H. and Andersen, R.: Algal Culturing Techniques, 2005th ed., edited by R. Andersen, Elsevier, San Diego., 2005.

Price, G. D., Badger, M. R., Woodger, F. J. and Long, B. M.: Advances in understanding the cyanobacterial CO_2-concentrating-mechanism (CCM): functional components, Ci transporters, diversity, genetic regulation and prospects for engineering into plants., J. Exp. Bot., 59, (7), 1441–61, doi:10.1093/jxb/erm112, 2008.

Prytherch, H. F.: Investigation of the physical conditions controlling spawning of oysters and the occurrence, distribution and settling of oyster larvae in the Milford Harbour, Connecticut, US Bur. Fish. Bull., (44), 429–503, 1929.

Ratti, S., Giordano, M. and Morse, D.: CO_2 -Concentrating Mechanisms of the Potentially Toxic Dinoflagellate *Protoceratium Reticulatum* (Dinophyceae, Gonyaulacales), J. Phycol., 43, (4), 693–701, doi:10.1111/j.1529-8817.2007.00368.x, 2007.

Raupach, M. R., Marland, G., Ciais, P., Le Quéré, C., Canadell, J. G., Klepper, G. and Field, C. B.: Global and regional drivers of accelerating CO_2 emissions., Proc. Natl. Acad. Sci. U. S. A., 104, (24), 10288–93, doi:10.1073/pnas.0700609104, 2007.

Raven. J., Caldeira. K., Elderfield. H., H.-G. and others: Ocean acidification due to increasing atmospheric carbon dioxide, R. Soc., (June), 2005.

Raven, J. A.: Effects on marine algae of changed seawtaer chemistry with increasing atmospheric CO_2, Biol. Environ. Proc. R. Irish Acad., 111, (1), 1–17, doi:10.3318/BIOE.2011.01, 2011.

Raven, J. A. and Geider, R. J.: Temperature and algal growth, New Phytol., 110, (4), 441–461,

doi:10.1111/j.1469-8137.1988.tb00282.x, 1988.

Raven, J. A. and Johnston, A.: Mechanisms of inorganic-carbon acquisition in marine phytoplankton and their implications for the use of other resources, Limnol. Oceanogr., 36, (8), 1707–1714, 1991.

Raven, J. A., Kumlbler, J. E. and Beardall, J.: Put out the light, and then put out the light, J. Mar. Biol. Assoc. United Kingdom, 80, (1), 1–25, 2000.

Raven, J. A, Giordano, M., Beardall, J. and Maberly, S. C.: Algal evolution in relation to atmospheric CO_2: carboxylases, carbon-concentrating mechanisms and carbon oxidation cycles., Philos. Trans. R. Soc. Lond. B. Biol. Sci., 367, (1588), 493–507, doi:10.1098/rstb.2011.0212, 2012.

Rees, A. P., Hope, S. B., Widdicombe, C. E., Dixon, J. L., Woodward, E. M. S. and Fitzsimons, M. F.: Alkaline phosphatase activity in the western English Channel: Elevations induced by high summertime rainfall, Estuar. Coast. Shelf Sci., 81, (4), 569–574, doi:http://dx.doi.org/10.1016/j.ecss.2008.12.005, 2009.

Reinfelder, J. R.: Carbon Concentrating Mechanisms in Eukaryotic Marine Phytoplankton, Ann. Rev. Mar. Sci., 3, (1), 291–315, doi:10.1146/annurev-marine-120709-142720, 2011.

Richier, S., Achterberg, E. P., Dumousseaud, C., Poulton, A. J., Suggett, D. J., Tyrrell, T., Zubkov, M. V. and Moore, C. M.: Phytoplankton responses and associated carbon cycling during shipboard carbonate chemistry manipulation experiments conducted around Northwest European shelf seas, Biogeosciences, 11, (17), 4733–4752, doi:10.5194/bg-11-4733-2014, 2014.

Riebesell, U.: Effects of CO_2 Enrichment on Marine Phytoplankton, J. Oceanogr., 60 (4), 719–729, doi:10.1007/s10872-004-5764-z, 2004.

Riebesell, U. and Jones, D.: Carbon fix for a diatom, Nature, 407, 959–960, 2002.

Riebesell, U. and Zondervan, I.: Reduced calcification of marine plankton in response to

increased atmospheric CO_2, Nature, 407, 2–5, 2000.

Riebesell, U., Wolf-Gladrow, D. A. and Smetacek, V.: Carbon dioxide limitation of marine phytoplankton growth rates, Nature, 361,(6409), 249–251 [online] Available from: http://dx.doi.org/10.1038/361249a0, 1993.

Riebesell, U., Schulz, K. G., Bellerby, R. G. J., Botros, M., Fritsche, P., Meyerhöfer, M., Neill, C., Nondal, G., Oschlies, a, Wohlers, J. and Zöllner, E.: Enhanced biological carbon consumption in a high CO_2 ocean., Nature, 450, (7169), 545–8, doi:10.1038/nature06267, 2007.

Riebesell, U., Körtzinger, A. and Oschlies, A.: Sensitivities of marine carbon fluxes to ocean change., Proc. Natl. Acad. Sci. U. S. A., 106, (49), 20602–9, doi:10.1073/pnas.0813291106, 2009.

Riebesell, U., Fabry, V. J., Hansson, L. and Gattuso, J.-P.: Guide to best practices for ocean acidification, edited by L. H. and J. –P. G. L. U. Riebesell, V. J. Fabry, Publications Office Of The European Union., 2010.

Riebesell, U., Tortell, P. D., Edited by Gattuso, J.-P. and Hansson, L.: Effects of ocean acidification on pelagic organisms and ecosystems, in: Ocean Acidification, Oxford University Press., 2011.

Roberts, K., Granum, E., Leegood, R. C. and Raven, J. A: Carbon acquisition by diatoms., Photosynth. Res., 93, (1–3), 79–88, doi:10.1007/s11120-007-9172-2, 2007.

Rogers, S. I. and Lockwood, S. J.: Observations on coastal fish fauna during a spring bloom of *Phaeocystis pouchetii* in the eastern Irish Sea, J. Mar. Biol. Assoc. United Kingdom, 70, (02), 249, doi:10.1017/S0025315400035360, 2009.

Rokitta, S. D. and Rost, B.: Effects of CO_2 and their modulation by light in the life-cycle stages of the coccolithophore *Emiliania huxleyi*, Limnol. Oceanogr., 57(2), 607–618, doi:10.4319/lo.2012.57.2.0607, 2012.

Rost, B. and Riebesell, U.: Coccolithophores and the biological pump :, edited by H. Thierstein and J. R. Young, Springer, Berlin., 2004.

Rost, B., Zondervan, I. and Riebesell, U.: Light-dependent carbon isotope fractionation in the coccolithophorid *Emiliania huxleyi*, Limnol. Oceanogr., 47(1), 120–128, doi:10.4319/lo.2002.47.1.0120, 2002.

Rost, B., Riebesell, U., Burkhardt, S. and Su, D.: Carbon acquisition of bloom-forming marine phytoplankton, Limnol. Oceanogr., 48, (1), 55–67, 2003.

Rost, B., Riebesell, U. and Sültemeyer, D.: Carbon acquisition of marine phytoplankton: effect of the photoperiodic length, Limnol., 51, (1), 12–20 [online] Available from: http://eprints.uni-kiel.de/5909/ (Accessed 27 July 2014a), 2006.

Rost, B., Richter, K.-U., Riebesell, U. and Hansen, P. J.: Inorganic carbon acquisition in red tide dinoflagellates, Plant, Cell Environ., 29, (5), 810–822, doi:10.1111/j.1365-3040.2005.01450.x, 2006b.

Rost, B., Zondervan, I. and Wolf-Gladrow, D.: Sensitivity of phytoplankton to future changes in ocean carbonate chemistry: current knowledge, contradictions and research directions, Mar. Ecol. Prog. Ser., 373, 227–237, doi:10.3354/meps07776, 2008.

Rousseau, V., Becquevort, S., Parent, J., Gasparini, S., Daro, M., Tackx, M. and Lancelot, C.: Trophic efficiency of the planktonic food web in a coastal ecosystem dominated by *Phaeocystis* colonies, J. Sea Res., 43, 357–372, 2000.

Rousseau, V., Chrétiennot-Dinet, M.-J., Jacobsen, A., Verity, P. and Whipple, S.: The life cycle of *Phaeocystis*: state of knowledge and presumptive role in ecology, Biogeochemistry, 83, (1–3), 29–47, doi:10.1007/s10533-007-9085-3, 2007.

Rubey, W. W.: Geologic history of sea water: an attempt to state the problem, Bull. Geol. Soc. Am., (62), 1111–48, doi:10.1130/0016-7606(1951)62, 1951.

Rutten, T. P. A, Sandee, B. and Hofman, A. R. T.: Phytoplankton monitoring by high performance flow cytometry: A successful approach?, Cytom. Part A, 64, (1), 16–26,

doi:10.1002/cyto.a.20106, 2005.

Sabine, C. L., Feely, R. A, Gruber, N., Key, R. M., Lee, K., Bullister, J. L., Wanninkhof, R., Wong, C. S., Wallace, D. W. R., Tilbrook, B., Millero, F. J., Peng, T.-H., Kozyr, A., Ono, T. and Rios, A. F.: The oceanic sink for anthropogenic CO_2., Science, 305(5682), 367–71, doi:10.1126/science.1097403, 2004.

Sakshaug, E., Bricaud, A., Dandonneau, Y., Falkowski, P. G., Kiefer, D. A., Legendre, L., Morel, A., Parslow, J. and Takahashi, M.: Parameters of photosynthesis: definations, theory and interpretation of results., J. Plankton Res., 19,(11), 1637–1670, doi:10.1093/plankt/19.11.1637, 1997.

Sarmiento, J. L., Slater, R., Barber, R., Bopp, L., Doney, S. C., Hirst, a. C., Kleypas, J., Matear, R., Mikolajewicz, U., Monfray, P., Soldatov, V., Spall, S. a. and Stouffer, R.: Response of ocean ecosystems to climate warming, Global Biogeochem. Cycles, 18, (3), doi:10.1029/2003GB002134, 2004.

Sathyendranath, S., Stuart, V., Nair, A., Oka, K., Nakane, T., Bouman, H., Forget, M. H., Maass, H. and Platt, T.: Carbon-to-chlorophyll ratio and growth rate of phytoplankton in the sea, Mar. Ecol. Prog. Ser., 383, 73–84, doi:10.3354/meps07998, 2009.

Savage, V. M., Gillooly, J. F., Brown, J. H., West, G. B. and Charnov, E. L.: Effects of Body Size and Temperature on Population Growth, Am. Nat., 163, (3), 429–441, doi:10.1086/381872, 2004.

Schlesinger, W. H.: Biogeochemistry: treatise on geochemistry, vol 8, 2005.

Schoemann, V., Becquevort, S., Stefels, J., Rousseau, V. and Lancelot, C.: *Phaeocystis* blooms in the global ocean and their controlling mechanisms: a review, J. Sea Res., 53, (1–2), 43–66, doi:10.1016/j.seares.2004.01.008, 2005.

Schulz, K. G., Riebesell, U., Bellerby, R. G. J., Biswas, H., Meyerhöfer, M., Müller, M. N., Egge, J. K., Nejstgaard, J. C., Neill, C., Wohlers, J. and Zöllner, E.: Build-up and decline of organic matter

during PeECE III, Biogeosciences, 5, (3), 707–718, doi:10.5194/bg-5-707-2008, 2008.

Schulz, K. G., Ramos, J. B., Zeebe, R. E. and Riebesell, U.: Biogeosciences CO_2 perturbation experiments : similarities and differences between dissolved inorganic carbon and total alkalinity manipulations, , Biogeosciences, 6, 2145–2153, 2009.

Schulz, K. G., Bellerby, R. G. J., Brussaard, C. P. D., Büdenbender, J., Czerny, J., Engel, A., Fischer, M., Koch-Klavsen, S., Krug, S. A., Lischka, S., Ludwig, A., Meyerhöfer, M., Nondal, G., Silyakova, A., Stuhr, A. and Riebesell, U.: Temporal biomass dynamics of an Arctic plankton bloom in response to increasing levels of atmospheric carbon dioxide, Biogeosciences, 10, (1), 161–180, doi:10.5194/bg-10-161-2013, 2013.

Sciandra, A, Harlay, J., Lefèvre, D., Lemée, R., Rimmelin, P., Denis, M. and Gattuso, J.: Response of coccolithophorid *Emiliania huxleyi* to elevated partial pressure of CO_2 under nitrogen limitation, Mar. Ecol. Prog. Ser., 261, 111–122, doi:10.3354/meps261111, 2003.

Shanks, A. L. and Trent, J. D.: Marine snow: sinking rates and potential role in vertical flux, Deep Sea Res. Part A. Oceanogr. Res. Pap., 27, (2), 137–143, doi:https://doi.org/10.1016/0198-0149(80)90092-8, 1980.

Shi, D., Xu, Y. and Morel, F. M. M.: Effects of the pH/pCO_2 control method on medium chemistry and phytoplankton growth, Biogeosciences, 6, (7), 1199–1207, doi:10.5194/bg-6-1199-2009, 2009.

Shi, D., Xu, Y., Hopkinson, B. M. and Morel, F. M. M.: Effect of Ocean Acidification on Iron Availability to Marine Phytoplankton, Science, (80)., 327, 676–679, 2010.

Silyakova, A., Bellerby, R. G. J., Schulz, K. G., Czerny, J., Tanaka, T., Nondal, G., Riebesell, U., Engel, A., De Lange, T. and Ludvig, A.: Pelagic community production and carbon-nutrient stoichiometry under variable ocean acidification in an Arctic fjord, Biogeosciences, 10, (7), 4847–4859, doi:10.5194/bg-10-4847-2013, 2013.

Smayda, T. J.: Normal and accelerated sinking of phytoplankton in the sea, Mar. Geol., 11(2), 105–122, doi:https://doi.org/10.1016/0025-3227(71)90070-3, 1971.

Smetacek, V. and Cloern, J. E.: On Phytoplankton Trends, Science, (80)., 319, (5868), 1346–1348 [online] Available from: http://www.jstor.org/stable/20053523, 2008.

Smyth, T. J., Fishwick, J. R., AL-Moosawi, L., Cummings, D. G., Harris, C., Kitidis, V., Rees, A., Martinez-Vicente, V. and Woodward, E. M. S.: A broad spatio-temporal view of the Western English Channel observatory, J. Plankton Res., 32, (5), 585–601, doi:10.1093/plankt/fbp128, 2010.

Sommer, U.: Comparison between steady state and non-steady state competition: Experiments with natural phytoplankton, Limnol. Oceanogr., 30, (2), 335–346, doi:10.4319/lo.1985.30.2.0335, 1985.

Sommer, U. and Lengfellner, K.: Climate change and the timing, magnitude, and composition of the phytoplankton spring bloom, Glob. Chang. Biol., 14, (6), 1199–1208, doi:10.1111/j.1365-2486.2008.01571.x, 2008.

Sommer, U., Adrian, R., Bauer, B. and Winder, M.: The response of temperate aquatic ecosystems to global warming: Novel insights from a multidisciplinary project, Mar. Biol., 159, (11), 2367–2377, doi:10.1007/s00227-012-2085-4, 2012.

Spilmont, N., Denis, L., Artigas, L. F., Caloin, F., Courcot, L., Créach, A., Desroy, N., Gevaert, F., Hacquebart, P., Hubas, C., Janquin, M. A., Lemoine, Y., Luczak, C., Migné, A., Rauch, M. and Davoult, D.: Impact of the *Phaeocystis* globosa spring bloom on the intertidal benthic compartment in the eastern English Channel: A synthesis, Mar. Pollut. Bull., 58, (1), 55–63, doi:10.1016/j.marpolbul.2008.09.007, 2009.

Stabell, O. B., Aanesen, R. T. and Eilertsen, H. C.: Toxic peculiarities of the marine alga *Phaeocystis pouchetii* detected by in vivo and in vitro bioassay methods, Aquat. Toxicol., 44, (4), 279–288,

doi:10.1016/S0166-445X(98)00081-2, 1999.

Stefels, J., Dijkhuizen, L. and Gieskes, W. W.: DMSP-lyase activity in a spring phytoplankton bloom off the Dutch coast, related to *Phaeocystis* sp. abundance, Mar. Ecol. Prog. Ser., 123, (1–3), 235–244, doi:10.3354/meps123235, 1995.

Strom, S.: Novel interactions between phytoplankton and microzooplankton : their influence on the coupling between growth and grazing rates in the sea, Hydrobioliga, 480, 41–54, 2002.

Sun, J., Hutchins, D. A., Seubert, E. L., Feng, Y., Caron, D. A. and Fu, F.-X.: Effects of changing pCO_2 and phosphate availability on domoic acid production and physiology of the marine harmful bloom diatom *Pseudo-nitzschia multiseries*, Limnol. Oceanogr., 56, (3) 829–840, doi:10.4319/lo.2011.56.3.0829, 2011.

Tang, D. L., Kawamura, H., Hai, D.-N. and Takahashi, W.: Remote sensing oceanography of a harmful algal bloom off the coast of southeastern Vietnam, J. Geophys. Res., 109, (3), 1–7, doi:10.1029/2003JC002045, 2004.

Tang, K. W., Jakobsen, H. H. and Visser, A. W.: *Phaeocystis globosa* (Prymnesiophyceae) and the planktonic food web: Feeding, growth, and trophic interactions among grazers, Limnol. Oceanogr., 46, (8), 1860–1870, doi:10.4319/lo.2001.46.8.1860, 2001.

Tango, P. J., Magnien, R., Butler, W., Luckett, C., Luckenbach, M., Lacouture, R. and Poukish, C.: Impacts and potential effects due to *Prorocentrum minimum* blooms in Chesapeake Bay, Harmful Algae, 4, (3), 525–531, doi:10.1016/j.hal.2004.08.014, 2005.

Tarling, G. A., Peck, V., Ward, P., Ensor, N. S., Achterberg, E., Tynan, E., Poulton, A. J., Mitchell, E. and Zubkov, M. V.: Effects of acute ocean acidification on spatially-diverse polar pelagic foodwebs: Insights from on-deck microcosms, Deep. Res. Part II Top. Stud. Oceanogr., 127, 75–92, doi:10.1016/j.dsr2.2016.02.008, 2016.

Tarran, G. A., Heywood, J. L. and Zubkov, M. V.: Latitudinal changes in the standing stocks of

nano- and picoeukaryotic phytoplankton in the Atlantic Ocean, Deep Sea Res. Part II Top. Stud. Oceanogr., 53, (14–16), 1516–1529, doi:10.1016/j.dsr2.2006.05.004, 2006.

Tatters, A. O., Fu, F. X. and Hutchins, D. A.: High CO_2 and silicate limitation synergistically increase the toxicity of *Pseudo-nitzschia fraudulenta*, PLoS One, (2), 7, doi:10.1371/journal.pone.0032116, 2012.

Tatters, A. O., Schnetzer, A., Fu, F., Lie, A. Y. A, Caron, D. and Hutchins, D. A: Short- versus long-term responses to changing CO_2 in a coastal dinoflagellate bloom: implications for interspecific competitive interactions and community structure., Evolution, 67, (7), 1879–91, doi:10.1111/evo.12029, 2013.

Taucher, J., Jones, J., James, A., Brzezinski, M. A., Carlson, C. A., Riebesell, U. and Passow, U.: Combined effects of CO_2 and temperature on carbon uptake and partitioning by the marine diatoms *Thalassiosira weissflogii* and *Dactyliosolen fragilissimus*, Limnol. Oceanogr., 60, (3), 901–919, doi:10.1002/lno.10063, 2015.

Teng, Y. C., Primeau, F. W., Moore, J. K., Lomas, M. W. and Martiny, A. C.: Global-scale variations of the ratios of carbon to phosphorus in exported marine organic matter, Nat. Geosci., 7, (12), 895–898, doi:10.1038/ngeo2303, 2014.

Tett, P., Gowen, R., Mills, D., Fernandes, T., Gilpin, L., Huxham, M., Kennington, K., Read, P., Service, M., Wilkinson, M. and Malcolm, S.: Defining and detecting undesirable disturbance in the context of marine eutrophication., Mar. Pollut. Bull., 55, (1–6), 282–97, doi:10.1016/j.marpolbul.2006.08.028, 2007.

Thoisen, C., Riisgaard, K., Lundholm, N., Nielsen, T. and Hansen, P.: Effect of acidification on an Arctic phytoplankton community from Disko Bay, West Greenland, Mar. Ecol. Prog. Ser., 520, 21–34, doi:10.3354/meps11123, 2015.

Thomas, M. K., Kremer, C. T., Klausmeier, C. A. and Litchman, E.: A Global Pattern of Thermal

Adaptation in Marine Phytoplankton, Science, (80)., 338, (6110), 1085–1088, doi:10.1126/science.1224836, 2012.

Thoms, S., Pahlow, M. and Wolf-Gladrow, D. A.: Model of the carbon concentrating mechanism in chloroplasts of eukaryotic algae., J. Theor. Biol., 208, (3), 295–313, doi:10.1006/jtbi.2000.2219, 2001.

Thomson, P. G., Davidson, A. T. and Maher, L.: Increasing CO_2 changes community composition of pico- and nano-sized protists and prokaryotes at a coastal Antarctic site, Mar. Ecol. Prog. Ser., 554, 51–69, doi:10.3354/meps11803, 2016.

Tilstone, G., Šedivá, B., Tarran, G., Kaňa, R. and Prášil, O.: Effect of CO_2 enrichment on phytoplankton photosynthesis in the North Atlantic sub-tropical gyre, Prog. Oceanogr., doi:10.1016/j.pocean.2016.12.005, 2016.

Torstensson, A., Chierici, M. and Wulff, A.: The influence of increased temperature and carbon dioxide levels on the benthic/sea ice diatom *Navicula directa*, Polar Biol., 35, (2), 205–214, doi:10.1007/s00300-011-1056-4, 2012.

Tortell, P., DiTullio, G., Sigman, D. and Morel, F.: CO_2 effects on taxonomic composition and nutrient utilization in an Equatorial Pacific phytoplankton assemblage, Mar. Ecol. Prog. Ser., 236, 37–43, doi:10.3354/meps236037, 2002.

Tortell, P. D., Rau, G. H. and Morel, F. M. M.: Inorganic carbon acquisition in coastal Pacific phytoplankton communities, Limnol. Oceanogr., 45, (7), 1485–1500, doi:10.4319/lo.2000.45.7.1485, 2000.

Tortell, P. D., Payne, C. D., Li, Y., Trimborn, S., Rost, B., Smith, W. O., Riesselman, C., Dunbar, R. B., Sedwick, P. and DiTullio, G. R.: CO_2 sensitivity of Southern Ocean phytoplankton, Geophys. Res. Lett., 35, (4), L04605, doi:10.1029/2007GL032583, 2008.

Trimborn, S., Lundholm, N., Thoms, S., Richter, K.-U., Krock, B., Hansen, P. J. and Rost, B.:

Inorganic carbon acquisition in potentially toxic and non-toxic diatoms: the effect of pH-induced changes in seawater carbonate chemistry., Physiol. Plant., 133, (1), 92–105, doi:10.1111/j.1399-3054.2007.01038.x, 2008.

Turner, J. T., Ianora, A., Esposito, F., Carotenuto, Y. and Miralto, A.: Zooplankton feeding ecology: does a diet of *Phaeocystis* support good copepod grazing, survival, egg production and egg hatching success?, J. Plankton Res., 24, (11), 1185–1195, doi:10.1093/plankt/24.11.1185, 2002.

Uitz, J. U., Huot, Y., Bruyant, F., Babin, M. and Claustre, H.: Relating phytoplankton photophysiological properties to community structure on large scales, Limnol. Oceanogr., 53, (2), 614–630, doi:10.4319/lo.2008.53.2.0614, 2008.

Utermöhl, H.: Zur vervollkommnung der quantitativen phytoplankton-methodik, Mitt. int. Ver. theor. angew. Limnol., 9, 1–38, 1958.

Verity, P. G.: Grazing experiments and model simulations of the role of zooplankton in *Phaeocystis* food webs, J. Sea Res., 43, (3–4), 317–343, doi:10.1016/S1385-1101(00)00025-3, 2000.

Verity, P. G., Brussaard, C. P., Nejstgaard, J. C., Van Leeuwe, M. A., Lancelot, C. and Medlin, L. K.: Current understanding of *Phaeocystis* ecology and biogeochemistry, and perspectives for future research, edited by M. A. van Leeuwe, J. Stefels, S. Belviso, C. Lancelot, P. G. Verity, and W. W. C. Gieskes, Springer Netherlands., 2007.

Vogt, M., O'Brien, C. J., Peloquin, J. A., Heinle, M., Gruber, N., Ajani, P., Andruleit, H., Arstegui, J., Beaufort, L., Estrada, M., Karentz, D., Kopczyska, E., Lee, R., Poulton, A. J., Pritchard, T. and Widdicombe, C.: Global marine plankton functional type biomass distributions: Coccolithophores, Earth Syst. Sci. Data, 5, (2), 259–276, doi:10.5194/essd-5-259-2013, 2013.

Wang, Y., Smith, W. O., Wang, X. and Li, S.: Subtle biological responses to increased CO_2 concentrations by *Phaeocystis globosa* Scherffel, a harmful algal bloom species, Geophys. Res.

Lett., 37, 1–5, doi:10.1029/2010GL042666, 2010.

Wannicke, N., Endres, S., Engel, A., Grossart, H.-P., Nausch, M., Unger, J. and Voss, M.: Response of *Nodularia spumigena* to pCO_2 – Part 1: Growth, production and nitrogen cycling, Biogeosciences, 9, (8), 2973–2988, doi:10.5194/bg-9-2973-2012, 2012.

Wassmann, P., Vernet, M., Mitchell, B. and Rey, F.: Mass sedimentation of *Phaeocystis pouchetii* in the Barents Sea , Mar. Ecol. Prog. Ser., 66, 183–195, doi:10.3354/meps066183, 1990.

Webb, W. L., Newton, M. and Starr, D.: Carbon dioxide exchange of *Alnus rubra*, Oecologia, 17(4), 281–291, doi:10.1007/BF00345747, 1974.

Welschmeyer: Fluorometric analysis of chlorophyll a in the presence of chlorophyll b and pheopigments, Limnol. Oceanogr., 39, (8), 1985–1992, 1994.

Widdicombe, C. E., Eloire, D., Harbour, D., Harris, R. P. and Somerfield, P. J.: Long-term phytoplankton community dynamics in the Western English Channel, J. Plankton Res., 32, (5), 643–655, doi:10.1093/plankt/fbp127, 2010.

Wolf-gladrow, B. D. A., Riebesell, U. L. F., Burkhardt, S. and Jelle, B.: Direct effects of CO_2 concentration on growth and isotopic composition of marine plankton, Tellus, 51B, 461–476, 1999.

Wollast, R.: “Evaluation and comparison of the global carbon cycle in the coastal zone and in the open ocean.” The sea., (10) 1998.

Woods, H. A. and Harrison, J. F.: Temperature and the chemical composition of poikilothermic organisms, Func. Ecol, (17), 237–245, 2003.

Wu, Y., Gao, K. and Riebesell, U.: CO_2-induced seawater acidification affects physiological performance of the marine diatom *Phaeodactylum tricornutum*, Biogeosciences, 7, (9), 2915–2923, doi:10.5194/bg-7-2915-2010, 2010.

Wu, Y., Campbell, D. A., Irwin, A. J., Suggett, D. J. and Finkel, Z. V.: Ocean acidification enhances the growth rate of larger diatoms, Limnol. Oceanogr., 59, (3), 1027–1034, doi:10.4319/lo.2014.59.3.1027, 2014.

Wynn-Edwards, C., King, R., Davidson, A., Wright, S., Nichols, P., Wotherspoon, S., Kawaguchi, S. and Virtue, P.: Species-Specific Variations in the Nutritional Quality of Southern Ocean Phytoplankton in Response to Elevated pCO_2, Water, 6, (6), 1840–1859, doi:10.3390/w6061840, 2014.

Xie, Y., Tilstone, G. H., Widdicombe, C., Woodward, E. M. S., Harris, C. and Barnes, M. K.: Effect of increases in temperature and nutrients on phytoplankton community structure and photosynthesis in the western English channel, Mar. Ecol. Prog. Ser., 519, 61–73, doi:10.3354/meps11101, 2015.

Xu, K., Fu, F.-X. and Hutchins, D. A: Comparative responses of two dominant Antarctic phytoplankton taxa to interactions between ocean acidification, warming, irradiance, and iron availability, Limnol. Ocean., 59, (6), 1919–1931, doi:10.4319/lo.2014.59.6.1919, 2014.

Yang, G. and Gao, K.: Physiological responses of the marine diatom *Thalassiosira pseudonana* to increased pCO_2 and seawater acidity., Mar. Environ. Res., 79, 142–51, doi:10.1016/j.marenvres.2012.06.002, 2012.

Zondervan, I., Rost, B. and Riebesell, U.: Effect of CO_2 concentration on the PIC/POC ratio in the coccolithophore *Emiliania huxleyi* grown under light-limiting conditions and different daylengths, J. Exp. Mar. Bio. Ecol., 272, (1), 55–70, doi:10.1016/S0022-0981(02)00037-0, 2002.